AD-A161 452 ISSUES IN FREQUENCY DOMAIN FEEDBACK CONTROL(U) ILLINOIS 1/5
UNIV AT URBANA DECISION AND CONTROL LAB
J S FREUDENBERG MAY 85 DC-81 N00014-84-C-0149

UNCLASSIFIED F/G 9/3 NL

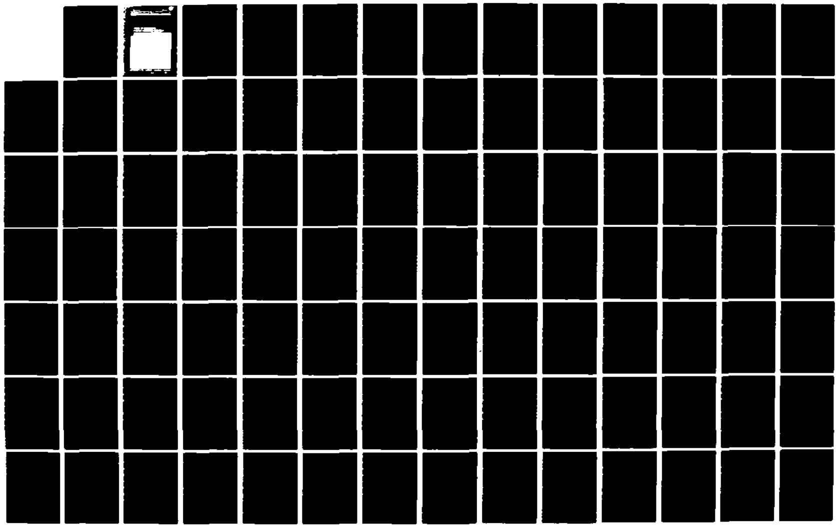

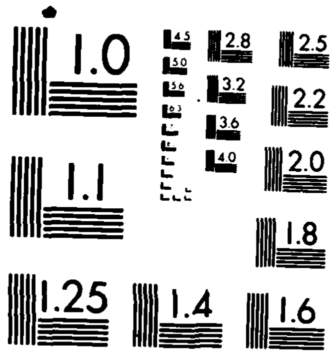
1.0
2.8
2.5
3.2
2.2
3.6
4.0
2.0
1.1
1.8
1.25
1.4
1.6

AD-A161 452

UNCLASSIFIED
SECURITY CLASSIFICATION OF THIS PAGE

AD-A161452

REPORT DOCUMENTATION PAGE

1a. REPORT SECURITY CLASSIFICATION UNCLASSIFIED	1b. RESTRICTIVE MARKINGS NONE
2a. SECURITY CLASSIFICATION AUTHORITY N/A	3. DISTRIBUTION/AVAILABILITY OF REPORT Approved for public release, distribution unlimited.
2b. DECLASSIFICATION/DOWNGRADING SCHEDULE N/A	
4. PERFORMING ORGANIZATION REPORT NUMBER(S) R-1043 UILU-ENG-85-2218 (DC-81)	5. MONITORING ORGANIZATION REPORT NUMBER(S) N/A
6a. NAME OF PERFORMING ORGANIZATION Coordinated Science Laboratory, Univ. of Illinois 6b. OFFICE SYMBOL (If applicable) N/A	7a. NAME OF MONITORING ORGANIZATION Joint Services Electronics Program
6c. ADDRESS (City, State and ZIP Code) 1101 W. Springfield Avenue Urbana, Illinois 61801	7b. ADDRESS (City, State and ZIP Code) Research Triangle Park, NC 27709
8a. NAME OF FUNDING/SPONSORING ORGANIZATION 8b. OFFICE SYMBOL (If applicable) N/A	9. PROCUREMENT INSTRUMENT IDENTIFICATION NUMBER N00014-84-C-0149
8c. ADDRESS (City, State and ZIP Code)	10. SOURCE OF FUNDING NOS. PROGRAM ELEMENT NO.: N/A; PROJECT NO.: N/A; TASK NO.: N/A; WORK UNIT NO.: N/A
11. TITLE (Include Security Classification) Issues in Frequency Domain Feedback Control	
12. PERSONAL AUTHOR(S) James Scott Freudenberg	
13a. TYPE OF REPORT Technical 13b. TIME COVERED FROM ______ TO ______	14. DATE OF REPORT (Yr., Mo., Day) May 1985 15. PAGE COUNT 415
16. SUPPLEMENTARY NOTATION N/A	
17. COSATI CODES FIELD / GROUP / SUB. GR.	18. SUBJECT TERMS (Continue on reverse if necessary and identify by block number)
19. ABSTRACT (Continue on reverse if necessary and identify by block number)	
20. DISTRIBUTION/AVAILABILITY OF ABSTRACT UNCLASSIFIED/UNLIMITED ☒ SAME AS RPT. ☐ DTIC USERS ☐	21. ABSTRACT SECURITY CLASSIFICATION UNCLASSIFIED
22a. NAME OF RESPONSIBLE INDIVIDUAL	22b. TELEPHONE NUMBER (Include Area Code) 22c. OFFICE SYMBOL NONE

DD FORM 1473, 83 APR EDITION OF 1 JAN 73 IS OBSOLETE.

UNCLASSIFIED

ISSUES IN FREQUENCY DOMAIN FEEDBACK CONTROL

BY

JAMES SCOTT FREUDENBERG

B.S., Rose-Hulman Institute of Technology, 1978
B.S., Rose-Hulman Institute of Technology, 1978
M.S., University of Illinois, 1982

THESIS

Submitted in partial fulfillment of the requirements
for the degree of Doctor of Philosophy in Electrical Engineering
in the Graduate College of the
University of Illinois at Urbana-Champaign, 1985

Urbana, Illinois

ISSUES IN FREQUENCY DOMAIN FEEDBACK CONTROL THEORY

James Scott Freudenberg, Ph.D.
Department of Electrical Engineering
University of Illinois at Urbana-Champaign, 1985

The purpose of this thesis is to examine several issues in the frequency domain theory of feedback control systems. Properties of both single loop and multiple loop systems are considered. For single loop systems the limitations on feedback properties imposed by right half plane poles and zeros of the plant are considered. The relation between open and closed loop properties of multiple loop systems is studied. A great deal of attention is given to how complex analyticity of matrix transfer functions limits feedback properties of multiple loop systems. An integral constraint generalizing Bode's gain-phase relation is presented.

ACKNOWLEDGMENTS

First, I would like to thank my parents, Jack and Sue Freudenberg, for much support and guidance over the years. I would also like to thank all my friends and relatives who put up with me while I was writing this thesis.

I would like to acknowledge many useful technical discussions with the personnel of the Honeywell Systems and Research Center, Minneapolis, where I spent an interesting summer in 1982. I would like to acknowledge Professor J. B. Cruz, Jr. and the personnel of the Decision and Control Group at the Coordinated Science Laboratory for providing an excellent environment in which to pursue a graduate education. In particular, I would like to thank Dixie Murphy for typing this thesis and Rose Harris for much help over the years.

Several members of the Mathematics Department at the University of Illinois were quite helpful in developing the ideas on the latter portion of this thesis. I had many useful discussions with Dave Pollack, who introduced me to complex projective space. The courses taught by Professor Phillippe Tondeur were very valuable in learning the ideas from geometry used herein. Professor Dick Bishop read and commented on portions of this thesis. Lastly, Professor Stephanie Alexander provided countless hours of help and encouragement.

I would like to express gratitude to Scientific American magazine. An article in this excellent magazine inspired me to apply geometric methods to the study of singular values and vectors. Judy R. also deserves much thanks for selling me the inspiration for Section 11.3.

Discussions with Gunter Stein, George Zames, and Bruce Francis helped clarify the ideas in Chapter 3 and especially in Chapter 4.

The final person I would like to thank is Professor Douglas P. Looze, without whose help and guidance (not to mention deprogramming abilities) this thesis would not have been possible.

Finally, I would like to acknowledge Murphy's Pub (and the denizens thereof) for five years of good times and friendship.

TABLE OF CONTENTS

CHAPTER 1

INTRODUCTION

Classical feedback theory has proven to be successful in the design of single-input single-output feedback systems. Recent years have seen a renewed effort to generalize this theory to multiple-input multiple-output systems. The purpose of this thesis is to attempt such generalizations for some selected topics from classical theory. Following are a brief summary of each chapter and a description of how the chapters relate to each other.

The purpose of Chapter 2 is to review the concepts from classical theory for which generalizations will be pursued in later chapters. The importance of each concept to the process of classical design is discussed, thus motivating work on extensions. Three concepts in particular are stressed.

First is the fact that certain closed loop transfer functions directly express the quality of a feedback design. Thus it is natural to state design specifications in terms of these transfer functions. Despite this fact, classical methods have focussed on the manipulation of gain and phase of the open loop transfer function. That this approach is successful is due, at least in part, to a second important characteristic of classical methods: that the relation between open and closed loop system properties is well-understood. Thus, the quality of a design may be evaluated from knowledge of the open loop transfer function; similarly, design specifications may be stated in terms of this function.

A third important idea from classical theory is that there exist hard limitations on the ability of a linear time-invariant system to achieve design specifications. The limitations of particular interest in this thesis are those known as the Bode integral relations and Bode gain-phase relations. These limitations manifest themselves as tradeoffs which must be performed among desirable system properties in different frequency ranges. Mathematically, the tradeoffs are due to the fact that transfer functions must be analytic in the complex frequency variable. This requirement imposes a great deal of structure upon transfer functions; it is this structure that allows one to prove that not all design goals are achievable.

The Bode relations and their interpretation in terms of design tradeoffs provide the scientific foundation for classical feedback theory. One way of viewing classical design is as a systematic process for exploring the set of designs possible given the various limitations due to the open loop plant and the conflicts among design specifications. This process involves a certain amount of trial and error; however, various rules of thumb are available to guide the designer. These are based upon knowledge of the relation between open and closed loop system properties and the unalterable properties of systems given by the Bode integral equations. Examples of rules of thumb are "high loop gain yields good disturbance rejection" and "loop roll-off near crossover should be no greater than 20 db/decade." Now, it is granted that such rules of thumb will generally be insufficient to carry out a complete system design. It appears their true significance is that they allow the designer to rapidly get in the

vicinity of a satisfactory design, after which a more detailed analysis must be made. For this reason, generalization of classical rules of thumb to multiple loop systems appears to be a worthy endeavor. Since the classical rules of thumb discussed above could each be given a theoretical justification, a first step will be to develop the necessary theory for multiple loop systems.

One advantage of working with open loop quantities is that various design limitations due to properties of the given plant are seen directly. Whether open or closed loop transfer functions are considered, however, it is important to express the design limitations in terms of the transfer functions evaluated along the imaginary axis, for this is where design specifications are imposed. Certain design limitations, namely those due to open right half plane poles and zeros of the plant, have commonly been considered in terms of their effect upon the gain and phase of the open loop transfer function along the imaginary axis. Recent years have seen renewed interest in expressing these limitations in terms of closed loop transfer functions. Existing results, however, have only been stated in terms of these functions evaluated at isolated points in the open right half plane. Thus, in Chapter 3, equivalent statements of these constraints are given in terms of closed loop properties along the imaginary axis. These statements, which are very much in the spirit of the Bode integral relations, show that tradeoffs among system properties in different frequency ranges must be performed.

Although insight into design limitations may be gained from the integral relations, they also show that direct design in terms of closed

loop transfer functions is complicated by the necessity of satisfying a fairly complicated set of constraints. This observation suggests that a criterion of merit for evaluating proposed design methods is the amount of insight provided into such constraints. Moreover, the ability to effectively perform the associated tradeoffs among design goals should also be present in any design technique. The purpose of Chapter 4 is to discuss the relative merits of design methods employing open loop transfer functions versus those employing closed loop transfer functions. In particular, it is conjectured that open loop based techniques might have certain advantages in dealing with limitations imposed by properties of the plant. It should be stressed, however, that the purpose of the discussion is not to reach any conclusive statements regarding the usefulness of any particular method. Rather, it is felt that a detailed examination of the issues such conjectures raise may be of importance in the development of design techniques. In the course of the discussion a class of recently proposed design methods, the H^{∞}-optimization techniques, are analyzed and found, for at least some problem statements, to be equivalent in many ways to other closed loop based methods. It is seen that the integral constraints developed in Chapter 3 are implicitly present in these design methods.

To summarize, Chapter 2 contains a review of known classical results and points out some highlights of the classical theory and methods. In Chapter 3, new results concerning classical design problems are developed. These results are applied, in Chapter 4, to discuss properties of various design schemes. With this background, sufficient motivation is provided for

developing extensions of the concepts described in Chapter 2 to multiple loop feedback systems.

A discussion of some previously obtained extensions of classical concepts is contained in Chapter 5. (The discussion, however, is limited to include only those extensions which are directly relevant to the purposes of this thesis.) As many authors have discussed, the fact that certain closed loop transfer functions directly express the quality of a feedback design holds for multiple loop as well as single loop systems. (One difference is that some nonstandard functions must be considered when multiple loop phenomena having no single loop analogue are encountered; see Chapter 5 for references to these results.) The focus of this thesis is on the other two concepts highlighted in Chapter 2, since it appears more work is needed in these areas. These two concepts are the relation of open to closed loop system properties and the tradeoffs between system properties in different frequency ranges imposed by the Bode integrals. It is shown in Chapter 5 that many previous extensions of these concepts hold only in special cases, for which the multiple loop design problem essentially reduces to a single loop problem. This reduction occurs when system properties and design goals are essentially the same in all loops of the system. Problem formulations are then given in which this simplifying assumption is not satisfied. In this way Chapter 5 also describes the class of design problems for which theory is to be developed in later chapters.

As stated previously, classical design emphasized shaping the gain and phase of the open loop transfer function. Although the generalization of gain to multiple loop systems is fairly straightforward,

the generalization of phase is not. In addition, multiple loop systems exhibit directionality, a property with no scalar analogue. The purpose of Chapter 6 is to discuss what role, if any, phase could play in multiple loop systems, and the relation of both gain and phase with the directionality properties of these systems. Emphasis in Chapter 6 is placed upon physical interpretations of the various parameters.

Another way of viewing the gain and phase of a scalar transfer function is as a set of coordinates completely specifying the value of the function. In Chapter 7 sets of coordinates for matrix transfer functions are discussed. These include the singular values and the measures of phase difference discussed in Chapter 6. Some relations between these coordinates and feedback properties are developed.

In Chapter 8 extensions of one of the important classical concepts are presented. This concept is that rules of thumb are available for relating open loop to closed loop properties of feedback systems. The novel results show that rules of thumb may be obtained for systems with both large and small levels of gain in different directions at the same frequency. As might be expected, feedback properties are a function of a certain measure of the coupling between high and low gain portions of the system. In addition, frequency regions analogous to gain crossover frequency in a single loop system are shown to exist.

For two-input two-output systems the results of Chapter 8 are expressed in the coordinates discussed in Chapters 6 and 7. Two examples are then presented. One is an example of a physical system. This example verifies that the results of Chapter 8 are indeed useful in analyzing systems of engineering interest.

The other example in Chapter 8 was specially constructed to reveal some behavior in multiple loop systems which appears to have no analogue in scalar systems. In particular, the limitations imposed by the Bode gain-phase relations appear to be violated. It is postulated that this behavior is due to a helpful interaction between the two loops of the system. The fact that no theoretical foundation for understanding such phenomena exists provides motivation for the major work of this thesis, which is to develop such a foundation.

Theoretical understanding of multiple loop systems is the topic of Chapters 9-12. Chapter 9 initiates this work by first analyzing how analytic function theory was used to derive constraints on scalar transfer functions. Although the Bode integral relations expressed these constraints in the form most useful to engineers, the information is also contained in the more familiar (to mathematicians) Cauchy-Riemann equations and Cauchy Integral Theorem. All these formulas show that the two coordinates needed to describe the value of a transfer function provide essentially only one degree of freedom to be manipulated in design.

Obviously in multiple loop systems the same equations may be applied to each element of a matrix transfer function written in standard coordinates. Unfortunately, these coordinates do not generally convey useful information about the quality of a feedback design. As shown in Chapters 6-8, other coordinates exist which do contain such information. It is not clear, however, how the constraints imposed by analyticity manifest themselves in these new coordinates. Thus it is necessary to study how the basic equations of complex variable theory transform under

changes of coordinates on matrix transfer functions. After this is understood, it will then be possible to express the Bode gain-phase relations in useful nonstandard coordinates.

Since a simple characterization of analyticity is given by the Cauchy-Riemann partial differential equations, study of these is undertaken first. It is shown, using differential equations, that knowledge of a singular value gives information about some property of the associated pair of singular vectors. The fact that the exact nature of this information is unclear motivates a study of how singular vectors change with frequency.

In Chapter 9 two special classes of singular vectors are singled out for study. The first class consists of those vectors for which the singular subspaces are constant, thus allowing scalar ideas about the relation of gain and phase to be generalized directly. The second class consists of so-called "minimum-energy" singular vectors. Thought experiments are discussed which suggest that these singular vectors exhibit motion only of the singular subspaces; such motion, in turn, is responsible for system behavior having no analogue in single loop systems.

Although differential equations describing the motion of singular vectors are developed in Chapter 9, the relation of a singular vector pair to its associated singular value remains difficult to analyze. To alleviate this difficulty, in Chapter 10 a study of the space in which singular vectors lie is undertaken. By showing that this space has the structure of a circle bundle over complex projective space, it is possible to separate the direction of a singular vector (i.e., the one-dimensional subspace in which it lies) from any given measure of its phase. Moreover, questions concerning

the existence of a general definition of phase may be settled. It is shown that a measure of phase difference between a pair of left and right singular vectors may be obtained from measures of the phase of each member of the pair.

In Chapter 11 the geometric framework developed in Chapter 10 for separating phase-like properties of singular vectors from directionality properties is used to analyze the differential equations derived in Chapter 9. It is shown that the tangent space to the unit sphere in $\mathbb{C}^n$ may be decomposed into the direct sum of two spaces. Each of these in turn corresponds to one of the two classes of singular vectors singled out in Chapter 9 for further study. This decomposition of the tangent space satisfies the definition of a connection in a principal fiber bundle.

Now, although this particular description of a connection arises naturally from the problem under study, it still does not seem to provide much insight. To remedy this, an equivalent description of the connection is developed in Chapter 11. This description does provide insight into the distinction between changes in the singular subspaces and changes in the phase difference between a pair of singular vectors. In addition, it is much more useful in performing computations.

One result of Chapter 11 is the derivation of some differential equations, involving a singular value and a measure of phase difference between its associated pair of singular vectors, which are analogous to the

familiar Cauchy-Riemann equations. It turns out, moreover, that the functions of interest generally do not satisfy these familar equations. The amount by which the Cauchy-Riemann equations fail to be satisfied may be quantified by the difference between two connection one-forms evaluated on tangent vectors to the paths through complex projective space which the singular vectors are constrained to traverse. By assigning coordinates to projective space, considerable insight is gained into the effects of nonconstant singular subspaces.

The final theoretical results of this thesis are contained in Chapter 12. In this chapter, the generalized Cauchy-Riemann equations developed in Chapters 9-11 are used in conjunction with Stokes' Theorem to derive a generalization of the Bode gain-phase relations to multiple-loop systems. The generalization is applicable to functions of the form $\sigma e^{j\Delta\theta}$, where σ is a singular value and $\Delta\theta$ is an appropriate measure of phase difference between the associated pair of singular vectors.

The generalized gain-phase relations show how the value of $\Delta\theta(j\omega)$ may be expressed as the sum of two integrals. The first integral is a function of the rate at which the singular value rolls off in the vicinity of $s = j\omega$, and is entirely analogous to the classical Bode integral relating the gain and phase of a single loop transfer function. The second integral, on the other hand, has no analogue in single loop systems. Interpretations of this term are also presented. These stress that the discrepancy between the actual value of $\Delta\theta(j\omega)$ and the value of the first integral is due to phase lead or lag being transferred among loops of the system.

Finally, in Chapter 13 the new integral relation developed in Chapter 12 is applied to analyze the example presented in Section 8.4. It was pointed out in the original discussion of this example that its anomalous behavior appeared to be due to a transfer of phase lead from the first to the second loop of the system. The new gain-phase relation allows this conjecture to be, if not verified, at least made quite plausible.

Concluding remarks are contained in Chapter 14.

CHAPTER 2

REVIEW OF CLASSICAL FEEDBACK CONCEPTS

2.1. Introduction and Motivation

The purpose of this chapter is to review classical feedback theory for linear time-invariant single-input single-output (SISO) control systems. The review is not intended to be complete. Rather some important concepts will be highlighted which have proved particularly useful in ascertaining design limitations. Extension of these concepts to multiple-input multiple-output (MIMO) systems will be pursued in later chapters of this thesis.

It should be emphasized that the purpose of this chapter is not to present new results. (New results in single loop feedback theory are given in Chapter 3.) Rather, in this chapter interpretations of existing results are presented, and a paradigm is seen to emerge. Three features of classical design are discussed in this chapter; a summary of these features was presented in Chapter 1. Additional discussion of classical design techniques is contained in Chapter 4.

One reason to carefully reexamine classical theory before attempting MIMO extensions is to insure that one is actually working with the key concepts, rather than concepts whose seeming importance is only illusory. To illustrate, recall that attempts to generalize the notion of gain and phase margins to MIMO systems met with difficulty. Extending the notion of the closest distance from the Nyquist locus to the critical point proved to be straightforward, however. Further examination, (e.g., [1, p. 1182]), showed that in fact gain and phase margins were only useful in assessing worst case robustness insofar as they approximated this closest distance.

Thus the difficulty in discovering MIMO gain and phase margins useful in worst case analysis is perhaps not surprising; it might be considered a fortuitous accident that these margins are even useful in SISO systems.

Another reason to discuss SISO systems is to point out certain properties of these systems which imposed limitations and tradeoffs in design. Later these properties will be examined in the context of MIMO systems to see if these limitations are still present, or whether the additional degrees of freedom available in MIMO design allow them to be overcome or at least allow tradeoffs to be made in a different manner.

2.2. Basic Equations for Feedback Systems

Consider a linear time-invariant single-input single-output feedback system as shown in Figure 2.1.

Here P(s) and F(s) are the transfer functions of the plant model and feedback compensator, respectively. The signal r(s) is the reference input, y(s) the system output, d(s) a disturbance input, and n(s) is sensor noise.

The output of the system is given by

$$y(s) = y_r(s) + y_d(s) + y_n(s) \tag{2.1}$$

$$y_r(s) = [1 + P(s)F(s)]^{-1} P(s)r(s) \tag{2.2}$$

$$y_d(s) = [1 + P(s)F(s)]^{-1} d(s) \tag{2.3}$$

$$y_n(s) = -[1 + P(s)F(s)]P(s)F(s)n(s) \quad . \tag{2.4}$$

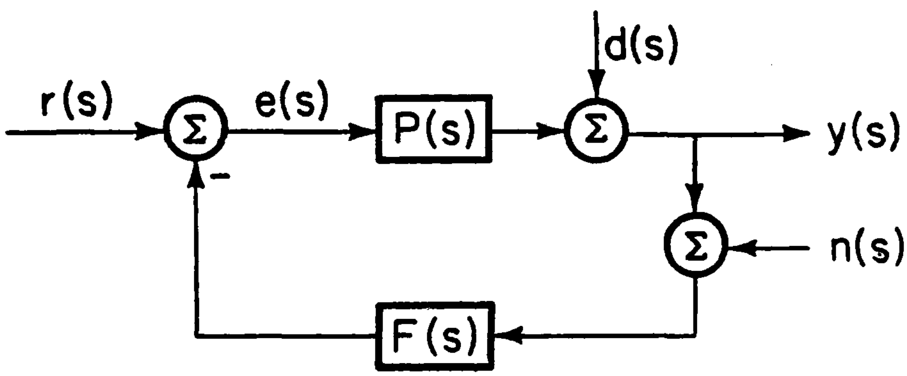

Figure 2.1. Feedback configuration.

Define the open loop transfer function

$$L(s) \triangleq P(s)F(s) \quad , \tag{2.5}$$

the system sensitivity function

$$S(s) \triangleq [1 + L(s)]^{-1} \quad , \tag{2.6}$$

and the complementary sensitivity function [2]

$$T(s) = [1 + L(s)]^{-1} L(s) \quad . \tag{2.7}$$

Assume that L(s) is free of unstable hidden modes. Then the feedback system is stable if S(s) is bounded in the closed right half plane. Note this assumption on L(s) implies that the closed right half plane poles and zeros of the plant and compensator must appear with at least the same multiplicity as that in L(s).

From (2.3) and (2.6) it follows that the response of the system to disturbance inputs is determined by the magnitude of the sensitivity function, $|S(j\omega)|$. Similarly, from (2.4) and (2.7) it follows that the response of the system to sensor noise is determined by the magnitude of the complementary sensitivity function, $|T(j\omega)|$. Therefore, the response of the system to disturbances of frequency ω can be made small by requiring that $|S(j\omega)| << 1$; the response to sensor noise can be made small by requiring that $|T(j\omega)| << 1$.

The benefits of feedback in reducing the effects of uncertainty in the plant model upon the system output can be assessed from [3]

$$E_c(s) \triangleq S'(s)E_o(s) \tag{2.8}$$

$$S'(s) \triangleq [1 + P'(s)F(s)]^{-1} \quad , \tag{2.9}$$

where $P'(s) \stackrel{\Delta}{=} [1 + \Delta(s)]P(s)$ is the true plant. The signals $E_c(s)$ and $E_o(s)$ are the deviations in the outputs of nominally equivalent closed and open loop systems caused by the model error $\Delta(s)$. If at some frequency

$$|S'(j\omega)| < 1 \tag{2.10}$$

then the closed loop system is said to possess the sensitivity reduction property at that frequency. Condition (2.10) is difficult to design for since it depends on the true unknown plant rather than the model. Nonetheless, at frequencies for which $|\Delta(j\omega)| < 1$, it is possible [4] to insure that (2.10) holds by requiring that $|S(j\omega)| \ll 1$. Thus it is possible to reduce the effects of sufficiently small levels of plant uncertainty by requiring the nominal sensitivity function to have small magnitude.

The sensitivity and complementary sensitivity functions are also related to the stability robustness properties of the system (see, e.g., [5], Table 1). In particular, suppose that the true plant is given, as above, by

$$P'(s) = [1 + \Delta(s)]P(s) \quad . \tag{2.11}$$

Assume that

(i) $P'(s)$ and $P(s)$ have the same number of unstable poles and

(ii) $\Delta(s)$ is otherwise arbitrary subject to a frequency dependent magnitude bound:

$$|\Delta(j\omega)| \leq M_{\Delta}(\omega) \qquad \forall\omega \quad . \tag{2.12}$$

Then if the nominal system ($\Delta(s) \equiv 0$) is stable, the true system is guaranteed to be stable if [4]

$$M_\Delta(\omega) < \frac{1}{|T(j\omega)|} \qquad \forall\omega \quad . \tag{2.13}$$

This bound requires that $|T(j\omega)|$ must be small at frequencies for which uncertainty may be large.

2.3. Closed Loop Transfer Functions and Feedback Properties

The preceding discussion has highlighted one important aspect of classical feedback theory. Properties of feedback systems which are important in design are expressed directly by various closed loop transfer functions. This fact motivates the statement of design specifications in terms of frequency dependent bounds on $|S(j\omega)|$ and $|T(j\omega)|$:

$$|S(j\omega)| \leq M_S(\omega) \qquad \forall\omega \tag{2.14}$$

$$|T(j\omega)| \leq M_T(\omega) \qquad \forall\omega \quad . \tag{2.15}$$

These bounds will generally be a function of the relative levels of disturbance inputs, sensor noise, and plant uncertainty. Note, however, that both $|S(j\omega)|$ and $|T(j\omega)|$ cannot be small at the same frequency. This fact follows from the identity

$$S(j\omega) + T(j\omega) \equiv 1 \quad . \tag{2.16}$$

Thus there exists, at each frequency, an algebraic tradeoff between the system properties of sensitivity reduction and disturbance rejection (which are achieved by requiring $|S(j\omega)| \ll 1$) and the properties of stability robustness and sensor noise rejection (achieved by requiring $|T(j\omega)| \ll 1$).

In engineering applications it commonly happens that levels of uncertainty and sensor noise become large at high frequencies. Disturbance rejection and nominal sensitivity reduction are generally desired over a low frequency band containing the frequency range of the reference input. Thus the algebraic tradeoff imposed by (2.16) is typically performed by requiring $M_S(\omega)$ to be small at low frequencies and $M_T(\omega)$ to be small at high frequencies. In addition neither $M_S(\omega)$ nor $M_T(\omega)$ should be excessively large at any frequency.

2.4. Design Limitations Imposed by Bode's Integral Theorem

There exist tradeoffs in feedback design in addition to those at each frequency imposed by (2.16). These tradeoffs must be performed between system properties in *different* frequency ranges, and are a consequence of physical realizability. In order to be physically realizable, a function of the complex frequency variable "s" must in fact be analytic in this variable; this follows from well-known properties of the Laplace transform. Thus, complex variable theory can be applied to study properties of feedback systems expressed by both open and closed loop transfer functions. One such application of the theory is the Nyquist stability criterion [6]. The use of complex variable theory to study limitations in the design of feedback systems was pioneered by Bode [7] after some early work by Norbert Wiener and students [8]. Interpretations of Bode's work in the context of control design were emphasized by Horowitz [9].

The tradeoffs analyzed by Bode are quantified by certain integral relations which must be satisfied by transfer functions of linear time invariant systems. One such tradeoff occurs among levels of sensitivity reduction in different frequency ranges. The following theorem was first proven by Bode; an extension to open loop unstable systems is presented in Chapter 3 of this thesis.

Theorem 2.1 (Bode Integral Theorem [7]): Assume that the open loop transfer function L(s) possesses no poles in the open right half plane. In addition, assume that

$$\lim_{R\to\infty} \sup_{\substack{|s| \geq R \\ \mathrm{Re}[s] \geq 0}} R|L(s)| = 0 \quad . \tag{2.17}$$

Then, if the closed loop system is stable, the sensitivity function must satisfy

$$0 = \int_0^\infty \log|S(j\omega)| \, d\omega \quad . \tag{2.18}$$

■

For a complete discussion of the design implications of Theorem 2.1, see Chapter 3. For now, note that (2.18) shows that on a plot of $\log|S(j\omega)|$ vs ω the sensitivity reduction area ($|S(j\omega)|<1$) must equal the area of sensitivity increase ($|S(j\omega)|>1$) in units of decibels × (radians/sec). Thus, the desirability of sensitivity reduction over, say, a low frequency range must be traded off against possibly undesirable effects of sensitivity increase at other frequencies. When realistic bandwidth constraints are imposed it can be shown (Chapter 3) that this tradeoff must take place primarily over a low frequency interval, despite the fact that the range of integration in (2.18) is infinite.

Theorem 2.1 illustrates another important theme in classical feedback theory. This theme is that there exist hard limitations on the achievable performance of any linear time-invariant feedback system. In the present case, (2.18) shows that if $L(s)$ must satisfy (2.17), then not all functions $S(s)$ can be realized as the sensitivity function of the closed loop system. In Chapter 3 it is shown that relations similar to (2.18) must be satisfied by $S(s)$ when the plant is nonminimum phase and by $T(s)$ when the plant is open loop unstable. In all these cases fixed properties of the open loop system restrict the achievable properties of the closed loop system. This may be one reason why classical design methods focussed upon shaping the gain and phase of the open loop transfer function despite the fact that it is the closed loop transfer function which directly expresses the quality of a feedback design. (Further discussion of this point is given by Horowitz [9, Sec. 6.13]. An extensive discussion is also presented in Chapter 4 of this thesis.)

2.5. Relations Between Open and Closed Loop System Properties

In any case, certainly one reason why classical loop shaping is successful is the fact that the relation between gain and phase of $L(j\omega)$ and closed loop properties is well understood.

From (2.6) and (2.7) the following relations between levels of open loop gain and closed loop properties can be deduced:

$$|L(j\omega)| \gg 1 \iff \begin{array}{c} |S(j\omega)| \ll 1 \\ \text{and} \\ |T(j\omega)| \approx 1 \end{array} \tag{2.19}$$

and

$$|L(j\omega)| \ll 1 \iff \begin{array}{c} |T(j\omega)| \ll 1 \\ \text{and} \\ |S(j\omega)| \approx 1 \end{array} \tag{2.20}$$

At frequencies for which the loop gain is approximately unity, closed loop properties can be approximated from knowledge of open loop phase:

$$\begin{array}{c} |L(j\omega)| \approx 1 \\ \text{and} \\ \measuredangle L(j\omega) \approx \pm 180° \end{array} \iff \begin{array}{c} |S(j\omega)| \gg 1 \\ \text{and} \\ |T(j\omega)| \gg 1 \end{array} \tag{2.21}$$

Approximations (2.19)-(2.21) yield well-known rules of thumb for classical design. Large loop gain is required for good sensitivity reduction and disturbance rejection properties, while small loop gain is required for sensor noise rejection and stability robustness. At frequencies for which $|L(j\omega)| \approx 1$ (e.g., gain crossover frequency, at which $|L(j\omega)| = 1$), the phase of the system should remain bounded sufficiently far away from ±180° to provide an adequate stability margin and to prevent amplifying both disturbance inputs and sensor noise.

Recall the discussion of the sensitivity and complementary sensitivity specifications (2.14) and (2.15). From that description of typical closed loop design specifications and the approximations (2.19)-(2.21) it follows that corresponding open loop gain and phase design specifications might appear as in Figure 2.2. These specifications reflect the fact that loop gains are <u>desired</u>

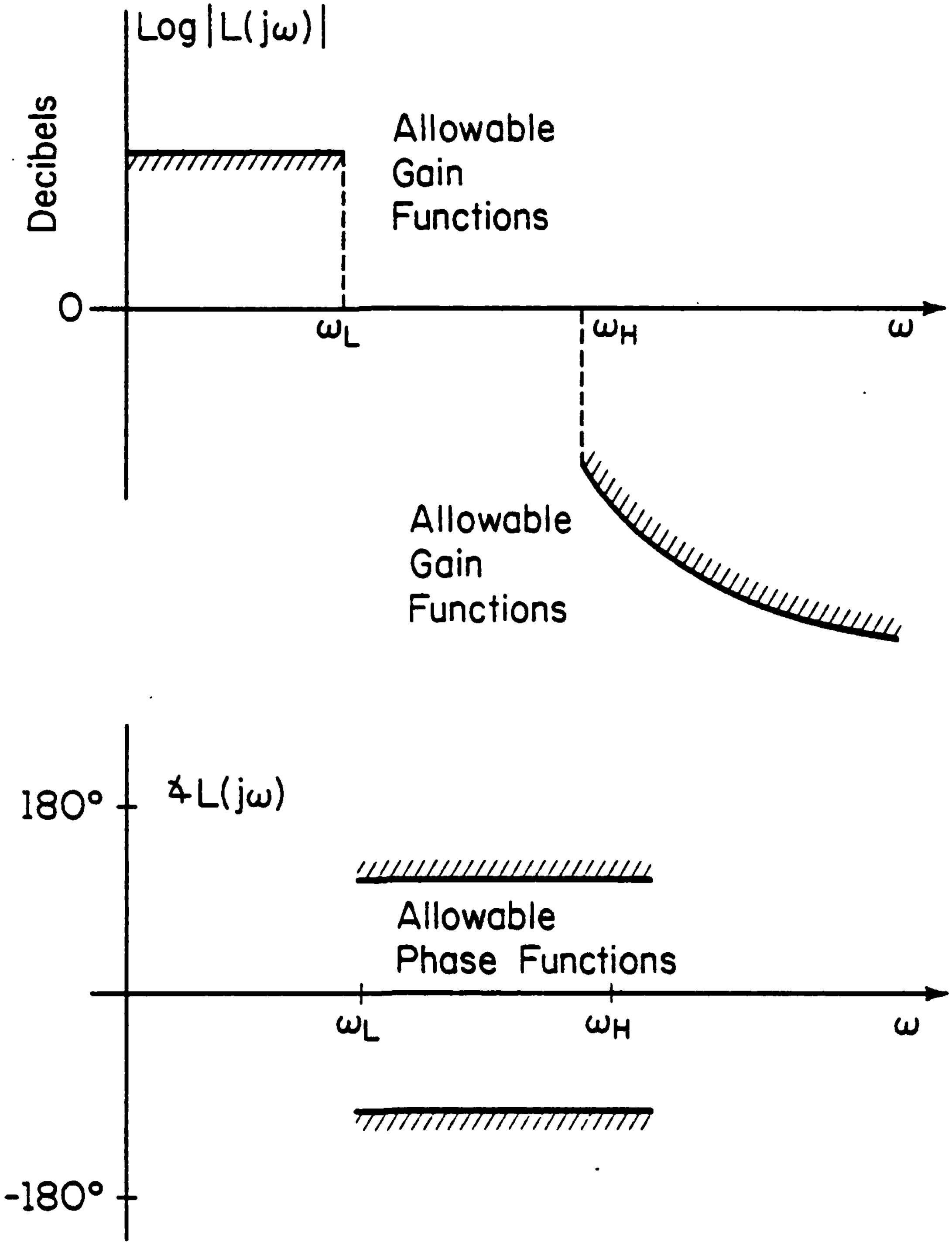

Figure 2.2. Gain and phase specifications.

to be high at low frequencies for good system performance and are required to be small at high frequencies in order to maintain stability robustness. At intermediate frequencies the phase of the system must be bounded away from ±180°. To maintain good sensitivity and disturbance rejection properties over as wide a frequency range as possible, ω_L should be close to ω_H.

2.6. Bode Gain-Phase Relations

The ability to achieve the specification just described is constrained by the fact that gain and phase cannot be assigned independently in design. The precise relation between gain and phase was stated in its most useful form by Bode [7]. Again, Horowitz [9] has discussed the implications for control design. A good recent discussion is given by Doyle and Stein [4].

Theorem 2.2 (Bode Gain-Phase Relation): Assume that L(s) has no poles or zeros in the closed right half plane; in addition, assume that L(s) has a power series expansion about the point at ∞:

$$L(s) = \sum_{i=0}^{\infty} \frac{c_i}{s^i} \quad . \tag{2.22}$$

Define

$$\nu = \log(\omega/\omega_o) \quad . \tag{2.23}$$

At each point $s = j\omega_o$ the following integral relation holds:

$$\measuredangle L(j\omega_o) = \frac{1}{\pi} \int_{-\infty}^{\infty} \frac{d \log|L(j\omega)|}{d\nu} \{\log \coth \frac{|\nu|}{2}\} \, d\nu \quad . \tag{2.24}$$

■

The above theorem gives conditions which, if satisfied, show that knowledge of $|L(j\omega)|\ \forall\omega$ (which implies knowledge of $\frac{d \log|L(j\omega)|}{d\nu}$) completely determines $\measuredangle L(j\omega)$. Thus, although two parameters or coordinates are needed to specify the value of a transfer function, for stable minimum phase systems there exists only one degree of freedom available to the designer. The presence of the weighting function (Figure 2.3)

$$\log \coth \frac{|\nu|}{2} = \log \left|\frac{\omega + \omega_o}{\omega - \omega_o}\right| \tag{2.25}$$

shows, however, that $\measuredangle L(j\omega_o)$ depends primarily on values of $\frac{d \log|L(j\omega)|}{d\nu}$ at frequencies near ω_o.

The implication of Theorem 2.2 for the design specification of Figure 2.2 is as follows. If the gain is decreasing at 20N db/decade at frequencies near ω_o, then the phase is approximately -90N°. Thus, in Figure 2.2 ω_L must be sufficiently less than ω_H so that the rate of gain decrease near gain crossover frequency is not much more than 20 db/decade, yielding a phase lag of not much more than -90°. Low frequency sensitivity reduction must be traded off against a sufficient stability margin near crossover. This is another example of a tradeoff which must be performed among system properties in different frequency ranges. Again, the tradeoff is due to the analyticity of transfer functions of physical systems. One difference between this tradeoff and that discussed in Section 2.4 is that the latter tradeoff was expressed in terms of a closed rather than an open loop transfer function.

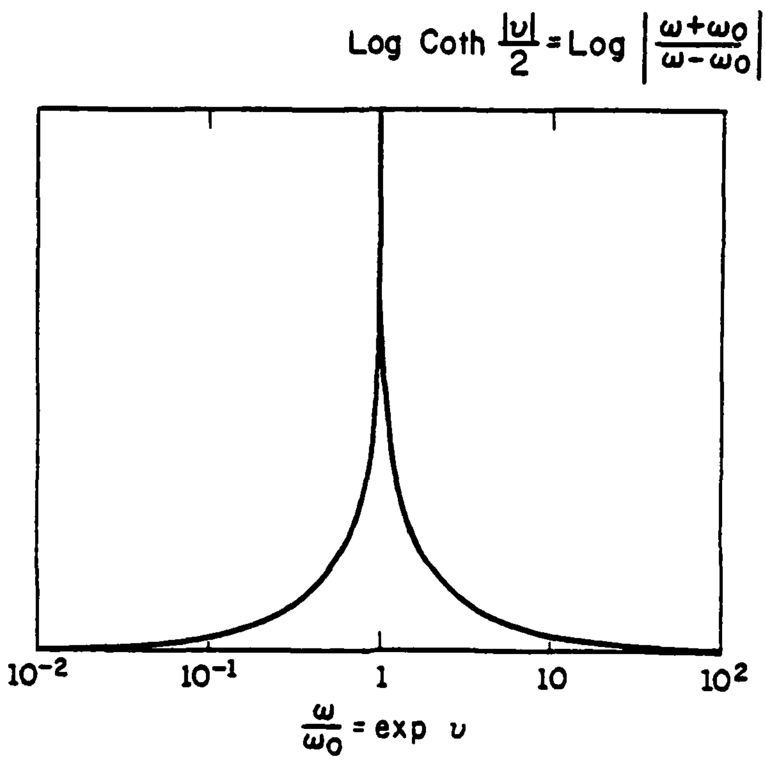

Figure 2.3. Weighting function in Bode gain-phase relation.

2.7. Summary

To summarize this chapter, several key concepts from classical feedback theory have been discussed. First, feedback properties can be assessed from various closed loop transfer functions. Second, despite this fact, classical design focussed on open loop quantities; this procedure was successful since the approximate relation between open and closed loop quantities is well understood. Third, properties of linear time-invariant systems constrain the class of achievable design specifications, whether these are imposed upon open or closed loop quantities, and impose tradeoffs in feedback design. Recognition of the existence of these tradeoffs, and the ability to deal insightfully with them in design, are crucial to the success of classical feedback theory. Tradeoffs can be seen to exist from classical Nyquist/Bode analysis techniques. Well-known rules of thumb associated with classical lead and lag compensation schemes show that tradeoffs cannot be avoided. However, these techniques are useful in exploring the set of possible designs and achieving a satisfactory compromise among design goals.

In the next chapter some new results concerning tradeoffs in SISO systems which are open loop unstable and/or nonminimum phase are presented.

CHAPTER 3

RIGHT HALF PLANE POLES AND ZEROS AND DESIGN TRADEOFFS IN FEEDBACK SYSTEMS

3.1. Introduction

A central issue in the design of feedback systems is that of sensitivity of the closed loop system to uncertainty in the plant model and to disturbance inputs. The system sensitivity function, denoted $S(s)$, has played a key role in the classical design and theory of feedback systems; its importance has been discussed by many authors [2-4,7,9-19]. Briefly, the magnitude of the sensitivity function evaluated along the $j\omega$-axis directly quantifies such feedback properties as output disturbance rejection and sensitivity to small parameter variations.

Another function which expresses important feedback properties is the complementary sensitivity function [2], defined as $T(s) \triangleq 1 - S(s)$. The magnitude of $T(s)$ along the $j\omega$-axis quantifies the response of the feedback system to sensor noise. In addition, this quantity has recently been used as a measure of the stability margin [4,11-14,20].

The importance of $|T(j\omega)|$ and $|S(j\omega)|$ to design properties motivates the expression of design limitations imposed by the open loop transfer function directly in terms of these quantities. For example, a well-known theorem of Bode [7,9] states that for stable open loop transfer functions with greater than one pole roll-off the integral overall frequencies of the log magnitude of the sensitivity function must equal zero. In the presence of bandwidth limitations this imposes a design tradeoff among system sensitivity properties in different frequency ranges ([9] and Section 3.3 below).

It has not been common, however, to formulate other limitations explicitly in terms of $|S(j\omega)|$ and $|T(j\omega)|$. For example, it has long bee recognized that the presence of right half plane poles and zeros in the open loop transfer function imposes limitations upon the design of feedback systems. These limitations are frequently expressed in terms of the effect on the phase of the open loop transfer function. Suppose the plant is nonminimum phase. Then, using classical analysis techniques, it can be seen qualitatively that requiring $|S(j\omega)|$ to be less than one over some frequency interval implies that $|S(j\omega)|$ is greater than one elsewhere. This fact is proven by Francis and Zames [21, Theorem 3]. These authors show that if the plant has a right half plane zero, then requiring $|S(j\omega)|$ to be arbitrarily small over some interval forces $|S(j\omega)|$ to be arbitrarily large elsewhere.

Despite the importance of $|S(j\omega)|$ and $|T(j\omega)|$ as measures of design quality, it has been more common to express limitations due to open right half plane poles and zeros as constraining the values of $S(s)$ and $T(s)$ at isolated points away from the $j\omega$-axis [2,15,16,20-22]. The purpose of this chapter is to present equivalent statements of the right half plane pole and zero constraints in terms of integral relations which must be satisfied by $|S(j\omega)|$ and $|T(j\omega)|$. These constraints show that desirable properties of the sensitivity and complementary sensitivity functions in one frequency range must be traded off against undesirable properties at other frequencies. These tradeoffs are a direct consequence of properties of linear time invariant systems. Thus the limitations discussed in this chapter are independent of any particular choice of design method.

The remainder of this chapter is organized as follows: Section 3.2 is devoted to the derivation of the integral relations from the right half plane pole and zero constraints. In Section 3.3 Bode's integral theorem, referred to above, is extended to open loop unstable plants and consequences for feedback design are discussed. Section 3.4 contains a discussion of the limitations imposed upon system sensitivity properties by the integral constraints due to open right half plane zeros. Section 3.5 contains a similar discussion of the limitations imposed upon the complementary sensitivity function by unstable open loop poles. The effect of the relative location of right half plane poles and zeros to frequency ranges of interest is discussed in Section 3.6. Some brief remarks on limitations in multivariable systems are found in Section 3.7. The chapter is summarized in Section 3.8. Results in this chapter have appeared in [23-25].

3.2. Right Half Plane Pole and Zero Constraints

Consider the linear time-invariant feedback system of Figure 3.1. Let the transfer functions of the plant model and the feedback compensator be denoted P(s) and F(s), respectively. The open loop transfer function is given by

$$L(s) \triangleq P(s)F(s) \quad . \tag{3.1}$$

The sensitivity function of this system is

$$S(s) = \frac{1}{1 + L(s)} \tag{3.2}$$

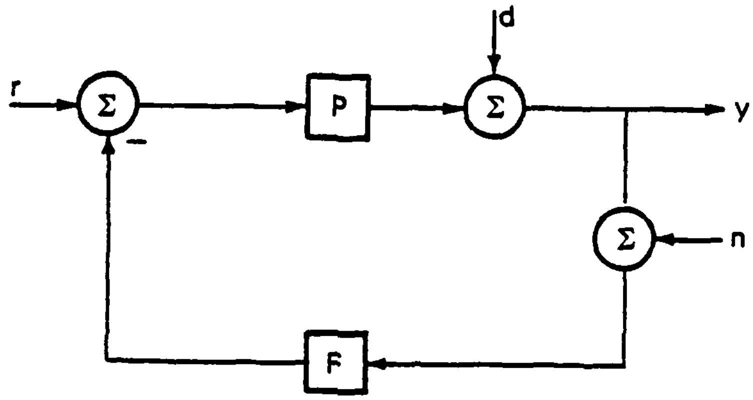

Figure 3.1. Feedback configuration.

and the complementary sensitivity function [2] is

$$T(s) \triangleq 1 - S(s) = \frac{L(s)}{1 + L(s)} \quad . \tag{3.3}$$

The response of the system of Figure 3.1 to disturbance inputs is given by

$$y_d(s) = S(s)d(s)$$

and the response to sensor noise is given by

$$y_n(s) = - T(s)n(s) \quad .$$

From these equations it is seen that, at a particular frequency, the effect of disturbances can be reduced by requiring that $|S(j\omega)| < 1$ at that frequency. Similarly, requiring $|T(j\omega)| < 1$ leads to a reduction in the effects of sensor noise at that frequency. Since $S(j\omega) + T(j\omega) = 1$ there is a well-known tradeoff between the two types of response at a given frequency. The integral relations to be derived in this section and Section 3.3 reveal that there also exist tradeoffs among feedback properties at <u>different</u> frequencies.

Assume that $L(s)$ is free of unstable hidden modes. Then the feedback system is stable if $S(s)$ is bounded in the closed right half plane. Note this assumption on $L(s)$ implies that the closed right half plane poles and zeros of the plant and compensator must appear with at least the same multiplicity in $L(s)$.

Assume also that $L(s)$ can be factored as

$$L(s) = \tilde{L}(s)B_p^{-1}(s)B_z(s)e^{-s\tau} \quad . \tag{3.4}$$

The term $e^{-s\tau}$, $\tau \geq 0$, represents a time delay if $\tau > 0$. The term

$$B_z(s) = \prod_{i=1}^{N_z} \frac{z_i - s}{\bar{z}_i + s} \tag{3.5}$$

is the Blaschke product of open right half plane zeros, including multiplicities:

$$\mathcal{Z} = \{z_i \ ; \ i=1,\ldots,N_z\} \quad . \tag{3.6}$$

Similarly,

$$B_p(s) = \prod_{i=1}^{N_p} \frac{p_i - s}{\bar{p}_i + s} \tag{3.7}$$

is the Blaschke product of open right half plane poles, including multiplicities:

$$\mathcal{P} = \{p_i \ ; \ i=1,\ldots,N_p\} \quad . \tag{3.8}$$

Finally, $\tilde{L}(s)$ is proper and has no poles or zeros in the open right half plane.

For later reference, consider the following class of functions. Given $F(s)$, define

$$M(R) \triangleq \sup_{\theta} \left| F(Re^{j\theta}) \right| \quad , \quad \theta \in [-\pi/2, \pi/2] \quad .$$

Then $F(s)$ is said to be in class $\mathcal{R}$ provided

$$\lim_{R \to \infty} \frac{1}{R} M(R) = 0 \quad . \tag{3.9}$$

Class $\mathcal{R}$ includes many functions of interest. If $L_o(s)$ is a proper rational function, then $\log L_o(s)$ and $\frac{d^i}{ds^i} \log L_o(s)$ are in class $\mathcal{R}$. Functions of the form $\log L(s)$ with $L(s) = L_o(s)e^{-s\tau}$, $\tau > 0$, are not. If, however, the feedback

system with sensitivity function (2.2) is stable, then log S(s) and $\frac{d^i}{ds^i}\log S(s)$ are in class $\mathcal{R}$ despite any time delay in L(s).

From (3.2) and (3.3) it is clear that right half plane poles and zeros of L(s) constrain the values of S(s) and T(s) at these points in the right half plane [15,16,20,22]. One way of expressing these constraints, following immediately from (3.2) and (3.3), is now given.

At each closed right half plane zero, z, of multiplicity m it follows that

$$\text{(A)}\qquad \begin{aligned} &S(z) = 1 \\ &\vdots \\ &\left.\frac{d^i}{ds^i} S\right|_{s=z} = 0 \quad i-1,\ldots,m-1 \end{aligned} \quad .$$

Similarly, at each closed right half plane pole, p, of multiplicity n it follows that

$$\text{(B)}\qquad \begin{aligned} &T(p) = 1 \\ &\vdots \\ &\left.\frac{d^i}{ds^i} T\right|_{s=p} = 0 \quad i=1,\ldots,n-1 \end{aligned} \quad .$$

Note that the above constraints can be expressed in terms of either S or T via the identity

$$S(s) + T(s) = 1 \quad . \tag{3.10}$$

Assume that the feedback system is stable. Then S(s) and T(s) have no poles in the closed right half plane. In order to express the constraints (A) due to open right half plane zeros in terms of $|S(j\omega)|$, it is

necessary to remove the zeros of $S(s)$ at the open right half plane poles of $L(s)$. Note the sensitivity function can be factored as

$$S(s) = \tilde{S}(s)B_p(s) \tag{3.11}$$

where $\tilde{S}(s)$ has no poles or zeros in the open right half plane. Since Blaschke products are all-pass of unit magnitude ($|B_p(j\omega)| = 1\ \forall\omega$), it follows that $|S(j\omega)| = |\tilde{S}(j\omega)|\ \forall\omega$. The constraints upon the sensitivity function at open right half plane zeros (A) can be expressed in terms of the sentivity function on the $j\omega$-axis as follows.

Theorem 3.1: Let $z = x + jy$ be an open right half plane zero, with multiplicity m, of the open loop transfer function $L(s)$. Assume that $\frac{d^i}{ds^i} \log \tilde{S}(s)$ is in class $\mathcal{R}$, $i=-,1,\ldots,m-1$. Then, if the corresponding feedback system is stable, the sensitivity function must satisfy the following integral constraints:*

$$\pi \log|B_p^{-1}(z)| = \int_{-\infty}^{\infty} \log|S(j\omega)|\ d\theta_z(\omega) \tag{3.12}$$

$$\pi \measuredangle B_p^{-1}(z) = \int_{-\infty}^{\infty} \measuredangle \tilde{S}(j\omega)\ d\theta_z(\omega) \tag{3.13}$$

$$\pi \frac{d^i}{ds^i} \log B_p^{-1}(s)\Big|_{s=z} = \int_{-\infty}^{\infty} \frac{d^i}{ds^i} \log \tilde{S}(s)\Big|_{s=j\omega} d\theta_z(\omega) \quad (i=1,\ldots,m-1) \quad . \tag{3.14}$$

The function $\theta_z(\omega)$ is given by

$$\theta_z(\omega) = \arctan\left[\frac{\omega - y}{x}\right] \quad . \tag{3.15}$$

■

Proof: A simple application of Poisson's Integral Formulas [26,27]. See Appendix A for details. ■

*The results of Theorems 3.1 and 3.3 remain valid even if $L(s)$ has $j\omega$-axis poles. Similarly, Theorem 3.2 remains valid if $L(s)$ has $j\omega$-axis zeros. This is discussed further in Appendix A.

In order to express the constraints (B) due to open right half plane poles in terms of $|T(j\omega)|$ it is necessary to remove any zeros of T(s) at the open right half plane zeros of L(s) as well as any time delay. Assume again that the feedback system is stable. Then the complementary sensitivity function can be factored as

$$T(s) = \tilde{T}(s)B_z(s)e^{-s\tau} \tag{3.16}$$

where $\tilde{T}(s)$ has no poles or zeros in the open right half plane. The fact that $B_z(s)$ and $e^{-s\tau}$ are all-pass functions of unit magnitude implies $|T(j\omega)| = |\tilde{T}(j\omega)|$. The constraints upon the complementary sensitivity function at open right half plane poles (B) can be expressed in terms of this function on the $j\omega$-axis as follows:

<u>Theorem 3.2</u>: Let $p = x + jy$ be an open right half plane pole, with multiplicity n, of the open loop transfer function L(s). Assume that $\frac{d^i}{ds^i} \log \tilde{T}(s)$ is in class $\mathcal{R}$, $i=0,1,\ldots,n-1$. Then, if the corresponding feedback system is stable, the complementary sensitivity function must satisfy the following integral constraints:

$$\pi \log|B_z^{-1}(p)| + \pi x\tau = \int_{-\infty}^{\infty} \log|T(j\omega)| \quad d\theta_p(\omega) \tag{3.17}$$

$$\pi \measuredangle B_z^{-1}(p) + \pi y\tau = \int_{-\infty}^{\infty} \measuredangle \tilde{T}(j\omega) \quad d\theta_p(\omega) \tag{3.18}$$

$$\pi \frac{d^i}{ds^i} (\log B_z^{-1}(s)e^{s\tau})\Big|_{s=p} = \int_{-\infty}^{\infty} \frac{d^i}{ds^i} \log \tilde{T}(s)\Big|_{s=j\omega} \cdot d\theta_p(\omega) \quad . \tag{3.19}$$

The function $\theta_p(\omega)$ is given by

$$\theta_p(\omega) = \arctan\left[\frac{\omega - y}{x}\right] \quad . \tag{3.20}$$

Proof: See Appendix A. ∎

Each of the integral relations of Theorems 3.1 and 3.2 places a constraint upon the sensitivity or complementary sensitivity funciton. For the purposes of this chapter the constraints which are most insightful are those given by (3.12) and (3.17). These constraints give the area under the $\log|S(j\omega)|$ and $\log|T(j\omega)|$ curves; the area is calculated using the $j\omega$-axis weighted by the location of a right half plane zero or pole, respectively. The weighting function

$$\theta_s(\omega) = \arctan\left[\frac{\omega - y}{x}\right] \quad , \quad s = x + jy$$

is shown in Figure 3.2.

It is of particular significance that (3.12) and (3.17) constrain the integrals of $\log|S(j\omega)|$ and $\log|T(j\omega)|$. This fact implies that feedback properties in different frequency ranges are not independent. To see this, note that since

$$\frac{d\theta_s(\omega)}{d\omega} = \frac{x}{x^2 + (y - \omega)^2} > 0$$

it follows that $\theta_s(\omega)$ is an increasing function of ω. Moreover, the terms on the left hand sides of equations (3.12) and (3.17) are nonnegative. These facts reveal that systems which reduce the response due to disturbances or sensor noise ($|S(j\omega)| < 1$ or $|T(j\omega)| < 1$) in some frequency range necessarily increase this response at other frequencies. Thus, feedback properties at different frequencies must be traded off against one another to achieve a satisfactory design. These tradeoffs will be discussed further in Sections 3.4 and 3.5.

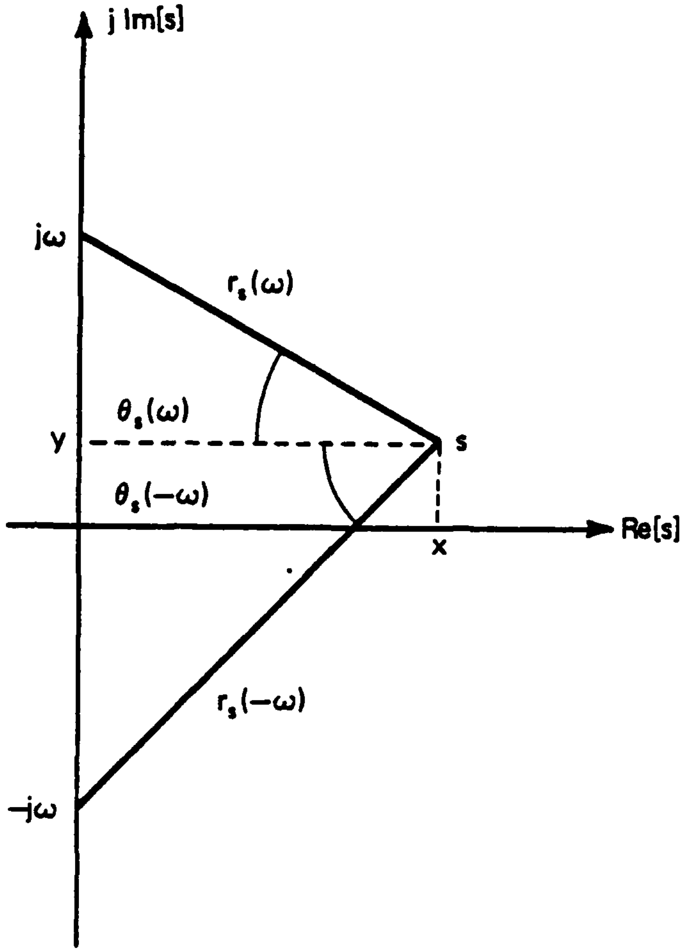

Figure 3.2. Geometry of weighting functions.

It seems intuitive that right half plane poles and zeros which are close to frequency ranges over which design objectives are given constitute a greater obstacle to the achievement of these objectives than if these poles and zeros were far away. The weighting function appearing in the integral relations verifies this intuition and yields a precise notion of the proximity of a zero or pole. The relation between the locations of zeros and poles and the corresponding weightings is discussed further in Section 3.6.

Finally, note that the weighted length of the $j\omega$-axis is finite (and equal to π). This implies, for example, that it is <u>not</u> possible to trade off a given amount of sensitivity reduction by allowing $|S(j\omega)|$ to exceed one by an arbitrarily small amount over an arbitrarily large frequency range. The amount by which $|S(j\omega)|$ exceeds one cannot be made arbitrarily small. The significance of this observation will become clear in Section 3.3, where an extension of the well-known Bode integral theorem is presented.

3.3. Generalization of Bode's Integral Theorem

The purpose of this section is to extend a well-known theorem of Bode [7] to open loop unstable systems. Bode's original result was valid only for open loop stable systems, despite a claim of Horowitz [9, p. 307] to the contrary. The implications of this result for feedback design have been discussed by Horowtiz [9] and others [3,18].

Bandwidth constraints in feedback design typically require that the loop gain be small above a specified frequency. In addition, it is frequently required that the loop gain possess greater than a one pole roll-off above that frequency. These constraints commonly arise due to the need to provide for stability robustness despite uncertainty in the plant model at high frequencies. Bandwidth constraints also arise due to limitations imposed by actuators and sensors. One way of quantifying such constraints is by requiring that

$$|L(j\omega)| \leq \frac{M}{\omega^{1+k}} \quad , \quad \omega > \omega_o \tag{3.21}$$

where $k > 0$ and $\frac{M}{\omega_o^{1+k}} \leq m$. The positive value of k insures that a greater than one pole roll-off is obtained while the value of m imposes a bound on the magnitude of the loop gain.

Bandwidth constraints such as (3.21) in turn impose a constraint upon the integral of the log magnitude of the sensitivity function. First, the requirement that the loop gain have greater than a one pole roll-off yields the following theorem:

Theorem 3.3: Assume that the open loop transfer function L(s) possesses finitely many open right half plane poles $\{p_i : i=1,\ldots,N_p\}$ including multiplicities. In addition, assume that

$$\lim_{R\to\infty} \sup_{\substack{|s|\geq R \\ \mathrm{Re}[s]\geq 0}} R|L(s)| = 0 \quad . \tag{3.22}$$

Then, if the closed loop system is stable, the sensitivity function must satisfy

$$\pi \sum_{i=1}^{N_p} \mathrm{Re}[p_i] = \int_0^\infty \log|S(j\omega)|d\omega \quad . \tag{3.23}$$

■

Proof: See Appendix A. ■

Note that Theorem 3.3 is valid for systems which include right half plane zeros and time delays in $L(s)$.

If $N_p = 0$, then Theorem 3.3 reduces to Bode's theorem. This theorem states that on a plot of $\log|S(j\omega)|$ versus ω the sensitivity reduction area ($\log|S(j\omega)| < 0$) must equal the area of sensitivity increase ($\log|S(j\omega)| > 0$) in units of decibels × (radians/sec).

If $N_p > 0$, then the area of sensitivity reduction is less than the area of sensitivity increase by an amount proportional to the sum of the distances from the unstable poles to the imaginary axis. This indicates that a portion of the loop gain which could otherwise contribute to sensitivity reduction must instead be used to pull the unstable poles into the left half plane.

By itself, Theorem 3.3 does not impose a meaningful design limitation since the necessary area of sensitivity increase can be obtained by allowing $|S(j\omega)|$ to exceed one by an arbitrarily small amount over an arbitrarily large frequency range. (In this respect Theorem 3.3 differs from Theorems 3.1 and 3.2.) However, only part of the bandwidth constraint (3.21) was used to obtain Theorem 3.3; namely, the fact that $k > 0$ implies (3.22) is satisfied. Practical bandwidth constraints also specify the value of m in

(3.21). Thus (3.21) implies there exists a frequency ω_c such that $\frac{M}{\omega_c^{1+k}} = \varepsilon < 1$. It follows that

$$|L(j\omega)| \leq \frac{M}{\omega^{1+k}} \leq \varepsilon \ , \ \omega \geq \omega_c \quad , \tag{3.24}$$

where $k > 0$. This property of the open loop transfer function yields the following bound.

Corollary: Assume that, in addition to (3.22), the transfer function L(s) satisfies the bound (3.24). Then

$$\int_{\omega_c}^{\infty} \log|S(j\omega)|d\omega \leq \frac{\log[\frac{1}{1-\varepsilon}]\cdot\omega_c}{k} \quad . \tag{3.25}$$

■

Proof: See Appendix A. ■

The bound (3.25) is crude and in fact is an optimistic estimate of the integral in question. Nonetheless, it indicates how bandwidth constraints which limit the loop gain as a function of frequency impose a tradeoff upon system sensitivity properties. Suppose that a given level of sensitivity reduction is desired over some low frequency range. Then (3.25) places an upper bound on the area of sensitivity increase which can be obtained at frequencies greater that ω_c and, therefore, a lower bound on the area of sensitivity increase which must be present at lower frequencies. This fact can be used to obtain a lower bound (greater than one) on the maximum value of sensitivity increase below ω_c. Note that the bound (3.25) can be increased only by relaxing the bandwidth specification. In practice this may not be possible due to the necessity of insuring stability robustness. Thus

a tradeoff is imposed among system sensitivity properties in different frequency ranges. The benefits of sensitivity reduction in one frequency range must be obtained at the cost of increased sensitivity at other frequencies whenever bandwidth constraints are imposed. The generalization of Bode's Theorem presented here shows that this cost is greater for open loop unstable systems.

3.4. Limitations on the Sensitivity Function due to Open Right Half Plane Zeros

In Section 3.2 it was shown that the presence of open right half plane zeros places constraints upon the system sensitivity function. These constraints show that if sensitivity reduction ($|S(j\omega)| < 1$) is present in some frequency range, then there necessarily exist other frequencies at which the use of feedback increases sensitivity ($|S(j\omega)| > 1$). The purpose of this section is to illustrate this requirement by deriving some lower bounds on the maximum amount of sensitivity increase given that a certain level of sensitivity reduction has been achieved over some frequency range.

For a given plant model P(s) suppose it is desired to design a feedback compensator F(s) such that a specified level of sensitivity reduction is obtained over a conjugate symmetric* range of frequencies Ω. Let the desired level of sensitivity reduction be given by

$$|S(j\omega)| \leq \alpha < 1 \qquad \forall\omega \in \Omega \quad . \tag{3.26}$$

Let z be an open right half plane zero of L(s) and let the weighted length of the frequency range Ω be denoted

* Conjugate symmetry implies that if $\omega \in \Omega$, then $-\omega \in \Omega$.

$$\Theta_z(\Omega) \triangleq \int_\Omega d\theta_z(\omega) \quad . \tag{3.27}$$

The weighted length of the complementary frequency range $\Omega^c = \{\omega : \omega \notin \Omega\}$ is given by

$$\Theta_z(\Omega^c) = \pi - \Theta_z(\Omega) \quad . \tag{3.28}$$

From Figure 3.3 it is clear that $\pi > \Theta_z(\Omega) > 0$ provided that $\Omega \neq \phi$ and $\Omega \neq \mathbb{R}$. It is also clear that if $\Omega_1 \subseteq \Omega_2$, then $\Theta_z(\Omega_2) \geq \Theta_z(\Omega_1)$.

Define the maximum sensitivity

$$\|S\|_\infty \triangleq \sup_\omega |S(j\omega)| \quad . \tag{3.29}$$

The following theorem gives a lower bound on the maximum sensitivity due to achievement of the sensitivity reduction level (3.26) for a nonminimum phase system. As this lower bound is greater than one, it follows that the closed loop system exhibits a sensitivity increase over some frequency range.

<u>Theorem 3.4</u>: Let the open loop transfer function L(s) have open right half plane poles and zeros given by (3.8) and (3.6). Suppose that the closed loop system is stable and that the level of sensitivity reduction (3.26) has been achieved. Then for each $z \in \mathcal{Z}$ the following bound must be satisfied:

$$\|S\|_\infty \geq \left(\frac{1}{\alpha}\right)^{\frac{\Theta_z(\Omega)}{\pi - \Theta_z(\Omega)}} \left|B_p^{-1}(z)\right|^{\frac{\pi}{\pi - \Theta_z(\Omega)}} \tag{3.30}$$

where $\Theta_z(\Omega)$ is given by (3.27).

<u>Proof</u>: From (3.12) ■

$$\pi \log|B_p^{-1}(z)| = \int_\Omega \log|S(j\omega)|d\theta_z(\omega) + \int_{\Omega^c} \log|S(j\omega)|d\theta_z(\omega) \quad . \tag{3.31}$$

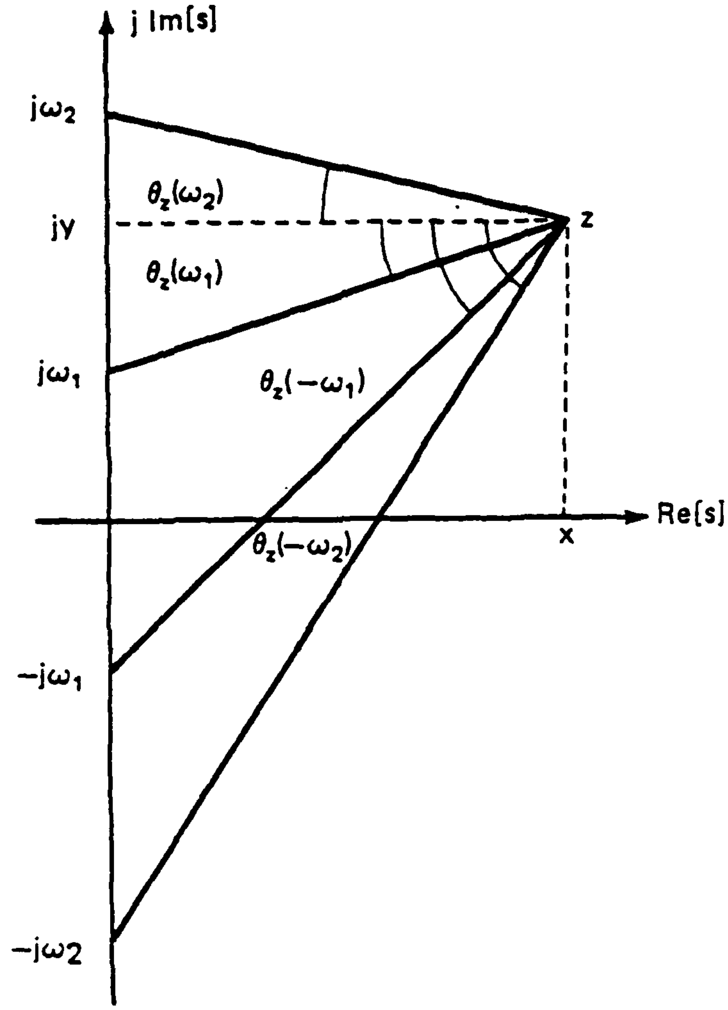

Figure 3.3. Geometry of weighted frequency interval.

Since $\sup_{\Omega}|S(j\omega)| \leq \alpha$ by design, and since $\sup_{\Omega^c}|S(j\omega)| \leq \|S\|_\infty$ by definition, it follows that

$$\pi \log|B_p^{-1}(z)| \leq \log(\alpha)\ \ \Theta_z(\Omega) + \log\|S\|_\infty\, \Theta_z(\Omega^c) \quad . \tag{3.32}$$

Exponentiating both sides of (3.32) yields the result. ∎

In general, a different lower bound is obtained for each zero (an exception being pairs of complex conjugate zeros). Note that a similar bound has been derived by Francis and Zames [21, Theorem 3]. The bound of Theorem 3.4 is less crude, and the proof and results are more insightful. In addition, although (3.30) is derived for the simple specification (3.26) the method readily extends to more general specifications. This is clear from the proof.

Inequalities (3.30) and (3.32) must be satisfied for each open right half plane zero of L(s). Before discussing the tightness of these inequalities the significance of each term will be briefly explained. First, however, note the facts that $\alpha < 1, |B_p^{-1}(z)| > 1$, and $\Theta_z(\Omega) < \pi$ imply that the right hand side of (3.30) is strictly greater than one. This verifies that the maximum sensitivity is indeed greater than one.

The term $\Theta_z(\Omega)$ given by (3.27) is the weighted length of the frequency range over which sensitivity reduction is desired; the term $\Theta_z(\Omega^c)$ given by (3.28) is the weighted length of the complementary frequency range. The relation between these weighted lengths and the location of the zero is discussed in Section 3.6. To illustrate, Figure 3.4 shows how the weighted length of the frequency interval $\Omega = [0,\omega_2]$ varies as a function of ω_2 for a zero at $s = 1$ and at $s = 1 + j$. From Figure 3.4 and inequalities (3.30) and (3.32), it is clear that a significant level of sensitivity reduction

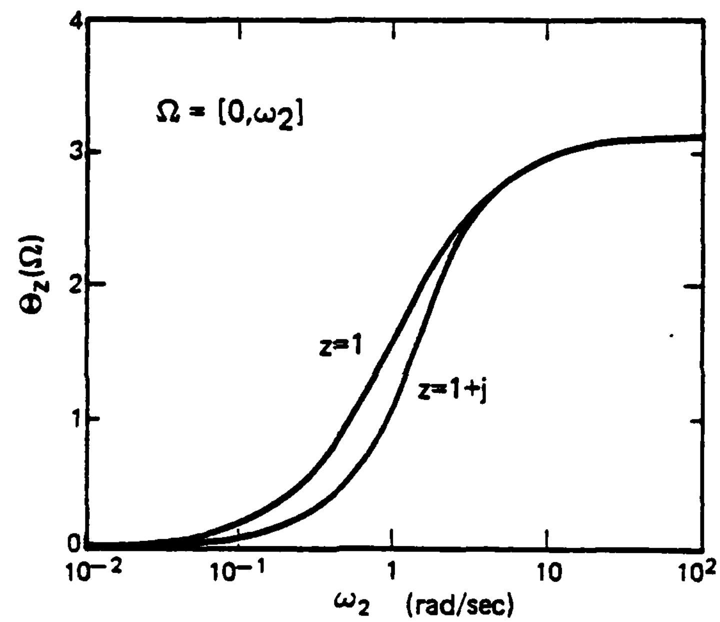

Figure 3.4. Weighted length of frequency interval.

at frequencies near a right half plane zero is necessarily accompanied by a large sensitivity increase at other frequencies. Moreover, suppose that sensitivity reduction is desired over all but a lightly weighted portion of the $j\omega$-axis. Then Theorem 3.4 shows that the accompanying sensitivity increase must be greater than if sensitivity is permitted to exceed one at more heavily weighted frequencies. The above comments are illustrated in Figure 3.5 by plotting the lower bound on $\log\|S\|_\infty$ for the frequency interval Ω = [0,1 rad/sec], zeros at $s=1$ and $s=1+j$, and various levels of sensitivity reduction. The system in this example is assumed to be open loop stable.

If the system is open loop unstable then the lower bound (3.30) on $\|S\|_\infty$ is increased as a function of the proximity of the unstable poles to the zero in question. This is a consequence of the fact that the weighted area under the $\log|S(j\omega)|$ curve is positive for open loop unstable systems. Thus the presence of unstable poles in the open loop transfer function tends to worsen the sensitivity performance of the closed loop system. Since

$$\pi\log|B_p^{-1}(z)| = \pi \sum_{i=1}^{N_p} \log\left|\frac{\bar{p}_i+z}{p_i-z}\right| \tag{3.33}$$

it follows (unsurprisingly) that systems with approximate right half plane pole-zero cancellations can have especially bad sensitivity properties. As an example, the magnitude of one term of (3.33) is plotted in Figure 3.6 versus various locations of a real pole for a zero at $s=1$. The effect of an unstable pole at $s=2$ upon the lower bound (3.30) for zeros at $s=1$ and $s=1+j$ and various levels of sensitivity reduction over the frequency

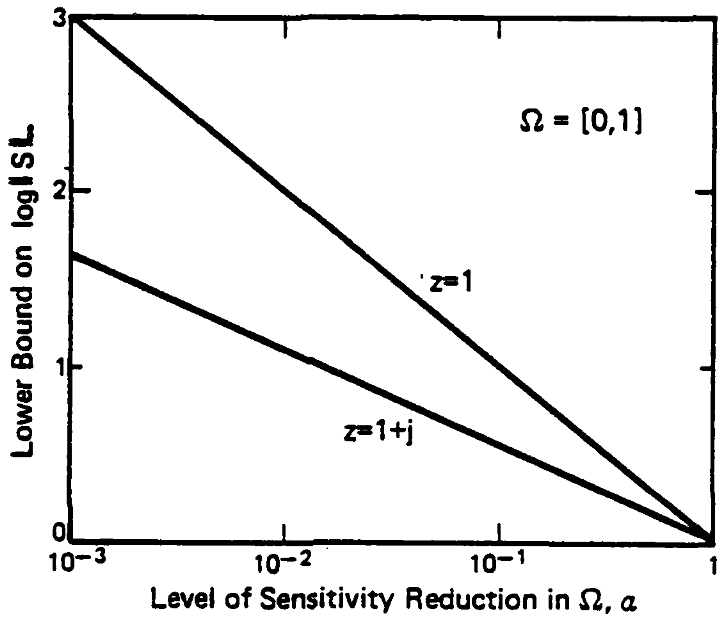

Figure 3.5. Lower bound on maximum sensitivity: Open loop stable.

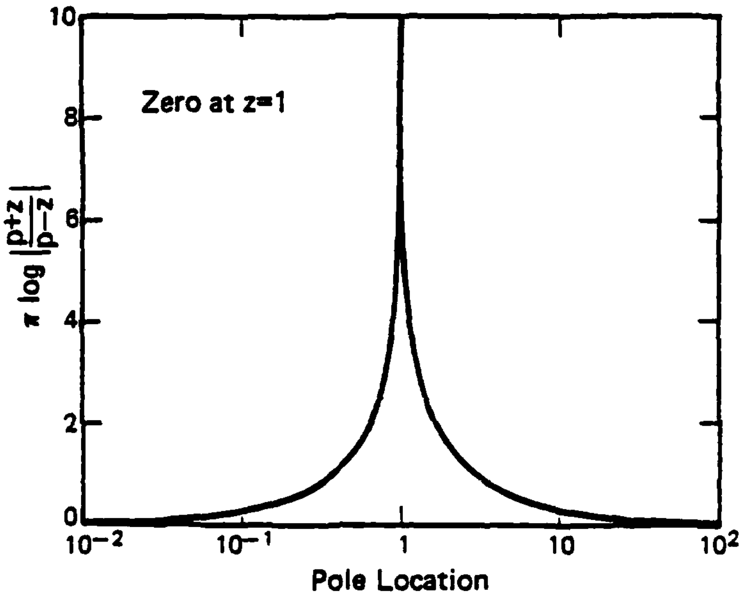

Figure 3.6. Effect of an unstable pole.

interval $\Omega = [0,1]$ is illustrated in Figure 3.7. This bound should be compared with that for an open loop stable system plotted in Figure 3.5.

In general, the bounds of Theorem 3.4 will not be tight for a variety of practical as well as theoretical reasons. Consider the bound (3.30) for a single zero. From (3.31) it follows that this bound is satisfied with equality by a function $\hat{S}(s)$ for which

$$|\hat{S}(j\omega)| = \begin{cases} \alpha & \omega \in \Omega \\ \|\hat{S}\|_\infty & \omega \in \Omega^c \end{cases} , \qquad (3.34)$$

where $\|\hat{S}\|_\infty$ is given by the right hand side of (3.30). The function $\hat{S}(s)$ is illustrated in Figure 3.8 for an open loop stable system with a zero at $s = 1 + j$ and a level of sensitivity reduction $\alpha = .1$ over the frequency interval [0,1 rad/sec]. This function has the minimum possible value of maximum sensitivity increase of all functions satisfying the sensitivity specification (3.26).

As mentioned earlier, a sensitivity function with a gain characteristic as in (3.34) and Figure 3.8 is in practice neither achievable nor desirable. It is not achievable due to the corresponding requirement of an infinite bandwidth open loop transfer function, nor desirable due to robustness considerations. In most cases robustness constraints will, at a minimum, require that

$$|S(j\omega) - 1| < \varepsilon \text{ for } \omega \in \Omega_3 \triangleq [\omega_3, \infty] \quad . \qquad (3.35)$$

The effect of the constraint (3.35) may be analyzed by a straightforward modification of Theorem 3.4. As $\varepsilon \to 0$, the bound (3.30) is replaced by

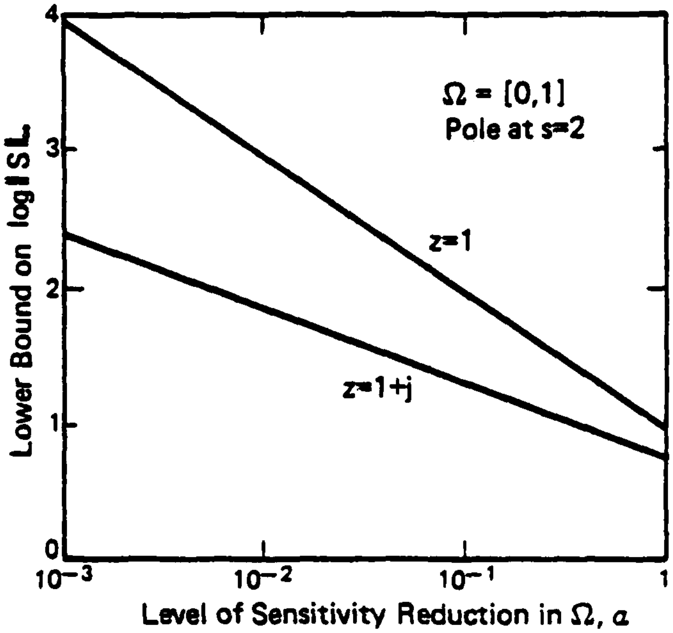

Figure 3.7. Effect of unstable pole on maximum sensitivity bound.

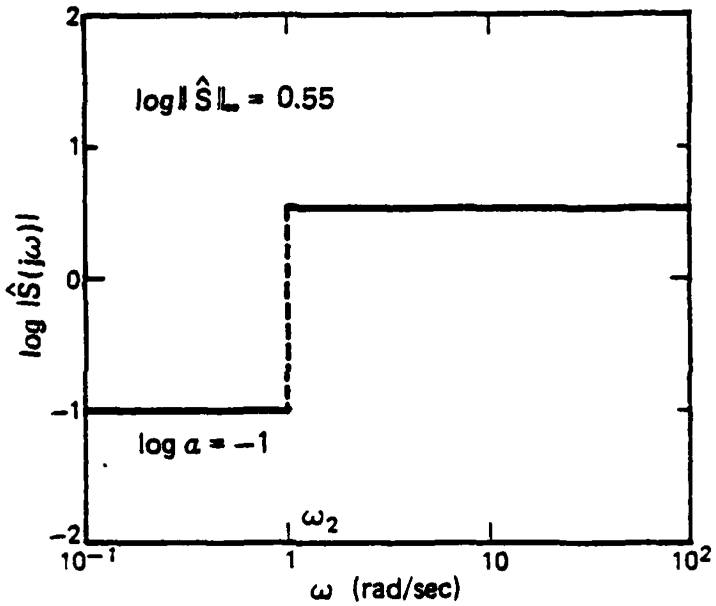

Figure 3.8. Sensitivity function achieving equality in (3.30).

$$\|S\|_\infty \geq \left(\frac{1}{\alpha}\right)^{\frac{\Theta_z(\Omega)}{\Theta_z(\Omega')}} \left|B_p^{-1}(z)\right|^{\frac{\pi}{\Theta_z(\Omega')}} \tag{3.36}$$

where $\Omega' \triangleq \Omega^c \cap [-\omega_3,\omega_3]$. As $\Theta_z(\Omega')$ is an increasing function of ω_3, it follows that for fixed values of z, α, ω_1 and ω_2 the minimum possible value of $\|S\|_\infty$ increases as ω_3 decreases. This minimum value would be attained by a design for which equality is achieved in (3.36). The gain characteristic of such a sensitivity function for the data of Figure 3.8 is plotted in Figure 3.9 for various values of ω_3. Note the effect of the weighting function upon the value of $\|S\|_\infty$ as a function of ω_3. For this example the increase in maximum sensitivity due to the requirement (3.35) is negligible for ω_3 sufficiently large.

Even though the gain characteristics of Figures 3.8 and 3.9 are discontinuous they may be approximated arbitrarily closely by stable rational functions. Thus, the bounds (3.30) or (3.36) would be tight if no other constraints on sensitivity were present. In order to realize these sensitivity functions by applying feedback around a given plant, however, integral relations (3.12)-(3.14) due to each open right half plane zero of L(s) must be satisfied. Thus, the sensitivity function constructed as in Figure 3.8 or 3.9 to satisfy (3.12) for one zero will not, in general, satisfy integral gain relations for other zeros. Recall that the sensitivity functions of Figures 3.8 and 3.9 are constructed to yield the minimum possible value of $\|S\|_\infty$ for the given sensitivity specification under the constraint imposed by a single zero. Thus, the implication of the preceding discussion is that this minimum possible value is optimistic and the lower bounds (3.30) and (3.36) cannot

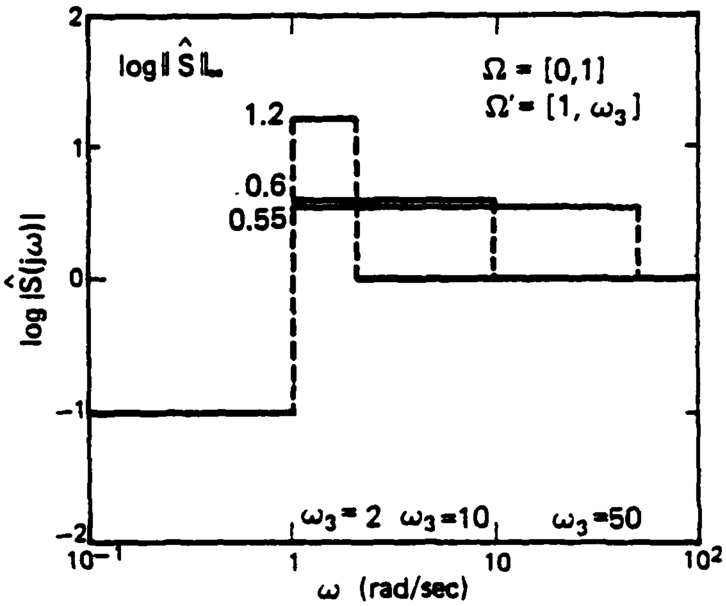

Figure 3.9. Sensitivity functions achieving equality in (3.36).

be tight. Finally, the practical need to limit complexity of the compensator will limit the ability to realize piecewise constant functions for which the bounds are tight.

The results of Theorem 3.4 can be useful in applications by allowing an estimate of the minimum price, in terms of sensitivity increase, which must be paid for a given level of sensitivity reduction over an interval. For example, given Ω, Ω' and α as in Figure 3.9, the minimum possible value of $\|S\|_\infty$ can be computed using the above procedure for each zero. If this value is too large for any zero then it may be necessary to reduce the level of sensitivity reduction α. Alternatively, the locations of the frequency intervals Ω and Ω' could be modified. There are, of course, other tradeoffs involved; for example, increasing the system bandwidth may not be permissible due to robustness considerations.

3.5. Limitations on the Complementary Sensitivity Function Imposed by Unstable Poles

In Section 3.2 it was shown that the presence of open right half plane poles places constraints upon the complementary system sensitivity function. These constraints show that there exists a tradeoff among system-sensor noise-rejection properties in different frequency ranges. This tradeoff can be thought of as dual to that imposed upon the sensitivity function by right half plane zeros.

Lower bounds on the maximum value of $|T(j\omega)|$ can be derived which are similar to those of Section 3.4. Specifications on sensor noise response,

analogous to (3.26) are usually imposed at high frequencies. Assumption of such a specification leads to a bound similar to (3.30). At low frequencies $|T(j\omega)|$ is usually constrained to be near unity by the requirement of small sensitivity. This fact can be used to construct a lower bound similar to (3.36).

One difference between the results of Sections 3.4 and 3.5 is that time delays worsen the tradeoff upon sensor noise reduction imposed by unstable poles. This is plausible for the following reasons. The use of feedback around an open loop unstable system is necessary to achieve stability. Time delays, as well as right half plane zeros, impede the processing of information around a feedback loop. Thus, it is reasonable to expect that limitations due to unstable poles are worse when time delays and/or right half plane zeros are present. Note in particular that the term due to the time delay in (3.17) is porportional to the product of the length of the time delay and the distance from the unstable pole in question to the $j\omega$-axis. This is consistent with the above interpretation.

It should also be noted that the reciprocal of the complementary sensitivity function has been interpreted as a measure of system stability margin against unstructured multiplicative uncertainty [4,11-14,20]. Under this interpretation, Theorem 3.2 shows that unstable poles also impose a tradeoff upon the size of this measure of stability margin in different frequency ranges. Thus, this stability margin cannot be large at all frequencies.

3.6. Dependence of Weightings upon Pole/Zero Location

In the previous sections it was shown that the weighted length of various frequency intervals is important in determining the tradeoffs imposed by right half plane poles and zeros via the integral relations of Theorems 3.1 and 3.2. Intuitively, the difficulty in achieving the benefits of feedback is a function of the proximity of such zeros and poles to frequency ranges over which design specifications are imposed. The fact that weighting functions appear in the integral relations justifies this intuition and allows the notion of proximity to be made precise.

The purpose of this section is to discuss the dependence of the weighting assigned to a frequency interval upon the relative location of the pole or zero and the interval. This dependence can be seen qualitatively from Figure 3.3. The quantitative analysis in this section should prove useful in constructing design specifications which reflect the tradeoff between benefits and cost of feedback imposed by right half plane poles and zeros. The discussion of this section uses weightings imposed by right half plane zeros, but identical results hold for weightings imposed by right half plane poles.

For purposes of illustration, consider the frequency interval

$$\Omega = [\omega_1,\omega_2] \cup [-\omega_2,-\omega_1] \quad . \tag{3.37}$$

Then (3.37) yields

$$\Theta_z(\Omega) = \theta_z(\omega_2) - \theta_z(\omega_1) + \theta_z(-\omega_1) - \theta_z(-\omega_2) \quad . \tag{3.38}$$

From Figure 3.3 and Equation (3.38) it is obvious that $\Theta_z(\Omega)$ is a monotonically increasing function of $\Delta\omega \triangleq \omega_2 - \omega_1$. For fixed values of ω_1 and z, a simple calculation reveals that

$$\frac{\partial\Theta_z(\Omega)}{\partial\Delta\omega} = x\{(\frac{1}{r_z(\omega_1+\Delta\omega)})^2 + (\frac{1}{r_z(-(\omega_1+\Delta\omega))})^2\} \quad , \tag{3.39}$$

where (see Figure 3.2)

$$r_s(\Omega) \triangleq \sqrt{x^2 + (y-\omega)^2} \quad , \quad s = x + jy \quad . \tag{3.40}$$

Equation (3.39) confirms that the severity of the tradeoff imposed by the integral relation (3.12) and estimated by the bound (3.30) becomes increasingly worse as the length of the frequency interval over which a given level of sensitivity reduction is desired is increased. For a real zero, the two terms on the right hand side of (3.39) are equal in magnitude and are monotonically decreasing functions of $\Delta\omega$. For a complex zero in the upper half plane the first term dominates, is an increasing function of $\Delta\omega$ until $r_z(\omega_1 + \Delta\omega) = \mathrm{Im}[z]$, and decreases thereafter (Figure 3.3). The second term is monotonically decreasing. These observations indicate that the greatest incremental degradation in performance due to an incremental increase in the length of an interval of sensitivity reduction occurs for values of $\Delta\omega$ such that ω_2 is in the vicinity of $y = \mathrm{Im}[z]$. This is verified for the frequency interval $\omega_1 = 0$, $\Delta\omega = \omega_2$ and zeros at $s = .1$ and $s = .1 + j$ in Figure 3.10.

Another interesting result is obtained by fixing the length of the frequency interval and varying the location of the interval relative to the zero. If $\Delta\omega < |z|$, then from Figure 3.3 it follows that as ω_1 is increased

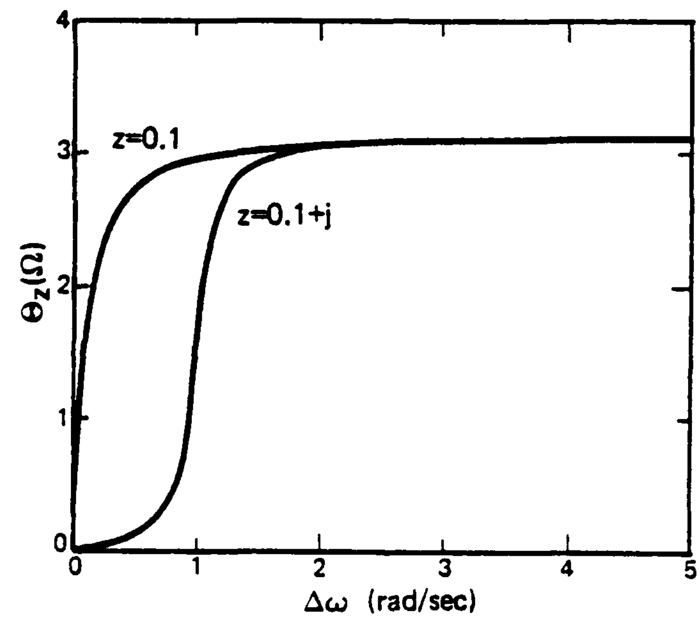

Figure 3.10. Weighted length of $\Omega = [0,\Delta\omega]$.

from 0 to ∞ the weighted length of the frequency interval increases and then decreases. This is verified quantitatively from

$$\frac{\partial\Theta_z(\Omega)}{\partial\omega_1} = x\{(\frac{1}{r_z(\omega_1+\Delta\omega)})^2 - (\frac{1}{r_z(\omega_1)})^2\}$$
$$+ x\{(\frac{1}{r_z(-(\omega_1+\Delta\omega))})^2 - (\frac{1}{r_z(-\omega_1)})^2\} . \qquad (3.41)$$

Again, for a real zero the two bracketed terms in (3.41) are equal and negative. For a complex zero in the upper half plane the second term is negative. The first term is monotonically decreasing and equal to zero for $\frac{\omega_1+\omega_2}{2} = y$. Together the contributions of the two terms indicate that the weighted length of the frequency interval reaches a maximum when the midpoint of the frequency interval is somewhat less than the imaginary component of the zero, with corresponding effect on the difficulty of achieving suitable sensitivity performance. This is illustrated in Figure 3.11 for a frequency interval $\Omega = [\omega_1, \omega_1+1]$ and zeros at $s = 1$ and $s = 1 + 10j$.

It is also interesting to consider the effect of varying the location of the zero relative to a fixed frequency interval. Of course, plant zeros cannot be varied in practice; however, this analysis can provide infromation as to which of several zeros causes the most difficulty in design.

A simple calcualtion shows that, for $z = x + jy$,

$$\frac{\partial\Theta_z(\Omega)}{\partial x} = \{\frac{(y-\omega_2)}{r_z(\omega_2)^2} - \frac{(y-\omega_1)}{r_z(\omega_1)^2} - \frac{(y+\omega_2)}{r_z(-\omega_2)^2} - \frac{(y+\omega_1)}{r_z(-\omega_1)^2}\} . \qquad (3.42)$$

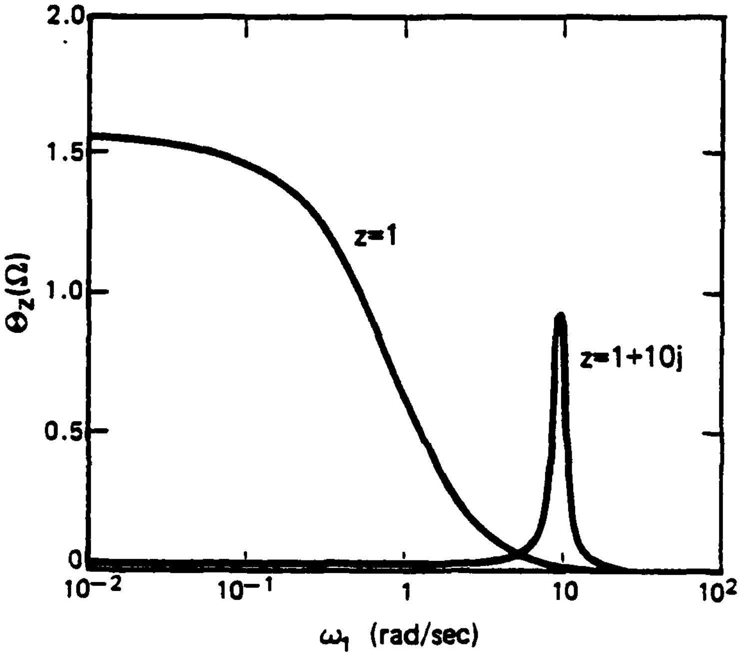

Figure 3.11. Weighted length of $\Omega = [\omega_1, \omega_1 + 1]$.

For a real zero, (3.42) reduces to

$$\frac{\partial \Theta_z(\Omega)}{\partial x} = \frac{2(\omega_2-\omega_1)(-x^2+\omega_1\omega_2)}{r_x(\omega_2)^2 \; r_x(\omega_1)^2} \quad . \tag{3.43}$$

From Figure 3.3 it is clear that as x is increased from zero, $\Theta_z(\Omega)$ first increases and then decreases. Equation (3.43) reveals that the maximum value of $\Theta_z(\Omega)$ is achieved for $x = \sqrt{\omega_1\omega_2}$. For a complex zero in the upper half plane, each of the two terms in (3.42) increases and then decreases as x is increased from zero. The first term is zero at $x = \sqrt{(y-\omega_1)(y-\omega_2)}$; the second term is zero at $x = \sqrt{(y+\omega_1)(y+\omega_2)}$. Thus, the maximum value of $\Theta_z(\Omega)$ is achieved at some intermediate value of x, which could be determined explicitly from (3.42). These results are illustrated in Figure 3.12 for the frequency interval $\Omega = [0.1,5]$ and zeros at $s = x$ and $s = x + 10j$.

Another simple calculation shows that

$$\begin{aligned}\frac{\partial \Theta_z(\Omega)}{\partial y} &= x\{\frac{-1}{r_z(\omega_2)^2} + \frac{1}{r_z(\omega_1)^2}\} + x\{\frac{1}{r_z(-\omega_2)^2} - \frac{1}{r_z(-\omega_1)^2}\} \\ &= \frac{x(\omega_2-\omega_1)(\omega_2+\omega_1-2y)}{r_z(\omega_2)^2 \; r_z(\omega_1)^2} - \frac{x(\omega_2-\omega_1)(\omega_2+\omega_1+2y)}{r_z(-\omega_2)^2 \; r_z(-\omega_1)^2} \quad .\end{aligned} \tag{3.44}$$

As y is increased from 0, the second term in (3.44) is negative; the first term is monotonically decreasing and is zero at $y = \frac{\omega_1+\omega_2}{2}$. Note that this result is consistent with (3.41).

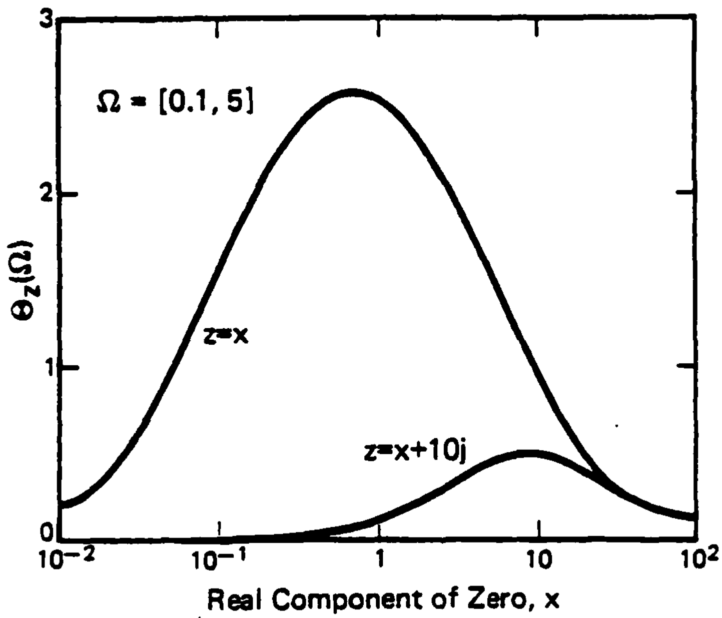

Figure 3.12. Weighted length of frequency interval as a function of real component of zero.

3.7. Remarks on Multivariable Systems

The purpose of this section is to briefly comment on the constraints that right half plane poles and zeros of a matrix open loop transfer function impose upon the corresponding matrix sensitivity and complementary sensitivity functions. Although the situation is more complicated than for single loop systems, some useful results can be obtained using the results of this paper. Again, the results are illustrated for the sensitivity function although analogous statements can be made about the complementary sensitivity function.

Let $L(s) \in \mathbb{C}^{n \times n}$ be a matrix of transfer functions and assume that the feedback system whose sensitivity function is the matrix $S(s) = [I + L(s)]^{-1}$ is stable. A commonly used measure of system sensitivity reduction [4,11-14] is the largest singular value, or matrix two-norm, of the sensitivity matrix. The results of this paper cannot, in general, be applied to singular values. Consider instead functions of the form

$$S_{vu}(s) = v^H S(s) u \quad , \tag{3.45}$$

where u and v are <u>constant</u> unit vectors in $\mathbb{C}^n$. The response of the system to disturbances entering in the direction spanned by u is given by $S(s)u$. The function $S_{vu}(s)$ is the component of this disturbance response appearing in the output direction spanned by v. Each function of the form (3.45) has the property that

$$|v^H S(j\omega) u| \leq \bar{\sigma}\,[S(j\omega)] = \|S(j\omega)\|_2 \quad . \tag{3.46}$$

Thus, to insure good sensitivity reduction properties at a given frequency, it is necessary (but not sufficient) to insure that $|v^H S(j\omega)u|$ is small at that frequency for a particular choice of u and v. For stable feedback systems, functions of the form (3.45) are analytic and bounded in the closed right half plane. Hence the results of this paper can be used to study the effect of right half plane transmission zeros upon the magnitude of $|v^H S(j\omega)u|$ and thus to indirectly study $\bar{\sigma}[S(j\omega)]$.

If $S_{vu}(s)$ has zeros in the right half plane, then these are either isolated or $S_{vu}(s) \equiv 0$. The latter case is trivial. If the zeros are isolated then they can be factored out using a Blaschke product as in (3.11) to form a function

$$\tilde{S}_{vu}(s) = S_{vu}(s)\; B^{-1}(s) \qquad , \tag{3.47}$$

which has no right half plane zeros and for which $|\tilde{S}_{vu}(j\omega)| = |S_{vu}(j\omega)|$.

One difference between the function $S_{vu}(s)$ and a scalar sensitivity function is that $S_{vu}(s)$ can possess right half plane zeros which are not due to unstable poles of L(s). For example, let

$$L(s) = \begin{bmatrix} \frac{1}{s+3} & \frac{2(s-2)}{s+3} \\ 0 & \frac{s-2}{s+3} \end{bmatrix} .$$

$$u = \begin{bmatrix} 0 \\ 1 \end{bmatrix} \qquad v = \begin{bmatrix} \frac{\sqrt{2}}{2} \\ \frac{\sqrt{2}}{2} \end{bmatrix} . \tag{3.48}$$

Then the function $S_{vu}(s)$ corresponding to (3.48) has a zero at $s=8$. This type of zero does not necessarily appear as a consequence of internal stability as do zeros at the poles of P(s) and F(s). Nonetheless, zeros of this type can be present in a given design and will be seen to worsen tradeoffs due to the transmission zeros of L(s).

If L(s) has a transmission zero at $s=z$, then it is easily verified that S(z) has an eigenvalue equal to one. Let w be a unit magnitude right eigenvector of S(z) corresponding to this eigenvalue. Then the unit vector u may be written as

$$u = \alpha w + \beta w_{\perp} \tag{3.49}$$

where α and β are complex scalars with $|\alpha|^2 + |\beta|^2 = 1$, and $w_{\perp}$ is a unit vector orthogonal to w. Then the magnitude of (3.45) at z is

$$|S_{vu}(z)| = |\alpha v^H w + \beta v^H S(z) w_{\perp}| \quad . \tag{3.50}$$

Lemma A.1 can be applied to show that

$$\pi \log|\alpha v^H w + \beta v^H S(z) w_{\perp}| + \pi \log|B^{-1}(z)| = \int_{-\infty}^{\infty} \log|S_{vu}(j\omega)| d\theta_z(\omega) \quad . \tag{3.51}$$

If the input direction u is equal to the right eigenvector w, then (3.51) reduces to

$$\pi \log|v^H w| + \pi \log|B^{-1}(z)| = \int_{-\infty}^{\infty} \log|S_{vu}(j\omega)| d\theta_z(\omega) \quad . \tag{3.52}$$

This equation shows how the presence of a right half plane zero constrains the magnitude of $v^H S(j\omega) w$ provided that v, the output direction of interest,

has a nonzero component in the direction of the eigenvector w. If in fact $v = w$, then $v^H w = 1$ and (3.52) is similar to the constraint (3.12). If v and w are orthogonal, however, then $v^H S(s)w$ has a zero at $s = z$. If this zero is isolated then it can be removed via the Blaschke product; the value of the resulting function $\tilde{S}_{vu}(s)$ is not constrained at $s = z$. Otherwise, $v^H S(s)w \equiv 0$. In either case there is no constraint imposed upon the weighted integral of $\log|S_{vu}(j\omega)|$. If $0 < |v^H w| \leq 1$, then a constraint is imposed whose severity decreases as $|v^H w|$ decreases.

The purpose of the above discussion is merely to show how some information about the effects of transmission zeros on closed loop sensitivity can be obtained and is not intended to be complete. For example, results can also be obtained using left eigenvectors of $S(z)$. It should be pointed out that the results of this section are consistent with those of Wall, Doyle and Harvey [19], who discuss multivariable right half plane zeros in terms of the extra phase lag they produce in certain directions.

3.8. Summary

In this chapter, limitations on feedback design due to right half plane poles and zeros of the open loop transfer function have been discussed. These limitations are expressed directly in terms of the magnitude of the sensitivity and complementary sensitivity functions evaluated along the $j\omega$-axis. This form of expressing the limitations should prove useful in that $|S(j\omega)|$ and $|T(j\omega)|$ are directly related to the quality of a feedback design. The Bode integral theorem has also been extended to the case of open loop unstable systems.

The limitations of Theorems 3.1-3.3 were interpreted as imposing tradeoffs among system properties in different frequency ranges. It should be pointed out that the origin of these tradeoffs is physical realizability. The property of realizability relevant to the present context is the fact that the Laplace transform of the impulse response of a physical system is a locally analytic function of the complex frequency variable. Thus the origin as well as the implications of the tradeoffs discussed above are significantly different from the well-known tradeoff between performance and robustness at a single frequency imposed by the algebraic relation $S(s) + T(s) = 1$.

CHAPTER 4

COMMENTS ON DIRECT DESIGN USING CLOSED LOOP TRANSFER FUNCTIONS

4.1. Introduction

As a prologue to attempting generalizations of classical single loop feedback theory to multiple loop systems, it is at least interesting to speculate upon why the existing theory developed as it did. One motivation for such speculation is that it might provide insight into how classical theory has avoided various pitfalls. This insight, in turn, might hopefully provide guidance into how these same pitfalls may be avoided in extensions to multiple loop systems. Of particular interest in this chapter will be the limitations on feedback properties quantified by the Bode integral relations discussed in Chapter 2 and the integral constraints due to right half plane poles and zeros discussed in Chapter 3. Recall that the ability to cope with these limitations and the tradeoffs they impose was the third important feature of classical methods pointed out in Chapter 2.

Return now to the first two features of classical methods discussed in Chapter 2. First it was observed that certain closed loop transfer functions evaluated along the $j\omega$-axis directly express the performance and robustness properties of a feedback system (a fact which has been noted by many authors for many years). Two transfer functions of particular interest are the sensitivity function and complementary sensitivity function, denoted $S(s)$ and $T(s) \triangleq 1 - S(s)$, respectively. Indeed, the values of $|S(j\omega)|$ and $|T(j\omega)|$ may reliably be used to judge the quality of a given feedback design. This fact, in turn, implies it is also natural to state design goals directly as bounds upon $|S(j\omega)|$ and $|T(j\omega)|$.

Despite the useful properties of closed loop transfer functions, classical control techniques in fact proceeded by shaping the open loop transfer function, $L(s) = P(s)F(s)$, where $P(s)$ and $F(s)$ are the plant and compensator transfer functions, respectively. That feedback design via open loop shaping is feasible is no doubt due to a second important feature of classical methods. This is the existence of rules of thumb for relating open and closed loop system properties.

At first it might seem odd that classical techniques focussed directly upon open loop, rather than closed loop, transfer functions. A little thought, however, suggests one (at least plausible) reason why this might have advantages. This reason is that the effect of various limitations imposed by properties of the open loop transfer function might be dealt with more readily, both in analysis and design, by methods employing open loop shaping. One might in fact conjecture that a tradeoff exists between design methods employing open loop transfer functions, in which design limitations are seen directly but feedback properties can only be assessed indirectly, and methods employing closed loop transfer functions, in which feedback properties may be directly assessed but plant limitations are not so readily seen.

The purpose of this chapter, then, is to investigate whether design techniques employing the open loop transfer function indeed do have any significant advantages over techniques directly employing closed loop transfer functions. Emphasis will be placed upon situations in which the class of achievable closed loop transfer functions is constrained by properties necessarily possessed by the open loop transfer function.

Many design problems could be used as a basis for the comparison undertaken in this chapter. The problem which is most convenient for the present purpose, due to the wealth of available literature, is the design of a system whose sensitivity function is to satisfy certain design goals despite limitations imposed by open loop system properties.

Finally, to return to the concerns voiced in the first paragraph of this section, suppose it is indeed true that open-loop based design techniques have important advantages in the design of single loop feedback systems. Then this might suggest that attempts to generalize closed-loop based design techniques to multiple loop feedback systems might not be as appropriate as attempts to generalize open-loop based techniques. Even if this conclusion is judged too strongly, it would nevertheless be of much interest to have knowledge of what information and insights are lost when open-loop techniques are abandoned. If this information and insight are indeed critical to the completion of a satisfactory design, then presumably they would have to be obtained from alternate sources and incorporated in any candidate design technique.

Portions of this chapter have appeared in preliminary form in [28].

4.2. The Sensitivity Design Problem

The purpose of this section is to discuss the design of a single loop feedback system whose sensitivity function is to satisfy certain design goals under bandwidth constraints imposed by properties of the plant and/or open loop transfer function. (Constraints due to nonminimum phase plants

are studied in Section 4.3.) It will be argued that realistic bandwidth constraints place nontrivial limitations upon the class of achievable sensitivity functions, that design methods directly employing the sensitivity function must face the problem of insuring that an admissible compensator will be obtained, and that design techniques employing the open loop transfer function may circumvent this difficulty by considering only admissible compensators from the outset.

The sensitivity function of a single-loop feedback system is given by $S(s) = [1 + P(s)F(s)]^{-1}$. This function is important in that $|S(j\omega)|$ is a measure of system response to disturbance inputs and of sensitivity to small variations in the plant parameters from their nominal values.

For purposes of discussion, consider a design specification requiring sensitivity reduction and disturbance rejection (i.e., requiring $|S(j\omega)| \ll 1$) over some low frequency range while also requiring that sensitivity not be excessively large at any frequency. This goal may be formulated quantitatively as imposing a frequency-dependent bound on the magnitude of the sensitivity function:

$$|S(j\omega)| \leq M(\omega) \qquad \forall\omega \tag{4.1}$$

$$M(\omega) = \begin{cases} M_H(\omega) & \omega \in [0, \omega_1] \qquad (4.1a) \\ M_S(\omega) & \omega > \omega_1 \quad . \qquad (4.1b) \end{cases}$$

Design constraints such as (4.1) are present in most practical problems, whether stated explicitly or only implicitly. As discussed in Chapters 2 and 3, it may well be that the bound (4.1) cannot be satisfied

due to some limitation imposed by properties of the open loop transfer function. In such cases it is relevant to ask whether it is possible to modify $M(\omega)$ appropriately so that a specification which is achievable and which also admits satisfactory designs is obtained. Toward this end, note that typically the value of $|S(j\omega)|$ is more critical to system performance at some frequencies than at others, and that satisfaction of design constraints is certainly more important at the more critical frequencies. Again, for the purpose of discussion, it will be assumed that the low frequency constraint $M_H(\omega)$ is a hard constraint to be satisfied, if at all possible, in order to achieve good system performance. The high frequency constraint $M_S(\omega)$, on the other hand, will be regarded as a soft constraint whose satisfaction, while desirable, is not as critical.

Recall it was conjectured in the previous section that certain difficulties faced by design methods employing closed loop transfer functions are either avoided or are encountered in a more tractable form by methods employing the open loop transfer function. The remainder of this section is devoted to discussing this conjecture in the case where the open loop transfer function must satisfy various bandwidth constraints. By bandwidth constraints is meant both frequency-dependent bounds on $|L(j\omega)|$ as well as requirements on the rate at which $|L(j\omega)| \to 0$ as $\omega \to \infty$. (If $L(s)$ is a rational transfer function then the latter requirement can be rephrased in terms of the order of the zero of $L(s)$ at infinity.)

First discussed is an argument of Horowitz [9, Section 6.13] concerning the feasibility of design by directly choosing the sensitivity function to satisfy design goals such as (4.1) while insuring the resulting

feedback compensator is proper. Now, as has recently been pointed out [16], any sensitivity function obtainable with an improper feedback compensator may be approximated as closely as desired by a sequence of strictly proper compensators. Thus objections based solely upon the inability to guarantee that a strictly proper compensator is obtained can readily be overcome. Realistic design constraints, however, impose much more severe limitations on the class of admissible compensators than mere propriety. The implications of these constraints for the method of design by direct choice of sensitivity function shall be discussed in detail after Horowitz' argument is reviewed.

Suppose that one directly chooses a function S(s) which is stable and satisfies the design constraint (4.1). Assume for simplicity that the plant is a stable, minimum phase rational function. Then a (possibly improper) feedback compensator yielding S(s) as the sensitivity function of the resulting design may be obtained from

$$F(s) = P^{-1}(s)[1 - S^{-1}(s)] \quad . \tag{4.2}$$

Now, in order to be realizable, this compensator must be at least proper. This requirement in turn may be translated into an algebraic constraint on the sensitivity function, as is now described. Again, this discussion is taken from Horowitz [9, Section 6.13].

Following Horowitz, let the plant have n poles and m zeros. Since physical plants are strictly proper, it follows that the pole-zero excess $e \triangleq n - m$ must be greater than zero. By straightforward manipulation, Horowitz shows that the sensitivity function must have the form

$$S(s) = \frac{s^n + \sum_{i=1}^{n} a_i s^{i-1}}{s^n + \sum_{i=1}^{n} b_i s^{i-1}} \tag{4.3}$$

where

$$a_i = b_i \quad ; \quad i=1,\ldots,m-1 \quad .$$

This fact, in turn, implies that the function $1 - S^{-1}(s)$ must have a zero of order (at least) e at $s = \infty$. The reason for this constraint may be seen from (4.2); it is necessary in order that the compensator F(s) be proper.

Horowitz then proceeds to point out the difficulty involved in choosing a function S(s) which satisfies both the design goals (4.1) as well as the constraints (4.3). Indeed, by fiddling with examples, one readily concludes that the problem is not trivial, and in fact seems nearly intractable for all but very small values of e.

To summarize, the requirement that a proper compensator be obtained translates into an algebraic constraint on the class of achievable sensitivity functions. The necessity of satisfying this constraint implies that attempts to design by directly choosing the sensitivity function will meet with difficulty. The problem is easily avoided, however, in open loop based design. Since the compensator F(s) is the design variable, one can trivially insure that F(s) is proper merely by choosing it to be so. Of course, one still has to verify that the resulting closed loop system is stable and that $|S(j\omega)|$ satisfies design goals. These may themselves not be trivial problems; however, classical Nyquist/Bode techniques have proven to be effective in

establishing the relationship between $L(j\omega)$ and $S(j\omega)$. Moreover, if a given design is judged unsatisfactory, classical techniques can provide insight into how the compensator might be modified to alter sensitivity properties.

Now, in [9], Horowitz ended his discussion after concluding that choosing $S(s)$ to satisfy both (4.1) and (4.3) is at best difficult. It is possible, however, to continue the analysis to show that, for $e \geq 2$, the goals (4.1) and constraint (4.3) may actually be mutually incompatible. Thus not only is the problem difficult, it may well be theoretically impossible. This can be shown by using the analyticity of $S(s)$ to translate the algebraic constraint on $S(\infty)$ into a constraint on $|S(j\omega)|$, $\forall\omega$. For $e \geq 2$, the Bode integral relation (Theorems 2.1 and 3.3) implies that

$$\int_0^\infty \log|S(j\omega)|d\omega = \sum_{i=1}^{N_p} \mathrm{Re}[p_i] \tag{4.4}$$

where $\{p_i \; ; \; i=1,\ldots,N_p\}$ is the set of unstable poles of $L(s)$. (Although not stated in the literature or in Chapter 3, there also exist integral constraints on the first $e-2$ derivatives of the sensitivity function.)

At this point it should be noted that the problem as posed thus far is not completely realistic. In practice, the class of admissible feedback compensators is constrained by requirements much more severe than mere propriety. In particular, not only is the order of the zero of $L(s)$ at infinity constrained, but also limitations on the bandwidth of $L(s)$ are present. These latter limitations in turn impose constraints on the bandwidth of the feedback compensator $F(s)$. (Also, note the approximation schemes of [16] are not applicable when the bandwidth of the compensator is constrained.) Two practical reasons why the bandwidth of the open loop

transfer function must be constrained are the natural bandwidth limitations of the plant and the necessity of rolling off the open loop gain to provide stability robustness (for example, to avoid exciting unmodelled high frequency dynamics). Thus in realistic situations S(s) must be chosen so that the resulting open loop transfer function satisfies a bandwidth constraint such as that discussed in Section 3.3,

$$|L(j\omega)| \le \frac{M}{\omega^{1+k}} \le \varepsilon \quad , \tag{4.5}$$

for $\omega > \omega_c$, $\varepsilon < 1$ and $k > 0$. As the Corollary in Section 3.3 shows, the tail of the integral in (4.4) must satisfy

$$\int_{\omega_c}^{\infty} \log|S(j\omega)|d\omega \le \frac{\log[\frac{1}{1-\varepsilon}]\omega_c}{k} \quad . \tag{4.6}$$

Thus, requiring that L(s) satisfy constraints such as (4.5) imposes even more severe limitations upon the class of achievable sensitivity functions. Hence, closed loop based design techniques are faced with the difficulty that candidate sensitivity functions must yield a compensator lying in a rather severely constrained class. Now, it is true that the class of function S(s) yielding such compensators may be characterized directly in terms of $|S(j\omega)|$ using (4.4) and (4.6). However, the problem is still nontrivial since it is difficult to look at a plot of $\log|S(j\omega)|$ and determine whether the necessary integral constraints are satisfied. The problem is particularly insidious since the value of $|S(j\omega)|$ is directly related to system performance. Since small values of $|S(j\omega)|$ indicate desirable sensitivity properties, the tendency would be to attempt a design for which the integral of $\log|S(j\omega)|$ in (4.4) is negative. Since increasing $|S(j\omega)|$ at some frequency results in poorer

performance at that frequency, one would like some insight into how this might be accomplished so that design quality is sacrificed no more than is absolutely necessary. Again, open loop based design techniques approach this problem by limiting the choice of candidate compensators to those which are admissible. Moreover, the Bode gain-phase relations and Nyquist plots may be used to provide insight into the fact that the rate at which loop gain rolls off affects the value of the sensitivity function. To summarize, the difficulty in satisfying constraints on admissible sensitivity functions is readily dispensed with and insight to aid in designing a compensator yielding satisfactory closed loop properties is available.

4.3. Design Limitations Due to Nonminimum Phase Plants

The purpose of this section is to discuss design limitations which are present as a consequence of the plant (more generally, the open loop transfer function) being nonminimum phase due to the presence of zeros in the open right half plane. These limitations restrict the class of achievable sensitivity specifications and thus pose obstacles to any design scheme whose goal is satisfaction of such specifications. As in the previous section, a comparison will be made between design techniques based upon the open loop transfer function, i.e., those which use the feedback compensator as the design variable, and a hypothetical design procedure which uses a candidate sensitivity function as the design variable. The latter technique must, of course, insure that the resulting feedback compensator yields no unstable pole/zero cancellations in the open loop transfer function. The

two design schemes compared may be referred to as "design by direct choice of the compensator" and "design by direct choice of the sensitivity function," respectively.

When a feedback system is designed around a nonminimum phase plant, internal stability requires that the feedback compensator possess no unstable poles at the right half plane zeros of the plant. This constraint on the class of admissible compensators implies that, to be achievable, the sensitivity function must satisfy the following algebraic constraints at each right half plane plant zero z of multiplicity m:

$$\begin{gathered} S(z) = 1 \\ \vdots \\ \left.\frac{d^i}{ds^i} S\right|_{s=z} = 0 \qquad i=1,\ldots,m-1 \quad . \end{gathered} \tag{4.7}$$

If a proposed sensitivity function violates (4.7), then the feedback compensator obtained from (4.2) will have one or more unstable poles at right half plane plant zeros. Experience with some examples should convince the reader that choosing a function S(s) satisfying one or more constraints (4.7) while also achieving design goals such as (4.1) may be quite difficult. (In fact, as shown in Chapter 3, it may well be impossible. This will be reviewed shortly.) To summarize, if the constraints (4.7) are not satisfied, then the compensator F(s) obtained from (4.2) will be inadmissible due to unstable pole-zero cancellations in L(s). On the other hand, if these constraints are satisfied, but the design goals (4.1) are not achieved, then it isn't clear that insight is provided into how S(s) might be modified to better achieve design goals while maintaining internal stability.

Classical design techniques based upon directly choosing the feedback compensator can, on the other hand, avoid the difficulty of satisfying the constraints (4.7) simply by selecting only candidate feedback compensators which have no poles at right half plane plant zeros. Insight into the relation between the feedback compensator and the resulting sensitivity function is available from Nyquist and Bode plots. In particular, the difficulty caused by the extra phase lag in $L(j\omega)$ contributed by the right half plane zeros is readily seen.

Although insight into the qualitative effects of right half plane plant zeros has long been available, only recently have precise quantitative statements of their impact upon feedback design been obtained. As shown in Chapter 3, the algebraic constraints (4.7) have equivalent expressions in terms of integral relations constraining the behavior of $\log S(j\omega)$. These relations are significant in that they express limitations due to right half plane zeros in terms of the sensitivity function evaluated along the $j\omega$-axis, where design specifications are imposed.

For example, the constraint $S(z) = 1$ is equivalent to (see Theorem 3.1)

$$\pi \log |B_p^{-1}(z)| = \int_{-\infty}^{\infty} \log|S(j\omega)|\, d\theta_z(\omega) \tag{4.8}$$

where $B_p(s)$ is the Blaschke product of unstable plant and compensator poles and

$$\frac{d\theta_z}{d\omega} = \frac{x}{x^2 + (y-\omega)^2} \quad , \qquad z = x + jy \quad . \tag{4.9}$$

(If z is complex, then there exists an additional constraint on $\measuredangle S(j\omega)$; if z has multiplicity greater than one, then there exist constraints on $\frac{d^i}{ds^i} \log S$). Before proceeding, some relevant observations concerning the integral constraint (4.8) will be reviewed.

First, since $|B_p^{-1}(z)| \geq 1$, and since (4.9) is positive $\forall\omega$, it follows that, if $|S(j\omega)| < 1$ over some frequency range, then <u>necessarily</u> there exist other frequencies for which $|S(j\omega)| > 1$. Thus a tradeoff exists among sensitivity properties in different frequency ranges. Moreover, since the weighted length of the $j\omega$-axis is finite (and equal to π), this tradeoff must be accomplished primarily over a finite frequency range.

Next, consider the implications of this tradeoff upon the ability of a feedback system to satisfy both (4.1) and (4.7). As shown in Chapter 3, one may derive a lower bound on $\|S\|_\infty \triangleq \sup_\omega |S(j\omega)|$, given that (4.1a) is satisfied. Using this lower bound, one may then analyze whether it is also possible to satisfy (4.1b). Thus one can actually prove that certain design specifications are unachievable given the constraints imposed by the right half plane plant zeros.

The question now arises as to whether the integral relations derived in Section 3.2 may provide sufficient insight to allow one to design by directly choosing the sensitivity function. Certainly some insight may be obtained from the function $\theta_z(\omega)$, which quantities the notion of proximity of a point on the $j\omega$-axis to a right half plane zero. The presence of this term in (4.8) shows that the price paid, in terms of sensitivity increase, for obtaining a given level of sensitivity reduction over a given frequency interval is a function of the location of that interval relative to the zero.

For example, at sufficiently high frequencies the weighting becomes very small. Hence the value of $|S(j\omega)|$ must be either very large or very small at those frequencies in order to contribute to the value of the integral (4.8). On the other hand, requiring sensitivity to be very small over a frequency range containing $y = \mathrm{Im}[z]$ can lead to large values of sensitivity elsewhere. This effect is exacerbated if $|S(j\omega)|$ is only allowed to exceed unity over frequency intervals whose weighted length is small.

Now consider the problem of design by directly choosing the sensitivity function when the plant has a single (real) right half plane zero x. For simplicity, assume that the plant is stable. Let $S_1(s)$ be a candidate sensitivity function. From the Lemma in Appendix A it follows that

$$\pi \log|S_1(x)| = \int_{-\infty}^{\infty} \log|S_1(j\omega)|\, d\theta_x(\omega) \quad .$$

This equation is significant since $S_1(s)$ has an internally stable realization only if $S_1(x) = 1$. Now, suppose this condition is not met, and assume further that $|S_1(x)| < 1$. (Since good sensitivity is achieved by requiring that $|S_1(j\omega)|$ is sufficiently less than one, this is surely the most likely case, at least in an initial attempt.) Now, if indeed $|S_1(x)| < 1$, it will be necessary to choose a new sensitivity function $S_2(s)$ with larger values of $|S_2(j\omega)|$ over some frequency range. The weighting function $\theta_x(\omega)$ yields at least some insight into how this may be done. For example, choosing a new sensitivity function whose magnitude is larger only at lightly weighted frequencies will not generally be effective; one must increase the magnitude at frequencies for which the weighting $\theta_x(\omega)$ is significant. If it turns out that

significantly large values of the weighting lie only within the frequency range over which sensitivity is desired to be small, then nontrivial compromises in system performance will have to be made. Whether enough insight is generally available from the weighting function $\theta_x(\omega)$ to enable such compromises to be made satisfactorily remains to be seen.

In any event, as will now be shown, the fact that P(s) was assumed to have only one zero in the right half plane facilitates design of S(s). This follows since each candidate sensitivity function may easily be modified to produce a new candidate function yielding an internally stable design. All that is necessary to perform the modification is to define the new function $\hat{S}_i(s) \triangleq \frac{S_i(s)}{S_i(x)}$. Of course, $|\hat{S}_i(j\omega)|$ and $|S_i(j\omega)|$ may have very different values. Suppose, however, that a function $S_i(s)$ is obtained which satisfies design goals sufficiently well and for which $S_i(x) \approx 1$. Then $\hat{S}_i(s)$ defined in this fashion will both yield an internally stable design and, since $|\hat{S}_i(j\omega)| = \frac{|S_i(j\omega)|}{|S_i(x)|}$, will likely come close to satisfying the design goals. Of course, this strategy works because the plant was assumed to have but a single right half plane zero. If more than one zero (even a complex conjugate pair of zeros) is present, then simple scaling will not generally yield a function satisfying all the necessary constraints.

Finally, consider once again the approach to this problem involving open loop shaping; i.e., "design by direct choice of the compensator." From a Nyquist diagram one can see that the frequency response of the open loop transfer function must eventually penetrate the unit circle centered at the critical point. Thus there will necessarily exist a frequency range for which $|S(j\omega)| > 1$; in particular, there will exist a peak in the sensitivity

function near the point on the Nyquist plot of $L(j\omega)$ closest to the critical point. The size of this peak may be varied via lead or lag compensation, but its existence will be unavoidable. Moreover, it can also be seen that, if the size of the peak is not to be excessively large, then the open loop gain must be rolled off before the phase lag produced by the zero becomes too great. Again, whether such insights are as readily available in the design procedure involving direct choice of the sensitivity function remains an open question.

4.4. Sensitivity Design via H^∞-Optimization

The purpose of this section is to discuss some properties of a recently proposed approach to the problem of feedback design. This approach, which utilizes H^∞-optimization methods, employs closed loop transfer functions directly in the design process. The specific design problem discussed in this section is, as in the rest of this chapter, the achievement of good sensitivity properties. The solution to the relevant H^∞-optimization problem is discussed at length by Zames and Francis [16]. It should be emphasized that the design goals in [16] are <u>not</u> the satisfaction of frequency-dependent norm bounds such as (4.1). Other authors, however, have considered satisfaction of norm bounds as the goal of H^∞-optimization. The results of [16] are used in the present analysis for availability and for convenience.

As discussed earlier in this chapter, feedback design methods which directly employ closed loop transfer functions may be faced with difficulties which are either avoided or rendered more tractable by classical methods

employing the open loop transfer function. Again, it is conjectured that there may be a real tradeoff between design techniques dealing directly with closed loop transfer functions, for which limitations imposed by properties of the open loop plant may only be dealt with indirectly, and design techniques dealing directly with open loop transfer functions, for which the feedback properties of a design may only be assessed indirectly. Thus, once the H^{∞} approach has been described, it will be examined to see whether difficulties in dealing with open loop plant limitations are present in this closed loop based design technique also.

The H^{∞} sensitivity minimization problem is to find, among all stabilizing feedback compensators, one for which a weighted infinity norm of the sensitivity function is minimized:

$$\min_F \|WS\|_{\infty} = \min_F \sup_{\omega} |W(j\omega)S(j\omega)| \quad . \tag{4.10}$$

The stable, minimum phase, weighting function $W(s)$ is to be supplied, via some procedure, by the designer.* For nonminimum phase plants, internal stability requires that the constraints (4.7) be satisfied at each open right half plane plant zero. Thus the optimization problem (4.10) is constrained by (4.7). However, the limitations on feedback design imposed by (4.7), which were interpreted in Section 4.3 as tradeoffs among levels of sensitivity along the $j\omega$-axis, are treated in this framework merely as algebraic constraints

*The reader is cautioned that the term weighting function has two uses in this chapter. These should be distinguishable by context. One use is to refer to the functions $\theta_z(\omega)$ and $\theta_p(\omega)$ which appear in the integral constraints due to right half plane zeros and poles (Theorems 3.1 and 3.2). The other use is to refer to the function $W(s)$ used as a design variable in the H^{∞}-optimization process.

imposed upon the sensitivity function at isolated points in the open right half plane. The significance of this distinction will become apparent below.

The solution to the problem (4.10) given in [16] shows that, given the existence of a nonminimum phase plant, the optimal unweighted sensitivity function has the form

$$S^*(s) = k^* B_P(s) B_{F^*}(s) W^{-1}(s) \quad , \tag{4.11}$$

where $B_P(s)$ is the Blaschke product of unstable plant poles. The Blaschke product $B_{F^*}(s)$ contains unstable poles of the optimal feedback compensator. There are at most one less of these poles than the number of open right half plane plant zeros. The unstable pole locations, as well as the value of the constant k^*, are determined by the constraints (4.7).

Since Blaschke products are allpass of unit magnitude, it follows from (4.11) that

$$|S^*(j\omega)| = |k^*| \cdot |W^{-1}(j\omega)| \quad . \tag{4.12}$$

Thus the weighting function determines the <u>shape</u> of the sensitivity function; i.e., its relative magnitude at different frequencies. The <u>level</u> of sensitivity reduction, however, is determined by the constraints (4.7) at the right half plane plant zeros.

One possible way to construct the weighting function is to choose

$$W(s) = \hat{M}^{-1}(s) \tag{4.13}$$

where $\hat{M}(s)$ is a stable minimum phase transfer function with $|\hat{M}(j\omega)| = M(\omega)$, $\forall\omega$, and $M(\omega)$ is given by the specification (4.1). Using this procedure, the H^∞-optimal solution satisfies the specification (4.1) if

$$\|WS^*\|_\infty = |W(j\omega)S^*(j\omega)| \leq 1 \qquad . \tag{4.14}$$

Moreover, if $\|WS^*\|_\infty > 1$, then the specification (4.1) is unachievable. Since the optimal weighted sensitivity function $W(s)S^*(s)$ is allpass (4.10)-(4.11), it follows in turn that if (4.1) is violated, then it is violated equally at all frequencies.

Now, one advantage of the H^∞-optimization procedure is that it guarantees the constraints (4.7) will be satisfied. The design goals (4.1), on the other hand, may well be violated, whether the weighting function is chosen to directly reflect these goals, as in (4.13), or not. This follows from the fact that, although the designer can specify the shape of the optimal unweighted sensitivity function, the level, or magnitude, is determined by the constant k^* which is determined by the locations of the right half plane plant zeros.

Suppose, then, that a weighting function has been chosen and the resulting optimal unweighted sensitivity function violates the design goals. In addition, suppose that it is desired to choose a new weighting function (perhaps by suitable modification of the existing weighting) so that the new optimal sensitivity satisfies, for example, the hard design specification (4.1a). Of course, this would entail violating the soft design specification (4.1b). In view of the presumed relative importance of the hard and soft specifications, this is not unreasonable provided the violation of (4.1b) is not excessive. The question which naturally arises is: At which frequencies, and by how much, should the weighting be modified in order to accomplish this task?

AD-A161 452 ISSUES IN FREQUENCY DOMAIN FEEDBACK CONTROL(U) ILLINOIS UNIV AT URBANA DECISION AND CONTROL LAB J S FREUDENBERG MAY 85 DC-81 N00014-84-C-0149 2/5

UNCLASSIFIED F/G 9/3 NL

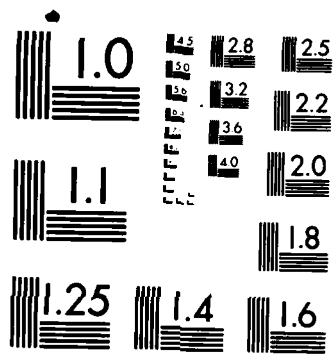

MICROCOPY RESOLUTION TEST CHART
NATIONAL BUREAU OF STANDARDS-1963-A

One might hope that some insight into this question would be furnished by the manner in which the current design violates the design specifications. Certainly classical design techniques provide some such insight. For example, looking at Nyquist and Bode plots not only reveals when a given design has poor sensitivity, but also gives information concerning how to use lead and/or lag compensation to modify the existing design. In addition, these techniques provide some insight into how the additional phase lag contributed by right half plane zeros complicates the design process. In particular, qualitative insight into how the location of the zero limits the frequency range over which large open loop gain may be achieved is provided.

Note, however, that H^∞ designs violate (4.1) even at those frequencies which are far away from any right half plane zeros and for which the value of $|S(j\omega)|$ contributes little to the tradeoff imposed by the integral constraint (4.8). While the fact that the specification is violated equally at all frequencies isn't necessarily bad by itself, it doesn't seem to furnish much insight into how difficult various portions of the specification are to satisfy. Consequently, it would seem that insight into how the weighting function might be modified must be obtained from other sources. This issue will be explored in the next section.

4.5. Relations Between $W(s)$ and $|S^*(j\omega)|$

In this section the relation between the weighting function and the optimal unweighted sensitivity function is investigated. The purpose is to examine issues which must be considered in attempting to modify the weighting

W(s) to obtain a sensitivity function satisfying frequency-dependent magnitude bounds, such as (4.1), over at least some frequencies.

First from (4.7) and (4.11) it may be seen that the following conditions must be satisfied at each right half plane plant zero z of multiplicity m:

$$\begin{aligned} 1 &= k^* B_P(z) B_{F*}(z) W^{-1}(z) \\ &\vdots \\ 0 &= \frac{d^i}{ds^i} B_P B_F W^{-1}\Big|_{s=z} \qquad i=1,\dots,m-1 \quad . \end{aligned} \tag{4.15}$$

From (4.15) it follows that if the plant possesses only one (real) right half plane zero (so that $B_{F*}(s) = 1$) then

$$|k^*| = |W(z) B_P^{-1}(z)| \quad . \tag{4.16}$$

If more than one zero is present, the value of $|k^*|$ increases as a function of the proximity of the unstable compensator poles to the zeros:

$$|B_{F*}^{-1}(z)| = \left| \prod_{i=1}^{N_{F*}} \frac{p_i + z}{p_i - z} \right| \geq 1 \quad .$$

Suppose, however, that the conditions

$$W(z_j) = W(z_k) \qquad \forall j,k \tag{4.17a}$$

and, at each zero of multiplicity $m > 1$,

$$0 = \frac{d^i}{ds^i} B_P \Big|_{s=z} W^{-1}(z) + B_P(z) \frac{d^i W^{-1}}{ds^i}\Big|_{s=z} \qquad i=1,\dots,m-1 \tag{4.17b}$$

are satisfied (which may not be possible for open loop unstable nonminimum

phase plants). Then (4.15) can be satisfied with $B_{F^*}(s) = 1$. Hence the optimal compensator is stable and $|k^*|$ again satisfies (4.16).

In any event, at each open right half plane zero the optimal unweighted sensitivity function must satisfy

$$|S^*(j\omega)| \geq |W(z)| \cdot |B_p^{-1}(z)| \cdot |W^{-1}(j\omega)| \tag{4.18}$$

with equality, holding if and only if (4.16) holds.

Motivated by the discussion of the previous section, suppose one wishes to modify an existing weighting function so that $|S^*(j\omega)|$ obtained from the new weighting satisfies a magnitude bound in some frequency range without becoming excessively large at other frequencies. From (4.11) and (4.15) it follows that simply scaling $W(s)$ by a constant leaves $S^*(s)$ unchanged. Thus in order to affect $|S^*(j\omega)|$ it is necessary to change the relative magnitude of $|W(j\omega)|$ at different frequencies. This will now be discussed.

Assume first that $P(s)$ has only one right half plane zero, so that (4.18) is an equality. Then (4.18) shows that $|S^*(j\omega)|$ is a function of both the magnitude of the weighting at the zero <u>and</u> the weighting along the $j\omega$-axis. If these quantities were independent, then one could reduce $|S^*(j\omega)|$ at some frequency simply by increasing the magnitude of the weighting at that frequency and/or by reducing the magnitude at the zero. Unfortunately, however, the magnitude of the weighting at the zero is <u>not</u> independent of its value along the $j\omega$-axis. In fact, $|W(j\omega)|$ is completely determined by $\{|W(j\omega)|, \forall\omega\}$. This follows since, at each open right half plane zero, z, of multiplicity m, the weighting satisfies the integral relations (see Appendix A):

$$\pi \log|W(z)| = \int_{-\infty}^{\infty} \log|W(j\omega)|\, d\theta_z(\omega) \qquad (4.19a)$$

$$\pi \measuredangle W(z) = \int_{-\infty}^{\infty} \measuredangle W(j\omega)\, d\theta_z(\omega) \qquad (4.19b)$$

$$\pi \frac{d^i}{ds^i} \log W\Big|_{s=z} = \int_{\infty}^{\infty} \frac{d^i}{ds^i} \log W\Big|_{s=j\omega} d\theta_z(\omega) \quad i=1,\ldots,m-1 \qquad (4.19c)$$

where $\frac{d\theta_z}{d\omega}$ is given by (4.9).

From (4.19a) it follows that increasing the magnitude of the weighting along the $j\omega$-axis can only <u>increase</u> the magnitude of the weighting at the zero. Similarly, $|W(z)|$ can be decreased only by <u>decreasing</u> $|W(j\omega)|$ over some frequency range. Hence, from the above discussion of (4.18) and its implications, it follows that attempts to modify the weighting to reduce $|S^*(j\omega)|$ will be complicated by these two opposing tendencies.

Thus, in order to modify $|W(j\omega)|$ to affect $|S^*(j\omega)|$ in some desired fashion, it appears necessary to have a good understanding of the relation between $|W(j\omega)|$ and $|W(z)|$. This relation is not completely transparent; however, some insight may be gained from (4.19a). For example, at high frequencies for which $\frac{d\theta_z}{d\omega}$ is small, changing $|W(j\omega)|$ will have relatively little effect upon the value of $|W(z)|$. Thus, attempting to meet a low frequency specification on $|S^*(j\omega)|$ by decreasing the weighting in a high frequency range will be effective only if $\frac{d\theta_z}{d\omega}$ is relatively large in this range. Otherwise the effect will be to increase sensitivity at high frequencies with very little attendant decrease at low frequencies.

If the plant has more than one right half plane zero, then in general the bound (4.18) will not be tight due to the presence of unstable

compensator poles. Nevertheless, if this lower bound is too large for any zero, the above comments apply to attempts to reduce the bound. Many plants with more than one right half plane zero (including all stable plants) can be used in a stable feedback system with a stable compensator. For these plants an alternate procedure is to require the weighting to satisfy (4.18). This requirement may also be stated in terms of $W(j\omega)$ using (4.19).

In Section 4.4 it was pointed out that design limitations due to nonminimum phase plants are treated in the H^∞ framework as constraints imposed at points in the right half plane, rather than along the $j\omega$-axis. From the preceding discussion, however, it appears that interpreting the constraints as tradeoffs imposed along the $j\omega$-axis is necessary if the weighting function is to be shaped to satisfactorily affect the sensitivity function. Moreover, it has been argued that it is necessary to consider the relation between $|W(j\omega)|$ and $|W(z)|$. Qualitative insights into this relation are available; however, whether these insights are sufficient to reliably produce a satisfactory design seems to be an open question.

4.6. Comparison between Design by Directly Choosing the Sensitivity Function and Design via H^∞-Optimization

Two procedures have now been discussed for designing a system with satisfactory sensitivity properties when the plant is nonminimum phase. Both these procedures employed a closed loop transfer function, specifically, the sensitivity function, in performing the design. The first, discussed in Section 4.3, consisted of iterating a candidate sensitivity function $S_1(s)$, until one which satisfied the constraints (4.7) was obtained. This technique

had the advantage that one could choose the level of sensitivity reduction $|S_1(j\omega)|$ and the disadvantage that an internally stable system is generally not obtained.

The second design scheme, discussed in Sections 4.4 and 4.5, was the H^∞-optimization method. This technique involved iterating a weighting function $W_1(s)$ in order to obtain a satisfactory sensitivity function, and had the advantage that an internally stable design is always achieved (albeit with generally improper and possible unstable compensators). The disadvantage of this technique is that the level of sensitivity reduction along the $j\omega$-axis is determined a posteriori via the optimization process, and consequently cannot be controlled directly.

The perceptive reader will have noticed, however, that the difficulty involved in both techniques arises from the same source; namely, the fact that the value of a stable minimum phase rational function at a point in the right half plane is <u>completely determined</u> by its values along the $j\omega$-axis. Consequently, these two quantities cannot be manipulated independently in design. Thus, although the two design procedures yield intermediate results with different properties, the ultimate problem which must be solved by each is the same. This may be shown explicitly using the following theorem.

<u>Theorem 4.1</u>: Let $P(s)$ be a nonminimum phase plant satisfying the assumptions of [16, Section II, C.1)]. Let $F(s)$ be a choice of feedback compensator and define the sensitivity function $S(s) = [1+P(s)F(s)]^{-1}$. Suppose that

(i) $S(s)$ has no poles in $\mathrm{Re}[s] \geq 0$,

(ii) $S(s)$ satisfies Condition (4.7) at the open right half plane zeros of $P(s)$ and, at each right half plane plant pole, p, of multiplicity n,

$$S(p) = 0$$
$$\vdots$$
$$\frac{d}{ds^i} S \Big|_{s=p} = 0 \qquad i=1,\ldots,n-1$$

(iii) $F(s)$ has $\leq N_P^z - 1$ unstable poles, where N_P^z is the total number of open right half plane zeros of $P(s)$,

(iv) $\exists\ \varepsilon > 0$ such that $\inf\limits_{Re[s] \geq 0} |\tilde{S}(s)| \geq \varepsilon$, where $\tilde{S}(s)$ is defined by (3.11),

(v) $\exists\ \alpha > 0$, $\ell \geq 0$, and $R > 0$ such that if $|s| > R$ and $Re[s] \geq 0$, then $|S(s)| \leq \alpha |s|^{\ell}$.

Conditions (i)-(v) are necessary and sufficient to insure a weighting function $W(s)$ exists which yields the compensator $F(s)$ as the solution to the weighted optimization problem (4.10). The appropriate weighting function is given by

$$W(s) = cB_P(s)B_F(s)S^{-1}(s) \tag{4.20}$$

where $B_P(s)$ is the Blaschke product of unstable plant poles, $B_F(s)$ is the Blaschke product of unstable compensator poles, $S(s)$ is the sensitivity function for the feedback $F(s)$, and $c \neq 0$ is an arbitrary constant. ∎

Proof: (Necessity) Suppose that $W(s)$ is a weighting function yielding an optimal conpensator $F^*(s) = F(s)$. Then it follows from (4.11) that

$$S^*(s) = kB_P(s)B_F(s)W^{-1}(s) \quad .$$

Since H^∞-optimal solutions are internally stable, (i) and (ii) are satisfied. From the fact that $F^*(s)$ has at most $N_P^z - 1$ unstable poles, it follows that $F(s)$ must satisfy (iii). Finally, from assumptions necessary to insure that $W(s)$ is a valid weighting function [16], (iv) and (v) are satisfied.

Sufficiency: Let $F(s)$ be a feedback compensator with $S(s)$ the corresponding sensitivity function, and suppose that assumptions (i)-(v) are satisfied. Then $W(s)$, given by (4.20), satisfies conditions the conditions in [16] to be a valid weighting function. By assumption (iii) the function $\hat{S}(s) \triangleq cB_P(s) B_F(s)W^{-1}(s)$, where c and $B_F(s)$ are as in (4.20), has the appropriate form (4.10). A simple calculation shows that $W(z) = cB_P(z)B_F(z)$ and $\frac{d^i}{ds^i} W\Big|_{s=z} = c \frac{d^i}{ds^i} B_P B_F\Big|_{s=z}$, $i=1,\ldots,m-1$. This follows from the fact that $S(s)$ must satisfy the constraints (4.7). Thus, the function $\hat{S}(s)$ satisfies these constraints also, and by the uniqueness result of [16], $S^*(s) = \hat{S}(s)$. It then follows that $F^*(s) = F(s)$. ■

Note that Conditions (i)-(ii) of Theorem 4.1 are necessary for internal stability while (iii)-(v) will be satisfied by any practical design. This theorem shows that the class of designs which may be obtained via H^∞ methods is very broad indeed.

Recall that the application of H^∞ techniques discussed in this chapter involves iterating on the weighting function $W_i(s)$ until a satisfactory optimal unweighted sensitivity function is obtained. Theorem 4.1 may now be used to show to what extent this procedure is equivalent to that discussed in Section 4.3 for design by iterating on candidate sensitivity functions.

Consider first the case of a plant with a single (real) right half plane zero, $z=x$, and assume for simplicity that the plant is stable. Then, the optimal unweighted sensitivity function is related to the weighting by $S^*(s) = W(x)W^{-1}(s)$. Thus the sequence of weightings $\{W_i\}$ used in the H^∞ procedure may also be used to construct candidate sensitivity functions for the direct sensitivity design procedure by setting $S_i(s) = W_i^{-1}(s)$. In

general, the constraint $S_i(x) = 1$ will not be satisfied; however, as in Section 4.3, the candidate sensitivity function $\hat{S}_i(s) \triangleq \frac{S_i(s)}{S_i(x)}$ will satisfy $\hat{S}_i(x) = 1$. Suppose, then, that one may construct the sequence of weighting functions so that $W_i(s)$ converges to a weighting for which the function $|W_i^{-1}(j\omega)|$ satisfies the design specification on sensitivity sufficiently well. Moreover, suppose that the corresponding value of $W_i(x)$ is approximately one. Then, the optimal unweighted sensitivity function $S_i^*(s) = W_i^{-1}(s)W_i(x)$ will likely also satisfy the design goals sufficiently well. Of course, the sequence of candidate sensitivity functions $\hat{S}_i(s)$ will converge to this same function. This follows easily from the fact that $\hat{S}_i(s) = W_i^{-1}(s) \cdot W_i(x) \approx S_i^*(s)$, since $W_i(x) \approx 1$.

Obviously, the above procedure may be reversed. One may construct a series of candidate sensitivity functions $S_i(s)$, as in Section 4.3, and then check to see if the constraint $S_i(x) = 1$ is satisfied. If not, then an internally stable design may be obtained by scaling: $\hat{S}_i(s) = \frac{S_i(s)}{S_i(x)}$. The function $\hat{S}_i(s)$ may then be used to construct a weighting function, as in Theorem 4.1. Of course, this weighting function will merely reproduce the design $\hat{S}_i(s)$; i.e., the weighting $W_i(s) \triangleq \hat{S}_i^{-1}(s)$ yields the optimal unweighted sensitivity function $S_i(s) = \hat{S}_i(s)$. Again, the success of this procedure depends upon the ability to choose a candidate sensitivity function for which $|S_i(j\omega)|$ satisfies design goals sufficiently well and for which $S_i(x) \approx 1$.

Thus, for the case of a single right half plane zero, design by iterating on the weighting function and by iterating on the sensitivity function directly are equivalent. The only possible advantage one technique

could have over the other is if it provided more insight. However, the problem faced by both procedures is the same, and is governed by the integral relations (4.8) and (4.19). It seems that, in each case, successful design rests on being able to gain insight from an integral relation.

If the plant has more than one right half plane zero (but is still assumed stable for simplicity of exposition), then simply scaling the candidate sensitivity function will not, in general, yield a new function satisfying the constraints at all the zeros. Choosing a candidate sensitivity function to satisfy constraints at more than one zero as well as some design goals would be difficult at best, despite any insights available from the integral relations. If, however, such a function were found, then a weighting constructed as in Theorem 4.1 would reproduce this function as the solution to the H^{∞}-optimization problem.

The way in which the H^{∞} approach deals with the case of more than one plant zero is different than the direct sensitivity design approach. The H^{∞} approach, however, violates accepted good design practice by using unstable poles in the compensator. These poles will be present unless the weighting function is chosen to satisfy the constraint (4.17), which may also be expressed in terms of integral relations using the lemma in Appendix A. A little inspection of (a) the constraints which a candidate sensitivity function must satisfy in order to yield an internally stable design and (b) the constraints which a weighting function must satisfy in order to yield a stable compensator reveals that essentially the same problem is faced by both techniques. Thus, again, it seems the two approaches are equivalent and the success of each hinges on the insights, or lack thereof, to be found in a set of integral relations.

The purpose of this section has been to point out that the H^{∞}-optimization approach to sensitivity design is remarkably similar to the method of "design by direct choice of sensitivity function." First, essentially any design obtained by one method may be obtained by the other. Second, the difficulty faced by both procedures is the same - the fact that one must consider certain integral relations relating $W(j\omega)$ and $W(x)$ or $S(j\omega)$ and $S(x)$. The success of either procedure seems to hinge on whatever insight into these relations may be gained.

4.7. Conclusions

The purpose of this chapter has been to examine the relative merits of two general approaches to feedback design. These two approaches are design employing open-loop transfer functions and design employing closed-loop transfer functions. The design problem chosen as a basis for comparison was that of obtaining a feedback system whose sensitivity function satisfies certain design specifications.

Two different closed loop based design methods were compared in this chapter, and found to be substantially equivalent when used to address the problem posed. In particular, both were complicated by the fact that the values of a stable minimum phase transfer function at points in the open right half plane are completely determined by the values of the function along the $j\omega$-axis. Even with whatever insights may be gained from the integral relations developed in Chapter 3, this difficulty appears nontrivial.

The preceding observations suggest that open loop based design techniques may have some real advantages, since the compensator may be chosen a priori to be within a given admissible class. This doesn't necessarily imply that open loop techniques are generally better than closed loop techniques; they are different, and must deal with problems in different ways. For example, using open loop techniques only allows one to evaluate closed loop behavior indirectly. Classical single-loop design methods utilized various rules of thumb to expedite this process. An attempt to generalize some of these rules of thumb to multiple-loop systems is discussed in Chapter 8. Again, as was stated in the introduction to this chapter, the purpose of the preceding discussion is not to completely discourage development of closed loop based design techniques. On the other hand, the discussion has pointed out some problems in which readily usable information seems to be lost in passing from open to closed loop methods. Clarification of these problems and related issues should help in the development of any design scheme.

One final remark will now be made. It is possible to interpret an iterative design process as an exploration of the set of possible designs. One purpose of such an exploration is to gain insight into the properties that this set possesses. (In particular, a distinction should be made between characterizations of possible designs which provide insight into the achievement of design goals and those characterizations which do not.) If such an exploration is done in conjunction with the development of design specifications, then the task of arriving at specifications which realistically reflect the essential tradeoffs inherent in the problem is facilitated. One

conclusion may be that the so-called "trial and error" aspect of classical design is present for a very good reason, and not necessarily as an indication of the lack of more precise methods. Another conclusion is that it may be unrealistic to impose design specifications based upon properties desired from a design until some idea of the properties available is obtained.

Finally, the viewpoint of the preceding paragraph suggests a reasonable criterion of merit by which proposed feedback design methods may be judged. This criterion is the ability of the method to efficiently yield insights into the class of feedback designs possible for a given plant. Of course, other properties must also be possessed by a technique in order for it to be generally useful.

CHAPTER 5

PREVIOUS MIMO RESULTS AND MOTIVATION FOR PRESENT WORK

5.1. Introduction

In Chapter 2 certain important concepts from classical control theory were discussed. The purpose of this chapter is to discuss previous work on the extension of these concepts to MIMO systems and to point out where further work needs to be done. Thus this chapter motivates the study of some specific problems to be proposed in the remainder of the thesis. The discussion will at first parallel closely that of Chapter 2. Portions of this chapter have appeared in [29].

5.2. Basic Equations for MIMO Feedback Systems

Consider a linear time-invariant multiple-input multiple-output (MIMO) feedback system as shown in Figure 5.1. This feedback structure is the same as that of Figure 2.1, for SISO systems, with the exception that all transfer functions are matrices and all signals are vectors. For simplicity, only square transfer function matrices are considered; such cases are sufficient to illustrate the ideas discussed in this thesis. Specifically, P(s) and F(s) are the transfer functions of the plant model and feedback compensator, respectively, and take values in $\mathbb{C}^{n\times n}$. The signal r(s) is the reference input; y(s), the system output; d(s), a disturbance input; and n(s), sensor noise. All signals take values in $\mathbb{C}^{n}$.

The output of the feedback system is again given by

$$y(s) = y_r(s) + y_d(s) + y_n(s) \tag{5.1}$$

$$y_r(s) = [I + P(s)F(s)]^{-1} P(s)r(s) \tag{5.2}$$

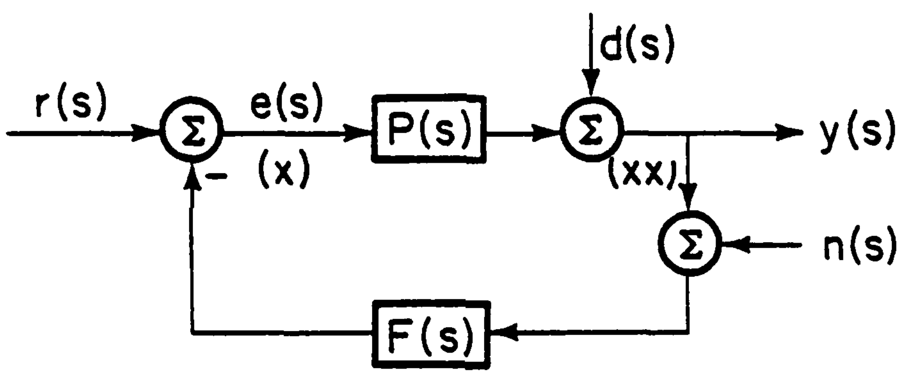

Figure 5.1. Feedback configuration.

$$y_d(s) = [I + P(s)F(s)]^{-1} d(s) \tag{5.3}$$

$$y_n(s) = - [I + P(s)F(s)]^{-1} P(s)F(s)n(s) \quad . \tag{5.4}$$

Define the open loop transfer function

$$L(s) \triangleq P(s)F(s) \quad , \tag{5.5}$$

the system sensitivity function

$$S(s) \triangleq [I + L(s)]^{-1} \quad , \tag{5.6}$$

and the complementary sensitivity function [2]

$$T(s) \triangleq [I + L(s)]^{-1} L(s) \quad . \tag{5.7}$$

Note the transfer functions, (5.5)-(5.7), are obtained by breaking the loop at the output of the plant (denoted by (xx) in Figure 5.1). Breaking the loop at the plant input yields a generally different set of transfer functions due to noncommutativity of matrix multiplication. These transfer functions are obtained by reversing the order of P(s) and F(s) in (5.5)-(5.7). Implications of this lack of commutativity will be discussed shortly. For later reference, define

$$L_1(s) \triangleq F(s)P(s) \tag{5.8}$$

$$S_1(s) \triangleq [I + L_1(s)]^{-1} \quad . \tag{5.9}$$

$$T_1(s) \triangleq [I + L_1(s)]^{-1} L_1(s) \quad . \tag{5.10}$$

Assume that L(s) and $L_1(s)$ are free of unstable hidden modes. Then the feedback system is <u>stable</u> if S(s) (equivalently $S_1(s)$) is bounded in the closed right half plane. Note the assumption on L(s) and $L_1(s)$ implies, as in the SISO case, that right half plane poles and zeros of the plant and

compensator must appear with at least the same multiplicity in L(s) and $L_1(s)$. In addition, this assumption imposes conditions on the left and right null spaces of L(s) and $L_1(s)$ evaluated at right half plane plant and compensator zeros. A similar condition holds for open right half plane poles.

One difference from SISO systems is that vector and matrix norms must be used to measure the magnitudes of signals and transfer functions. In this thesis attention will be restricted to the standard Euclidean vector norm and the induced matrix two-norm. This matrix norm is also referred to as the singular value norm; a discussion of relevant properties of singular values is contained in Appendix B.

From (5.3) and (5.6) it follows that the response of the system to disturbance inputs is determined by the sensitivity function with the loop broken at the plant output. Since

$$\bar{\sigma}[S(j\omega)] = \max_{\substack{u \in \mathbb{C}^n \\ \|u\|_2 = 1}} \|S(j\omega)u\|_2 \quad , \tag{5.11}$$

it follows that the response of the system to disturbances at frequency ω can be made small by requiring that $\bar{\sigma}[S(j\omega)] << 1$. Note (5.11) implies that the response to a disturbance will be small independently of the subspace of $\mathbb{C}^n$ in which it lies. Similarly, the response of the system sensor noise is determined by T(s), and can be made small by requiring $\bar{\sigma}[T(j\omega)] << 1$.

The benefits of feedback in reducing the effects of uncertainty in the plant model upon the system output can be assessed from [3]

$$E_c(s) = S'(s)E_o(s) \tag{5.12}$$

$$S'(s) \triangleq [I + P'(s)F(s)]^{-1} \tag{5.13}$$

where $P'(s) \triangleq [I + \Delta(s)]P(s)$ is the true plant. The signals $E_c(s)$ and $E_o(s)$ are the deviations in the outputs of nominally equivalent open and closed loop systems caused by the model error $\Delta(s)$. If at some frequency

$$\bar{\sigma}[S'(j\omega)] < 1 \quad , \tag{5.14}$$

then the closed loop system is said to possess the sensitivity reduction property at that frequency. Condition (5.14) is difficult to design for since it depends on the true unknown plant rather than the model. Nonetheless, at frequencies for which $\bar{\sigma}[\Delta(j\omega)] < 1$ it is possible [4] to insure that (5.14) holds by requiring the nominal sensitivity function to have small magnitude. (Although this approach may fail dramatically [10] when the uncertainty cannot be assumed arbitrarily small, or when uncertainty is present which cannot be modelled as above.)

The sensitivity and complementary sensitivity functions are also related to stability robustness properties of the system (see, e.g. [5], Table 1). Suppose that uncertainty is modelled as occurring at the output of the plant:

$$P'(s) = [I + \Delta_o(s)]P(s) \quad . \tag{5.15}$$

Assume that

(i) $P'(s)$ and $P(s)$ have the same number of unstable poles and

(ii) $\Delta_o(s)$ is otherwise arbitrary subject to a frequency dependent norm bound

$$\bar{\sigma}[\Delta_o(j\omega)] \leq M_\Delta(\omega) \qquad \forall\omega \quad . \tag{5.16}$$

Then if the nominal system ($\Delta_o(s) \equiv 0$) is stable, the true system is guaranteed to be stable if [4]

$$M_\Delta(\omega) < \frac{1}{\bar{\sigma}[T(j\omega)]} \qquad \forall\omega \quad . \tag{5.17}$$

This bound requires that $\bar{\sigma}[T(j\omega)]$ be small at frequencies for which uncertainty modelled in (5.15), is large.

An important difference between SISO and MIMO systems is the fact that stability margins in the latter are generally different at different points in the feedback loop. Mathematically this occurs because matrix multiplication is not in general commutative, as was pointed out in the above discussion of transfer functions obtained by breaking the loop at different points (Eqs. (5.5)-(5.7) compared to (Eqs. (5.8)-(5.10)). To illustrate, suppose that uncertainty is modelled as occurring at the plant input

$$P'(s) = P(s)[I + \Delta\ (s)] \tag{5.18}$$

rather than at the plant output as in (5.15). Under assumptions analogous to (i) and (ii), if the nominal system is stable, the true system is guaranteed to be stable if [4]

$$M_\Delta(\omega) \leq \frac{1}{\bar{\sigma}[T_1(j\omega)]} \qquad \forall\omega \tag{5.19}$$

where $T_1(s)$ is given by (5.10). Thus, MIMO systems can have small stability margins in one loop location despite having good margins elsewhere. Moreover, when uncertainty is present at both the input and the output to the plant, the system can be close to instability despite good margins against uncertainty occurring at each point separately. Such phenomena are examples of MIMO system behavior which has no analogue in SISO systems. Examples are found in [10]. A framework for analyzing robustness against uncertainty occurring in different loop locations has been developed by Doyle [30] and Doyle, Wall and Stein [5].

5.3. Special Cases in which SISO Concepts Generalize to MIMO Systems

The above discussion has shown that the first concept from SISO theory discussed in Chapter 2 generalizes readily to MIMO systems. Closed loop properties can be determined by examining certain closed loop transfer function matrices. This point of view is stressed in [4,11-14].

Differences are that more matrices must be considered, including some nonstandard ones [5,30] when uncertainty is present at more than one location in the loop. Attention in this thesis will be restricted to uncertainty modelled as occurring at only one location in the loop so that matrices such as (5.6)-(5.7) or (5.9)-(5.10) suffice to determine feedback properties.

The second theme from SISO feedback theory is that the relation between open and closed loop system properties can be approximated fairly well. Under certain conditions this relation extends to MIMO systems. First some terminology will be introduced.

From the definition of singular values of a matrix $M \in \mathbb{C}^{n \times n}$

$$\bar{\sigma}[M] = \max_{\substack{u \in \mathbb{C}^n \\ \|u\|_2 = 1}} \|Mu\|_2 \tag{5.20}$$

and

$$\underline{\sigma}[M] = \min_{\substack{u \in \mathbb{C}^n \\ \|u\|_2 = 1}} \|Mu\|_2 \quad . \tag{5.21}$$

Equations (5.20) and (5.21) motivate the following terminology. When M is a transfer function matrix, $M = M(s)$, evaluated at some frequency ω, then the gain of the underlying system is said to be large in all directions at that frequency, provided that $\underline{\sigma}[M(j\omega)]>>1$. Similarly, the gain is said to be small in all directions, provided that $\bar{\sigma}[M(j\omega)]<<1$. If at some frequency $\underline{\sigma}[M(j\omega)]<<1<<\bar{\sigma}[M(j\omega)]$, then the system has both large and small gain (in different directions) at that frequency. Use of singular values to generalize the notion of gain has been discussed by several authors; an early reference is MacFarlane and Scott-Jones [31].

From (5.6) and (5.7) the following relations between levels of open loop gain and closed loop properties can be deduced:

$$\underline{\sigma}[L(j\omega)]>>1 \iff \begin{matrix} \bar{\sigma}[S(j\omega)]<<1 \\ \text{and} \\ T(j\omega) \approx I \end{matrix} \tag{5.22}$$

and

$$\bar{\sigma}[L(j\omega)]<<1 \iff \begin{matrix} \bar{\sigma}[T(j\omega)]<<1 \\ \text{and} \\ S(j\omega) \approx I \end{matrix} \quad . \tag{5.23}$$

Thus, at frequencies for which open loop gain is either large in all directions or small in all directions, the SISO rules of thumb (2.19) and (2.20) for relating open to closed loop properties generalize directly. When neither of these assumptions on the gain of $L(j\omega)$ hold, then previous results only suffice to relate open to closed loop properties in special cases, e.g., diagonal systems.

Another important concept from classical feedback theory was the existence of tradeoffs among various design goals. These tradeoffs are also present in MIMO systems although their exact nature is much more complicated. Known generalizations of <u>analytic</u> tradeoffs among system properties in <u>different</u> frequency ranges will be described first.

Tradeoffs imposed by open right half plane poles and zeros upon the sensitivity and complementary sensitivity functions were described briefly in Chapter 3. An advantage of these results was that they showed that open right half plane poles and zeros affect feedback properties only in certain directions. A generalization (due to Doug Looze) of Bode's integral theorem (Theorems 2.1 and 3.3) is now given.

<u>Theorem 5.1</u>: Assume that the open loop transfer function matrix $L(s)$ possesses finitely many open right half plane poles $\{p_i \,;\, i=1,\dots,N_p\}$ including multiplicities. In addition, assume that each element $L_{ij}(s); i,j=1,\dots,n$ satisfies

$$\lim_{R\to\infty} \sup_{\substack{|s|\geq R \\ \mathrm{Re}[s]\geq 0}} R|L_{ij}(s)| = 0 \qquad (5.24)$$

Then, if the closed loop system is stable, the determinant of the sensitivity function must satisfy

$$\pi \sum_{i=1}^{M_p} \mathrm{Re}[p_i] = \int_0^\infty \log|\det[S(j\omega)]|d\omega \quad . \tag{5.25}$$

■

<u>Proof</u>: See Appendix C. ■

<u>Corollary 5.2</u>: Assume the hypothesis of Theorem 5.1 is satisfied. Then, the singular values of the sensitivity function must satisfy

$$\pi \sum_{i=1}^{N_p} \mathrm{Re}[p_i] = \sum_{i=1}^{n} \int_0^\infty \log\sigma_i[S(j\omega)]d\omega = 0 \quad . \tag{5.26}$$

■

<u>Proof</u>: See Appendix C. ■

Corollary 5.2 shows that a tradeoff between sensitivity reduction and sensitivity increase exists for MIMO systems as well as SISO systems. The difference is that the tradeoff is averaged over all singular values of $S(j\omega)$. Presumably sensitivity properties could be traded off among different directions as well as among different frequency ranges, although no insight is given into how this might be achieved. Note, however, that if

$$\sigma_i[S(j\omega)] = \sigma_j[S(j\omega)] \ \forall i \neq j \text{ and } \forall \omega \quad , \tag{5.27}$$

then the tradeoff for open loop stable systems is exactly the same as in the SISO case. For open loop unstable systems the additional penalty due to the right half plane poles of $L(s)$ can apparently be averaged over all loops of the system or can be concentrated more or less in some loops. Again, no insight into how to achieve this is available.

In summary, Corollary 5.2 indicates that tradeoffs analogous to those found in SISO systems are present, but that they can be made between different directions as well as between frequency ranges. When the behavior of the feedback system is assumed to be the same in all directions, (i.e., (5.27) holds) the tradeoffs reduce to those found in SISO systems, with the exception noted when the system is open loop unstable. As pointed out, little is known about the general case.

The Bode gain-phase relations (Theorem 2.2) have also been studied in the context of MIMO systems (Doyle and Stein [4]), although again the results are primarily useful for systems which have nearly identical properties in all directions. Doyle's results utilize the fact that eigenvalues and singular values satisfy the inequality

$$\underline{\sigma}[M] \leq |\lambda_i[M]| \leq \bar{\sigma}[M] \ , \ \forall i \qquad . \tag{5.28}$$

Thus, if one can show that $|\lambda_i[S(j\omega)]|>>1$ for some i, then it follows that $\bar{\sigma}[S(j\omega)]>>1$. Since

$$\lambda_i[S(j\omega)] = \frac{1}{1+\lambda_i[L(j\omega)]} \tag{5.29}$$

one can study the relation between gain and phase of the eigenvalues of $L(j\omega)$ near crossover to see if tradeoffs such as those imposed by the SISO gain-phase relations are present.

A complete analysis is given in [4, pp. 9-10]; the conclusion is that the relation between $\dfrac{d \log|\lambda_i(j\omega)|}{d\nu}$ and $\measuredangle\lambda_i(j\omega)$ is the same as for a SISO transfer function if $\lambda_i(s)$ has no right half plane branch points.

If $\lambda_i(s)$ has branch points, then the relation holds averaged over all the eigenvalues defined on the same Riemann surface. These relations are most informative about feedback properties in the special case that $\bar{\sigma}[L(j\omega)] = |\lambda_i[L(j\omega)]| = \underline{\sigma}[L(j\omega)]$ in the vicinity of crossover. If this condition holds, then the tradeoff is the same as that for SISO systems. When there exist different levels of gain in different directions, then generally

$$\bar{\sigma}[L(j\omega)] > |\lambda_i[L(j\omega)]| > \underline{\sigma}[L(j\omega)] \quad \forall i \tag{5.30}$$

and the eigenvalue magnitudes need not even closely approximate the singular values. Thus, the gain in some loops could decrease rapidly near crossover with no corresponding rapid decrease in the $|\lambda_i[L(j\omega)]|$. No insight into this situation is provided, however.

The other class of tradeoffs found in SISO systems was <u>algebraic</u>. Those tradeoffs exist between system properties at any given frequency and follow from an identity which generalizes to MIMO systems as

$$S(s) + T(s) \equiv I \quad . \tag{5.31}$$

The algebraic tradeoffs discussed in Chapter 2 extend to MIMO systems in the following manner. If good sensitivity reduction and disturbance rejection properties are present <u>in all directions</u> at a given frequency ($\bar{\sigma}[S(j\omega)] \ll 1$), then from (5.31), good sensor noise rejection and large stability margins cannot be present <u>in any direction</u> ($T(s) \approx I$). A similar statement holds if $\bar{\sigma}[T(j\omega)] \ll 1$.

In summary, the relation between open and closed loop system properties, and the analysis of tradeoffs among system properties extends readily to MIMO systems only when these properties are constrained to be approximately the same in all directions. These cases may be viewed merely as special instances for which no uniquely MIMO system properties are present. The usefulness of these results will be limited to cases for which

(i) the plant has approximately equal bandwidth in all directions or loops,

(ii) only <u>unstructured</u> uncertainty, sensor noise, and disturbance inputs are present; that is, the magnitudes of these quantities are approximately the same in all directions.

Condition (i) will hold whenever $\bar{\sigma}[P(j\omega)] = \underline{\sigma}[P(j\omega)]\ \forall\omega$. Now, recall that the classical design methods focussed on modifying open loop properties via a suitable choice of compensation to achieve the desired closed loop properties. Obviously, this process is expedited if insight into the relation between open and closed loop properties is available. If Condition (i) fails, in particular, if the open loop plant has both large and small gain in some frequency range, then design will be complicated by lack of necessary insight.

Condition (ii) holds for uncertainty, as modelled in (5.16). This condition will also hold for disturbance inputs and sensor noise which are arbitrary, subject only to frequency dependent norm bounds:

$$\|d(j\omega)\|_2 \leq M_d(\omega) \qquad \forall\omega \tag{5.32}$$

and

$$\|n(j\omega)\|_2 \leq M_n(\omega) \qquad \forall\omega \quad . \tag{5.33}$$

If Condition (ii) fails to hold, then one is led to consider design goals on S(s) and T(s) which specify different properties in different loops. To see this, some simple models for structured uncertainty, sensor noise, and disturbance inputs are considered in the next section.

5.4. Structure in MIMO Systems and Failure of SISO Generalizations

In MIMO systems it is reasonable to expect that levels of disturbance inputs and/or sensor noise may be significantly different in different directions over the same frequency range. To illustrate, suppose that sensors in some loops are noisy at a lower frequency than sensors in other loops, while the level of disturbance inputs is approximately the same in all loops at any given frequency. This situation can be modelled mathematically by assuming the sensor noise can be separated into two components:

$$n(s) = n_s(s) + n_u(s) \quad . \tag{5.34}$$

The component $n_s(s)$ lies in a k-dimensional subspace $\mathcal{N}_s$ of $\mathbb{C}^n$ and represents structured sensor noise. The component $n_u(s)$ represents an additional unstructured component, and is assumed to lie in $\mathbb{C}^n$. Suppose that the levels of the two components of sensor noise and the level of disturbance inputs are bounded as

$$\|n_s(j\omega)\|_2 \leq M_s(\omega) \qquad \forall\omega \tag{5.35}$$

$$\|n_u(j\omega)\|_2 \leq M_u(\omega) \qquad \forall\omega \tag{5.36}$$

$$\|d(j\omega)\|_2 \leq M_d(\omega) \qquad \forall\omega \quad . \tag{5.37}$$

Next, suppose that the ratios of the bounds on the two components of sensor noise compared to the bound on the disturbance inputs is as shown in Figure 5.2. This figure indicates that the structured component of the sensor noise becomes relatively larger at a lower frequency than does the unstructured component. Thus, the following design specification on S(s) and T(s) is motivated. First, let $\mathbb{P}_s$ be an orthogonal projection [32] onto the subspace $\mathbb{N}_s$ of $\mathbb{C}^n$. Then, $\mathbb{P}_s^{\perp} = I - \mathbb{P}_s$ is an orthogonal projection onto $\mathbb{N}_s^{\perp}$, the orthogonal complement of $\mathbb{N}_s$. The design specification is thus:

$$\bar{\sigma}[S(j\omega)] \ll 1 \qquad \omega \leq \omega_1 \tag{5.38a}$$

$$\bar{\sigma}[T(j\omega)\mathbb{P}_s] \ll 1 \qquad \omega_2 \leq \omega \leq \omega_3 \tag{5.38b}$$

$$\bar{\sigma}[S(j\omega)\mathbb{P}_s^{\perp}] \ll 1 \qquad \omega_1 \leq \omega \leq \omega_3 \tag{5.38c}$$

$$\bar{\sigma}[T(j\omega)] \ll 1 \qquad \omega_4 \leq \omega \quad . \tag{5.38d}$$

This specification provides for disturbance rejection in all directions in the low frequency range $[0,\omega_1]$ for which disturbances dominate the sensor noise in all directions. At frequencies greater than ω_2 sensor noise in the subspace $\mathbb{N}_s$ should be rejected, since the level of sensor noise dominates the level of disturbance inputs at these frequencies. On the other hand, disturbances in the subspace $\mathbb{N}_s^{\perp}$ should be rejected at frequencies less than ω_3. This follows since the level of disturbances in this subspace still dominates sensor noise levels at these frequencies. Finally, at frequencies greater than ω_4, sensor noise should be rejected in all directions.

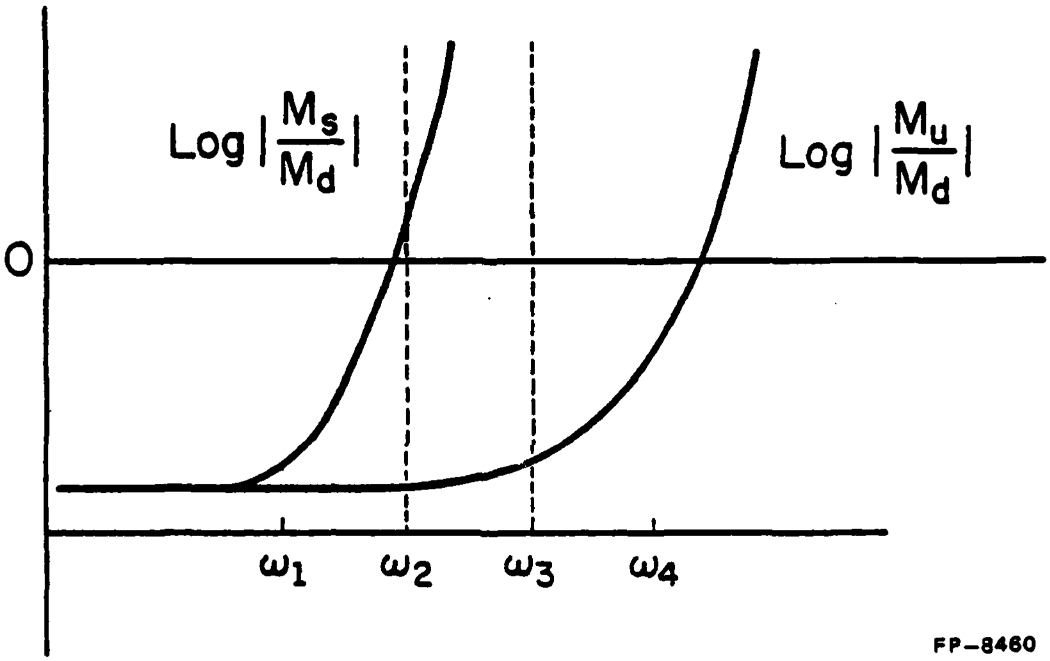

Figure 5.2. Relative levels of sensor noise to disturbance inputs.

Thus in this example the physical nature of the extraneous inputs dictated the design of a system with significantly different properties in different directions over the frequency range $[\omega_2,\omega_3]$.

Design specifications such as that just discussed can also arise when structured uncertainty is present. To see this, consider uncertainty modelled as occurring at the plant output as in (5.15) with $\Delta_o(s) \in \mathbb{C}^{n\times n}$ given by

$$\Delta_o(s) = \alpha(s)\, YX^H + \Delta_r(s) \quad . \tag{5.39}$$

Here, YX^H is a constant matrix of rank k whose k nonzero singular values are equal to one, $\alpha(s)$ is a scalar transfer function satisfying

$$|\alpha(j\omega)| \leq M_\alpha(\omega) \qquad \forall\omega \tag{5.40}$$

and $\Delta_r(s)$ represents residual unstructured uncertainty with

$$\bar{\sigma}[\Delta_r(j\omega)] \leq M_r(\omega) \qquad \forall\omega \quad . \tag{5.41}$$

The first term in (5.39) represents structured uncertainty which becomes large at lower frequencies than the remaining unstructured component. For example, since the uncertainty is modelled as occurring at the plant output, this might represent unmodelled sensor dynamics in the ith loop (in which case $YX^H = \mathrm{diag}[0,\ldots 0,1,0,\ldots 0]$ with the one in the ith position). A similar model using uncertainty occurring at the plant input, as in (5.18), could be used to represent unmodelled actuator dynamics.

The proof of the stability robustness theorem in [4, p. 7] can be followed to show that stability is guaranteed, provided that

$$\bar{\sigma}[\Delta_0(j\omega)T(j\omega)]<1 \qquad \forall\omega \quad . \tag{5.42}$$

At frequencies for which $\Delta_0(j\omega) \approx \alpha(j\omega)YX^H$, it follows that

$$M_\alpha(\omega) < \frac{1}{\bar{\sigma}[YX^H\ T(j\omega)]} \tag{5.43}$$

must hold. Suppose that $M_\alpha(\omega) >> 1$, and let $\mathbb{P}_X$ be an orthogonal projection onto $\mathbb{N}_X$, the column space of X^H. It follows that (5.43) implies

$$\bar{\sigma}[\mathbb{P}_X\ T(j\omega)] << 1 \quad . \tag{5.44}$$

Thus, $T(j\omega)$ must be small, but only in a k-dimensional subspace of $\mathbb{C}^n$. Specifically, the range of $T(j\omega)$ must be restricted to the subspace $\mathbb{N}_X^\perp$, the null space of the structured uncertainty.

From (5.31) it follows that (5.44) implies

$$\mathbb{P}_X S(j\omega) \approx \mathbb{P}_X \quad . \tag{5.45}$$

Thus, $S(j\omega)$ is approximately the identity on a k-dimensional subspace of $\mathbb{C}^n$. Although the subspace containing disturbances which cannot be rejected is not specified, the response to these disturbances is constrained to lie in the subspace $\mathbb{N}_X$. As in the discussion of structured sensor noise, $S(j\omega)$ can still reject disturbances lying in an $(n-k)$-dimensional subspace.

5.5. Summary

The above discussion has pointed out that there exist many cases of interest for which the closed loop system has significantly different properties in different directions over some frequency range. It was also pointed out that several important classical concepts have not been extended to MIMO systems which possess such properties. One such concept is an understanding of the relation between open and closed loop system properties. Such understanding is necessary to shape the open loop transfer function via the choice of feedback compensator. Another such concept is the statement of various tradeoffs among system properties in different frequency ranges. Precise statements of these tradeoffs are necessary to assess whether a given design specification is achievable by a linear time-invariant design. Both these questions will be addressed, although not solved completely, in the remainder of this thesis. First, the role of phase in MIMO systems will be discussed.

CHAPTER 6

GAIN, PHASE, AND DIRECTIONS IN MIMO SYSTEMS (PHYSICAL INTERPRETATIONS)

6.1. Introduction

The purpose of this chapter is to discuss generalizations of the classical SISO system concepts of gain and phase to MIMO systems. In addition, the concept of direction of a vector signal will be discussed. Directionality has, of course, no analogue in SISO system theory.

First, the physical meaning of a transfer function is discussed as it relates to the steady-state response of a linear time-invariant system to sinusoidal inputs. Next, the meaning of the direction of a vector signal is discussed, along with a measure of distance between signals lying in different directions. The concept of the gain of an SISO transfer function is discussed, along with the generalization to MIMO systems. Although the use of the singular value decomposition (SVD) to exhibit a canonical set of gains is well-known (see, e.g., [4],[31]) this idea is reviewed for completeness.

Generalization of the concept of phase to MIMO systems has not been as straightforward. On the one hand, the importance of the phase concept has been called into question. In particular, it has been shown (e.g., [1] and the discussion in Section 2.1) that the concept of phase margin is not of primary importance even in the single loop case. On the other hand, several different definitions of phase have been proposed by MacFarlane and co-workers ([14],[33]). Given these observations, perhaps the most accurate assessment is that a generally accepted concept of phase in multiple loop systems is not yet available. Rather than attempt such a definition, in this chapter, some physical interpretations of phase in single loop system are first

explored. Multiple loop systems are then examined to see if similar interpretations are available in the general case. The approach which will be taken is based upon the way in which vector-valued sinusoidal signals interact when added together. Portions of this chapter will appear in [34].

6.2. Properties of Transfer Functions

The response of a linear time invariant system to an input is a function of both the input and the initial conditions. If these initial conditions are equal to zero, then the response may be calculated from the transfer function of the system. Let this transfer function be denoted by $L(s) \in \mathbb{C}^{n\times n}$ and consider inputs of the form

$$u(t) = ke^{s_o t} \tag{6.1}$$

where $k \in \mathbb{C}^n$ is a constant vector and $s_o = x_o + jy_o$ is the complex frequency of the input. Entries of k can, of course, be complex; note, however, that (6.1) can be rewritten

$$u(t) = \begin{bmatrix} r_1 e^{s_o t + \phi_1} \\ r_2 e^{s_o t + \phi_2} \\ \vdots \\ r_n e^{s_o t + \phi_n} \end{bmatrix} \tag{6.2}$$

where each $r_i \geq 0$ and different values of ϕ_i imply phase differences between the components of the sinusoidal signal.

The Laplace transform of $u(t)$ is given by

$$u(s) = k \frac{1}{s-s_o} \quad . \tag{6.3}$$

The frequency response of the system, given the input $u(s)$, is

$$y(s) = L(s)u(s) \quad . \tag{6.4}$$

The corresponding time response will, in general, have contributions from the poles of $L(s)$ as well as the pole $s = s_o$ of the input. For stable systems the former contributions go to zero in the steady state and the time response is given by

$$y(t) = L(s_o)u(t) \quad . \tag{6.5}$$

In fact it can be shown [35] that the input $u(t)$ can be augmented with a set of delta functions and derivatives of delta functions so that the steady state is reached at $t = 0^+$. Thus, (6.5) illustrates the manner in which properties of transfer functions are related to the time responses of the system to complex exponential inputs.

6.3. Directions of Vector Signals

From (6.4) and (6.5) one can see that the action of a transfer function matrix upon an input (6.1) is solely a function of the (one-dimensional) subspace of $\mathbb{C}^n$ spanned by k. That is, choosing an input $\hat{u}(t) = c\, u(t)$, with c a complex scalar, yields an output $\hat{y}(t) = c\, y(t)$. Since linear systems are being studied, this is an obvious remark; however, this is the first manifestation of an idea which will recur throughout the remainder of this thesis. Namely, given a one-dimensional subspace of $\mathbb{C}^n$

there exist <u>two</u> degrees of freedom in specifying a vector within that subspace. One degree of freedom corresponds to the magnitude of the vector; the other is analogous to phase. Many system properties of interest depend only on the subspace in which a signal lies. For now, discussion will be limited to making precise the notion of the direction of a vector signal.

The set of <u>directions</u> in $\mathbb{C}^n$ will be defined as the set of one-dimensional subspaces of $\mathbb{C}^n$. The following notation is convenient: Given a nonzero vector in $\mathbb{C}^n$ denoted by a small letter, e.g., k, then the one-dimensional subspace of $\mathbb{C}^n$ spanned by this vector will be denoted by a capital script letter, e.g., $\mathcal{K}$. (This convention will later be extended to subspaces of dimension greater than one.) Thus, the direction of a signal is given by the one-dimensional subspace of $\mathbb{C}^n$ which it spans.

A method of measuring the distance between directions, or one-dimensional subspaces of $\mathbb{C}^n$, will be needed. It is standard [36] to define the angle ϕ between two one-dimensional subspaces $\mathcal{C}_1$ and $\mathcal{C}_2$ of $\mathbb{C}^n$ from

$$\cos\phi = \frac{|c_2^H c_1|}{\|c_1\|_2 \|c_2\|_2} \tag{6.6}$$

where c_i is an arbitrary nonzero vector in $\mathcal{C}_i$. Note that $0 \leq \phi \leq \frac{\pi}{2}$. Thus ϕ is a measure of angular distance between the subspaces $\mathcal{C}_1$ and $\mathcal{C}_2$. For $\phi = 0$, the two subspaces are identical; for $\phi = \pi/2$, the two subspaces are orthogonal. The concept of angles between subspaces of $\mathbb{C}^n$ can also be extended to subspaces of dimension greater than one [36].

6.4. Gain in SISO and MIMO Systems

For SISO systems the gain is a frequency-dependent function which gives the ratio of the magnitude of the system output to that of the input. Thus, for scalar inputs of the form (6.1):

$$\begin{aligned} \text{gain} &= \frac{|y(t)|}{|u(t)|} \\ &= \frac{|L(s_o)u(t)|}{|u(t)|} \\ &= |L(s_o)| \quad . \end{aligned} \tag{6.7}$$

For MIMO systems, gain is a function of the direction of the input as well as the frequency. Thus, for a vector input of the form (6.1):

$$\begin{aligned} \text{gain} &= \frac{\|y(t)\|}{\|u(t)\|} \\ &= \frac{\|L(s_o)k\|}{\|k\|} \end{aligned} \tag{6.8}$$

where the standard Euclidean vector norm is used. In view of the directional dependence of the gain it is only natural to ask which directions yield the largest and smallest values of gain. This question is answered using the singular value decomposition (SVD) [37-39]. This canonical form of a matrix is given by (dropping the functional dependence on s_o):

$$L = V\Sigma U^H \quad . \tag{6.9}$$

A complete discussion of the SVD is contained in Appendix B. A summary is given here for the case in which the singular values are distinct. The singular values of L are given by the nonnegative square roots of the eigenvalues of L^HL. It is assumed here that $L(s_o) \in \mathbb{C}^{n\times n}$: thus, these eigenvalues are identical to those of LL^H. (The symbol L^H is read "L-Hermitian" and is

the complex conjugate of the transpose of L.) The right singular vectors of L are the columns of U and are the eigenvectors of $L^H L$. The left singular vectors of L are the columns of V and are the eigenvectors of LL^H. Assuming that the singular values are distinct, the right singular vectors are unique up to multiplication by a unit magnitude constant $e^{j\alpha}$. The left singular vectors are then uniquely determined from the relation

$$Lu_i = \sigma_i v_i \quad . \tag{6.10}$$

Note that choosing a different right singular vector

$$\hat{u}_i = e^{j\alpha} u_i \tag{6.11}$$

implies that the new left singular vector is given by

$$\hat{v}_i = e^{j\alpha} v_i \quad . \tag{6.12}$$

It is common to order the singular values so that

$$\sigma_1 \geq \sigma_2 \geq \cdots \geq \sigma_n \geq 0 \tag{6.13}$$

and to define

$$\bar{\sigma} \triangleq \sigma_1 \quad , \quad \underline{\sigma} \triangleq \sigma_n \quad . \tag{6.14}$$

The singular values and vectors have many useful properties which they inherit from properties of the eigenvalues and eigenvectors of Hermitian matrices. For example, the matrices U and V are unitary: $UU^H = I$, $VV^H = I$. Thus, the sets of right and left singular vectors form an orthonormal basis for $\mathbb{C}^n$. The singular values possess the following min-max property [37-39]:

$$\sigma_i = \min_{\mathcal{S}_i} \max_{\substack{u \in \mathcal{S}_i \\ u \neq 0}} \frac{\|Lu\|_2}{\|u\|_2} \qquad \dim \mathcal{S}_i = n-i+1 \quad . \tag{6.15}$$

The minimum in (6.15) is taken over all subspaces of $\mathbb{C}^n$ of the appropriate dimension while the maximum is taken over all nonzero vectors within the given subspace. Thus, in particular,

$$\bar{\sigma}[L] = \max_{\substack{u \in \mathbb{C}^n \\ u \neq 0}} \frac{\|Lu\|_2}{\|u\|_2} = \|L\|_2 \tag{6.16}$$

and

$$\underline{\sigma}[L] = \min_{\substack{u \in \mathbb{C}^n \\ u \neq 0}} \frac{\|Lu\|_2}{\|u\|_2} \quad . \tag{6.17}$$

If $\det L \neq 0$, then

$$\underline{\sigma}[L] = \frac{1}{\|L^{-1}\|_2} \quad . \tag{6.18}$$

Thus, at each frequency, the singular value decomposition gives the directions of the inputs to the system which are multiplied by a canonical set of gains, the values of those gains, and, via (6.10), the directions of the resulting outputs. Finally, the above discussion shows that letting L vary as a function of s causes the singular vectors to vary in accordance with the min-max principle (6.15).

6.5. Phase in SISO Systems

The value of a scalar transfer function is given at a specific frequency by its gain and phase. The concept of gain has been generalized to matrix transfer functions as described above; however, the concept of phase has presented more difficulty. In order to arrive at a useful notion of phase in an MIMO system it is instructive to examine the different ways in which the term phase is used in SISO systems and focus on those which are most relevant to feedback design. To do this, consider the way in which scalar signals interact when added together.

Suppose one is given two nonzero scalar exponential signals with the same complex frequency:

$$u_1(t) = c_1 e^{s_o t}$$

and (6.19)

$$u_2(t) = c_2 e^{s_o t} \quad .$$

The phase difference between these two signals may be uniquely defined (modulo 2π) as

$$\Delta\theta = \measuredangle\, \bar{c}_2\, c_1 \quad . \tag{6.20}$$

The importance of the phase difference is that it governs how the signals interfere when added together. This may be seen from

$$\begin{aligned} |u_1(t) + u_2(t)| &= e^{x_o t}\, |c_1 + c_2| \\ &= e^{x_o t} \sqrt{|c_1|^2 + |c_2|^2 + 2\mathrm{Re}\, \bar{c}_2 c_1} \\ &= e^{x_o t} \sqrt{|c_1|^2 + |c_2|^2 + 2|c_1||c_2| \cos \Delta\theta} \end{aligned} \tag{6.21}$$

For example, if the phase difference is $(2k + 1)\pi$, k an integer, then the signals interfere purely destructively and

$$|u_1(t) + u_2(t)| = e^{x_o t}\big||c_1| - |c_2|\big| \quad . \tag{6.22}$$

If the phase difference is $2k\pi$, then the signals interfere purely constructively and

$$|u_1(t) + u_2(t)| = e^{x_o t}[|c_1| + |c_2|] \quad . \tag{6.23}$$

If the phase difference is not an integer multiple of π, then the magnitude of the sum of the two signals is bounded below and above by (6.22) and (6.23). From (6.3), equations analogous to (6.21)-(6.23) also hold in the frequency domain; i.e.,

$$|u_1(s) + u_2(s)| = \left|\frac{1}{s-s_o}\right| \sqrt{|c_1|^2 + |c_2|^2 + 2|c_1||c_2| \cos \Delta\theta} \quad . \tag{6.24}$$

The importance of the relation between phase difference and signal interference in feedback systems should be obvious from the definition of e(s) in Figure 2.1.

Note that it is possible to compute the phase difference between $u_1(t)$ and $u_2(t)$ by first computing the phases of $u_1(t)$ and $u_2(t)$ individually and then subtracting. First, define

$$\theta_1 \triangleq \measuredangle u_1(t)\big|_{t=0} = \measuredangle c_1$$

and (6.25)

$$\theta_2 = \measuredangle u_2(t)\big|_{t=0} = \measuredangle c_2 \quad .$$

This definition leads to another way of representing the signals:

$$u_1(t) = |c_1|e^{s_o t+\theta_1}$$
$$u_2(t) = |c_2|e^{s_o t+\theta_2} \quad . \qquad (6.26)$$

Thus, the phase difference between two signals may be defined in two equivalent ways - either from (6.20) or from

$$\Delta\theta = \theta_2 - \theta_1 \quad . \qquad (6.27)$$

Note, in particular, that the phase difference between the two signals is invariant under rotations of the coordinate system in the complex plane used to measure the phases of the individual signals; the phases of the individual signals are not invariant, however.

6.6. Phase in MIMO Systems

For vector signals no standard definition of phase or phase difference exists. The possibility of such definitions is studied mathematically in Chapter 10. A reasonable approach based upon physical considerations seems to be to generalize the notion of phase difference by considering the way in which two vector signals interfere when added together. Thus, consider (6.19) with c_1 and $c_2 \in \mathbb{C}^n$. The analogue to (6.21) is (using Euclidean vector norms):

$$\|u_1(t) + u_2(t)\| = e^{x_o t}\sqrt{\|c_1\|^2 + \|c_2\|^2 + 2\mathrm{Re}\; c_2^H c_1} \quad . \qquad (6.28)$$

Equation (6.28) shows that the interference of $u_1(t)$ and $u_2(t)$ is governed by the term Re $c_2^H c_1$. Defining

$$\theta \triangleq \measuredangle\, c_2^H c_1 \tag{6.29}$$

and recalling the definition of the angle between one-dimensional subspaces of $\mathbb{C}^n$, (6.28) becomes

$$\|u_1(t) + u_2(t)\| = e^{x_o t} \sqrt{\|c_1\|^2 + \|c_2\|^2 + 2\|c_1\|\|c_2\| \cos\phi \cos\theta} \quad , \tag{6.30}$$

where ϕ is the angle between the subspaces spanned by u_1 and u_2. Comparing (6.3) with (6.21) reveals that the interference between two vector signals depends upon the angle ϕ. If the two subspaces are orthogonal ($\phi = \frac{\pi}{2}$), then

$$\|u_1(t) + u_2(t)\| = e^{x_o t} \sqrt{\|c_1\|^2 + \|c_2\|^2} \quad . \tag{6.31}$$

Thus, in this case the signals do not interfere at all. If $\phi < \pi/2$, then interference can occur; for purely constructive interference

$$\|u_1(t) + u_2(t)\| = \|u_1(t)\| + \|u_2(t)\| \tag{6.32}$$

and for purely destructive interference

$$\|u_1(t) + u_2(t)\| = \big|\|u_1(t)\| - \|u_2(t)\|\big| \tag{6.33}$$

it must be that the two signals lie in the same direction ($\phi = 0$). In addition, $\theta = 2k\pi$ is required for (6.32) and $\theta = (2k+1)\pi$ radians are required for (6.33). If $0 < \phi < \pi/2$, then interference takes place between one signal and that component of the other signal which lies in the same direction.

The preceding discussion suggests that a natural generalization of phase difference to vector signals is given by the angle θ which determines how the signals interfere. If the signals lie in orthogonal directions, then θ is undefined. This is only natural since signals in orthogonal directions cannot interfere.

Now that a definition of phase difference between two vector signals has been proposed, does there exist a definition of the phase of a vector signal? One way to attempt this would be to fix a vector $w \in \mathbb{C}^n$, e.g., one of the standard basis vectors, and then define the phase of a vector signal as (compare with (6.25))

$$\text{phase}[u(t)] \triangleq \measuredangle\, w^H u(t)\Big|_{t=0} \quad . \tag{6.34}$$

This definition could be used to define the phase of all vector signals in directions not orthogonal to that of w. Computing phase difference between two signals $u_1(t)$ and $u_2(t)$ using (6.34) would thus be identical to computing the phase difference between the components of $u_1(t)$ and $u_2(t)$ lying in the direction of w. By defining

$$\theta_1 \triangleq \measuredangle w^H u_1(t)\Big|_{t=0}$$

and (6.35)

$$\theta_2 \triangleq \measuredangle w^H u_2(t)\Big|_{t=0}$$

a measure of phase difference is given by

$$\tilde{\theta} \triangleq \theta_2 - \theta_1 \quad . \tag{6.36}$$

This definition will not, in general, yield the same value of phase difference as that given by (6.29) and, in addition, does not have as nice a physical interpretation. Nonetheless, this definition of phase difference will be useful in later chapters.

The natural definition of phase difference (6.29) will be found useful in studying properties of MIMO feedback systems. The relation between (6.29) and matrix transfer functions is now explained. From (6.5) it can be seen that the phase difference between an input (6.1) and the resulting output of the system whose transfer function is given by L(s) is given by

$$\begin{aligned}\theta(s_o) &= \measuredangle u^H(t)y(t) \\ &= \measuredangle u^H(t)L(s_o)u(t) \quad . \end{aligned} \tag{6.37}$$

The angle between the direction of the input and that of the resulting output is given by

$$\begin{aligned}\cos\phi(s_o) &= \frac{|u^H(t)y(t)|}{\|u(t)\| \; \|L(s_o)u(t)\|} \\ &= \frac{|u^H(t)L(s_o)u(t)|}{\|u(t)\| \; \|L(s_o)u(t)\|} \quad . \end{aligned} \tag{6.38}$$

Given an input of the form (6.1), with k a unit vector, the quantity

$$k^H \, L(s_o)k \equiv \|L(s_o)k\| \quad \cos\phi(s_o)e^{j\theta(s_o)}$$

thus relates the gain of the system in the direction K, the angle between the directions of the input and the resulting output, and the phase difference between the input and output.

Given a matrix $M \in \mathbb{C}^{n \times n}$ the set

$$\{u^H M u \; : \; \|u\|_2 = 1 \; , \; u \in \mathbb{C}^n\} \tag{6.39}$$

is defined to be the numerical range [40] of the matrix. This set has been identified as important in system theory. For example, a necessary condition for (strict) positive realness [41] of a transfer function matrix is that the numerical range of L(s), $Re[s] \geq 0$, be confined to the (open) right half plane. Thus, in order to be strict positive real, a transfer function matrix must have the property that $|\theta| < \frac{\pi}{2}$ and $\phi < \frac{\pi}{2}$ for all inputs and all s with $Re[s] \geq 0$.

In the next section two parameterizations of matrix transfer functions will be developed. These parameterizations will use angles and phase shifts as defined in this chapter.

CHAPTER 7

CHANGES OF BASIS AND PARAMETERIZATIONS OF MATRIX TRANSFER FUNCTIONS

7.1. Introduction

The purpose of this chapter is to introduce a change of basis in the spaces of inputs to and outputs from a system described by a transfer function matrix. As discussed in Section 7.2 this leads to transformed open and closed loop system matrices displaying information contained in the singular value decomposition (SVD) of the open loop transfer function. In particular the angles between singular subspaces and the phase differences between singular vectors, quantities introduced in Chapter 6, are displayed.

Using these parameters lower bounds on $\bar{\sigma}[S(j\omega)]$ are derived. Implications on the possible values of these parameters given that an upper bound on $\bar{\sigma}[S]$ is satisfied are discussed in Section 7.3. In Section 7.4 some useful parameterizations for transfer functions of two-input two-output systems are discussed.

7.2. A Change of Basis

Let the singular value decomposition of the open loop transfer function matrix, $L(s) \in \mathbb{C}^{n\times n}$, be given by (suppressing dependence on s):

$$L = V\Sigma U^H \tag{7.1}$$

with singular values

$$\Sigma = \mathrm{diag}[\sigma_1 \; \dots \; \sigma_n] \tag{7.2}$$

left singular vectors

$$V = [v_1 \mid \ldots \mid v_n] \tag{7.3}$$

and right singular vectors

$$U = [u_1 \mid \ldots \mid u_n] \quad . \tag{7.4}$$

In contrast to convention the singular values are not necessarily assumed to be numbered in decreasing order of magnitude. The singular values and vectors must still satisfy the equation,

$$Lu_i = \sigma_i v_i \quad , \tag{7.5}$$

however. Degrees of freedom available in selecting the singular vectors are discussed in Appendix B.

It will be convenient to write the spaces of inputs and outputs in the orthonormal basis for $\mathbb{C}^n$ furnished by the right singular vectors. (The left singular vectors could also be used for this, of course.) With this change of basis the matrix L is transformed into:

$$\tilde{L} = U^H V \Sigma \quad . \tag{7.6}$$

Note $$\tilde{L} = ULU^H \tag{7.7}$$

and $$\tilde{L} = U^H L U \quad . \tag{7.8}$$

The sensitivity and complementary sensitivity functions become

$$\begin{aligned} \tilde{S} &= [I + \tilde{L}]^{-1} \\ &= [I + U^H V \Sigma]^{-1} \end{aligned} \tag{7.9}$$

and

$$\begin{aligned}\tilde{T} &= [I + \tilde{L}]^{-1} \tilde{L} \\ &= [I + U^H V\Sigma]^{-1} U^H V\Sigma\end{aligned} \tag{7.10}$$

and are related to S and T via

$$S = U\tilde{S}U^H \tag{7.11}$$

and

$$T = U\tilde{T}U^H \quad . \tag{7.12}$$

The transformation from L, S and T to $\tilde{L}$, $\tilde{S}$ and $\tilde{T}$ just presented is both a similarity transformation, preserving the eigenvalues of the matrices involved, and a unitary transformation, preserving the singular values. The former fact implies that absolute stability properties of the closed loop system are preserved since these can be assessed from the determinant [42] or the eigenvalues [43] of S(s) and T(s). The latter fact implies that information about closed loop system properties, such as stability margins and disturbance response, is preserved.

Writing L in terms of the individual singular values and vectors (7.2)-(7.4) yields

$$\begin{aligned}\tilde{L} &= U^H V\Sigma \\ &= \begin{bmatrix} u_1^H v_1 \sigma_1 & u_1^H v_2 \sigma_2 & \cdots & u_1^H v_n \sigma_n \\ u_2^H v_1 \sigma_1 & u_2^H v_2 \sigma_2 & & \vdots \\ \vdots & & & \vdots \\ u_n^H v_1 \sigma_1 & \cdots & & u_n^H v_n \sigma_n \end{bmatrix} \quad .\end{aligned} \tag{7.13}$$

This expression is appealing in that it displays the angles between singular subspaces given by

$$\cos \phi_i \triangleq |u_i^H v_i| \tag{7.14}$$

and the phase difference between left and right singular vectors defined by

$$\theta_i \triangleq \measuredangle u_i^H v_i \quad . \tag{7.15}$$

(Physical interpretations of ϕ_i and θ_i are presented in Chapter 6.) Note that if the singular values are distinct, then all the ϕ_i are uniquely determined and $0 \leq \phi_i \leq \pi/2$. If $\phi_i \neq \pi/2$ then the θ_i are defined and uniquely determined (modulo 2π). If there exist singular values with multiplicity greater than one, then the directions of the corresponding singular vectors are no longer uniquely defined. Given a choice of right singular vectors, however, the left singular vectors are uniquely determined vis (7.5). Thus, it is possible to define ϕ_i and θ_i using this choice of singular vectors.

The transformations (7.6), (7.9) and (7.10) are useful in relating properties of the open loop singular values and subspaces to those of the closed loop system. This relation will be studied in detail in Chapter 8 for the case when there exist large gains in some directions and small gains in other directions over the same frequency range. A relation which holds for the general case is presented in Section 7.3.

7.3. A Lower Bound on Closed Loop Sensitivity

In this section, a lower bound on $\bar{\sigma}[S(j\omega)]$, the largest singular value of the system sensitivity function, is obtained in terms of the open loop singular values and the parameters ϕ_i and θ_i from (7.14) and (7.15). First, a more general relation is obtained using the numerical range of $L(j\omega)$ defined in Section 6.6.

From the definition of the sensitivity function (Chapter 5) and various properties of singular values, it follows that (again suppressing dependence on s):

$$\|S\|_2 = \bar{\sigma}[S]$$

$$= \bar{\sigma}[(I + L)^{-1}]$$

$$= \frac{1}{\underline{\sigma}[I + L]}$$

$$\|S\|_2 = \frac{1}{\min\limits_{\substack{w \in \mathbb{C}^n \\ \|w\|_2 = 1}} \|(I + L)w\|_2} \quad . \tag{7.16}$$

From (7.16) it follows that, given any unit vector $w \in \mathbb{C}^n$, a lower bound on the magnitude of the sensitivity matrix may be obtained from

$$\|S\|_2 \geq \frac{1}{\|(I + L)w\|_2} \quad . \tag{7.17}$$

The lower bound (7.17) can be written as

$$\|S\|_2 \geq \frac{1}{\sqrt{1 + \|Lw\|_2^2 + 2\mathrm{Re}[w^H Lw]}} \quad . \tag{7.18}$$

Now, recall $w^H Lw$ is an element of the numerical range of L (Section 6.6). Define

$$\rho = \|Lw\|_2 \tag{7.19a}$$

$$z = \frac{Lw}{\rho} \tag{7.19b}$$

$$\phi = \arccos |w^H z| \tag{7.19c}$$

$$\theta = \measuredangle w^H z \quad . \tag{7.19d}$$

Then, (7.18) becomes

$$\|S\|_2 \geq \frac{1}{\sqrt{1+\rho^2+2\rho\cos\phi\cos\theta}} \quad . \tag{7.20}$$

Now, if $\phi = 0$, i.e., if w is an eigenvector of L, it follows that $\rho e^{j\theta}$ is an eigenvalue of L and the relation between the gain ρ and phase difference θ is exactly as in the case of SISO systems. If $\phi > 0$, however, the relation is no longer as in the SISO case. Apparently, $\rho e^{j\theta} \approx -1$ can occur without necessarily causing $\bar{\sigma}[S]$ to become unbounded or even large, provided that ϕ is sufficiently large. Of course, inputs in directions other than those given by w could produce a large output from the sensitivity function. Nonetheless, (7.20) could be useful in showing that certain open loop system properties necessarily lead to poor feedback properties. Moreover, (7.20) can be used to study necessary properties of systems which satisfy bounds on $\bar{\sigma}[S]$, e.g., optimal linear quadratic-state feedback regulators designed under certain assumptions (see, e.g., [4, p. 13]).

Note that (7.17) can be evaluated for w, a right singular vector of L. In this case (7.20) becomes

$$\|S\|_2 \geq \frac{1}{\sqrt{1 + \sigma_i^2 + 2\sigma_i \cos\phi_i \cos\theta_i}} \quad . \tag{7.21}$$

This bound is useful in studying the relationship between the canonical set of open loop gains given by the singular values and feedback properties. For example, if $\|S\|_2 \leq 1$, then it follows that, for each i,

$$\sigma_i + 2\cos\phi_i \cos\theta_i > 0 \quad . \tag{7.22}$$

One possible application of this bound would be to study properties of linear quadratic-state feedback regulators, for which under certain assumptions (7.22) is guaranteed to hold. Analysis of (7.22) or an analogous bond obtained from the more general inequality (7.20) could lead to new interpretations of the guaranteed properties of these designs.

7.4. Parameterizations for Two-Input Two-Output Systems

In this section, two useful parameterizations of transfer function matrices for two-input two-output systems are described. Such parameterizations are undoubtedly also possible for larger systems. The emphasis in this thesis, however, will be to ascertain whether useful insights are obtained for simple cases. If useful results can be obtained for simple cases, then this will motivate further work on larger systems.

Suppose W is a unitary matrix in $\mathbb{C}^{2\times 2}$ and suppose further that the diagonal elements of W are nonzero. (It can easily be verified that $w_{11} = 0$, if and only if $w_{22} = 0$.) Then W can be parameterized as

$$W = \begin{bmatrix} \cos\phi\ e^{j\theta_1} & -\sin\phi\ e^{-j\psi} e^{j\theta_2} \\ \sin\phi\ e^{j\psi} e^{j\theta_1} & \cos\phi\ e^{j\theta_2} \end{bmatrix}, \tag{7.23}$$

where $\phi \in [0,\pi/2)$ and the θ_i and ψ can be chosen to lie in the interval $(-\pi,\pi]$. (Note these parameters are not the same as those of (7.14)-(7.15).) This parameterization may be used in the SVD (7.1):

$$\begin{aligned} L &= V\Sigma U^H \\ &= [v_1 \mid v_2] \begin{bmatrix} \sigma_1 & 0 \\ 0 & \sigma_2 \end{bmatrix} \begin{bmatrix} u_1^H \\ \hline u_2^H \end{bmatrix} \\ &= \begin{bmatrix} \cos\phi_v\ e^{j\theta_{v1}} & -\sin\phi_v\ e^{-j\psi_v}\ e^{j\theta_{v2}} \\ \sin\phi_v\ e^{j\psi_v}\ e^{j\theta_{v1}} & \cos\phi_v\ e^{j\theta_{v2}} \end{bmatrix} \begin{bmatrix} \sigma_1 & 0 \\ 0 & \sigma_2 \end{bmatrix} \\ &\quad \begin{bmatrix} \cos\phi_u\ e^{j\theta_{u1}} & -\sin\phi_u\ e^{-j\psi_u}\ e^{j\theta_{u2}} \\ \sin\phi_u\ e^{j\psi_u}\ e^{j\theta_{u1}} & \cos\phi_u\ e^{j\theta_{u2}} \end{bmatrix}^H . \end{aligned} \tag{7.24}$$

Note, that (7.24) contains 10 parameters; this is apparently too many since eight numbers suffice to specify a 2×2 complex matrix. Inspection reveals that the value of L depends only on the quantities

$$\tilde{\theta}_i \triangleq \theta_{vi} - \theta_{ui} \qquad i=1,2 \qquad . \tag{7.25}$$

Thus (7.24) can be written

$$L = V\Sigma U^H$$

$$= \begin{bmatrix} \cos\phi_v & -\sin\phi_v\, e^{-j\psi_v} \\ \sin\phi_v\, e^{j\psi_v} & \cos\phi_v \end{bmatrix} \begin{bmatrix} \sigma_1\, e^{j\tilde{\theta}_1} & 0 \\ 0 & \sigma_2\, e^{j\tilde{\theta}_2} \end{bmatrix} \begin{bmatrix} \cos\phi_u & -\sin\phi_u\, e^{-j\psi_u} \\ \sin\phi_u\, e^{j\psi_u} & \cos\phi_u \end{bmatrix}^H \quad . \tag{7.26}$$

From (6.35)-(6.36) it can be seen that $\tilde{\theta}_1$ is the difference in phase between the components of u_1 and v_1 lying in the direction of the standard basis vector $e_1 = \begin{bmatrix} 1 \\ 0 \end{bmatrix}$. Thus, $\tilde{\theta}_1$ does not measure how an input in the direction u_1 will interfere with the resulting output which is in the direction v_1. Rather $\tilde{\theta}_1$ determines how the indicated components of u_1 and v_1 interfere. Similar remarks can be made about the meaning of $\tilde{\theta}_2$ using the basis vector $e_2 = \begin{bmatrix} 0 \\ 1 \end{bmatrix}$.

The angles ϕ_u and ψ_u indicate how an input written in the standard basis is multiplied by the singular value gains. Similarly, the angles ϕ_v and ψ_v indicate how the resulting output is distributed between the standard basis directions. Thus, although the phases $\tilde{\theta}_i$ do not have as nice an interpretation as those given by $\measuredangle u_i^H v_i$, the corresponding parameterization

of the singular subspaces is useful for relating properties of the SVD to design goals stated in terms of the physical loops of the system.

Parameterizations can also be obtained for the matrix U^HV in (7.6), the expression for $\tilde{L}$. Thus, if $u_i^Hv_i \neq 0$, U^HV may be parameterized as

$$U^HV = \begin{bmatrix} u_1^Hv_1 & u_1^Hv_2 \\ u_2^Hv_1 & u_2^Hv_2 \end{bmatrix}$$

$$= \begin{bmatrix} \cos\phi\ e^{j\theta_1} & -\sin\phi\ e^{-j\psi}\ e^{j\theta_2} \\ \sin\phi\ e^{j\psi}\ e^{j\theta_1} & \cos\phi\ e^{j\theta_2} \end{bmatrix} , \qquad (7.27)$$

where $\cos\phi = |u_i^Hv_i|$ is the cosine of the angle between each set of left and right singular subspaces; $\phi \in [0,\pi/2)$. Since $\phi < \pi/2$, the phase differences $\theta_i = \measuredangle u_i^Hv_i$ are defined and may be chosen so that $\theta_i \in (-\pi,\pi]$. The quantity ψ is <u>not</u> well defined, however, due to a lack of uniqueness in the choice of singular vectors (Appendix B). Thus it may be assumed that $\psi \equiv 0$. To justify this, recall that if $\sigma_1 \neq \sigma_2$, there exist well-defined one-dimensional right singular subspaces $\mathfrak{U}_1$ and $\mathfrak{U}_2 \subseteq \mathbb{C}^2$. The right singular vectors may be chosen as any unit vectors within these subspaces; the left singular vectors are then completely determined from (7.5). Suppose that for a particular choice $u_1 \in \mathfrak{U}_1$ it so happens that $\psi \neq 0$; i.e., $\measuredangle u_2^Hv_1 \neq \theta_1$. Then choose $\hat{u}_1 = e^{-j\psi}u_1$ (which from (7.5) implies $\hat{v}_1 = e^{-j\psi}v_1$); it follows that $\measuredangle u_2^H\hat{v}_1 = \theta_1$ and $\psi = 0$.

Finally, (7.27) can be used in (7.6) to obtain

$$\tilde{L} = U^H V \Sigma$$

$$= \begin{bmatrix} \cos\phi & -\sin\phi \\ \sin\phi & \cos\phi \end{bmatrix} \begin{bmatrix} \sigma_1 e^{j\theta_1} & 0 \\ 0 & \sigma_2 e^{j\theta_2} \end{bmatrix} \quad . \tag{7.28}$$

This transformation of L displays useful information concerning how inputs to L in the direction of the right singular subspaces interfere with the resulting outputs when added together.

Although there are only five parameters displayed in (7.28) eight parameters are still needed to completely specify the matrix. The reason is that three parameters are needed to specify the basis of right singular vectors. Ordinarily four parameters are needed for this; e.g.,

$$U = \begin{bmatrix} \cos\phi_u e^{j\theta u_1} & -\sin\phi_u e^{j\psi u} e^{j\theta u_2} \\ \sin\phi_u e^{j\psi} e^{j\theta u_1} & \cos\phi_u e^{j\theta u_2} \end{bmatrix} \quad . \tag{7.29}$$

It will be recalled, however, that θ_{u_1} was adjusted to make the parameter ψ in (7.27) equal to zero. On the other hand, fixing $\theta_{u_1} = \theta_{u_2} \equiv 0$ implies that ψ is well determined. Thus in the former case, L is completely determined by

$$\{\sigma_1, \sigma_2, \theta_1, \theta_2, \phi, \phi_u, \psi_u, \theta_{u_2}\} \tag{7.30}$$

while in the latter case L is completely determined by

$$\{\sigma_1, \sigma_2, \theta_1, \theta_2, \phi, \psi, \phi_u, \psi_u\} \quad . \tag{7.31}$$

The five parameters in (7.28) appear to be the most useful in approximating feedback system properties in terms of open loop system parameters. However, as the discussion of structured design specifications for MIMO systems showed (Chapter 5), information about the directions of the right singular subspaces is important in stating design goals. Thus both parameterizations display valuable design information.

CHAPTER 8

SYSTEMS WITH HIGH AND LOW GAINS AT THE SAME FREQUENCY

8.1. Introduction

The purpose of this chapter is to provide approximations to the sensitivity and complementary sensitivity functions of an MIMO feedback system in terms of properties of the open loop transfer function. The case considered is that in which, over some frequency range, this transfer function has much higher levels of gain in some directions than in others. Motivation for studying this case was provided by the discussion of structured disturbance inputs, sensor noise, and modelling uncertainty in Chapter 5. The assumption of such structure naturally leads to systems whose open loop transfer function has, at the same frequency, high levels of gain in directions for which good performance is desired and small gain in other directions to provide stability robustness and/or sensor noise rejection. An additional motivation is provided by the observation that a given plant may naturally possess different bandwidths in different directions. To facilitate design of a compensator, it is useful to know how this property affects the closed loop system. Finally, when the plant has an unequal number of inputs and outputs, one of the two open loop transfer functions, $L = PF$ or $L_1 = FP$, will necessarily have less than full rank. Hence, such a system will also necessarily have different bandwidths in different directions.

Portions of this chapter have appeared in [29] and [44] and will appear in [45].

8.2. Approximations to S and T in Terms of Open Loop System Properties

It is desired to study systems which, at the same frequency, possess much higher levels of gain in some directions than in others. Thus it is convenient to partition the singular value decomposition (SVD) of the open loop transfer function as (suppressing dependence on the complex frequency variable s):

$$L = [V_1 \mid V_2] \begin{bmatrix} \Sigma_1 & 0 \\ 0 & \Sigma_2 \end{bmatrix} \begin{bmatrix} U_1^H \\ \hline U_2^H \end{bmatrix}$$

or (8.1)

$$L = V_1\Sigma_1U_1^H + V_2\Sigma_2U_2^H$$

where $\underline{\sigma}[\Sigma_1] >> \bar{\sigma}[\Sigma_2]$ and with V_1, $U_1 \in \mathbb{C}^{n\times k}$, $V_2, U_2 \in \mathbb{C}^{n\times(n-k)}$, $\Sigma_1 \in \mathbb{C}^{k\times k}$, and $\Sigma_2 \in \mathbb{C}^{(n-k)\times(n-k)}$. Inputs to the open loop system lying in the subspace $\mathfrak{U}_i$ (the column space of U_i) are amplified by the level of gain given by the singular values of Σ_i and appear as outputs in the subspace $\mathfrak{V}_i$ (the column space of V_i). This partition suggests that L be referred to as consisting of a high gain subsystem $(V_1\Sigma_1U_1^H)$ and a low gain subsystem $(V_2\Sigma_2U_2^H)$ (with the caveat that the partition need not correspond to physical subsystems).

It is convenient to write the spaces of inputs and outputs in the basis of right singular vectors; i.e., the columns of U. The matrices L and S written with respect to this basis are given by

$$\begin{aligned} \tilde{L} &= U^H L U \\ &= U^H V \Sigma \end{aligned} \tag{8.2}$$

and

$$\tilde{S} = U^H S U$$
$$= (I + U^H V \Sigma)^{-1} \quad . \tag{8.3}$$

Since $\tilde{L}$ and $\tilde{S}$ are related to L and S by a unitary transformation, the singular values of $\tilde{L}$ and $\tilde{S}$ are the same as those of L and S. Note that (8.2) and (8.3) are also similarity transformations; thus eigenvalues are also preserved. This fact is appealing since various system properties quantified by singular values and eigenvalues are preserved under the transformations.

Rewriting (8.2) in terms of the partition (8.1) yields

$$\tilde{L} = \begin{bmatrix} U_1^H V_1 \Sigma_1 & U_1^H V_2 \Sigma_2 \\ U_2^H V_1 \Sigma_1 & U_2^H V_2 \Sigma_2 \end{bmatrix} \quad . \tag{8.4}$$

The matrices $U_i^H V_j$ give a measure of the alignment of the subspaces $\mathcal{U}_i$ and $\mathcal{V}_j$ (the column spaces of U_i and V_j). The singular values of $U_i^H V_j$ are the cosines of the canonical angles between the subspaces $\mathcal{U}_i$ and $\mathcal{V}_j$ (see Appendix D for a discussion of these angles). The canonical angles generalize the usual notion of angle when the subspaces are one-dimensional. If all the canonical angles are equal to zero then $\mathcal{U}_i = \mathcal{V}_i$. If all these angles are equal to $\pi/2$ then $\mathcal{U}_i \cap \mathcal{V}_i = \phi$, the empty set. Similarly the singular values of $U_i^H V_j$, $i \neq j$, are the sines of the canonical angles. In system terms the matrix $U_i^H V_j$ indicates how much of the output of the transfer function L lying in the subspace $\mathcal{V}_j$ is due to inputs lying in the subspace $\mathcal{U}_i$. If, at some frequency, $U_i^H V_j = 0$, $i \neq j$, then the high gain and low gain subsystems are decoupled (at the given frequency). Note that in terms of the feedback

system of Figure 5.1 this means that the output of the high gain subsystem is fed completely back to the input of this subsystem. A similar statement holds for the low gain subsystem. If $U_j^H V_i \neq 0$, $i \neq j$, then part of the output of the high gain subsystem is fed back to the input of the low gain subsystem (and conversely). The effect of this behavior upon the sensitivity and complementary sensitivity functions will now be examined.

The transformed sensitivity matrix (8.3) may be written in terms of the partition (8.4) of $\tilde{L}$ into subsystems as

$$\tilde{S} = \begin{bmatrix} I + U_1^H V_1 \Sigma_1 & U_1^H V_2 \Sigma_2 \\ U_2^H V_1 \Sigma_1 & I + U_2^H V_2 \Sigma_2 \end{bmatrix}^{-1} . \tag{8.5}$$

Using a standard formula for the inverse of a partitioned matrix, the transformed sensitivity function can be written as (assuming $\det A \neq 0$ and $\det C \neq 0$):

$$\tilde{S} = \begin{bmatrix} A^{-1} + BC^{-1}D & -BC^{-1} \\ -C^{-1}D & C^{-1} \end{bmatrix} \tag{8.6}$$

where

$$A \triangleq I + U_1^H V_1 \Sigma_1 \tag{8.7a}$$

$$B \triangleq (I + U_1^H V_1 \Sigma_1)^{-1}\, U_1^H V_2 \Sigma_2 \tag{8.7b}$$

$$C \triangleq (I + U_2^H V_2 \Sigma_2) - U_2^H V_1 \Sigma_1 (I + U_1^H V_1 \Sigma_1)^{-1}\, U_1^H V_2 \Sigma_2 \tag{8.7c}$$

$$D \triangleq U_2^H V_1 \Sigma_1 (I + U_1^H V_1 \Sigma_1)^{-1} . \tag{8.7d}$$

If the gain in both subsystems is sufficiently greater than one, then $S \approx 0$ and $T \approx I$. If the gain in both subsystems is sufficiently small,

then $S \approx I$ and $T \approx 0$. These approximations were discussed in Chapter 5. The following theorem yields an approximation to S and T when the gain in one subsystem is sufficiently large and the gain in the other subsystem is sufficiently small.

In the following it will be assumed that none of the canonical angles is equal to $\pi/2$; i.e., it is assumed that $\det[U_i^H V_i] \neq 0$. An analysis of this special case can be performed using the pseudoinverse of $U_i^H V_i$; however, the resulting expressions are complicated. In Section 8.4 the analysis of this case is performed for two-input two-output systems.

Theorem 8.1: Assume $\det[U_1^H V_1] \neq 0$. Then, if

$$\underline{\sigma}[\Sigma_1] >> \bar{\sigma}[(U_1^H V_1)^{-1}] \tag{8.8}$$

and

$$\bar{\sigma}[\Sigma_2] << \underline{\sigma}[V_2^H U_2] \tag{8.9}$$

the sensitivity function and complementary sensitivity function are approximated by the following equivalent expressions:*

$$S \approx \begin{cases} U_2(V_2^H U_2)^{-1} V_2^H & \text{(8.10a)} \\ U_2(V_2^H U_2)^{-1}(V_2^H U_1) U_1^H + U_2 U_2^H & \text{(8.10b)} \\ V_1(V_1^H U_2)(V_2^H U_2)^{-1} V_2^H + V_2 V_2^H & \text{(8.10c)} \end{cases}$$

*A caveat is in order concerning approximations (8.10)-(8.11) as well as those in the remainder of this chapter. For example, (8.10) does not imply that S is singular, rather, just that $\bar{\sigma}[S - U_2(V_2^H U_2)^{-1} V_2^H]$ may be made arbitrarily small. How small is "small enough" depends on the specific application; e.g., the magnitude of the disturbances to be rejected. Similarly, the amounts by which the gain $\underline{\sigma}[\Sigma_1]$ must exceed $\bar{\sigma}[(U_1^H V_1)^{-1}]$ and by which the gain $\bar{\sigma}[\Sigma_2]$ must be below $\underline{\sigma}[V_2^H U_2]$ in order to insure (8.10)-(8.11) hold will depend upon the application. Again, similar remarks hold for the other approximations in this chapter.

$$T \approx \begin{cases} V_1(U_1^H V_1)^{-1} U_1^H & (8.11a) \\ U_2(U_2^H V_1)(U_1^H V_1)^{-1} U_1^H + U_1 U_1^H & (8.11b) \\ V_1(U_1^H V_1)^{-1}(U_1^H V_2) V_2^H + V_1 V_1^H & (8.11c) \end{cases}$$

■

Proof: See Appendix E. ■

Expression (8.10a) shows that the response of the feedback system to disturbances lying in the subspace $\mathcal{V}_1$ (which contains the output of the high gain subsystem) can be made arbitrarily small. Similarly, the disturbance response is confined to the subspace $\mathcal{U}_2$ (which contains the input to the low gain subsystem). The magnitude of the sensitivity function is

$$\bar{\sigma}[S] \approx \frac{1}{\cos \bar{\alpha}} \tag{8.12}$$

where $\bar{\alpha}$ is the largest canonical angle between the subspaces $\mathcal{U}_2$ and $\mathcal{V}_2$. Thus in order that the system response to disturbances not be excessively large it is necessary that the high gain and low gain subsystems should be sufficiently decoupled. Expression (8.10b) shows that the disturbance response of the system consists of two components. First, disturbances in the subspace $\mathcal{U}_2$ are fed directly through to the output of the system. This is analogous to the SISO case for which $|L| \ll 1$ implies $y_d \approx d$. Second, disturbances in the subspace $\mathcal{U}_1$ are amplified by the system; the resulting output lies in the subspace $\mathcal{U}_2$. The amount of amplification is given by the singular values of the matrix $(V_2^H U_2)^{-1}(V_2^H U_1)$, which in turn are equal to the tangents of the canonical angles between the subspaces $\mathcal{U}_2$ and $\mathcal{V}_2$. This behavior (which has no analogue in SISO systems) is apparently due to a

component of the output from the high gain subsystem being fed into the input of the low gain subsystem and conversely. Equation (8.10c) may be used to decompose the disturbance response in terms of the outputs of the high and low gain subsystems.

Remarks similar to those above can be made about the system response to sensor noise. This may be accomplished using approximations (8.11) to the complementary sensitivity function.

Consider now the problem of structured sensor noise posed in Section 5.4 and the resulting design specification (5.38). Suppose the attempt is made to satisfy this specification by requiring the gain of the system to be small on $\mathcal{N}_s$, the subspace of the input containing the structured component of the sensor noise. This may be stated by requiring $\mathcal{U}_2 \approx \mathcal{N}_s$ and $\bar{\sigma}[\Sigma_2] << 1$. Then approximation (8.11a) shows that this procedure does indeed prevent n_s, the structured component of the sensor noise, from producing a response in the system output. Moreover, maintaining large gain ($\underline{\sigma}[\Sigma_1] >> 1$) in the orthogonal subspace $\mathcal{N}_s^{\perp} \approx \mathcal{U}_1$ insures that the disturbance response will be confined to the subspace $\mathcal{U}_2$.

In order, however, to prevent the system from amplifying disturbances and sensor noise in some directions with greater than unity gain, it is necessary that the interaction between high and low gain subsystems be small. Thus in addition to the requirements $\bar{\sigma}[\Sigma_2] << 1$, $\mathcal{U}_2 \approx \mathcal{N}_s$ and $\underline{\sigma}[\Sigma_1] >> 1$ it is necessary to require $\mathcal{V}_2 \approx \mathcal{U}_2$. Hence, the use of both high and low gains in a design can achieve some of the feedback properties expected from the SISO case, but only if the subsystems are approximately decoupled.

If the gain in both subsystems is sufficiently greater than one, then, as discussed in Section 5.3, the approximations $S \approx 0$ and $T \approx I$ hold.

When the gain in one subsystem has been "rolled off" while that in the other is still large, then Theorem 8.1 may be used to approximate feedback properties. Recall the condition for the low gain subsystem to be rolled off is $\bar{\sigma}[\Sigma_2] << \underline{\sigma}[V_2^H U_2] \leq 1$. This condition guarantees that the matrix $V_2^H U_2 + \Sigma_2 \approx V_2^H U_2$. Note this is a more stringent requirement than the SISO analogue which required that $|L| << 1$ in order to guarantee $1 + L \approx 1$.

This discussion motivates the investigation of whether a frequency region analogous to gain crossover frequency in SISO systems exists. Presumably such a region would exist for crossover of each of the low and high gain subsystems. This is now investigated.

<u>Lemma 8.2</u>: Assume $\det[U_1^H V_1] \neq 0$ and $\det[V_2^H U_2 + \Sigma_2] \neq 0$. Then if

$$\underline{\sigma}[\Sigma_1] >> \bar{\sigma}[(U_1^H V_1)^{-1}] \tag{8.13}$$

the transformed sensitivity function (8.6) is approximated by

$$\tilde{S}_{11} \approx \Sigma_1^{-1}(U_1^H V_1)^{-1}[I - (U_1^H V_2)\Sigma_2(V_2^H U_2 + \Sigma_2)^{-1}(V_2^H U_1)] \tag{8.14a}$$

$$\tilde{S}_{12} \approx -\Sigma_1^{-1}(U_1^H V_1)^{-1}(U_1^H V_2)\Sigma_2(V_2^H U_2 + \Sigma_2)^{-1}(V_2^H U_2) \tag{8.14b}$$

$$\tilde{S}_{21} \approx (V_2^H U_2 + \Sigma_2)^{-1}(V_2^H U_1) \tag{8.14c}$$

$$\tilde{S}_{22} \approx (V_2^H U_2 + \Sigma_2)^{-1}(V_2^H U_2) \tag{8.14d}$$

■

<u>Proof</u>: See Appendix E. ■

<u>Theorem 8.3</u>: Assume $\det[U_1^H V_1] \neq 0$ and $\det[V_2^H U_2 + \Sigma_2] \neq 0$. Then if $\underline{\sigma}[\Sigma_1]$ is sufficiently large the sensitivity function and complementary sensitivity function are approximated by the following equivalent expressions:

$$S \approx \begin{cases} U_2(V_2^H U_2 + \Sigma_2)^{-1} V_2^H & (8.15a) \\ U_2(V_2^H U_2 + \Sigma_2)^{-1}[(V_2^H U_1)U_1^H + (V_2^H U_2)U_2^H] & (8.15b) \\ [V_2(V_2^H U_2) + V_1(V_1^H U_2)](V_2^H U_2 + \Sigma_2)^{-1} V_2^H & (8.15c) \end{cases}$$

$$T \approx \begin{cases} V_1(U_1^H V_1)^{-1} U_1^H + U_2(V_2^H U_2)^{-1}\Sigma_2(V_2^H U_2 + \Sigma_2)^{-1} V_2^H & (8.16a) \\ V_1 V_1^H + [-V_1(V_1^H U_2) + V_2\Sigma_2](V_2^H U_2 + \Sigma_2)^{-1} V_2^H & (8.16b) \\ U_1 U_1^H + U_2(V_2^H U_2 + \Sigma_2)^{-1}[-(V_2^H U_1)U_1^H + \Sigma_2 U_2^H] & (8.16c) \end{cases}$$

■

Proof: See Appendix E. ■

Lemma 8.2 shows that the frequency range for which there exists i, $1 \leq i \leq n$, such that $\underline{\sigma}[\Sigma_2] \leq \sigma_i[V_2^H U_2] \leq \bar{\sigma}[\Sigma_2]$, plays a role analogous to scalar gain crossover frequency. Near gain crossover frequency in SISO systems knowledge of open loop gain is insufficient to allow the approximation of feedback properties. Similarly, at frequencies for which the conditions

$$\bar{\sigma}[\Sigma_2] \ll \underline{\sigma}[U_2^H V_2] \quad (8.17)$$

and

$$\underline{\sigma}[\Sigma_2] \gg \bar{\sigma}[U_2^H V_2] \quad (8.18)$$

both fail to hold, knowledge of open loop singular values does not provide sufficient information to determine feedback properties. For SISO systems the magnitude of the sensitivity and complementary sensitivity functions are determined by open loop phase. Some generalizations of this were presented in Section 7.3. Further generalizations are given later in this chapter.

Note that the magnitude of $\bar{\sigma}[(V_2{}^H U_2 + \Sigma_2)^{-1}]$ is related, via (8.14a,b), to the level of gain required in the high gain subsystem to insure that the component of the disturbance response lying in the subspace $\mathcal{U}_1$ is small.

The following lemma and theorem are a counterpart to Lemma 8.2 and Theorem 8.3 for the frequency range over which the high gain subsystem is being rolled off.

Lemma 8.4: Assume $\det[U_2{}^H V_2] \neq 0$; then if

$$\bar{\sigma}[\Sigma_2] \ll \underline{\sigma}[(U_2{}^H V_2)^{-1}] \tag{8.19}$$

the transformed sensitivity matrix (8.6) is approximated by (assuming the indicated inverse exists):

$$\tilde{S}_{11} \approx [I + U_1{}^H V_1 \Sigma_1 - (U_1{}^H V_2 \Sigma_2)(U_2{}^H V_1 \Sigma_1)]^{-1} \tag{8.20a}$$

$$\tilde{S}_{12} \approx -[I + U_1{}^H V_1 \Sigma_1 - (U_1{}^H V_2 \Sigma_2)(U_2{}^H V_1 \Sigma_1)]^{-1}(U_1{}^H V_2 \Sigma_2) \tag{8.20b}$$

$$\tilde{S}_{21} \approx -(U_2{}^H V_1 \Sigma_1)[I + U_1{}^H V_1 \Sigma_1 - (U_1{}^H V_2 \Sigma_2)(U_2{}^H V_1 \Sigma_1)]^{-1} \tag{8.20c}$$

$$\tilde{S}_{22} \approx I + (U_2{}^H V_1 \Sigma_1)[I + U_1{}^H V_1 \Sigma_1 - (U_1{}^H V_2 \Sigma_2)(U_2{}^H V_1 \Sigma_1)]^{-1}(U_1{}^H V_2 \Sigma_2) \tag{8.20d}$$

∎

Proof: See Appendix E. ∎

Theorem 8.5: Assume $\det[U_2{}^H V_2] \neq 0$ and $\det(I + U_1{}^H V_1 \Sigma_1) \neq 0$. Then if $\bar{\sigma}[\Sigma_2]$ is sufficiently small, the sensitivity function and complementary sensitivity function are approximated by the following equivalent expressions

$$S \approx \begin{cases} U_2(V_2^H U_2)^{-1} V_2^H + V_1(U_1^H V_1)^{-1}(I + U_1^H V_1 \Sigma_1)^{-1} U_1^H & (8.21a) \\ U_2 U_2^H + [U_1 - U_2(U_2^H V_1)\Sigma_1](I + U_1^H V_1 \Sigma_1)^{-1} U_1^H & (8.21b) \\ V_2 V_2^H + V_1(I + \Sigma_1 U_1^H V_1)^{-1}[V_1^H - \Sigma_1(U_1^H V_2)V_2^H] & (8.21c) \end{cases}$$

$$T \approx \begin{cases} V_1 \Sigma_1 (I + U_1^H V_1 \Sigma_1)^{-1} U_1^H & (8.22a) \\ V_1 \Sigma_1 (I + U_1^H V_1 \Sigma_1)^{-1}[(U_1^H V_1)V_1^H + (U_1^H V_2)V_2^H] & (8.22b) \\ [U_1(U_1^H V_1) + U_2(U_2^H V_1)]\, \Sigma_1 (I + U_1^H V_1 \Sigma_1)^{-1} U_1^H & (8.22c) \end{cases}$$

■

Proof: See Appendix E. ■

Theorem 8.5 shows that the frequency range for which there exists i, $1 \leq i \leq n$, such that $\underline{\sigma}[\Sigma_1] \leq \sigma_i[(U_1^H V_1)^{-1}] \leq \bar{\sigma}[\Sigma_1]$, plays a role analogous to scalar gain crossover frequency when the high gain subsystem is being rolled off. Comments similar to those following Theorem 8.3 can be made concerning system properties in this frequency range.

The approximations to the sensitivity and complementary sensitivity functions given by Theorem 8.1-8.3 may be used to obtain approximations to the singular values of these matrices. Recall that $\mathfrak{U}_1$ and $\mathfrak{V}_1$ are k-dimensional subspaces of $\mathbb{C}^n$ and $\mathfrak{U}_2$ and $\mathfrak{V}_2$ are (n-k)-dimensional.

From (8.10a) it follows that k singular values of S are small, while (n-k) singular values are approximated by

$$\sigma_i[S] \approx \frac{1}{\cos \alpha_i} \qquad i=1,\ldots,n-k \tag{8.23}$$

where $\{\alpha_i\ ;\ i=1,\ldots,n-k\}$ are the canonical angles between the subspaces $\mathfrak{U}_2$ and $\mathfrak{V}_2$. Similarly, from (8.11a) it follows that (n-k) singular values of T are small, while k singular values are approximated by

$$\sigma_i[T] \approx \frac{1}{\cos \beta_i} \qquad i=1,\ldots,k \tag{8.24}$$

where $\{\beta_i\ ;\ i=1,\ldots,k\}$ are the canonical angles between the subspaces $\mathfrak{U}_1$ and $\mathfrak{V}_1$. Assume that $n-k \leq k$. Then from Appendix D it follows that 2k-n nonsmall singular values of T are approximately one while the remaining nonsmall singular values are approximately equal to the nonsmall singular values of S. A similar statement holds if $n-k \geq k$ except that n-2k singular values of S are approximately one.

From (8.15a) it follows that the (n-k) nonsmall singular values of S are approximated by

$$\sigma_i[S] \approx \sigma_i[(V_2^H U_2 + \Sigma_2)^{-1}] \quad i=1,\ldots,n-k \quad . \tag{8.25}$$

The approximation of the singular values of T is more difficult since the approximations (8.16) are not in the form of a singular value decomposition as are those in (8.15). However, some useful information may still be obtained. For example, let the singular values of S and T be numbered in order of decreasing magnitude. Then, from the identity $T+S = I$ and Theorem 6.6 of Stewart [37], it follows that

$$|\sigma_i[S] - \sigma_i[T]| \leq 1 \quad . \tag{8.26}$$

In particular, when $\sigma_i[S]$ is large so is $\sigma_i[T]$.

One alternate approximation to the singular values of T may be obtained from (8.16b). Since the nonzero singular values of $V_1 V_1^H$ are equal to one it follows that $\sigma_i[T]$ is large if and only if

$$\sigma_i\{[-V_1(V_1{}^H U_2) + V_2\Sigma_2]\ (V_2{}^H U_2 + \Sigma_2)^{-1} V_2{}^H\}$$

is large. In this case

$$\sigma_i[T] \approx \sqrt{\sigma_i^2[(V_1{}^H U_2)(V_2{}^H U_2 + \Sigma_2)^{-1}] + \sigma_i^2[\Sigma_2(V_2{}^H U_2 + \Sigma_2)^{-1}]} \quad . \tag{8.27}$$

This approximation is useful when it is desired to detect large values of $\sigma_i[T]$, since the approximation is valid exactly in this case. Similar approximations to $\sigma_i[T]$ and $\sigma_i[S]$ may be obtained from Theorem 8.5. The approximation analogous to (8.25) is given by

$$\sigma_i[T] \approx \sigma_i[\Sigma_1(I + U_1{}^H V_1\Sigma_1)^{-1}] \quad . \tag{8.28}$$

Note that $\sigma_i[S]$ is large if and only if $\sigma_i\{[U_1 - U_2(U_2{}^H V_1)\Sigma_1]\ (I + U_1{}^H V_1\Sigma_1)^{-1} U_1{}^H]\}$ is large. In this case

$$\sigma_i[S] \approx \sqrt{\sigma_i^2[(I + U_1{}^H V_1\Sigma_1)^{-1}] + \sigma_i^2[(U_2{}^H V_1)\ \Sigma_1(I + U_1{}^H V_1\Sigma_1)^{-1}]} \quad . \tag{8.29}$$

8.3. Two-Input Two-Output Systems

The purpose of this section is to specialize the results of Section 8.2 to systems with two inputs and two outputs. In order to accomplish this a parameterization of such matrices introduced in Section 7.4 will prove useful.

Consider the transformed open loop transfer function (8.2):

$$\tilde{L} = U^H V \Sigma$$

$$= \begin{bmatrix} u_1^H v_1 \sigma_1 & u_1^H v_2 \sigma_2 \\ u_2^H v_1 \sigma_1 & u_2^H v_2 \sigma_2 \end{bmatrix} \quad . \tag{8.30}$$

Assume first that $u_1^H v_1 \neq 0$. (Since $U^H V$ is a unitary matrix this is equivalent to the condition that $u_2^H v_2 \neq 0$.) Then the parameterization (7.28) may be applied to (8.30):

$$\tilde{L} = \begin{bmatrix} \cos\phi \; \sigma_1 \; e^{j\theta_1} & -\sin\phi \; \sigma_2 \; e^{j\theta_2} \\ \sin\phi \; \sigma_1 \; e^{j\theta_1} & \cos\phi \; \sigma_2 \; e^{j\theta_2} \end{bmatrix} \quad . \tag{8.31}$$

The transformed sensitivity function (8.3) may be written as

$$\tilde{S} = \frac{\begin{bmatrix} 1 + \sigma_2 \; e^{j\theta_2} \cos\phi & \sigma_2 \; e^{j\theta_2} \sin\phi \\ -\sigma_1 \; e^{j\theta_1} \sin\phi & 1 + \sigma_1 \; e^{j\theta_1} \cos\phi \end{bmatrix}}{1 + \sigma_2 \cos\phi \; e^{j\theta_2} + \sigma_1 \; e^{j\theta_1} (\cos\phi + \sigma_2 \; e^{j\theta_2})} \quad . \tag{8.32}$$

The following are specializations of Theorems 8.1, 8.2 and 8.5 to systems with two inputs and two outputs.

<u>Corollary 8.6</u>: Assume $\cos\phi \neq 0$. Then if

$$\sigma_1 >> \frac{1}{\cos\phi} \tag{8.33}$$

and

$$\sigma_2 << \cos\phi \tag{8.34}$$

the magnitudes of the sensitivity and complementary sensitivity functions are approximated by

$$\bar{\sigma}[S] \approx \frac{1}{\cos\phi} \tag{8.35}$$

$$\bar{\sigma}[T] \approx \frac{1}{\cos\phi} \quad . \tag{8.36}$$

■

Proof: Follows easily from (8.10a), (8.11a) and the fact that $|u_1^H v_1| = |u_2^H v_2| = \cos\phi$. ■

Corollary 8.7: Assume $\cos\phi \neq 0$ and $\cos\phi + \sigma_2 e^{j\theta_2} \neq 0$. Then if σ_1 is sufficiently large the magnitude of the sensitivity function is approximated by

$$\bar{\sigma}[S] \approx \frac{1}{|\cos\phi + \sigma_2 e^{j\theta_2}|} \quad . \tag{8.37}$$

■

Proof: Follows from (8.15a) by noting

$$\bar{\sigma}[U_2(V_2^H U_2 + \Sigma_2)^{-1} V_2^H] = \frac{1}{|v_2^H u_2 + \sigma_2|}$$

and from

$$\begin{aligned} |v_2^H u_2 + \sigma_2| &= |\cos\phi \, e^{-j\theta_2} + \sigma_2| \\ &= |\cos\phi + \sigma_2 e^{j\theta_2}| \quad . \end{aligned}$$

■

Corollary 8.8: Assume that $\cos\phi \neq 0$ and $|1 + \cos\phi \, \sigma_1 e^{j\theta_1}| \neq 0$. Then if σ_2 is sufficiently small the magnitude of the complementary sensitivity function is approximated by

$$\bar{\sigma}[T] \approx \frac{\sigma_1}{|1 + \cos\phi\ \sigma_1\ e^{j\theta_1}|} \quad . \tag{8.38}$$

■

Proof: Follows from (8.22a) by an argument similar to the proof of Corollary 8.7. ■

From Corollary 8.7 it may be seen that at frequencies for which $\sigma_2 \approx \cos\phi$ it is important to keep θ_2 bounded away from $\pm\pi$. Thus such frequencies bear the same relation to the low gain subsystem as gain crossover frequency does to an SISO system. Similarly from Corollary 8.8 it follows that at frequencies for which $\sigma_1 \approx \frac{1}{\cos\phi}$ it is important to maintain θ_1 bounded away from $\pm\pi$. Thus for each subsystem there exists a generalization of the concept of crossover frequency; moreover, at such frequencies the value of a generalized measure of phase difference must be kept bounded away from $\pm\pi$ in order to maintain good feedback properties.

The results of Section 8.2 and the Corollaries of this section are valid only if the canonical angles between subspaces $\mathfrak{U}_1$ and $\mathfrak{V}_1$ (equivalently $\mathfrak{U}_2$ and $\mathfrak{V}_2$) are less than $\frac{\pi}{2}$. An analysis of feedback properties may also be performed in this case; however, the expressions are rather complicated. For systems with two inputs and two outputs, however, the expressions are simple enough to be insightful. An analogue to Theorem 8.1 is now presented. Note that the condition $\det[U_2^H V_2] \neq 0$ imposed in that theorem reduces to $u_2^H v_2 \neq 0$.

Theorem 8.9: Assume $u_2^H v_2 = 0$. Then there exist two cases:

(a) If $\sigma_1\sigma_2 >> 1$, then the sensitivity function is approximated by

$$S \approx \left(\frac{-u_2^H v_1}{\sigma_2}\right) u_2 u_1^H + \left(\frac{-u_1^H v_2}{\sigma_1}\right) u_1 u_2^H \tag{8.39}$$

(b) If $\sigma_1\sigma_2 << 1$, then

$$S \approx I - (\sigma_1 u_2^H v_1) u_2 u_1^H - (\sigma_2 u_1^H v_2) u_1 u_2^H \quad . \tag{8.40}$$

■

Proof: Follows easily from noting that $u_2^H v_2 = 0$ implies

$$\tilde{S} = \frac{\begin{bmatrix} 1 & -u_1^H v_2 \sigma_2 \\ -u_2^H v_1 \sigma_1 & 1 \end{bmatrix}}{(1 + \sigma_1\sigma_2)} \tag{8.41}$$

■

The preceding theorem shows that if $\cos\phi = 0$ and $\sigma_1 >> 1 >> \sigma_2$ then $\bar{\sigma}[S]$ will necessarily be large. In case (a), $\bar{\sigma}[S] \approx \frac{1}{\sigma_2}$, and in case (b), $\bar{\sigma}[S] \approx \sigma_1$. (This follows since $|u_i^H v_j| = 1$, $i \neq j$.) In either case feedback properties are poor. This is plausible since, as shown in Collary 8.6, $\bar{\sigma}[S]$ becomes larger as the angle ϕ becomes smaller. Finally, it might be expected that some sort of unusual feedback behavior would occur when $\cos\phi = 0$. This is plausible since (i) if this condition holds the outputs of each subsystem are being fed completely into the inputs of the other subsystem and (ii) the two subsystems have very different properties in terms of levels of gain. Thus, as a signal travels around the loop it is multiplied, alternately, by high and low levels of gain.

For later reference the approximations to $\bar{\sigma}[T]$ and $\bar{\sigma}[S]$ given by (3.27) and (8.29) will now be stated in terms of the parameterization (8.31). From (8.27) it follows that

$$\bar{\sigma}[T] \approx \frac{\sqrt{(\sin\phi)^2 + \sigma_2^2}}{|\cos\phi + \sigma_2 e^{j\theta_2}|} \tag{8.42}$$

and from (8.29)

$$\bar{\sigma}[S] \approx \frac{\sqrt{1 + \sigma_1^2(\sin\phi)^2}}{|1 + \cos\phi\ \sigma_1\ e^{j\theta_1}|} \quad . \tag{8.43}$$

8.4. An Example of a Multivariable System Phenomenon

In this section an example of a transfer function describing a two-input two-output system will be given. The immediate purpose of this example is to illustrate the approximations developed in Sections 8.2 and 8.3. A secondary purpose is to provide motivation. It will be seen that this example possesses feedback properties having no analogue in scalar systems. Developing the theoretical framework necessary to understand this behavior is the primary goal of this dissertation.

Consider the open loop transfer function

$$L(s) = \begin{bmatrix} \dfrac{1.5 \times 10^5}{(s + 10)} & \dfrac{.78}{(s + .01)^2} \\ \dfrac{-7.071 \times 10^6(s + .1)}{(s + 10)^3} & \dfrac{.64}{(s + .01)^2} \end{bmatrix}$$

The gain in the second loop of this system, given by $\left|\dfrac{1}{(s + .01)^2}\right|$, is large until $\omega = .01$ rad/sec, and then decreases with a two-pole roll-off ($\approx$ 40 db/decade). The gain in the first loop is large until $\omega = .01$ rad/sec, and then decreases at a rate of 20 db/decade. The effect on the open loop singular values is shown in Figure 8.1. The largest singular value corresponds to the gain in the first loop while the smallest singular value

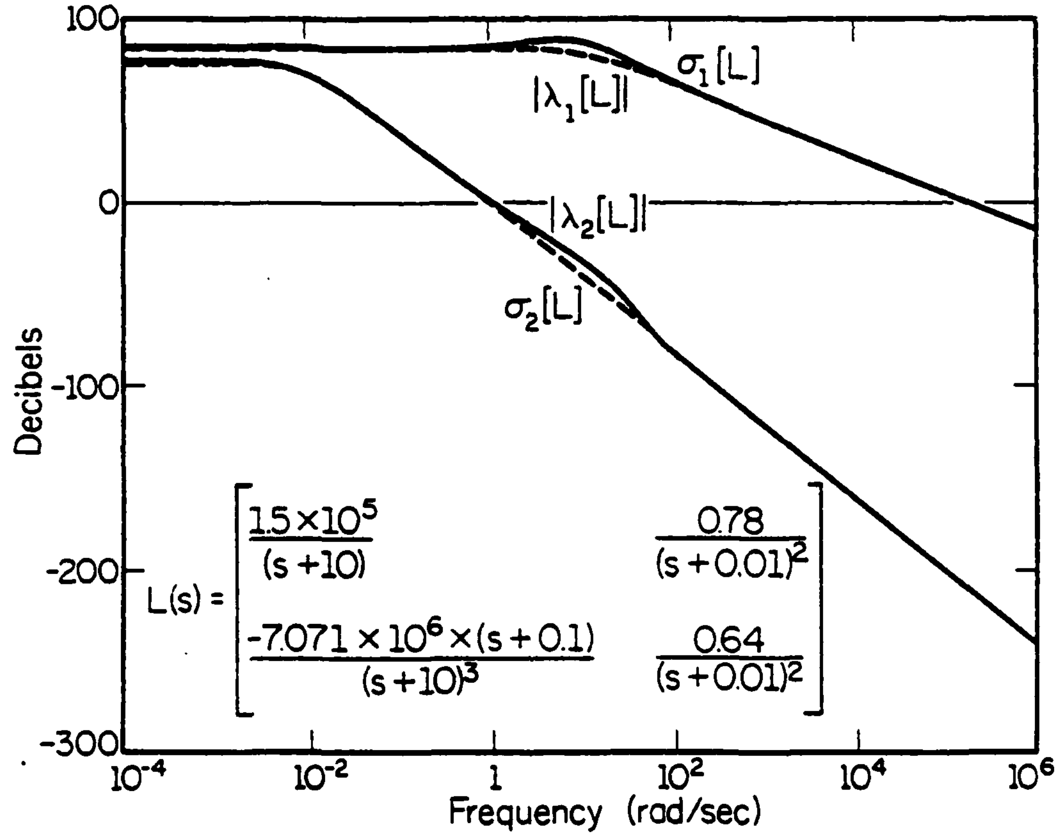

Figure 8.1. Singular values and magnitudes of eigenvalues - open loop system.

corresponds to the gain in the second loop. In the frequency range over which $\sigma_1 >> \sigma_2$ the right singular subspaces are aligned with the standard basis directions (Figure 8.2). This fact greatly facilitates analysis of this example. First the angle ϕ_v, which is a measure of the interaction between the two physical loops of the system, may be identified with the angle ϕ between the left and right singular subspaces (Figures 8.3 and 8.4). (Recall ϕ can be interpreted as a measure of interaction between high gain and low gain subsystems.) A second consequence is that the two measures of phase difference given by θ_i (7.15) and $\tilde{\theta}_i$ (7.25) are very nearly equal in this example (Figures 8.5 and 8.6).

The singular values of the sensitivity function are plotted in Figure 8.7. (The approximation (8.37) is indistinguishable from $\bar{\sigma}[S] = \sigma_1[S]$ on the scale of this plot.) Note the two peaks of $\approx$ 8 db each in $\bar{\sigma}[S]$. From Figure 8.4 it may be seen that the second of these corresponds to a large value of ϕ, as expected from Corollary 8.6. The first peak is in the crossover frequency range in which $\sigma_2 \approx \cos\phi$; the value of this peak may be approximated from Corollary 8.7.

This example illustrates some interesting phenomena not present in SISO systems. If $\sigma_2 \, e^{j\theta_2}$ were a stable minimum phase transfer function with a two-pole roll-off in the vicinity of gain crossover (e.g., $\frac{1}{(s + .01)^2}$), then the value of θ_2 would be $\approx -179°$. This follows from the Bode gain-phase relation (2.24). From the approximation (8.37) it would follow that $\bar{\sigma}[S] \approx 34$ db. Instead $\bar{\sigma}[S] \approx 8$ db. The immediate reason for this may be seen from Figure 8.5. As the gain in the second loop of this system begins to roll-off, the phase difference θ_2 becomes increasingly negative. This might be expected based on intuition from SISO systems. Upon reaching $\approx -160°$,

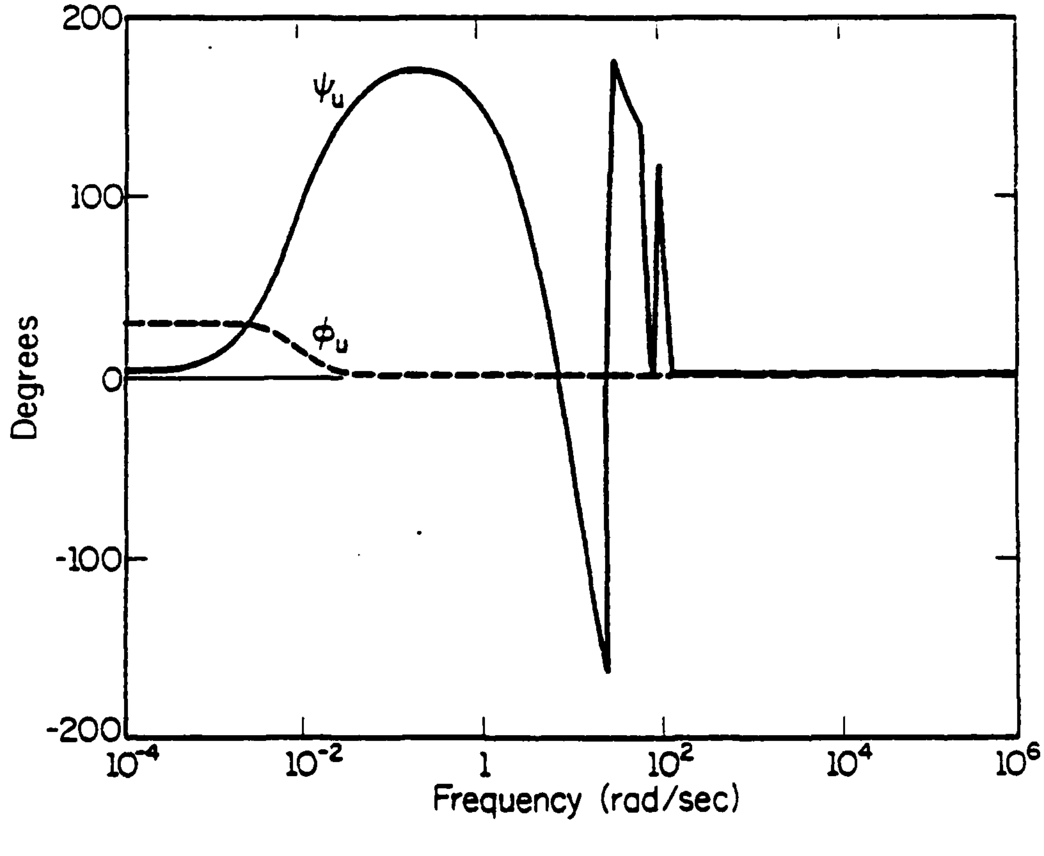

Figure 8.2. Right singular subspaces - open·loop system.

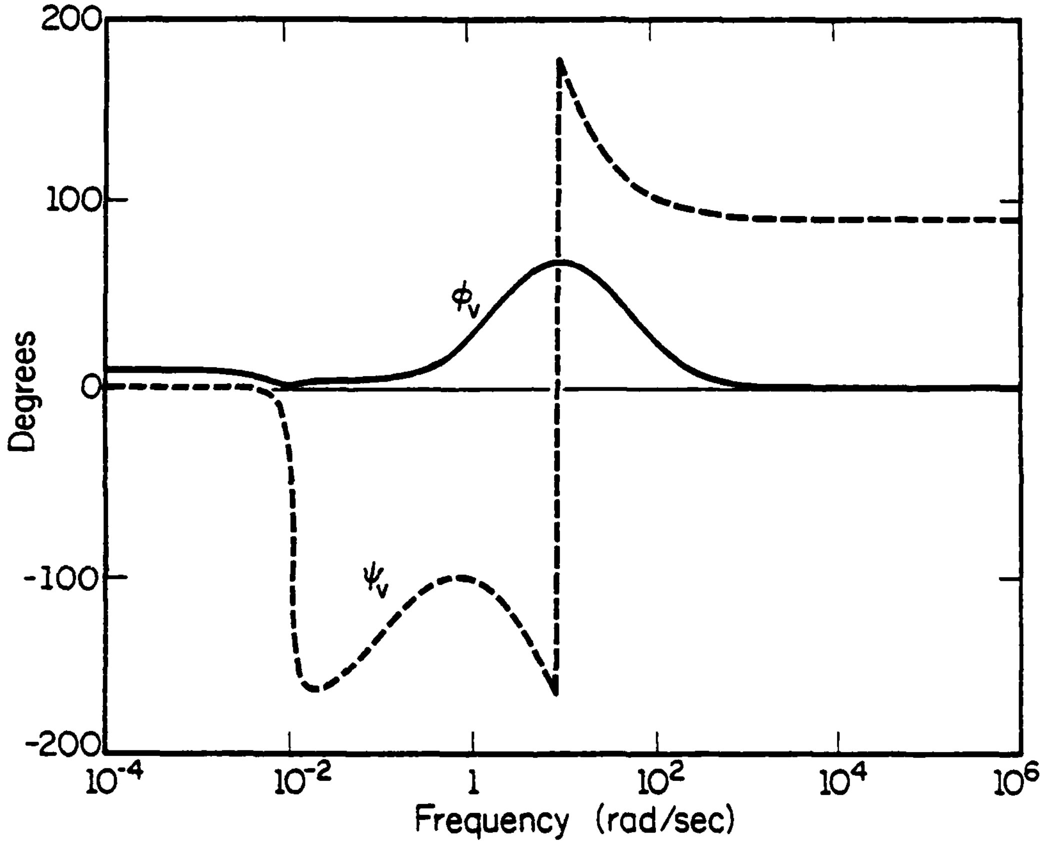

Figure 8.3. Left singular subspaces - open loop system.

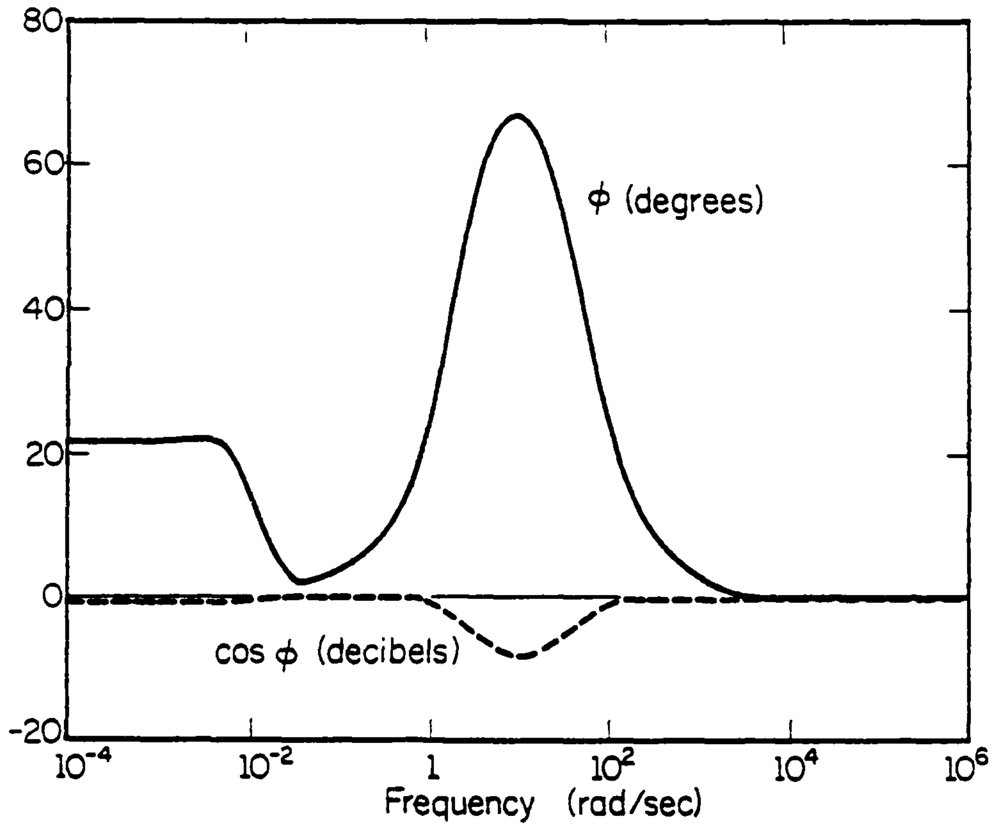

Figure 8.4. Angle between singular subspaces - open loop system.

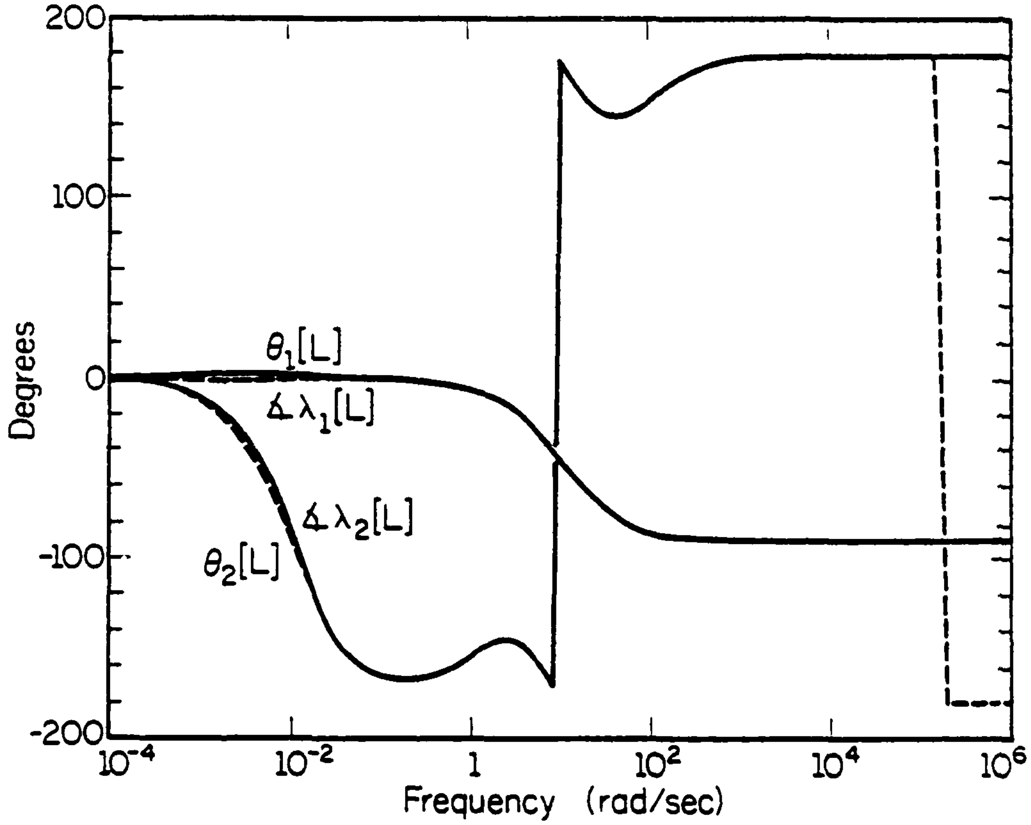

Figure 8.5. Measures of phase difference between singular vectors and phases of eigenvalues - open loop system.

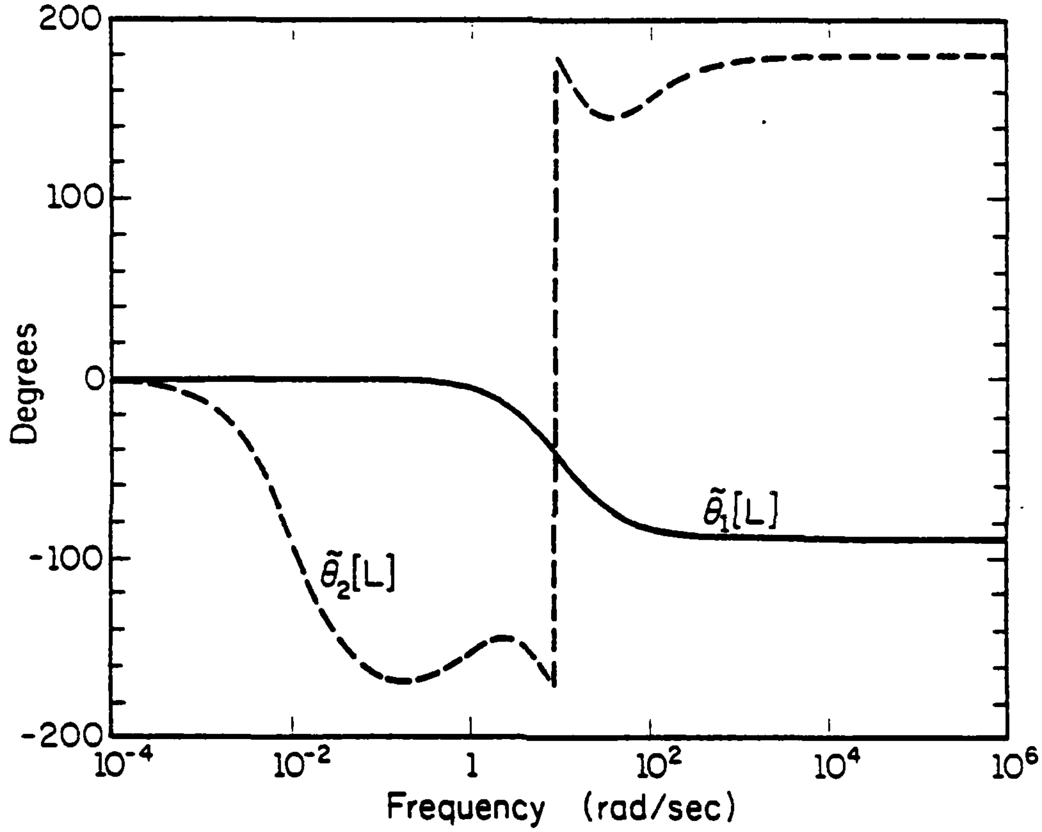

Figure 8.6. Phase differences between "ith" components of "ith" pair of singular vectors - open loop system.

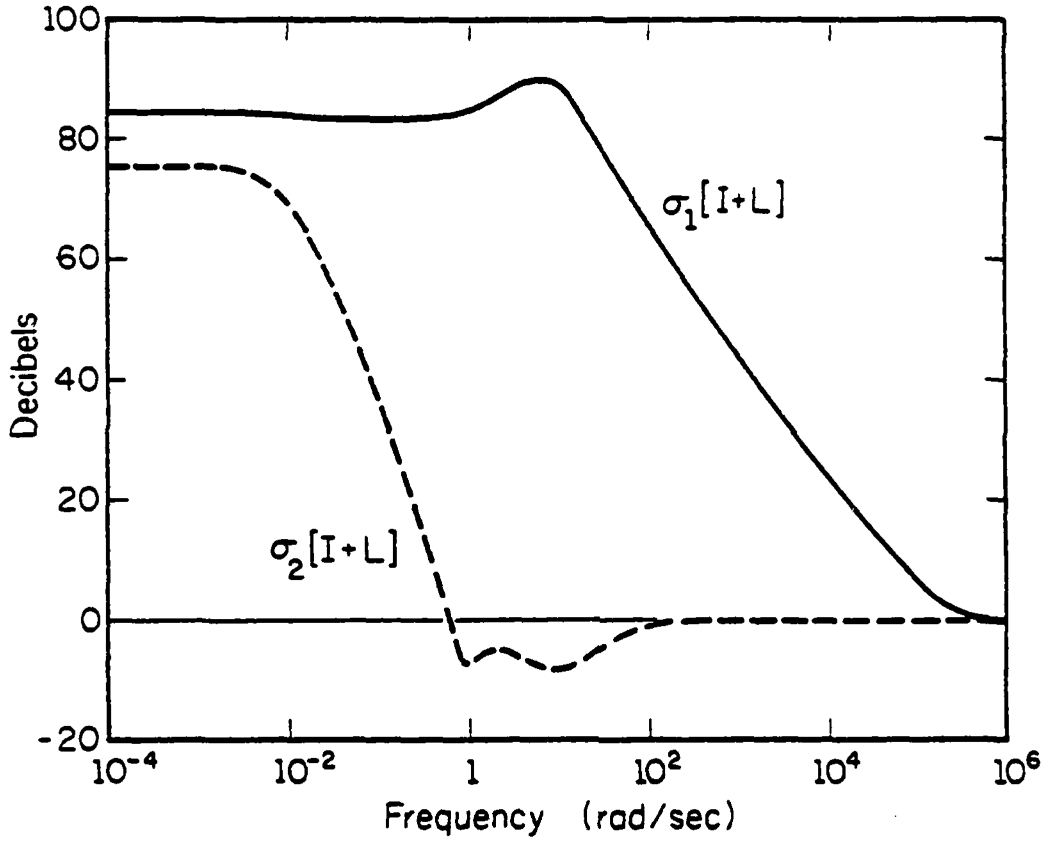

Figure 8.7. Singular values of return difference matrix.

however, θ_2 actually increases to $\approx -140°$ in the vicinity of crossover. In this respect it is as though a phase lead filter were present in the second loop of the system. On the other hand, if such a filter were present in an SISO system the 40 db/decade decrease in gain could not be maintained.

It is interesting to note that a phase lead filter is present in the first loop of the system and that the leading action occurs in the frequency range over which the unusual increase in θ_2 occurs. It is difficult to see a direct relation between these two phenomena. One can easily establish, though, that the increase in the gain $|L_{21}(j\omega)|$ associated with the lead filter is responsible for the increased interaction between the two loops of the system and thus for the increase in ϕ. It is as though the phase lead present in the first loop of the system were being manifest in the second loop via some sort of helpful loop interaction. Additional evidence for this was provided by the observation of a tradeoff between the magnitudes of the two peaks in $\bar{\sigma}[S]$. Increasing the ratio $|L_{21}|/|L_{11}|$ by a constant caused the angle ϕ to become larger, the second peak to increase in magnitude, and the first peak to decrease. Decreasing this ratio produced the opposite effect. The measure of interaction ϕ became smaller, the phase θ_2 became more negative, and the second peak decreased at the expense of an increase in the first peak.

This example illustrates phenomena such as helpful loop interactions which have no analogue in SISO systems. Moreover, these interactions appear to yield additional tradeoffs among feedback properties in different frequency ranges. An extended analysis of this example will be performed in a later chapter, after the development of MIMO generalizations of the Bode gain-phase relations.

8.5. A Practical Example

The purpose of this section is to analyze an example of a practical feedback system using the results of Sections 8.2 and 8.3. One reason for doing so is to verify that the approximations of these sections are valid for systems of physical (as opposed to academic) interest. Another reason is to illustrate how the approximations might be used in design.

The example considered is described in [46]. It consists of a laser beam whose direction is controlled by two mirrors. Since the transfer functions given in [46] did not yield the plots contained therein, the transfer functions were modified so that plots similar to the ones given were obtained.

The open loop transfer function for this system is

$$L(s) = \frac{(2600)(2\pi)^2}{s^2} \begin{bmatrix} 1 & 0 \\ \frac{(-1.825s + 19.5\pi)}{(s + 300\pi)} & 2.52 \end{bmatrix} \begin{bmatrix} G_\alpha & 0 \\ 0 & G_y \end{bmatrix} \tag{8.44a}$$

$$G_\alpha = (172.8) \left(\frac{s + 1068.7}{s + 7480.7}\right) \left(\frac{s + 188.5}{s}\right) \tag{8.44b}$$

$$G_y = (1.782) \left(\frac{s + 166.2}{s + 1163.7}\right) \left(\frac{s + 62.8}{s}\right) \quad . \tag{8.44c}$$

Bode plots of the elements of L(s) are found in Figures 8.8-8.10. Note the differences in the bandwidth of the two loops. Gain crossover for L_{11} is $\approx$ 2300 rad/sec, gain crossover for L_{22} $\approx$ 410 rad/sec, and gain crossover for L_{21} is $\approx$ 4000 rad/sec. These plots show the existence of a

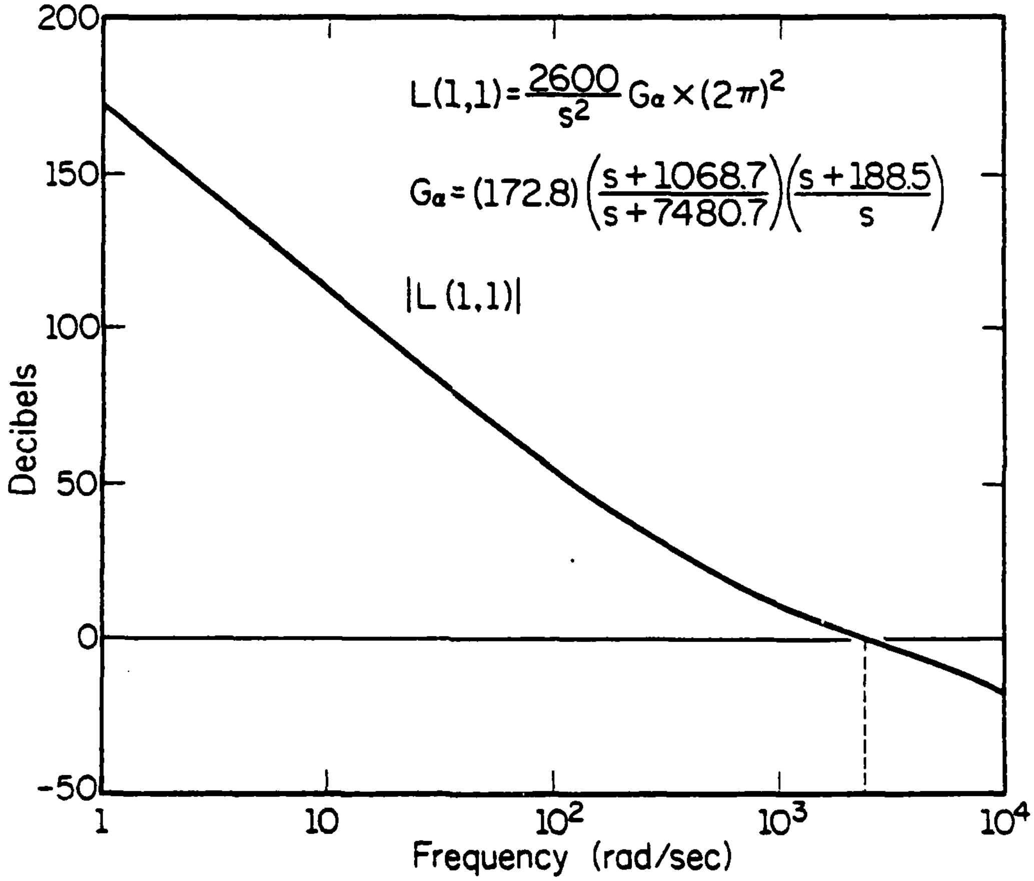

Figure 8.8.a. Gain of L(1,1).

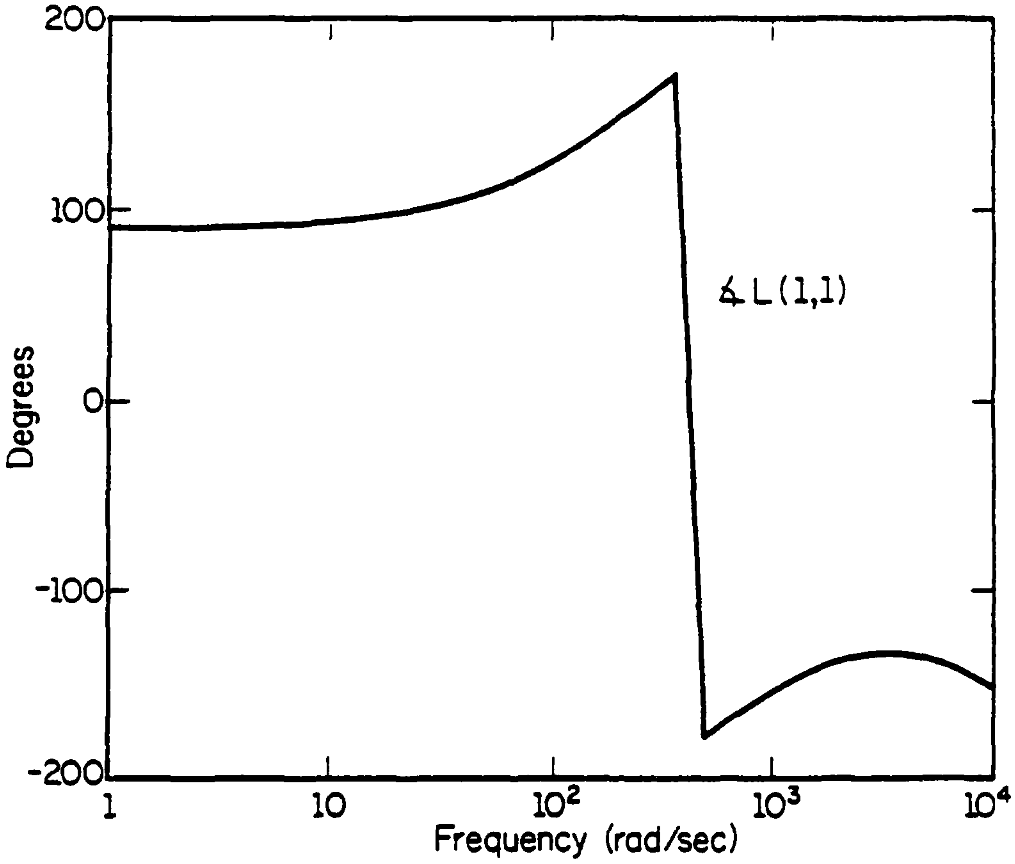

Figure 8.8.b. Phase of L(1,1).

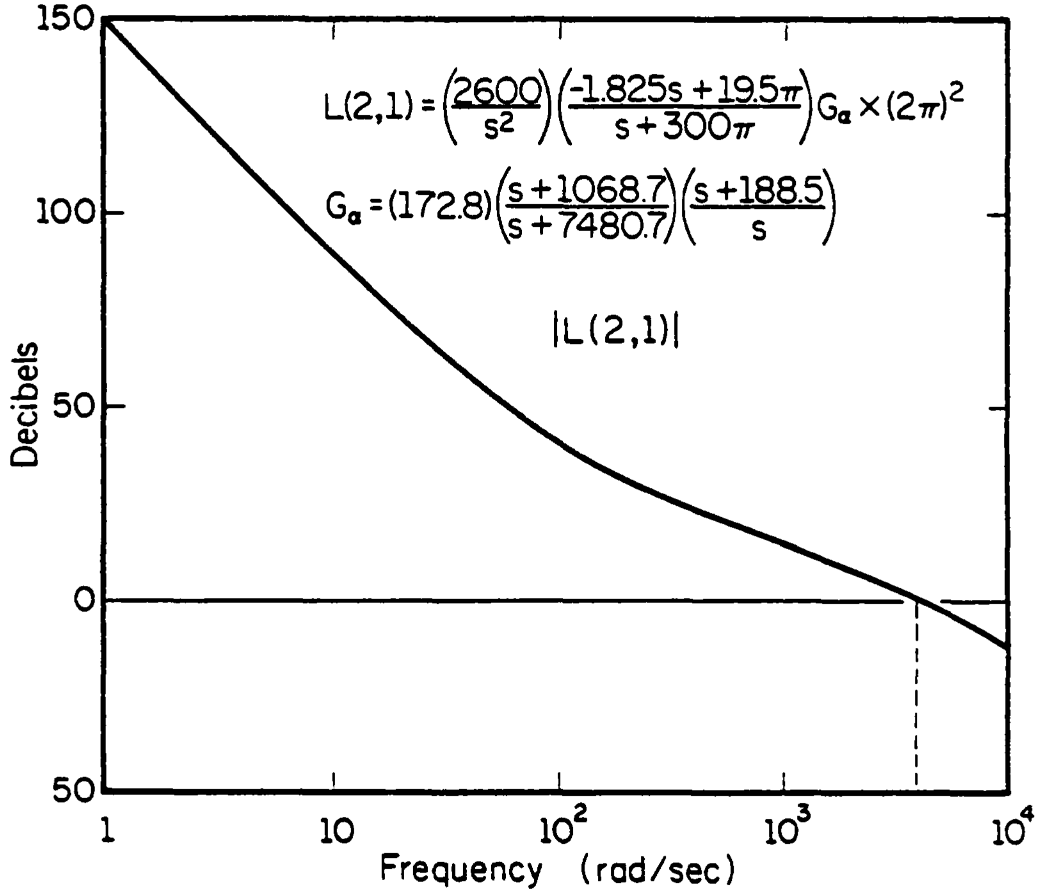

Figure 8.9.a. Gain of L(2,1).

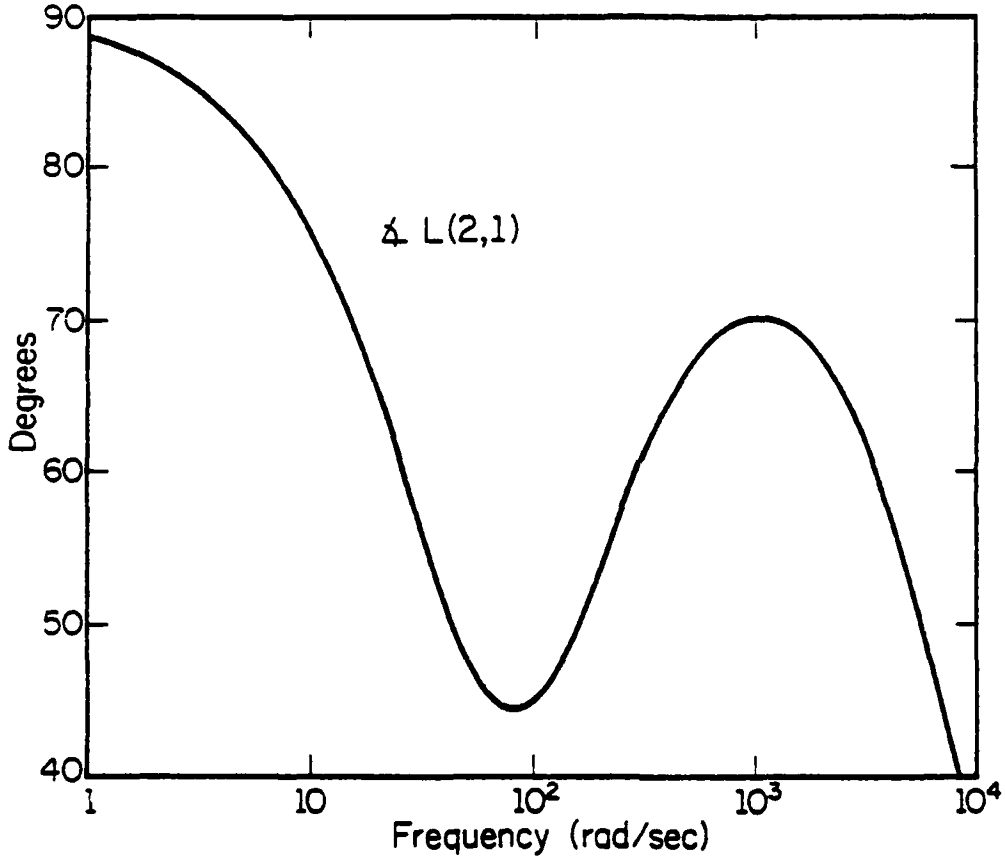

Figure 8.9.b. Phase of L(2,1).

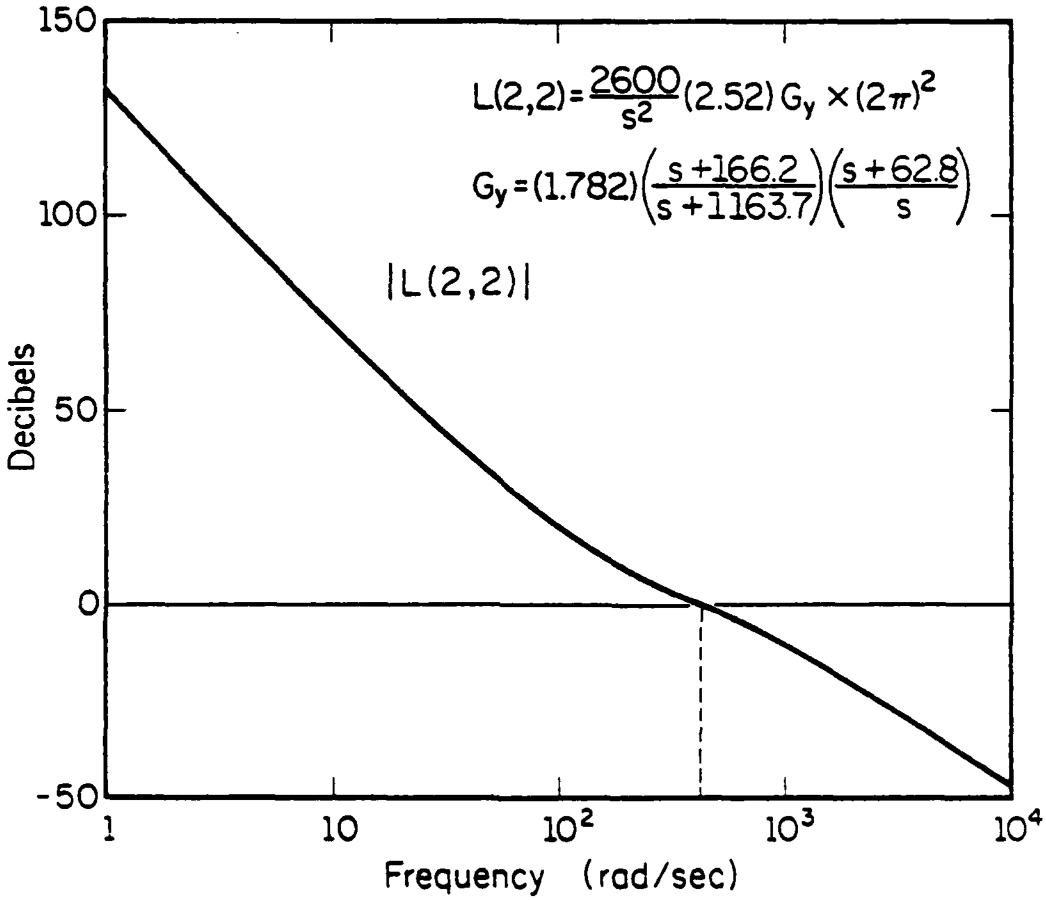

Figure 8.10.a. Gain of L(2,2).

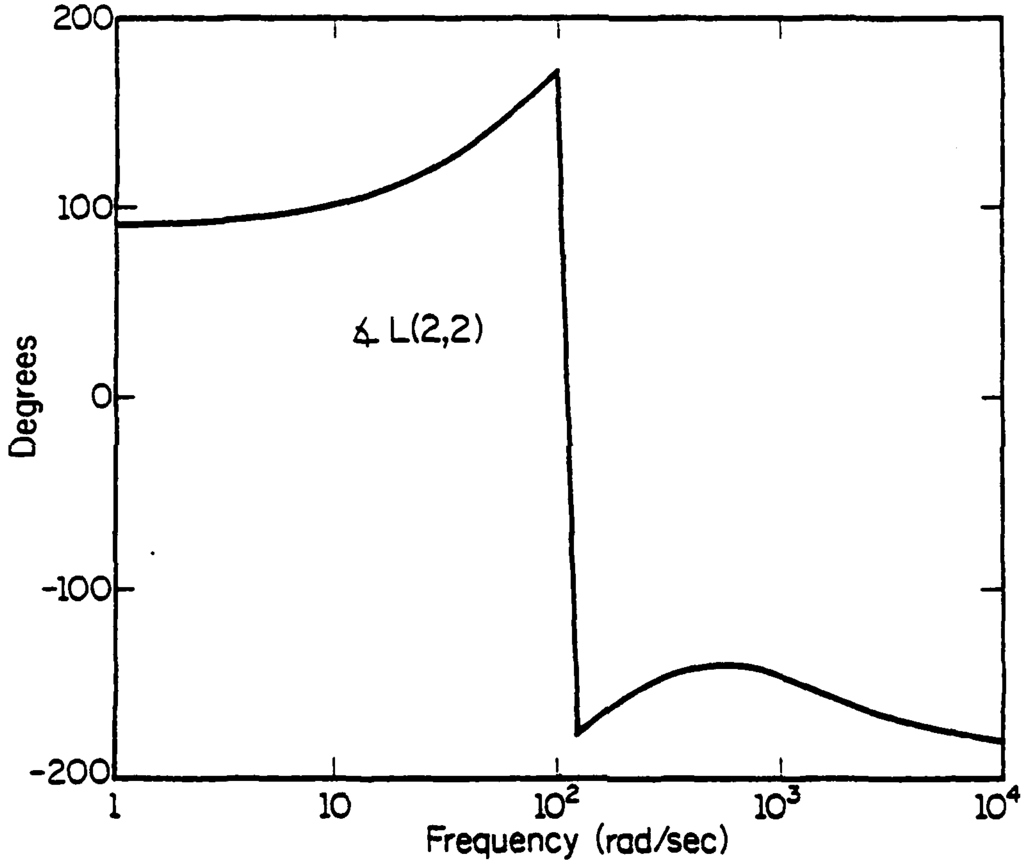

Figure 8.10.b. Phase of L(2,2).

frequency range over which the gain in the first loop of the system is large while that in the second loop has been rolled off. Moreover, the large L_{21} element implies the two loops are rather strongly coupled over this frequency range. The singular values of L(s) are plotted in Figure 8.11. Note that the difference in bandwidth between the two loops of the system corresponds to a difference in the bandwidth of the singular values. Thus it should be possible to apply the approximations of Section 8.3 to estimate feedback properties.

First, note that the angle ϕ between singular subspaces is large (Figure 8.12) and is related to the coupling between loops introduced by the L_{21} element. To see this, observe that the right singular subspaces are aligned with the standard basis directions. This follows from the small value of ϕ_u (from the parameterization 7.26) in Figure 8.13. Since inputs to the individual loops of the system are thus aligned closely with inputs in the right singular subspaces, it follows that the left singular vectors may be approximated from

$$\sigma_1 v_1 = Lu_1$$

$$= \begin{bmatrix} L_{11} & L_{12} \\ L_{21} & L_{22} \end{bmatrix} \begin{bmatrix} \cos\phi_u \\ \sin\phi_u \, e^{j\psi_u} \end{bmatrix} \tag{8.45}$$

$$\Rightarrow \quad \sigma_1 = \left\| \begin{bmatrix} L_{11} \cos\phi_u \\ L_{21} \cos\phi_u + L_{22} \sin\phi_u \, e^{j\psi_u} \end{bmatrix} \right\|_2 \quad . \tag{8.46}$$

Since $\cos\phi_u \approx 1$ and $|L_{22}| << |L_{21}|$, it follows that

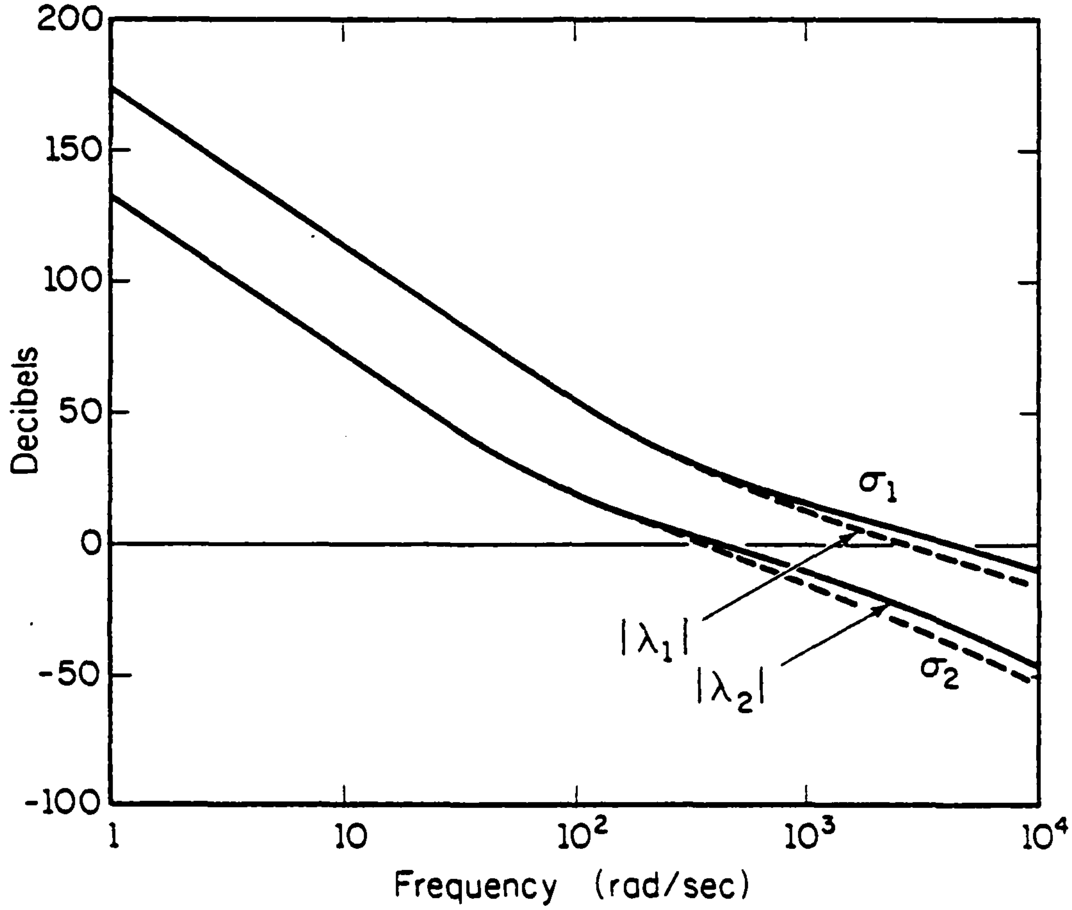

Figure 8.11. Open loop singular values and eigenvalue magnitudes.

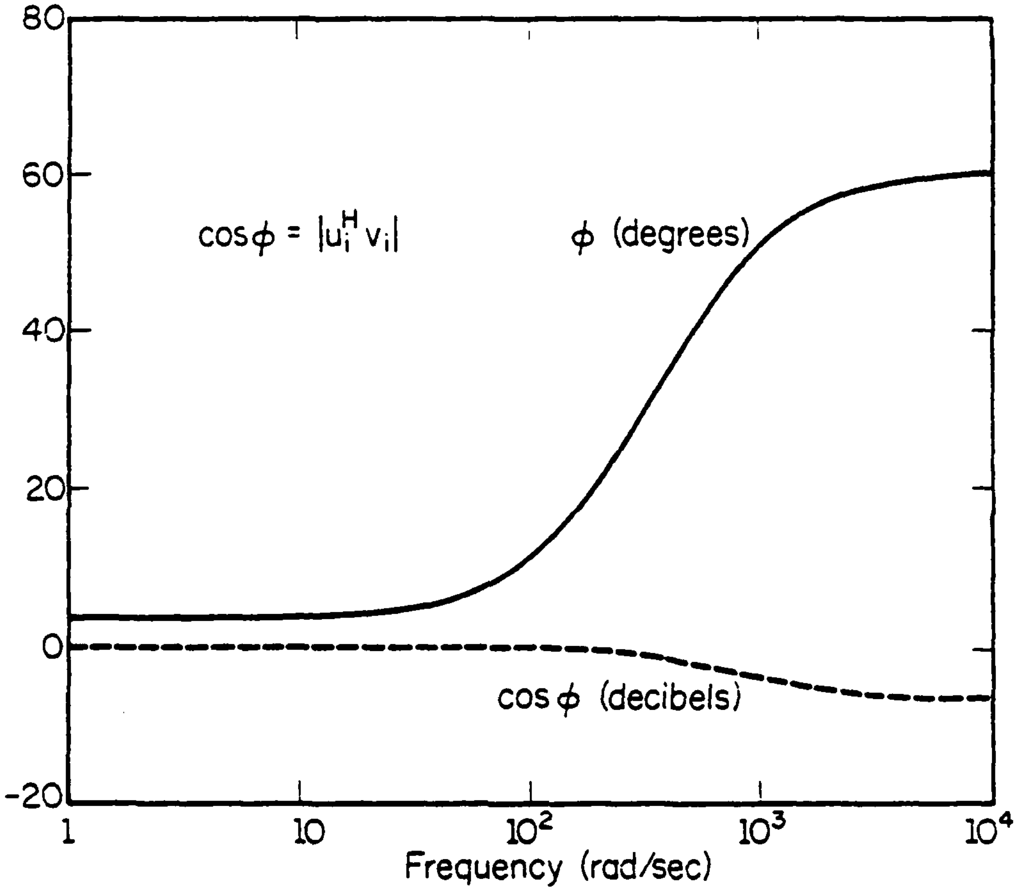

Figure 8.12. Angle between singular subspaces.

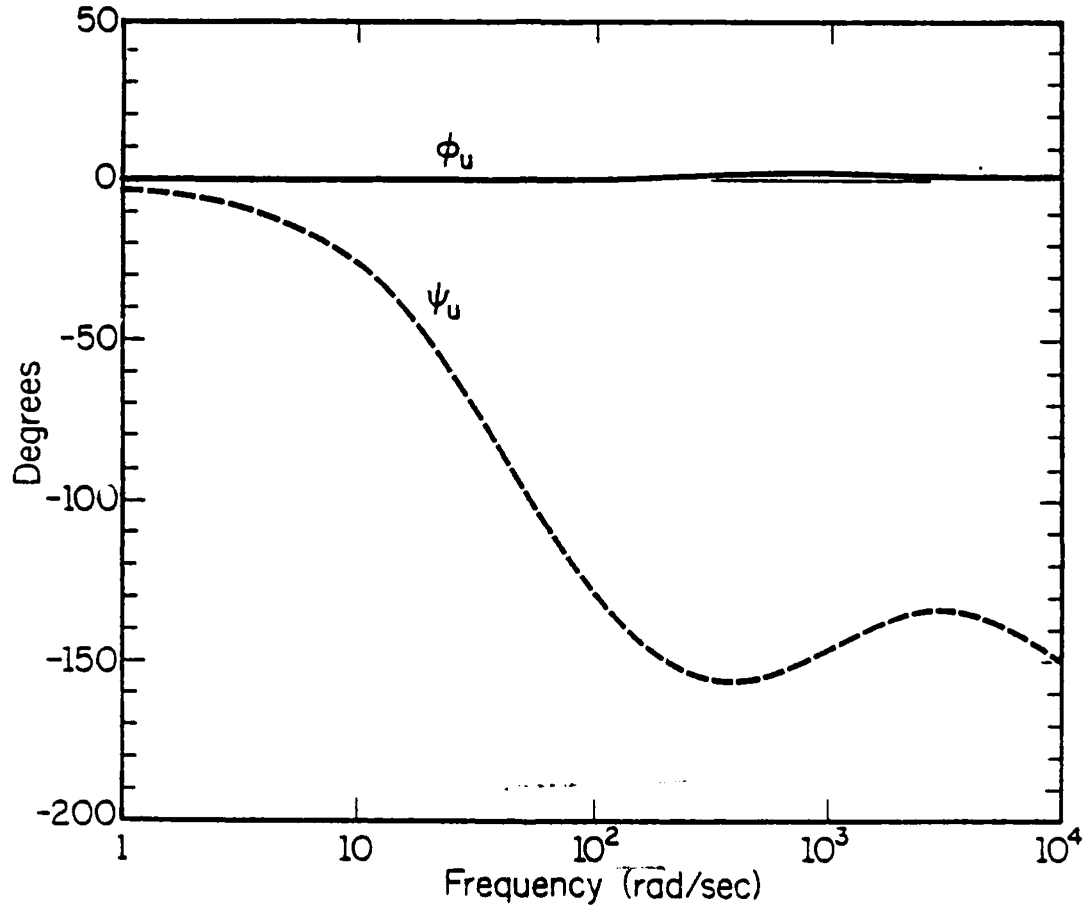

Figure 8.13. Right singular subspaces.

AD-A161 452 ISSUES IN FREQUENCY DOMAIN FEEDBACK CONTROL(U) ILLINOIS UNIV AT URBANA DECISION AND CONTROL LAB J S FREUDENBERG MAY 85 DC-81 N00014-84-C-0149 3/5

UNCLASSIFIED F/G 9/3 NL

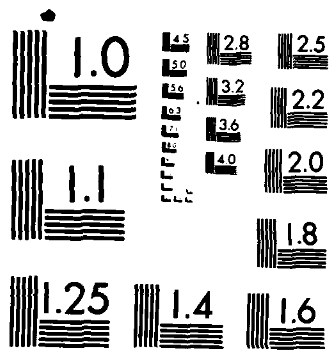

MICROCOPY RESOLUTION TEST CHART
NATIONAL BUREAU OF STANDARDS-1963-A

$$\sigma_1 \approx \sqrt{|L_{11}|^2 + |L_{21}|^2} \quad . \tag{8.47}$$

Thus

$$\cos\phi_v = |v_{11}| \approx \frac{|L_{11}|}{\sqrt{|L_{11}|^2 + |L_{21}|^2}} \tag{8.48}$$

and

$$\psi_v = \measuredangle L_{21} - \measuredangle L_{11} \quad . \tag{8.49}$$

This may be verified from Figures 8.8, 8.9 and 8.14.

Comparing the relative magnitudes of L_{11} and L_{21} (Figures 8.8 and 8.9) it can be seen that ϕ_v is at least 45°. (Note that a similar procedure cannot easily be applied to estimate $\cos\phi_v$ using the smaller singular value. This is because the approximation analogous to (8.46) $\Rightarrow$ (8.47) must deal with products of large and small numbers. Such products cannot easily be estimated.) Next, since $\cos\phi = |u_i^H v_i| \approx |e_i^H v_i|$, it follows that $\phi \approx \phi_v$. Thus the identification of the right singular subspaces with the physical loops of the system implies that the coupling between these loops produces coupling between the high gain and low gain subsystems defined in (8.1). Since Corollary (8.6) shows that $\bar{\sigma}[S] \approx \frac{1}{\cos\phi}$ it follows that the large level of coupling between loops will cause poor sensitivity properties in the appropriate frequency range. (This approximation may be verified from Figures 8.12 and 8.15.) In fact, there exists a tradeoff between coupling and poor sensitivity. This was pointed out in [46]; however, the analysis was made entirely a posteriori by direct evaluation of the singular value decomposition of the sensitivity matrix. Note the SVD of the sensitivity matrix is available from (3.17):

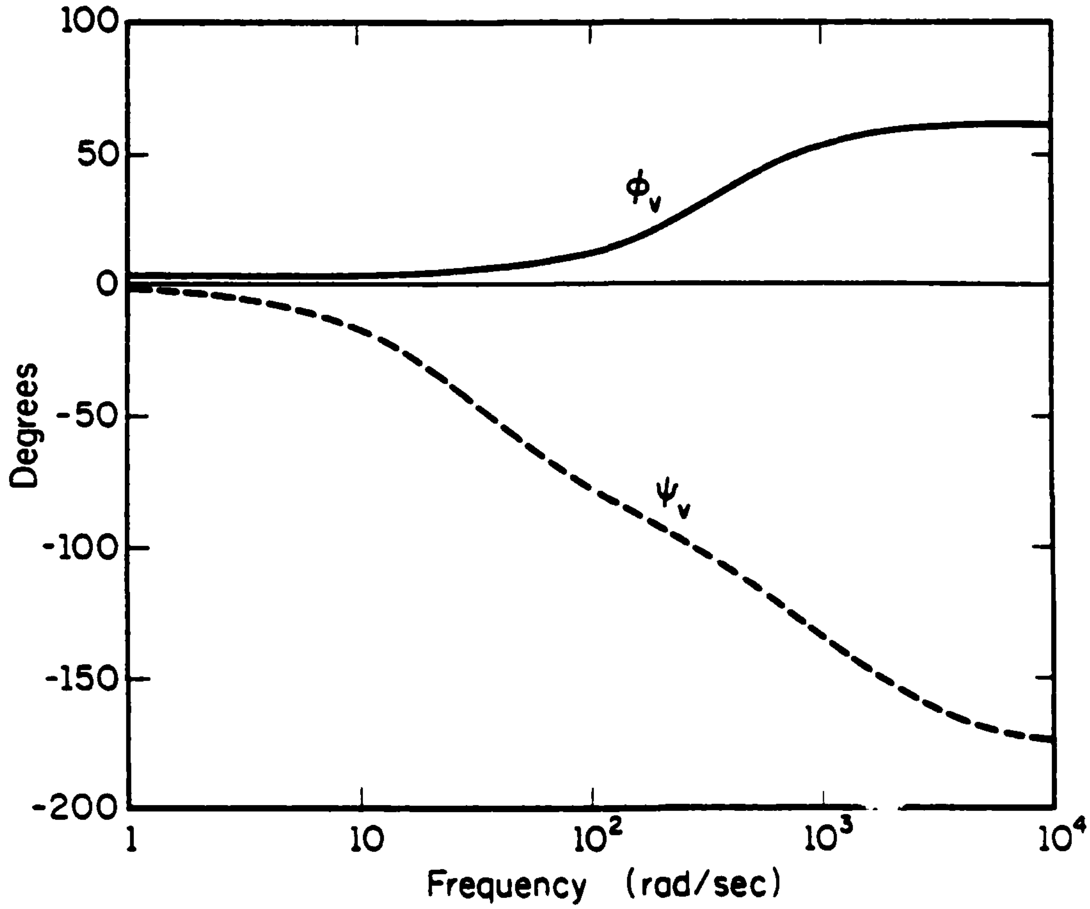

Figure 8.14. Left singular subspaces.

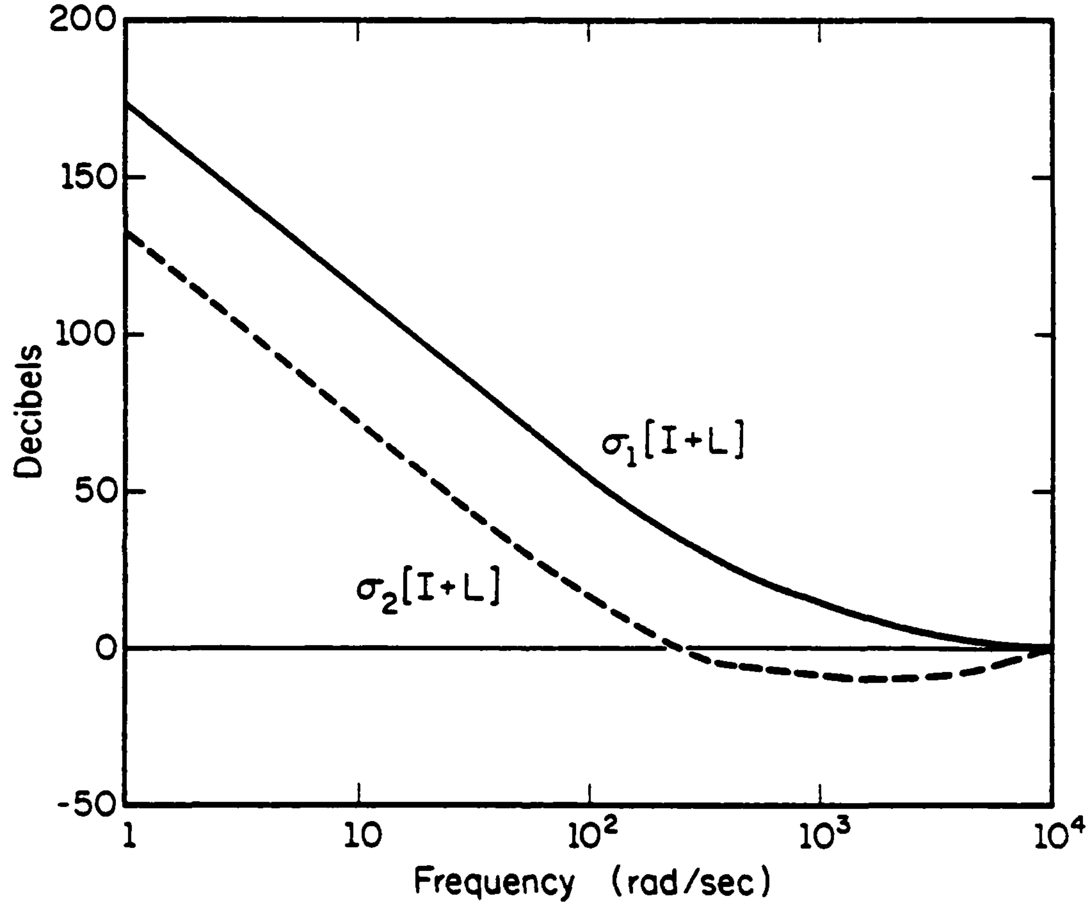

Figure 8.15. Singular values of return difference matrix.

$$S \approx S_{app} = u_2(v_2^H u_2)^{-1} v_2^H \quad . \tag{8.50}$$

Since the right singular subspaces approximate the standard basis directions, it follows that the measures of phase difference θ_i and $\tilde{\theta}_i$ (defined in (7.15) and (7.25)) are approximately equal. This may be verified by comparing Figures 8.16 and 8.17. Thus (8.50) is in turn approximated by

$$S \approx S_{app} \approx \begin{bmatrix} 0 \\ 1 \end{bmatrix} [-\sin\phi_v \; e^{j\psi_v} \quad \cos\phi_v] \; (\frac{e^{-j\theta_2}}{\cos\phi}) \quad . \tag{8.51}$$

Thus, in the frequency range where $\bar{\sigma}[S] \approx \frac{1}{\cos\phi}$, it follows that the rank one destabilizing perturbation of smallest norm [46], is given by

$$E \approx -(\cos\phi \; e^{j\theta_2}) \begin{bmatrix} 0 & -\sin\phi_v \; e^{-j\psi_v} \\ 0 & \cos\phi_v \end{bmatrix} \quad . \tag{8.52}$$

The above discussion shows that much valuable information about feedback properties may be obtained from analysis of the open loop transfer function in the frequency range over which the gain in the first loop is large and that in the second has been rolled off. In Section 8.3 approximations to feedback properties were presented for the frequency ranges in which the two open loop singular values were being rolled off. The approximations to $\bar{\sigma}[S]$ given by (8.37) and (8.43) are plotted in Figure 8.18. (Actually the inverses of these are plotted to be consistent with [46].) The approximations are valid to within a few dB; certainly they are much closer than those obtained from using single-loop analysis (Figure 8.19). Note that since L is triangular, the same results are obtained using the eigenvalues of L to

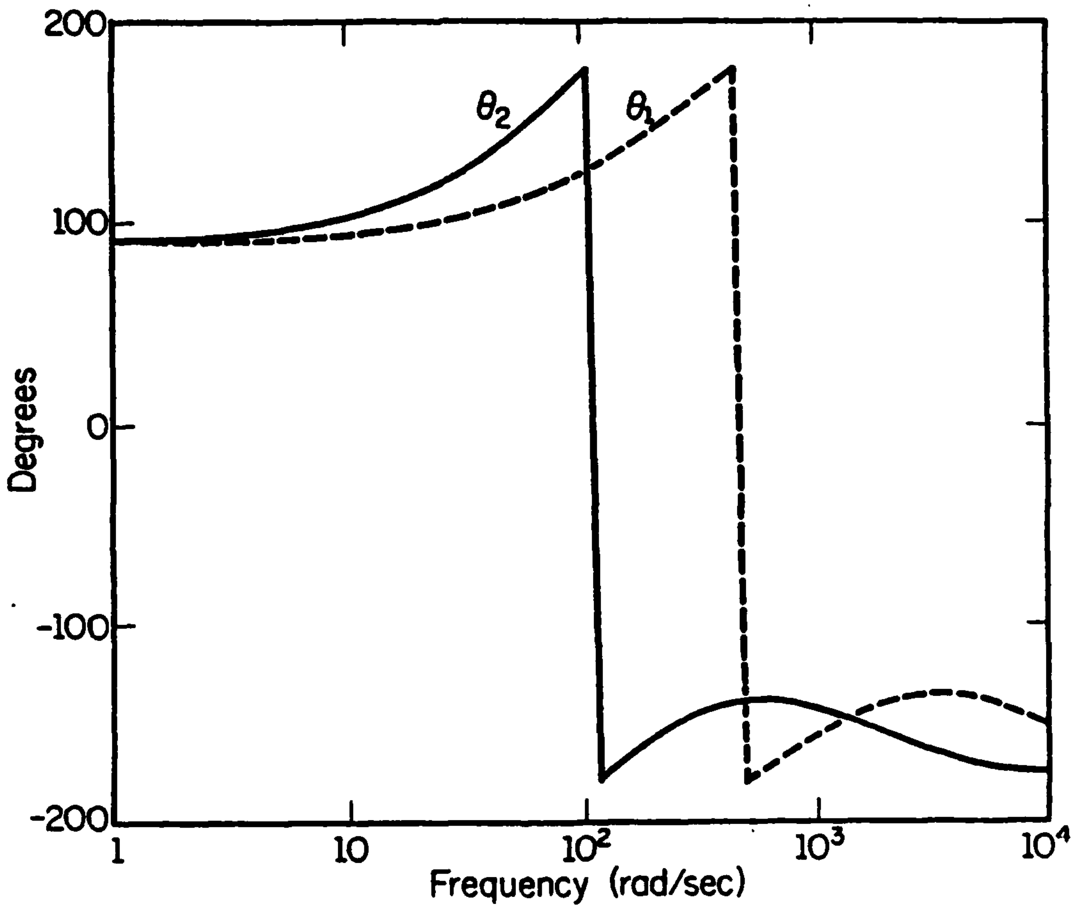

Figure 8.16. Phase differences $\measuredangle u_i^H v_i$.

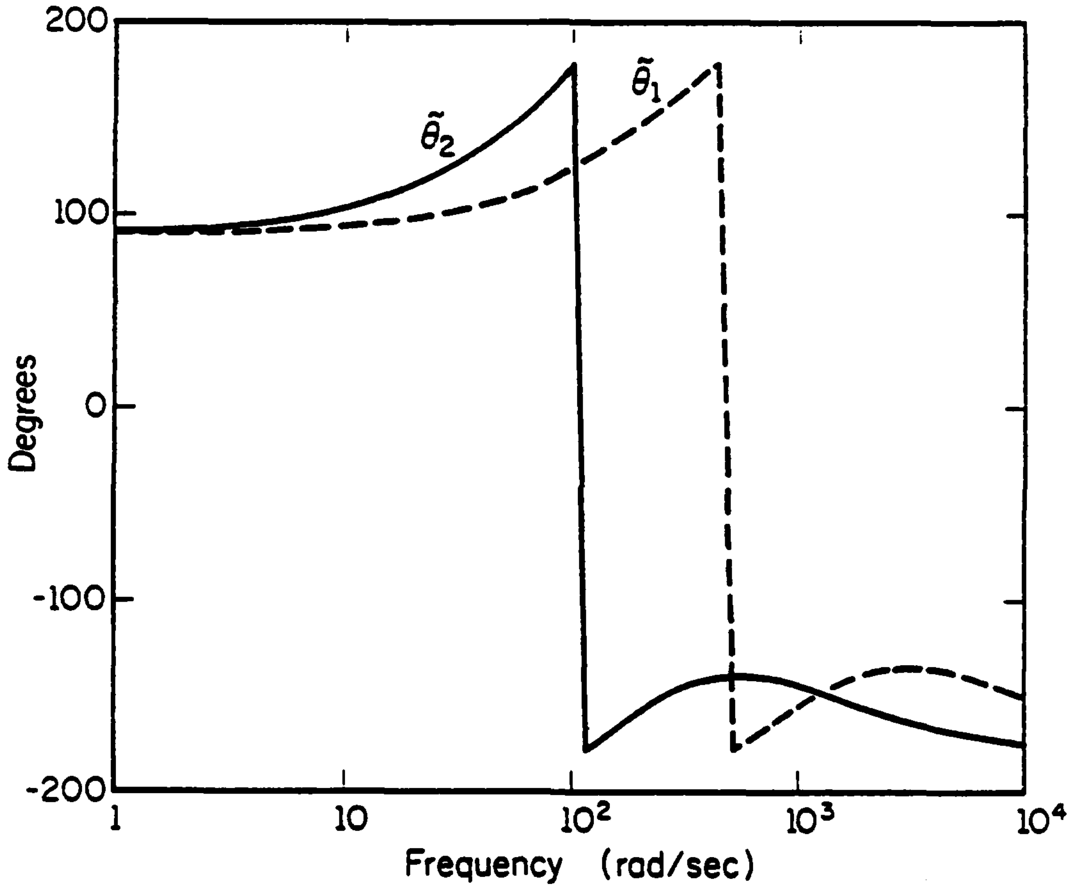

Figure 8.17. Phase differences $\tilde{\theta}_i = \measuredangle e_i^H v_i - \measuredangle e_i^H u_i$.

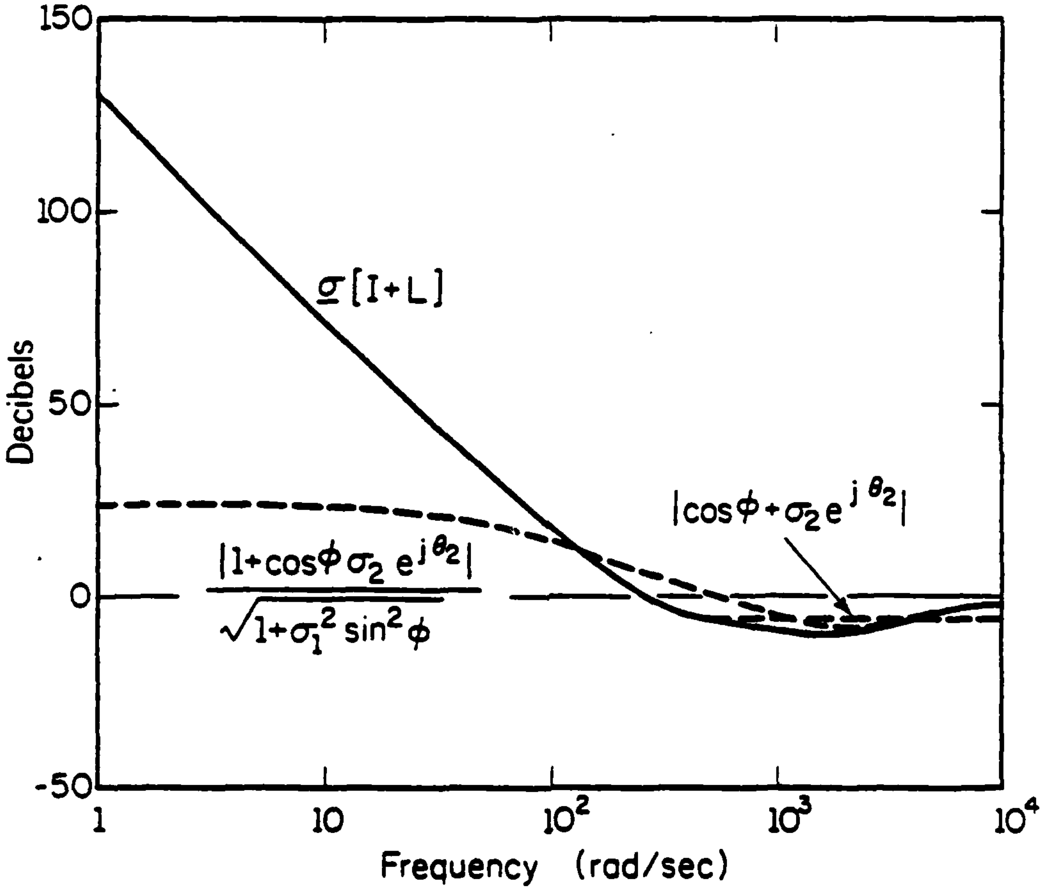

Figure 8.18. $\underline{\sigma}[I + L]$ and two approximations.

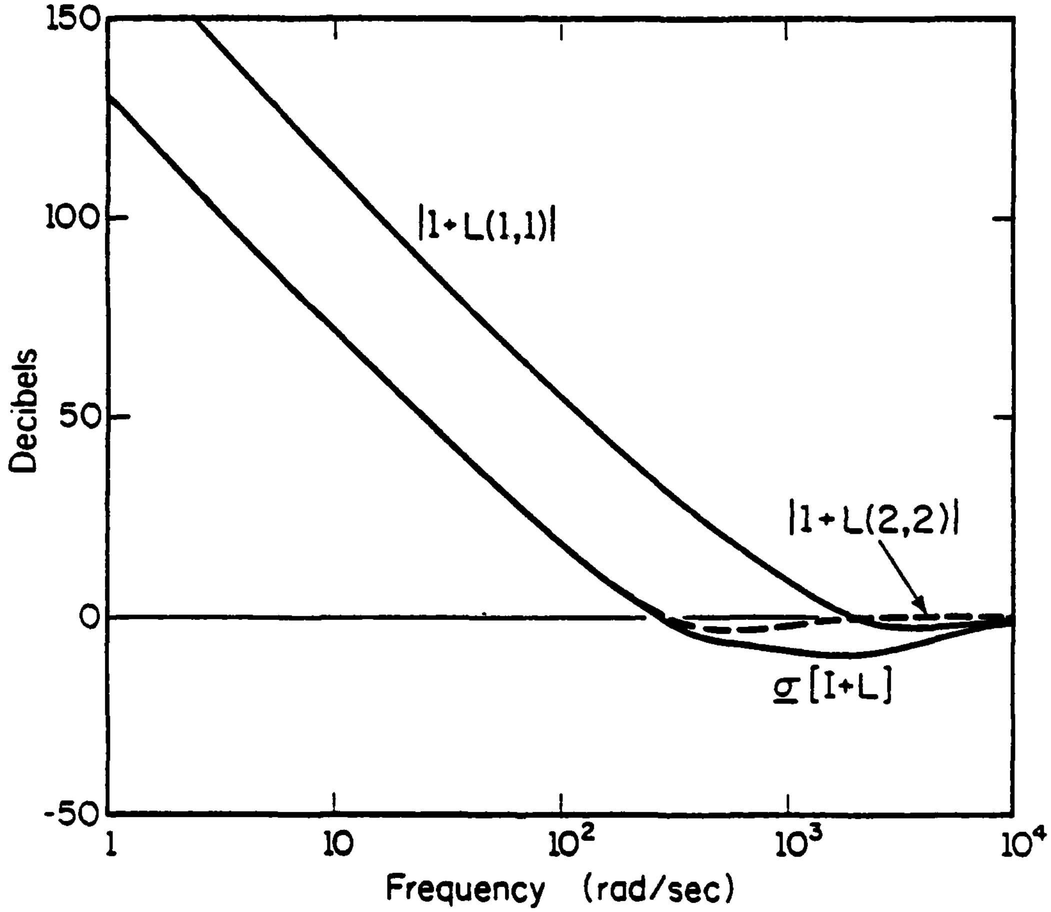

Figure 8.19. Single loop stability margins vs. singular value stability margin.

estimate feedback properties. The gains of the eigenvalues are plotted in Figure 8.11 while the phases are indistinguishable from the parameters θ_i plotted in Figure 8.16. Incidentally, this correspondence, together with the fact that the open loop singular values roll off at approximately the same rate as the eigenvalues (Figure 8.11), shows that the Bode gain phase relations are approximately satisfied by the functions $\sigma_i \, e^{j\theta_i}$. As demonstrated by the example in Section 8.4, there is no a priori reason why this should be true, especially since there is a significant amount of coupling present in the system.

The preceding discussion has shown that much valuable information about feedback properties may be obtained from analysis of the open loop transfer function. This fact has several advantages. First, these feedback properties may be determined a priori before a design is completed, rather than a posteriori as in [46]. This could reduce the number of iterations needed to achieve a satisfactory design. Second, the existence of a tradeoff between the level of coupling and good feedback properties can be seen and quantified. These two facts together serve to point out the usefulness of this method of analysis, since the tradeoff between desirable system properties may be made in part at an early stage in the design process. Thus the results of Sections 8.2 and 8.3 yield rules of thumb concerning the effect of coupling high and low gain subsystems. These rules may be used to gain a feel for the set of possible designs which is more efficient than resorting to trial and error. This characteristic is very much in the spirit of classical methods.

Finally, as discussed in [46], the reason that coupling was introduced into this design was to improve some open loop system properties (reducing torque requirements). The results of this chapter show how such open loop phenomena may be related to feedback properties.

8.6. Systems with Three Inputs and Three Outputs

The purpose of this section is to present some results for relating open to closed loop properties of systems with three inputs and three outputs. It will be seen that there exist both similarities to and differences from the two input two output cases.

Consider a system with three inputs and three outputs and suppose the open loop transfer function has much larger gain in one direction than in others. Then, as in (8.1), L(s) may be written

$$L = V_1\Sigma_1U_1^H + V_2\Sigma_2U_2^H \quad . \tag{8.53}$$

Since the subspaces $\mathfrak{U}_1$ and $\mathfrak{V}_1$ are one-dimensional, the matrices in (8.53) may be written $U_1 = u_1$, $V_1 = v_1$, $\Sigma_1 = \sigma_1$, $U_2 = [u_2 \mid u_3]$, $V_2 = [v_2 \mid v_3]$ and $\Sigma_2 = \mathrm{diag}[\sigma_2,\sigma_3]$. Suppose that the singular values are numbered so that $\sigma_1 >> \sigma_2 \geq \sigma_3$. Then, assuming the conditions in Theorem 8.3 are satisfied, it follows that the sensitivity function may be approximated by

$$S \approx S_{app} \triangleq U_2(V_2^HU_2 + \Sigma_2)^{-1}V_2^H \quad . \tag{8.54}$$

As in (7.15), let

$$\theta_i \triangleq \measuredangle\, u_i^H v_i \qquad i=1,\ldots,3 \tag{8.55}$$

and define

$$\hat{v}_i \triangleq e^{-j\theta_i}\, v_i \qquad i=1,\ldots,3 \quad . \tag{8.56}$$

Note the vectors u_i and v_i satisfy the relation

$$\hat{v}_i^H\, Lu_i = \sigma_i\, e^{j\theta_i} \quad . \tag{8.57}$$

Finally, define the matrices

$$\Theta = [\Theta_1 \mid \Theta_2] \triangleq \mathrm{diag}[\theta_1, \theta_2, \theta_3] \tag{8.58}$$

and

$$\begin{aligned} \hat{V} &= [\hat{V}_1 \mid \hat{V}_2] = V\, e^{j\Theta} \\ &= [\hat{v}_1 \mid \hat{v}_2 \mid \hat{v}_3] \quad . \end{aligned} \tag{8.59}$$

In terms of (8.59) the approximation (8.54) becomes

$$S_{app} = U_2(\hat{V}_2^H U_2 + \Sigma_2\, e^{j\Theta_2})^{-1} \hat{V}_2^H \quad . \tag{8.60}$$

Now from (8.60) it follows that

$$\begin{aligned} \bar{\sigma}[S] \approx \bar{\sigma}[S_{app}] &= \bar{\sigma}[(\hat{V}_2^H U_2 + \Sigma_2\, e^{j\Theta_2})^{-1}] \\ &= \frac{1}{\underline{\sigma}[(\hat{V}_2^H U_2 + \Sigma_2\, e^{j\Theta_2})]} \quad . \end{aligned} \tag{8.61}$$

In general it may be difficult to obtain simpler expressions for $\bar{\sigma}[S_{app}]$. Note, however, that lower bounds on $\bar{\sigma}[S_{app}]$ may be obtained from upper bounds on $\underline{\sigma}[S_{app}^{-1}]$. If any such lower bound is large, then the system has poor feedback properties. Thus, write

$$S_{app}^{-1} = \begin{bmatrix} \hat{v}_2^H u_2 + \sigma_2\, e^{j\theta_2} & \hat{v}_3^H u_2 \\ \hat{v}_2^H u_3 & \hat{v}_3^H u_3 + \sigma_3\, e^{j\theta_3} \end{bmatrix} . \tag{8.62}$$

From (8.62) it follows that an upper bound on $\underline{\sigma}[S_{app}^{-1}]$ is given by the norm of each row and of each column of S_{app}^{-1}. Define

$$\cos\phi_i = |u_i^H \hat{v}_i| . \tag{8.63}$$

Then (8.61) and (8.62) imply

$$\bar{\sigma}[S_{app}] \geq \max \begin{cases} 1/\sqrt{|\cos\phi_2 + \sigma_2\, e^{j\theta_2}|^2 + |\hat{v}_2^H u_3|^2} \\ 1/\sqrt{|\cos\phi_2 + \sigma_2\, e^{j\theta_2}|^2 + |\hat{v}_3^H u_2|^2} \\ 1/\sqrt{|\cos\phi_3 + \sigma_3\, e^{j\theta_3}|^2 + |\hat{v}_2^H u_3|^2} \\ 1/\sqrt{|\cos\phi_3 + \sigma_3\, e^{j\theta_3}|^2 + |\hat{v}_3^H u_2|^2} \end{cases} . \tag{8.64}$$

It is also possible to obtain upper and lower bounds on $\bar{\sigma}[S_{app}]$ using the relation

$$\frac{1}{\sqrt{2}} \|S_{app}\|_F \leq \bar{\sigma}[S_{app}] \leq \|S_{app}\|_F \tag{8.65}$$

where $\|M\|_F = \sqrt{\sum_{i,j} |M_{ij}|^2} = \sqrt{\sum_{i=1}^{n} \sigma_i^2}$ is the Frobenius norm of M. From

$$S_{app} = \frac{\begin{bmatrix} \cos\phi_3 + \sigma_3 e^{j\theta_3} & -\hat{v}_3^H u_2 \\ -\hat{v}_2^H u_3 & \cos\phi_2 + \sigma_2 e^{j\theta_2} \end{bmatrix}}{(\cos\phi_3 + \sigma_3 e^{j\theta_3})(\cos\phi_2 + \sigma_2 e^{j\theta_2}) - (\hat{v}_3^H u_2)(\hat{v}_2^H u_3)} \tag{8.66}$$

it follows that

$$\|S_{app}\|_F^2 = \frac{[|\cos\phi_3 + \sigma_3 e^{j\theta_3}|^2 + |\cos\phi_2 + \sigma_2 e^{j\theta_2}|^2 + |\hat{v}_3^H u_2|^2 + |\hat{v}_2^H u_3|^2]}{|(\cos\phi_3 + \sigma_3 e^{j\theta_3})(\cos\phi_2 + \sigma_2 e^{j\theta_2}) - (\hat{v}_3^H u_2)(\hat{v}_2^H u_3)|^2} . \tag{8.67}$$

The bounds (8.64)-(8.67) may be used to relate feedback properties to those of the open loop system, although the results are not as conclusive as those for two-input two-output systems in Section 8.3. Nonetheless, one can point out some differences between systems with two inputs and outputs and those with three inputs and outputs. For example, the quantities $|\cos\phi_i + \sigma_i e^{j\theta_i}|$ can be small without necessarily causing poor feedback properties to appear. Suppose $|\cos\phi_3 + \sigma_3 e^{j\theta_3}| \approx 0$. From (8.64) and (8.67) it follows that $\bar{\sigma}[S_{app}]$ will be large unless both $|\hat{v}_3^H u_2|$ and $|\hat{v}_2^H u_3|$ are bounded sufficiently away from zero. Note this implies two conditions. First, in order that $|\hat{v}_2^H u_3|$ and $|\hat{v}_3^H u_2|$ be as large as possible, outputs of L(s) due to inputs in the subspace $\mathcal{U}_2$ = {column space of $U_2 = [u_2 \mid u_3]$} should lie primarily in $\mathcal{U}_2$ as well. Second, there must exist coupling within the low gain subsystem; i.e., part of the output of L(s) due to an input in the direction spanned by u_2 (respectively, u_3) must be fed back into the direction spanned by u_3 (respectively, u_2).

Note also that if $|\cos\phi_3 + \sigma_3 e^{j\theta_3}| \approx 0$ and if $\sigma_2 >> 1$ then it follows from (8.65) and (8.67) that $\bar{\sigma}[S_{app}] >> 1$ independently of the magnitudes of $|\hat{v}_3^H u_2|$ and $|\hat{v}_2^H u_3|$. This makes sense because in this case outputs from the low gain subsystem represented by $\sigma_3 v_3 u_3^H$ can only be fed into a subsystem $\sigma_2 v_2 u_2^H$ with much higher levels of gain.

Suppose that there exists a range of frequencies over which $\sigma_1 >> \sigma_2 >> \sigma_3$. The MIMO generalizations of crossover frequency discussed in Section 8.2 may be applied to σ_1 and σ_3. Does there exist an analogue of crossover frequency for σ_2? To study this, note that the conditions $\sigma_1 >> \sigma_2 >> \sigma_3$ and $\sigma_3 << |\hat{v}_3^H u_3|$ imply

$$S_{app} \approx \frac{\begin{bmatrix} \hat{v}_3^H u_3 & -\hat{v}_3^H u_2 \\ -\hat{v}_2^H u_3 & \hat{v}_2^H u_2 + \sigma_2 e^{j\theta_2} \end{bmatrix}}{(\hat{v}_3^H u_3)(\hat{v}_2^H u_2 + \sigma_2 e^{j\theta_2}) - (\hat{v}_3^H u_2)(\hat{v}_2^H u_3)} \quad . \tag{8.68}$$

If $\sigma_2 >> |\hat{v}_2^H u_2|$, then $\bar{\sigma}[S_{app}] \approx \frac{1}{\cos\phi_3}$ as shown in Theorem 8.1. To obtain a generalization of MIMO crossover for σ_2, note that the denominator in (8.68) must be bounded away from zero. This motivates definition of crossover for σ_2 as being that frequency for which

$$\sigma_2 = \left| \frac{(\hat{v}_2^H u_2)(\hat{v}_3^H u_3) - (\hat{v}_3^H u_2)(\hat{v}_2^H u_3)}{\hat{v}_3^H u_3} \right| \quad . \tag{8.69}$$

Note that the numerator in (8.69) is equal to $|\det[\hat{V}_2^H U_2]|$. Recall the singular values of $\hat{V}_2^H U_2$ are equal to the cosines of the canonical angles

between the subspaces $\mathcal{U}_2$ and $\mathcal{V}_2$. Denote these angles by $\bar{\alpha}$ and $\underline{\alpha}$. Then (8.69) becomes

$$\sigma_2 = \frac{\cos\bar{\alpha} \cdot \cos\underline{\alpha}}{\cos\phi_3} \quad . \tag{8.70}$$

Note that $\cos\bar{\alpha} \leq \cos\phi_3 \leq \cos\underline{\alpha}$. Thus (8.70) gives a more accurate indication of crossover for σ_2 than the conditions $\cos\bar{\alpha} \leq \sigma_2 \leq \cos\underline{\alpha}$ imposed in Section 8.2. Also note that, although the value of θ_2 is important when (8.70) holds, θ_2 should not necessarily be bounded away from $\pm\pi$. This follows since the quantity $[-(\hat{v}_3^H u_2)(\hat{v}_2^H u_3)]$ can achieve complex values.

The results of this section have shown that it is possible to obtain approximations to feedback properties for higher dimensional systems. The results are not as conclusive, however, and this area definitely needs further research.

8.7. Summary

The purpose of this chapter has been to generalize one of the important aspects of classical feedback theory to MIMO systems. This aspect was the ability to approximate feedback properties in terms of the open loop transfer function. As described in Section 8.5, the results of this chapter may be used to obtain rules of thumb useful in design.

The results may also be used to gain information about various design procedures. For example, linear quadratic-state feedback designs are guaranteed, under certain conditions (e.g., [4, p. 13]), to possess

the property that $\bar{\sigma}[S(j\omega)] \leq 1, \forall\omega$. Some implications of this fact are pointed out in Section 7.3. The results of Section 8.2 show that it is not possible to use this design procedure to obtain a design with strongly coupled high and low gain subsystems.

Finally, note that the results of this chapter are based upon algebraic system properties; i.e., properties which are related at a given frequency by an algebraic equation. Based upon these results, it might be conjectured that a rule of thumb for good design is that coupling between subsystems with different levels of gain is always to be avoided. Certainly this would be true if system properties at different frequencies could be manipulated independently.

The various Bode integral and gain-phase relations show that system properties at different frequencies are not independent even for SISO systems. Thus the existence of coupling between high and low gain subsystems might be used to affect the value of some system parameter which might not appear, a priori, to depend upon coupling. This is best demonstrated by the example in Section 8.4. This example exhibited feedback properties which appeared to violate intuition based upon SISO Bode gain-phase relations. In order to achieve this, however, it was necessary to introduce coupling into the system. Thus the rule of thumb conjectured above fails when feedback properties constrained by the analyticity of transfer functions are considered. Describing such constraints is the subject of the remainder of this thesis.

CHAPTER 9

DIFFERENTIAL EQUATIONS FOR SINGULAR VALUES AND VECTORS

9.1. Introduction and Motivation

In Chapter 2, several Bode integral relations were introduced and their implications for design were discussed. In Chapter 3, one Bode relation was generalized and new integral relations were presented. Recall that these relations show not all design specifications are achievable and, therefore, tradeoffs among desirable system properties in different frequency ranges must be performed.

Although the Bode integrals are precise _quantitative_ statements, their greatest value may lie in the _qualitative_ insight they afford into system properties. This insight allowed the development of various rules of thumb useful in feedback design. As an example, consider the Bode gain-phase relation (Theorem 2.2). This relation shows that the open loop gain cannot be rolled off much faster than 20 db/decade near crossover frequency. The weighting function (2.25), however, shows that the value of phase near crossover is relatively independent of the gain behavior at frequencies much more than a decade or so away. (However, see [47] for discussion of a case where this rule of thumb fails to hold.) In any event, the integral relations and interpretations developed by Bode provide the theoretical foundation upon which the practice of feedback design is based.

The problem of deciding whether a given design specification is achievable can be restated as: Under what conditions is a given function of the complex frequency variable realizable as the transfer function of a

linear time invariant system? From well-known properties of the Laplace transform, it follows that one such condition is that the function must be locally analytic in the frequency variable. This fact is significant in that the mathematical tools used to derive the Bode integral relations are found in analytic function theory. It is apparent that the same tools must play a role in any attempt to extend these integral relations to MIMO systems.

First, note one way of viewing the Bode gain-phase relations (Theorem 2.2) is that they show how partial knowledge or partial specification of a transfer function can suffice to completely determine the function. Thus, although two real parameters or coordinates are necessary to describe a transfer function (e.g., gain and phase), there is in essence only one degree of freedom available for design.

Arguments based upon degrees of freedom can be made for MIMO systems as well. Consider a matrix transfer function written in standard coordinates; each element of this matrix is a scalar transfer function. Hence, the Bode gain-phase relations can be applied to each of these scalar functions to show that, of the $2n^2$ real coordinates needed to describe a transfer function matrix in $\mathbb{C}^{n\times n}$, there exist only n^2 degrees of freedom. The difficulty with this observation is that the gain and phase of these elements do not generally yield useful information about feedback properties.

It was argued in Chapters 6-8 of this thesis that certain parameterizations of the singular value decomposition of the open loop transfer function matrix <u>are</u> useful in assessing feedback properties.

These parameters include the singular values, parameters describing the directions of system inputs and outputs, and various measures of phase difference. In Section 7.4, two parameterizations of transfer function matrices in $\mathbb{C}^{2\times 2}$ were presented. Each of these parameterizations involved eight real coordinates; the above argument using standard coordinates and scalar gain-phase relations shows that these eight new coordinates must also only represent four degrees of freedom. An example giving some indication of the relation among these parameters was presented in Chapter 8, Section 8.4. The fact that these parameters do appear to be related to feedback properties motivates study of how the property of local analyticity is preserved under coordinate transformations.

The most useful statement of the dependence among system parameters is given by the gain-phase relations. There are other equations which must be satisfied by analytic functions which are more simple to treat mathematically than are the gain-phase relations. These include the Cauchy-Riemann equations, Laplace's equation, and Cauchy's integral formula. The manner in which these equations are preserved after coordinate transformations will thus be investigated first.

The remainder of this chapter is organized as follows. In Section 9.2 some elementary properties of analytic functions are reviewed and the question of whether singular values possess any of these properties is addressed. In Section 9.3, formulas for the derivatives of singular vectors are presented. It is shown that singular values and singular vectors are not independent quantities. Knowledge of singular values indeed determines some properties of the singular vectors. This relationship will be investigated in detail in later chapters of this thesis.

9.2. Analytic Function Theory and Singular Values

The mathematical tool used by Bode in deriving the integral relations discussed in the previous section was complex variable theory. This theory was applicable since transfer functions are locally analytic in the complex frequency variable. It is not apparent, however, that the same tools may be applied to study singular values of matrix transfer functions. Since singular values are real they cannot, by definition, be even locally analytic functions of s.

Recall that one interpretation of the scalar gain-phase relations emphasized that, along the $j\omega$-axis, knowledge of the gain of a transfer function suffices to determine the phase as well. This follows since gain and phase are not independent quantities under the conditions of Theorem 2.2. The last observation motivates the question: Does knowledge of a singular value of a transfer function matrix suffice to determine any other properties of the matrix?

The Bode gain-phase relations express the interdependence of scalar gain and phase in the form which is most useful in applications to feedback theory. It is mathematically more tractable, however, first to study this interdependence as expressed by the Cauchy-Riemann equations and properties of harmonic functions. To do this requires some results from complex variable theory. Background information is found in [26] and [48].

Definition 9.1. [48, p. 34]: Let D be an open subset of $\mathbb{C}$, the complex plane. Then, a function $f : D \to \mathbb{C}$ is analytic if f is continuously differentiable in D; i.e., if the derivative of f with respect to s exists and is continuous at all points of D. ∎

Definition 9.2. [48, p. 40]: A region is an open connected subset of the complex plane. ∎

Theorem 9.3. [48, p. 42]: Let g and h be real-valued functions defined on a region D of the complex s-plane, $s = x + jy$. Suppose that g and h have continuous first partial derivatives. Then, the function $f : D \to \mathbb{C}$, defined by $f(s) \triangleq g(s) + jh(s)$, is analytic if and only if g and h satisfy the Cauchy-Riemann equations:

$$\frac{\partial g}{\partial x} = \frac{\partial h}{\partial y}$$

$$\frac{\partial g}{\partial y} = -\frac{\partial h}{\partial x} \quad .$$

Equivalently,

$$\frac{\partial f}{\partial x} = \frac{1}{j}\frac{\partial f}{\partial y} \quad . \tag{9.1}$$

∎

If f(s) is analytic and nonzero on some region D then,

$$\log f = \log|f| + j\measuredangle f \tag{9.2}$$

is also analytic on D. Moreover, the log magnitude and phase of f satisfy the Cauchy-Riemann equations:

$$\begin{aligned} \frac{\partial \log|f|}{\partial x} &= \frac{\partial \measuredangle f}{\partial y} \\ \frac{\partial \log|f|}{\partial y} &= -\frac{\partial \measuredangle f}{\partial x} \quad . \end{aligned} \tag{9.3}$$

Equations (9.3) can be used to show that knowledge of the gain of a transfer function $f(s)$ in a simply connected region D where $f(s)$ is analytic and nonzero suffices to determine the phase of $f(s)$ up to an arbitrary constant. Given the value of $\measuredangle f$ at some point $s_o \in D$, the value at any other point $s \in D$ can be computed by a line integral. Let $\gamma: [0,1] \rightarrow D$ be a piecewise smooth path with $\gamma(0) = s_o$ and $\gamma(1) = s$. Then, $\measuredangle f(s)$ can be found by integrating the differential form

$$\begin{aligned} d\measuredangle f &= \frac{\partial \measuredangle f}{\partial x} dx + \frac{\partial \measuredangle f}{\partial y} dy \\ &= -\frac{\partial \log|f|}{\partial y} dx + \frac{\partial \log|f|}{\partial x} dy \end{aligned} \tag{9.4}$$

along γ. Thus,

$$\begin{aligned} \measuredangle f(s) &= \measuredangle f(s_o) + \int_\gamma d\measuredangle f \\ &= \measuredangle f(s_o) + \int_0^1 \left[\frac{\partial \measuredangle f}{\partial x}\frac{\partial x}{\partial t} + \frac{\partial \measuredangle f}{\partial y}\frac{\partial y}{\partial t}\right] dt \quad . \end{aligned} \tag{9.5}$$

Using the Cauchy-Riemann equations shows that the integral in (9.5) is determined by $|f|$:

$$\measuredangle f(s) = \measuredangle f(s_o) + \int_0^1 \left[-\frac{\partial \log|f|}{\partial y}\frac{\partial x}{\partial t} + \frac{\partial \log|f|}{\partial x}\frac{\partial y}{\partial t}\right] dt \quad . \tag{9.6}$$

The fact that $\measuredangle f(s)$ is well-defined in a simply connected region follows from the fact that the line integral in (9.5) is independent of the path γ. Path independence in a simply connected region is guaranteed, provided that the differential form (9.4) satisfies* the condition

*The elementary properties of differential forms used in this chapter can be found in [49].

$d^2 \measuredangle f = 0$, or

$$d^2 \measuredangle f = \left(\frac{\partial^2 \measuredangle f}{\partial y \partial x} - \frac{\partial^2 \measuredangle f}{\partial x \partial y} \right) dx \wedge dy \quad . \tag{9.7}$$
$$= 0$$

Note that (9.7) is equivalent to the familiar condition that mixed second partial derivatives are equal.

From the Cauchy-Riemann equations it follows that (9.7) is also equivalent to the requirement that $\log|f|$ satisfy Laplace's equation:

$$\frac{\partial^2 \log|f|}{\partial x^2} + \frac{\partial^2 \log|f|}{\partial y^2} = 0 \quad . \tag{9.8}$$

Definition 9.4. [48, p. 41]: A function with continuous second partial derivatives satisfying Laplace's equation is said to be harmonic. ■

If D is a simply connected region and $g : D \to \mathbb{R}$ is harmonic on D, then it can be shown [48, p. 43] that there exists another harmonic function $h : D \to \mathbb{R}$ such that the function $f : D \to \mathbb{C}$ defined by $f \triangleq g + jh$ is analytic on D. Such a function is termed a harmonic conjugate of g. It is a fact that the real part of any function analytic on some region D is harmonic on D and the imaginary part of the analytic function is a harmonic conjugate. In particular, on simply connected regions over which the logarithm of a transfer function, $\log f(s)$, is analytic, it follows that the phase, $\measuredangle f(s)$, is a harmonic conjugate of the log magnitude, $\log|f(s)|$.

Since singular values are a generalization of gain to MIMO systems, one might conjecture that each singular value is the magnitude of some locally analytic function (as is the gain of a scalar transfer function).

From the preceding discussion this conjecture would be true, provided that $\log \sigma_i$ is locally a harmonic function. The following example shows the conjecture is false, however.

Example 9.5: (Due to Doug Looze.)

Let

$$M(s) = \begin{bmatrix} s & 0 \\ 2 & s \end{bmatrix} .$$

The singular values of M(s) are given by

$$\sigma_1 = 1 + \sqrt{|s|^2 + 1}$$

$$\sigma_2 = -1 + \sqrt{|s|^2 + 1}$$

from which it may be verified that

$$\frac{\partial^2 \log\sigma_1}{\partial x^2} + \frac{\partial^2 \log\sigma_1}{\partial y^2} = \left(\frac{1}{\sqrt{|s|^2 + 1}}\right)^3$$

$$\frac{\partial^2 \log\sigma_2}{\partial x^2} + \frac{\partial^2 \log\sigma_2}{\partial y^2} = -\left(\frac{1}{\sqrt{|s|^2 + 1}}\right)^3 .$$

Proof: See Appendix F. ∎

The fact that $\log \sigma_i$ is not, in general, harmonic shows that σ_i cannot, in general, be the magnitude of some analytic function. In particular, knowledge of σ_i in a simply connected region does not suffice

to determine the value of a harmonic conjugate in the same way that the log magnitude of a scalar transfer function determined the phase of the function. Nonetheless, it can be shown that knowledge of a singular value of a matrix transfer function does determine other properties of the matrix. This will be seen from expressions for the derivative of a singular value.

Since singular values are not analytic in the complex frequency variable $s = x + jy$, it follows by definition that the derivative of a singular value with respect to s does not exist. Partial derivatives with respect to x and y do exist, however, although some care must be taken for the case of multiple singular values. A thorough discussion of the existence of partial derivatives of singular values and vectors is contained in Appendix G. To illustrate the discussion of this section and Section 9.3, it is sufficient to consider only distinct singular values. Proof of the existence of derivatives is deferred to Appendix G. The following formula for the derivative of a singular vector was originally derived in [10] but is given here for the sake of completeness.

Recall (Appendix B) that the square of each singular value is an eigenvalue of the matrix $[M(s)]^H M(s)$ with eigenspace given by the right singular subspace:

$$[M(s)]^H M(s) u_i(s) = \sigma_i^2 u_i(s) \quad . \tag{9.9}$$

From (9.9) it follows that (suppressing dependence on s):

$$u_i^H \frac{\partial M^H M}{\partial x} u_i - \sigma_i^2 \equiv 0$$

$$\Rightarrow \quad \sigma_i^2 \left[\frac{\partial u_i^H}{\partial x} u_i + u_i^H \frac{\partial u_i}{\partial x} \right] + u_i^H \frac{\partial M^H M}{\partial x} u_i - 2\sigma_i \frac{\partial \sigma_i}{\partial x} = 0 \quad . \tag{9.10}$$

Since u_i is, by definition, a unit vector:

$$u_i^H u_i \equiv 1$$

$$\Rightarrow \quad \frac{\partial u_i^H u_i}{\partial x} = 0$$

$$\Rightarrow \quad \mathrm{Re}\left[u_i^H \frac{\partial u_i}{\partial x} \right] \triangleq \frac{1}{2} \left[\frac{\partial u_i^H}{\partial x} u_i + u_i^H \frac{\partial u_i}{\partial x} \right] = 0 \quad . \tag{9.11}$$

Substituting (9.11) into (9.10) yields:

$$2\sigma_i \frac{\partial \sigma_i}{\partial x} = u_i^H \left[\frac{\partial M^H}{\partial x} M + M^H \frac{\partial M}{\partial x} \right] u_i$$

$$\Rightarrow \quad \frac{\partial \sigma_i}{\partial x} = \mathrm{Re}\left[v_i^H \frac{\partial M}{\partial x} u_i \right] \quad . \tag{9.12}$$

Similarly,

$$\frac{\partial \sigma_i}{\partial y} = \mathrm{Re}\left[v_i^H \frac{\partial M}{\partial y} u_i \right] \quad . \tag{9.13}$$

The fact that $M(s)$ is locally analytic implies that each element of $M(s)$ must satisfy the Cauchy-Riemann equations. This in turn yields:

Lemma 9.6: Let u and v be vectors in $\mathbb{C}^n$. Then if each element of $M(s)$ is analytic at $s = x + jy \in \mathbb{C}$, it follows that

$$\mathrm{Re}\left[v^H \frac{\partial M}{\partial x} u\right] = \mathrm{Im}\left[v^H \frac{\partial M}{\partial y} u\right]$$

and (9.14)

$$\mathrm{Re}\left[v^H \frac{\partial M}{\partial y} u\right] = -\mathrm{Im}\left[v^H \frac{\partial M}{\partial x} u\right] \qquad . \qquad \blacksquare$$

<u>Proof</u>: The Cauchy-Riemann Equations (9.1) yield:

$$\frac{\partial M}{\partial x} = \frac{1}{j}\frac{\partial M}{\partial y}$$

$$\Rightarrow \qquad v^H \frac{\partial M}{\partial x} u = \frac{1}{j} v^H \frac{\partial M}{\partial y} u \qquad . \tag{9.15}$$

Taking real and imaginary parts of (9.15) yields the result. ■

Note the similarity of Equations (9.14) to the Cauchy-Riemann Equations (9.1). Together with Equations (9.12)-(9.13), Lemma 9.6 shows that each singular value of a matrix locally analytic in s determines a differential form defined by (dropping the subscript "i" for convenience):

$$A \triangleq \frac{1}{\sigma}\,\mathrm{Im}\left[v^H \frac{\partial M}{\partial x} u\right] dx + \frac{1}{\sigma}\,\mathrm{Im}\left[v^H \frac{\partial M}{\partial y} u\right] dy$$

$$= \frac{-1}{\sigma}\,\mathrm{Re}\left[v^H \frac{\partial M}{\partial y} u\right] dx + \frac{1}{\sigma}\,\mathrm{Re}\left[v^H \frac{\partial M}{\partial x} u\right] dy \tag{9.16}$$

$$A = -\frac{\partial \log\sigma}{\partial y}\, dx + \frac{\partial \log\sigma}{\partial x}\, dy \qquad .$$

Recall that a differential form (9.4), similar to (9.16), was found to relate the gain and phase of a scalar transfer function. Again, one might conjecture there exists some function θ such that $A \equiv d\theta$. By the Poincaré Lemma [49, p. 94], such a function θ exists if and only if $dA = 0$. But, as Example 9.5 has shown, this is generally impossible; the

condition $dA = 0$ is equivalent to the Laplacian of $\log \sigma$ being equal to zero and this is not generally true.

The preceding discussion shows that the differential form (9.16) does not arise from the differential of any function (in geometric language, [49], the form is not exact). In particular, there exists no function θ for which $\log \sigma + j\theta$ is locally analytic. Hence σ cannot, in general, be the magnitude of a locally analytic function. Nonetheless, knowledge of a singular value does determine other properties of the matrix M. Thus one may now pose the question: What is the significance of the differential form A in (9.16) which is determined by $\sigma(x,y)$? To answer this question requires a discussion of the derivatives of the singular vectors.

9.3. Derivatives of Singular Vectors

In this section, formulas for the partial derivatives of singular vectors are presented. As in Section 9.2, questions of existence are relegated to Appendix G; similarly, the discussion in this section is restricted to singular values of multiplicity one.

First, recall the one degree of freedom which exists in choosing each pair of left and right singular vectors. This degree of freedom is discussed in detail in Appendix B but is reviewed here for convenience.

Corresponding to each singular value σ_i of multiplicity one there exist uniquely defined one-dimensional right and left singular subspaces denoted $\mathfrak{U}_i$ and $\mathfrak{V}_i$, respectively. These subspaces are determined

by a min-max principle inherited from properties of Hermitian matrices. One can choose the right singular vector as an arbitrary unit vector $u_i \in \mathfrak{U}_i$. If $\sigma_i \neq 0$, then the left singular vector is uniquely determined by the conditions that $v_i \in \mathfrak{V}_i$ and that $\sigma_i \equiv v_i^H M u_i$ is a positive real number. To illustrate the degree of freedom available, let u_i be one choice of right singular vector and let v_i be the corresponding left singular vector. Then, choosing a different right singular vector $\hat{u}_i = e^{j\alpha} u_i$ yields a different left singular vector $\hat{v}_i = e^{j\alpha} v_i$.

Now, consider the singular vectors along a curve in the complex plane: $\gamma(t) = x(t) + jy(t)$. Since it was assumed that the singular values are distinct along $\gamma(t)$, it follows by continuity that this property holds in a neighborhood of each point in the image of γ. The results of Appendix G can then be applied to show that the singular vectors may be chosen to be differentiable in (x,y) in some neighborhood of each point in the image of γ. One can think of the motion of a singular vector along $\gamma(t)$ as being decomposed into two components. One component measures how the appropriate <u>singular subspace</u> is changing along γ and is well determined by the min-max characterization of singular values and vectors. The other component is a function of which unit vector in the subspace is being "chosen" as <u>the</u> singular vector. Note that this component would be arbitrary (subject to smoothness) if the <u>convention</u> that $\sigma_i = v_i^H M u_i$ be positive real were not imposed; obviously, $\sigma_i = |v_i^H M u_i|$ for any unit vectors in the appropriate subspaces. A helpful picture to keep in mind is that of a vector which moves along a path in space (motion of the singular subspace) as well as "spins" as it moves (motion within the singular subspace). This analogy will be made precise in Chapter 10. First, formulas for partial derivatives of singular vectors will be discussed.

Let u_i and v_i be right and left singular vectors corresponding to a singular value σ_i of multiplicity one. Write the derivatives of u_i and v_i with respect to x as (a similar formula holds for the derivatives with respect to y)

$$\frac{\partial u_i}{\partial x} = \sum_{k=1}^{n} u_k \left(u_k^H \frac{\partial u_i}{\partial x} \right) \tag{9.17}$$

$$\frac{\partial v_i}{\partial x} = \sum_{k=1}^{n} v_k \left(v_k^H \frac{\partial v_i}{\partial x} \right) \quad . \tag{9.18}$$

Using various properties of the singular values and vectors yields, for $i \neq k$

$$M^H M u_i = \sigma_i^2 u_i$$

$$\Rightarrow \quad \frac{\partial M^H M}{\partial x} u_i + M^H M \frac{\partial u_i}{\partial x} = 2\sigma_i \frac{\partial \sigma_i}{\partial x} u_i + \sigma_i^2 \frac{\partial u_i}{\partial x}$$

$$\Rightarrow \quad u_k^H \frac{\partial M^H M}{\partial x} u_i + \sigma_k^2 u_k^H \frac{\partial u_i}{\partial x} = 0 + \sigma_i^2 u_k^H \frac{\partial u_i}{\partial x}$$

$$\Rightarrow \quad u_k^H \frac{\partial u_i}{\partial x} = \left(\frac{1}{\sigma_i^2 - \sigma_k^2} \right) \left\{ u_k^H \frac{\partial M^H}{\partial x} M u_i + u_k^H M^H \frac{\partial M}{\partial x} u_i \right\}$$

$$\Rightarrow \quad u_k^H \frac{\partial u_i}{\partial x} = \left(\frac{1}{\sigma_i^2 - \sigma_k^2} \right) \left\{ \sigma_i u_k^H \frac{\partial M^H}{\partial x} v_i + \sigma_k v_k^H \frac{\partial M}{\partial x} u_i \right\} \quad . \tag{9.19}$$

Similarly,

$$v_k^H \frac{\partial v_i}{\partial x} = \left(\frac{1}{\sigma_i^2 - \sigma_k^2} \right) \left\{ \sigma_k u_k^H \frac{\partial M^H}{\partial x} v_i + \sigma_i v_k^H \frac{\partial M}{\partial x} u_i \right\} \quad . \tag{9.20}$$

From (9.11) it follows that

$$\mathrm{Re}\left[u_i^H \frac{\partial u_i}{\partial x}\right] = 0$$

and (9.21)

$$\mathrm{Re}\left[v_i^H \frac{\partial v_i}{\partial x}\right] = 0 \quad .$$

It remains to calculate $\mathrm{Im}\left[u_i^H \frac{\partial u_i}{\partial x}\right]$ and $\mathrm{Im}\left[v_i^H \frac{\partial v_i}{\partial x}\right]$. From the identity

$$v_i^H M u_i \equiv \sigma_i$$

$$\Rightarrow \quad \frac{\partial v_i^H}{\partial x} M u_i + v_i^H \frac{\partial M}{\partial x} u_i + v_i^H M \frac{\partial u_i}{\partial x} = \frac{\partial \sigma_i}{\partial x}$$

$$\Rightarrow \quad \sigma_i \left[\frac{\partial v_i^H}{\partial x} v_i + u_i^H \frac{\partial u_i}{\partial x}\right] + \mathrm{Re}\left[v_i^H \frac{\partial M}{\partial x} u_i\right] + j\mathrm{Im}\left[v_i^H \frac{\partial M}{\partial x} u_i\right] = \frac{\partial \sigma_i}{\partial x}$$

$$\Rightarrow \quad \left[v_i^H \frac{\partial v_i}{\partial x} - u_i^H \frac{\partial u_i}{\partial x}\right] = \frac{j}{\sigma_i} \mathrm{Im}\left[v_i^H \frac{\partial M}{\partial x} u_i\right] \quad . \tag{9.22}$$

Note that the right hand side of (9.22) shows that the left hand side is independent of the choice of singular vectors.

The degree of freedom available in the choice of singular vectors manifests itself in the differential equations governing their behavior. To see this, consider a path $\gamma = x + jy : [0,1] \to \mathbb{C}$. In Appendix G it is shown, using results of Kato [32], that there exists a unit vector $u_i(t)$ defined along $\gamma(t)$ with the properties that $u_i(t)$ is analytic in t and that $u_i(t) \in \mathcal{U}_i(t)$, the ith right singular subspace. Thus $u_i(t)$ is one possible choice of the ith right singular vector. Let $\beta(t)$ be an arbitrary real valued function analytic in t. It follows that another choice of ith right singular vector, also analytic in t, is given by

$$\hat{u}_i(t) \triangleq e^{j\beta(t)} u_i(t) \quad .$$

Note that

$$\frac{d\hat{u}_i}{dt} = e^{j\beta}\frac{du_i}{dt} + e^{j\beta}\, j\,\frac{d\beta}{dt}\, u_i$$

$$= e^{j\beta}\frac{du_i}{dt} + \hat{u}_i\, j\,\frac{d\beta}{dt} \quad .$$

Thus

$$\hat{u}_i^H \frac{d\hat{u}_i}{dt} = \hat{u}_i^H e^{j\beta}\frac{du_i}{dt} + j\,\frac{d\beta}{dt}$$

$$= u_i^H \frac{du_i}{dt} + j\,\frac{d\beta}{dt} \quad .$$

Since u_i and $\hat{u}_i$ are unit vectors, $u_i^H \frac{du_i}{dt}$ and $\hat{u}_i^H \frac{d\hat{u}_i}{dt}$ must be purely imaginary. Hence the lack of uniqueness in choosing the right singular vector indeed manifests itself in the differential equation governing the vector. The right singular vector may be chosen so that the component of its derivative given by $u_i^H \frac{du_i}{dt}$ is any arbitrary function of t, subject only to differentiability requirements.

It remains to verify that this is indeed the only degree of freedom available in choosing the differential equations governing the singular vector pair. To see this, first note that once the component $u_i^H \frac{du_i}{dt}$ is specified it follows that $v_i^H \frac{dv_i}{dt}$ is completely determined from the equation

$$v_i^H \frac{dv_i}{dt} - u_i^H \frac{du_i}{dt} = \frac{j}{\sigma_i}\,\mathrm{Im}[v_i^H \frac{dM}{dt} u_i] \quad .$$

Second, note that $\frac{du_i}{dt}$ and $\frac{dv_i}{dt}$ are <u>not</u> functions of the choices of right and left singular vectors u_k and v_k, $k \neq i$. This follows since the projection operators $u_k u_k^H$ and $v_k v_k^H$ in (9.17) and (9.18) are functions <u>only</u> of the singular subspaces $\mathfrak{U}_k$ and $\mathfrak{V}_k$.

To summarize, one can construct a pair of left and right singular vectors along any path $\gamma(t)$ (over which the corresponding singular value is distinct) by integrating the differential equations

$$\frac{du_i}{dt} = \sum_{k=1}^{n} u_k (u_k^H \frac{du_i}{dt})$$

$$\frac{dv_i}{dt} = \sum_{k=1}^{n} v_k (v_k^H \frac{dv_i}{dt}) \quad .$$

In these equations the terms $u_k(u_k^H \frac{du_i}{dt})$ and $v_k(v_k^H \frac{dv_i}{dt})$ for $k \neq i$ are completely determined from (9.19) and (9.20) and similar equations in y. The terms $u_i(u_i^H \frac{du_i}{dt})$ and $v_i(v_i^H \frac{dv_i}{dt})$ possess one degree of freedom. Once this degree of freedom is utilized in choosing the component $u_i^H \frac{du_i}{dt}$ or $v_i^H \frac{dv_i}{dt}$ (or some combination thereof), the remaining component is completely determined from (9.22) and a similar equation in y.

Given an initial condition $u_i(0)$, let $u_i^*(t)$ denote the right singular vector obtained by setting $u_i^H \frac{du_i}{dt} \equiv 0$ and integrating the resulting differential equation along $\gamma(t)$. Note that, of all possible choices of $u_i(t)$ along γ, the choice $u_i^*(t)$ yields the minimum possible magnitude of $\left\| \frac{du_i}{dt} \right\|_2$. This follows since $u_i^{*H} \frac{du_i^*}{dt} \equiv 0$ by construction and the other components can change only by a multiple of $e^{j\beta(t)}$ for some real valued $\beta(t)$. Thus, $u_i^*(t)$ changes along γ only enough to remain in the correct singular subspace and no more.

With this choice of right singular vector the left singular vector is completely determined; from (9.22)

$$v_i^H \frac{dv_i}{dt} = \frac{j}{\sigma_i} \operatorname{Im} \left[v_i^H \frac{dM}{dt} u_i \right] \quad . \tag{9.23}$$

The magnitude of $\frac{1}{\sigma_i} \operatorname{Im}[v_i^H \frac{dM}{dt} u_i]$ indicates how much the left singular vector chosen as described deviates from the "minimum energy" left singular vector obtained by setting $v_i^H \frac{dv_i}{dt} = 0$.

Of all possible choices of singular vectors, the choice such that either $v_i^H \frac{dv_i}{dt} = 0$ or $u_i^H \frac{du_i}{dt} = 0$ yields the minimum possible value of $\left\|\frac{du_i}{dt}\right\|_2 + \left\|\frac{dv_i}{dt}\right\|_2$ subject to (9.22). This fact should have significance since

$$
\begin{aligned}
&\frac{1}{\sigma_i} \operatorname{Im}[v_i^H \frac{dM}{dt} u_i] \\
&= \frac{1}{\sigma_i} \operatorname{Im}[v_i^H \frac{\partial M}{\partial x} u_i]\frac{dx}{dt} + \frac{1}{\sigma_i} \operatorname{Im}[v_i^H \frac{\partial M}{\partial y} u_i]\frac{dy}{dt} \\
&= -\frac{\partial \log\sigma_i}{\partial y}\frac{dx}{dt} + \frac{\partial \log\sigma_i}{\partial x}\frac{dy}{dt} \qquad (9.24) \\
&= A_i(\frac{d\gamma}{dt})
\end{aligned}
$$

where the last equality follows by evaluating the differential form (9.16) on the tangent vector to the curve γ.

Thus the quantity $\frac{1}{\sigma_i} \operatorname{Im}[v_i^H \frac{dM}{dt} u_i]$, which measures the deviation of the singular vector pair from the pair which moves just enough to remain in the proper singular subspaces, is determined by the singular value σ_i. In answer to the question posed at the end of Section 9.2 it can be said that the singular value determines some property of the singular vector pair.

Now, recall the two components of singular vector motion discussed above. An analogy was made between these two components and vectors in $\mathbb{R}^3$ which move in space as well as "spin" as they move. If the spin component can be identified with $u_i^H \frac{du_i}{dt}$, then setting this component equal to zero implies the vector is not spinning as it moves. The following discussion will hopefully clarify this.

One can consider spinning as a generalization of the following situation. Suppose that along $\gamma(t)$ the right singular subspace $\mathcal{U}_i$ is constant ($u_j^H \frac{du_i}{dt} = 0$, $i \neq j$). Then, $u_i(t) = e^{j\theta(t)} u_i$, where u_i is constant, and $u_i^H \frac{du_i}{dt} = j \frac{d\theta}{dt}$. The change in θ along γ can be thought of as spinning or twisting of the singular vector. (Think of a pencil being held in a fixed direction, but being twisted about its lengthwise axis.) Now it is clear that for the case of a <u>constant</u> singular subspace, $u_i^H \frac{du_i}{dt} = 0 \Rightarrow u_i(t) =$ constant. Now, intuition suggests that a motion analogous to spinning takes place even if the singular subspace is not constant. In particular, $u_i^H \frac{du_i}{dt}$ should be a measure of the spinning and $u_i^H \frac{du_i}{dt} = 0$ should mean that $u_i(t)$ is not spinning. Consider a thought experiment: Suppose $\gamma(t)$ is a closed curve; i.e., $\gamma : [0,1] \to \mathbb{C}$, $\gamma(0) = \gamma(1)$. If the singular vector does not spin then will $u_i(1) = u_i(0)$ when (9.17) is integrated with $u_i^H \frac{du_i}{dt} = 0$? Clearly, this will be the case if the singular subspace is constant; thus, if $u_i(1) \neq u_i(0)$ it must be due to the motion of the singular subspace along γ. These questions will be pursued shortly.

In earlier chapters it was argued that certain measures of phase difference between singular vectors have interpretations in terms of feedback system properties. The fact that each singular value, via (9.24), constrains a quantity which determines the difference in components $u_i^H \frac{du_i}{dt}$ and $v_i^H \frac{dv_i}{dt}$ suggests that this measure of phase difference might be related to these components. Thus in the attempt to generalize Bode gain-phase relations to MIMO systems it would appear that understanding the property of singular vector pairs governed by $\frac{1}{\sigma_i} \mathrm{Im}[v_i^H \frac{dM}{dt} u_i]$ may be of significance.

9.4. Summary

The purpose of the preceding discussion has been to motivate further investigations of the property of each singular vector pair determined by the singular value. To summarize, in SISO systems, once gain is specified then phase is determined and this has important design implications. In MIMO systems gain and gain directions, as quantified by singular values and subspaces, as well as certain measures of phase difference between singular vectors have design implications. Now, each singular value determines some property of the associated singular vector pair; intuitively this should have something to do with the measure of phase difference between the pair of singular vectors. In order to pursue this question, it is convenient to assign coordinates to the singular vectors and to use these coordinates to study the solutions to the differential equations governing these vectors. This is pursued in the next chapter.

Finally, a formula for the Laplacian of the logarithm of a singular value will be presented. For simplicity it will be assumed that the singular values are all distinct.

Theorem 9.7: Assume that M(s) is a matrix of transfer functions taking values in $\mathbb{C}^{n\times n}$ and assume that each element of M(s) is analytic at s_o. In addition assume that $M(s_o)$ is nonsingular and that the singular values of $M(s_o)$ are distinct and ordered so that $\sigma_1 > \sigma_2 > \ldots > \sigma_n > 0$. Then the Laplacian of the logarithm of each singular value is given by

$$\nabla^2 \log\sigma_i \triangleq \frac{\partial^2 \log\sigma_i}{\partial x^2} + \frac{\partial^2 \log\sigma_i}{\partial y^2}$$

$$= \sum_{k \neq i} \frac{1}{(\sigma_i^2 - \sigma_k^2)} \left\{ \left|v_k^H \frac{\partial M}{\partial x} u_i\right|^2 + \left|v_k^H \frac{\partial M}{\partial y} u_i\right|^2 + \left|v_i^H \frac{\partial M}{\partial x} u_k\right|^2 + \left|v_i^H \frac{\partial M}{\partial y} u_k\right|^2 \right\} . \quad (9.25)$$

■

<u>Proof</u>: See Appendix H. ■

Note (9.25) proves that, in general, log σ_i is not a harmonic function. In particular, at points for which $\nabla^2 \log\sigma_i < 0$, it follows that log σ_i is locally superharmonic [50]. This means that σ_i can have local maxima but no local minima. Similarly, if $\nabla^2 \log\sigma_i > 0$, it follows that log σ_i is locally subharmonic and can have local minima but no local maxima. By contrast, recall that harmonic functions can have no local maxima or minima. Note that the largest singular value is always subharmonic and that the smallest singular value is always superharmonic.

A final motivation for the additional study of singular vectors may be obtained by comparing (9.25) to the formulas (9.17)-(9.20) for the derivatives of the singular vectors. Obviously, if the singular subspaces are constant, $v_k^H \frac{\partial v_i}{\partial x}$, $v_k^H \frac{\partial v_i}{\partial y}$, $u_k^H \frac{\partial u_i}{\partial x}$ and $u_k^H \frac{\partial u_i}{\partial y}$, $\forall k \neq i$, must all equal zero. From (9.19) and (9.20), it follows that $v_k^H \frac{\partial M}{\partial x} u_i$, etc., must also equal zero. Consequently, $\nabla^2 \log\sigma_i = 0$, $\forall i$. Thus properties of singular values, (i.e., the extent to which log σ_i fails to be harmonic) are related to that component of singular vector motion given by the motion of the singular subspaces.

CHAPTER 10

MATHEMATICAL STRUCTURE OF SINGULAR VECTORS, I

10.1. Introduction

The purpose of this chapter is to develop a mathematical framework within which to study properties of the singular vectors obtained from the singular value decomposition of a matrix transfer function. Once these properties have been described they will be used, in Chapter 11, to explain the meaning of the differential form

$$\begin{aligned}
&\left[v_i^H \frac{\partial v_i}{\partial x} - u_i^H \frac{\partial u_i}{\partial x}\right] dx + \left[v_i^H \frac{\partial v_i}{\partial y} - u_i^H \frac{\partial u_i}{\partial y}\right] dy \\
&\quad = \frac{j}{\sigma_i} \operatorname{Im}\left[v_i^H \frac{\partial M}{\partial x} u_i\right] dx + \frac{j}{\sigma_i} \operatorname{Im}\left[v_i^H \frac{\partial M}{\partial y} u_i\right] dy \\
&\quad = j\left[-\frac{\partial \log \sigma_i}{\partial y} dx + \frac{\partial \log \sigma_i}{\partial x} dy\right]
\end{aligned} \tag{10.1}$$

which was introduced in Chapter 9.

First, it will be shown that the unit sphere in $\mathbb{C}^n$, the space in which singular vectors lie, has the mathematical structure of a principal fiber bundle. Using this structure, various notions of the phase of a singular vector and the phase difference between a pair of singular vectors can be introduced. A complete set of coordinates for the singular vectors may be obtained from the phase coordinates just described as well as a set of coordinates for the complex projective space $\mathbb{C}P^{n-1}$. This space consists of the directions in $\mathbb{C}^n$, a concept introduced in Chapter 6.

10.2. Fiber Bundles and Singular Vectors

In order to study the differential equations governing the motion of singular vectors, it is first necessary to describe the structure of the space in which these vectors lie. The relevant space is the unit sphere in $\mathbb{C}^n$; in this section it is shown that the unit sphere has the structure of a principal fiber bundle. This structure naturally allows a unit vector to be described by giving its direction (see Chapter 6) as well as a parameter analogous to phase.

First, the set of directions in $\mathbb{C}^n$ will be described as points in complex projective space, a manifold with complex dimension (n-1).

Definition 10.1 [51, p. 47; 52, p. 114]: For each integer n identify $\mathbb{R}^{2n}$ with $\mathbb{C}^n$ and denote the points by $z = (z_1, \ldots, z_n)$. Then the unit sphere $S^{2n-1} \subseteq \mathbb{C}^n$ is given by

$$S^{2n-1} = \{(z_1, \ldots, z_n) \mid \sum_{i=1}^{n} |z_i|^2 = 1\}. \tag{10.2}$$

Define an equivalence relation on S^{2n-1} by $z \sim z'$ if and only if there exists a complex number λ with $|\lambda| = 1$ such that $z = \lambda z'$. The quotient space $S^{2n-1}/\sim$ is denoted by $\mathbb{C}P^{n-1}$ and is termed (n-1)-dimensional complex projective space. Given $z \in S^{2n-1}$ the corresponding point in $\mathbb{C}P^{n-1}$ is denoted $[z]$. ■

The vectors in a given equivalence class can be distinguished by assigning to each a number analogous to phase. This may be done by choosing an arbitrary vector z in the equivalence class and defining the phase of other vectors $\hat{z} \in [z]$ by the rule

$$\theta(\hat{z}) = \measuredangle\, z^H \hat{z}. \tag{10.3}$$

In particular each equivalence class may be placed in one-to-one correspondence with the unit circle S^1 by defining a point on the unit circle in the complex plane by $e^{j\theta}$, $\theta \in (-\pi, \pi]$.

The above observations may be used to show the unit sphere in $\mathbb{C}^n$ has the structure of a principal fiber bundle. A layman's description of fiber bundles and their application to physics is found in [53]; a precise treatment is found in [54]. The basic definitions and properties of fiber bundles are now described. Following the mathematical preliminaries a discussion of their relevance to the study of singular vectors will be given. The following definitions are taken from [54]. In the interest of brevity, not all terms will be defined; however, references to the relevant pages of [54] will be given.

Definition 10.2 [54, p. 26]: A principal fiber bundle (PFB) consists of a manifold P (called the total space), a Lie group G [54, p. 18], a base manifold M, and a projection map $\pi : P \to M$ such that (A), (B), and (C) are satisfied.

(A) The group G acts freely and differentiably on P to the right [54, p. 26].

(B) The map $\pi : P \to M$ is onto and $\pi^{-1}(\pi(p)) = \{pg : g \in G\}$. If $x \in M$, then $\pi^{-1}(x)$ is called the fiber above x.

(C) For each $x \in M$ there is an open set U_α with $x \in U_\alpha$ and a diffeomorphism [54, p. 7] $T_\alpha : \pi^{-1}(U_\alpha) \to U_\alpha \times G$ of the form $T_\alpha(p) = (\pi(p), s_\alpha(p))$ where $s_\alpha : \pi^{-1}(U_\alpha) \to G$ has the property $s_\alpha(pg) = s_\alpha(p)g$ for all $g \in G$, $p \in \pi^{-1}(U_\alpha)$. The map T_α is called a local trivialization. ∎

Note (C) states that locally the PFB must look like the product of the base space with the Lie group.

Definition 10.3 [54, p. 27]: Let $T_\alpha : \pi^{-1}(U_\alpha) \to U_\alpha \times G$ and $T_\beta : \pi^{-1}(U_\beta) \to U_\beta \times G$ be two local trivializations of a PFB $\pi : P \to M$ with group G. The transition function from T_α to T_β is the map $g_{\alpha\beta} : U_\alpha \cap U_\beta \to G$ defined, for $x = \pi(p) \in U_\alpha \cap U_\beta$, by $g_{\alpha\beta}(x) = s_\alpha(p)[s_\beta(p)]^{-1}$. Note that $g_{\alpha\beta}(x)$ is independent of the choice of $p \in \pi^{-1}(x)$ because

$$s_\alpha(pg)[s_\beta(pg)]^{-1} = s_\alpha(p)g[s_\beta(p)g]^{-1} = s_\alpha(p)[s_\beta(p)]^{-1}.$$

The following properties hold:

(i) $g_{\alpha\alpha}(y) = e$ for all $y \in U_\alpha$, where e is the identity element of the group G.

(ii) $g_{\beta\alpha}(y) = [g_{\alpha\beta}(y)]^{-1}$ for all $y \in U_\alpha \cap U_\beta$.

(iii) $g_{\alpha\beta}(y) g_{\beta\gamma}(y) g_{\gamma\alpha}(y) = e$ for all $y \in U_\alpha \cap U_\beta \cap U_\gamma$. ∎

The transition functions describe how the products $U_\alpha \times G, U_\beta \times G$, etc. piece together to form the total space P. Thus P may be considered as the space obtained from the disjoint union $(U_\alpha \times G) \cup (U_\beta \times G) \cup \ldots$ by identifying the point $(x,g) \in U_\alpha \times G$ with $(x,g') \in U_\beta \times G$ if $g = g_{\alpha\beta}(x)g'$.

Definition 10.4 [54, p. 27]: A local section of a PFB $\pi : P \to M$ with group G is a map $\rho_\alpha : U_\alpha \to P$ ($U_\alpha \subset M, U_\alpha$ open) such that $\pi \circ \rho_\alpha = 1_\alpha \equiv$ the identity function on U_α. ∎

Theorem 10.5 [54, p. 27]: There is a natural correspondence between local sections and local trivializations. ∎

Proof: If $\rho_\alpha : U_\alpha \to P$ is a local section, then define $T_\alpha : \pi^{-1}(U_\alpha) \to U_\alpha \times G$ by $T_\alpha(\rho_\alpha(x)g) = (x,g)$. Conversely, given a local trivialization $T_\alpha : \pi^{-1}(U_\alpha) \to U_\alpha \times G$, define a local section $\rho_\alpha : U_\alpha \to P$ by $\rho_\alpha(x) = T_\alpha^{-1}(x,e)$, where e is the identity element of G. ∎

Definition 10.6 [54, p. 27]: If T_α is a local trivialization with $U_\alpha = M$ (i.e., $T_M : P \to M \times G$), then T_M is called a global trivialization, and the PFB is called trivial if such a T_M exists. A local section $\rho_\alpha : U_\alpha \to P$ is called a global section if $U_\alpha = M$. Global sections correspond to global trivializations. ∎

In the present case the total space is the unit sphere in $\mathbb{C}^n$, identified with $S^{2n-1} \subset \mathbb{R}^{2n}$, and the base manifold is complex projective space $\mathbb{C}P^{n-1}$. The Lie group is the scalar unitary group

$$U(1) \triangleq \{e^{j\theta};\ \theta \in \mathbb{R}\} \tag{10.4}$$

and the projection map is that taking a unit vector in $\mathbb{C}^n$ to its equivalence class via the relation in Definition 10.1.

Condition (A) of Definition 10.2 means, for the present purpose, that for each element $g = e^{j\theta} \in U(1)$ there exists a mapping $R_g : S^{2n-1} \to S^{2n-1}$ defined by $R_g(z) = ze^{j\theta}$, $z \in S^{2n-1}$, and that this mapping is nicely behaved. Condition (B) means that each fiber of the bundle looks like the Lie group $U(1)$ and thus like the unit circle S^1. This motivates referring to the set of unit vectors in $\mathbb{C}^n$ as a circle bundle over complex projective space. Condition (C) may be interpreted as stating that locally it is possible to define the phase of a vector signal. This is now discussed.

The discussion preceding (10.3) shows how one might place each fiber in one-to-one correspondence with the interval $(-\pi, \pi]$ and thus with the Lie group $U(1)$. This suggests one way to construct local trivializations. The definition of $\theta(\hat{z})$ in (10.3) can obviously be extended to all vectors not orthogonal to the reference vector z; thus the neighborhood U_α in (C) can be extended to include all points in $\mathbb{C}P^{n-1}$ representing subspaces of

$\mathbb{C}^n$ not orthogonal to that spanned by z. The corresponding diffeomorphism $T_z : \pi^{-1}(U_z) \to U_z \times G$ is given by

$$T_z(y) = ([y], e^{j\theta_z(y)}) \tag{10.5}$$

with

$$\theta_z(y) \overset{\Delta}{=} \measuredangle\, z^H y, \quad \theta_z \in (-\pi, \pi].$$

Note that $\theta_z(ye^{j\theta_1}) = \theta_z(y) + \theta_1$ as required. Again, this construction shows that it is possible to define the phase of unit vectors in $\mathbb{C}^n$ locally and that the domain of definition can be extended to include all vectors not orthogonal to a given reference vector.

From Chapter 6 recall that $\theta_z(y)$, defined in (10.5), has the following physical interpretation. Given two sinusoidal vector signals $y(t) = ye^{s_o t}$ and $z(t) = z\, e^{s_o t}$, then $\theta_z(y)$ determines how the signals interfere when added together:

$$\begin{aligned} \|y(t) + z(t)\|_2 &= e^{x_o t}\sqrt{2}\sqrt{1 + \mathrm{Re}\, z^H y} \\ &= e^{x_o t}\sqrt{2}\sqrt{1 + |z^H y| \cos\theta_z(y)}\ . \end{aligned} \tag{10.6}$$

If z and y lie in orthogonal subspaces, then no interference takes place; thus it is reasonable that this definition of phase cannot be extended to a global definition.

The concept of a local section (Definition 10.4) can be viewed as a local choice of a reference, or phase zero, vector in each fiber. This can be seen from the proof of Theorem 10.5; the reference vector in the fiber over [y] is given by

$$\rho_z([y]) = T_z^{-1}([y], 1). \tag{10.7}$$

It follows, given a local trivialization and the local section defined by (10.7), that a unit vector w may be decomposed as

$$w = \rho_z([w])e^{j\theta_z(w)} \quad . \tag{10.8}$$

Suppose that a global trivialization (Definition 10.6) existed. This would imply the existence of a definition of phase valid for all unit vectors in $\mathbb{C}^n$; by Theorem 10.5 this would also imply the existence of a continuous choice of reference vector in each direction of $\mathbb{C}^n$.

Note if such a global trivialization existed, then, by definition, there would exist a homeomorphsim $T : S^{2n-1} \rightarrow \mathbb{C}P^{n-1} \times S^1$. Now it is a fact from topology that homeomorphisms preserve the property of simple connectedness. The existence of the map T would therefore imply that either a) both S^{2n-1} and $\mathbb{C}P^{n-1} \times S^1$ are simply connected, or b) neither space has this property. It can be shown, however, [55, p. 43] that the unit sphere S^m is simply connected if and only if $m > 1$. Thus the unit sphere in $\mathbb{C}^n$, $n > 1$, is simply connected while S^1 (and thus the product space $\mathbb{C}P^{n-1} \times S^1$) is not. This contradiction shows that no map T with the desired properties exists. Thus it is not possible to obtain either a method of defining phase of vector signals which is valid globally nor (equivalently) does there exist a continuous choice of phase-zero reference vectors.

The preceding concepts will now be illustrated by using the standard basis vectors for $\mathbb{C}^n$, $\{e_i = [0\ 0\ \ldots\ \overset{i}{1}\ \ldots\ 0]^T;\ i = 1,\ldots,n\}$ to define local trivializations, transition functions, and local sections.

Consider a vector $p = [p_1, \ldots, p_n]^T \in S^{2n-1}$ and assume that $e_i^H p \neq 0$. Then p lies in the domain of definition of the local trivialization defined by

$$T_i(p) = ([p], e^{j\theta_i(p)}) \tag{10.9}$$

where

$$\begin{aligned} \theta_i(p) &\triangleq \angle\, e_i^H p \\ &= \angle\, p_i . \end{aligned} \tag{10.10}$$

The transition functions $g_{ik}([p])$ and local sections $\rho_i([p])$ may be computed using an <u>arbitrarily</u> chosen vector $\hat{p}$ in the equivalence class [p]. The transition functions are given by

$$g_{ik}([p]) = \exp[j \angle\, \bar{\hat{p}}_k \hat{p}_i] \tag{10.11}$$

where $\hat{p}_k$ and $\hat{p}_i$ are the kth and ith components of the vector $\hat{p}$. The local sections may be defined, as in the proof of Theorem 10.5, by

$$\rho_i([p]) = \exp[-j \angle\, \hat{p}_i] \cdot \hat{p}. \tag{10.12}$$

Choosing the local section $\rho_i([p])$ as in (10.12) may be viewed as choosing for a reference vector in each subspace that vector with the ith component positive real. This is possible provided the fiber above [p] is within the domain of definition of T_i; i.e., provided $p_i \neq 0$. Note that the local sections are related by

$$\rho_k([p]) = \rho_i([p]) g_{ik}([p]) \tag{10.13}$$

while the phase coordinates in different local trivializations are related by

$$e^{j\theta_i(p)} = g_{ik}([p]) e^{j\theta_k(p)} . \tag{10.14}$$

Since the unit sphere in $\mathbb{C}^n$ may be identified with $S^{2n-1} \subseteq \mathbb{R}^{2n}$, it follows that 2n-1 real coordinates are needed to describe a vector in $\mathbb{C}^n$. Suppose a vector lies within the domain of definition of the local trivialization T_i. Then T_i may be used to assign a coordinate analogous to scalar phase to this vector. Thus unit vectors not orthogonal to e_i may be specified by giving the appropriate point in $\mathbb{C}P^{n-1}$ plus the phase coordinate corresponding to T_i.

A method for assigning the 2n-2 real coordinates needed to describe a point in $\mathbb{C}P^{n-1}$ is now developed. Note in particular that this assignment is completely independent of the local trivialization used to distinguish vectors in the fiber above the point.

First, consider the unit sphere in $\mathbb{C}^2$. The set of equivalence classes under the relation given in Definition 10.1 may be mapped onto the unit sphere $S^2 \subseteq \mathbb{R}^3$ via a procedure similar to one given by Auslander and MacKenzie [64]. Coordinates on $\mathbb{C}P^1$ may then be identified with the latitude and longitude of points on S^2.

Indeed, let $p = [p_1 \;\; p_2]^T$ be a unit vector in $\mathbb{C}^2$. The points of the projective space $\mathbb{C}P^1$ may be placed in one-to-one correspondence with the extended complex plane via the mapping

$$z(p) = \frac{p_2}{p_1} . \tag{10.15}$$

Note z(p) is a function only of the subspace spanned by p. Moreover, it is not essential to construct the correspondence using the components of p written in the standard basis. Any other basis would do; this fact will be used later.

By mapping the extended plane onto the unit sphere, it is thus possible to place the points of $\mathbb{C}P^1$ in one-to-one correspondence with $S^2 \subseteq \mathbb{R}^3$. Defining ϕ and Ψ by

$$\tan\phi \triangleq \left|\frac{p_2}{p_1}\right|, \qquad 0 \leq \phi \leq \pi/2$$

and (10.16)

$$\Psi \triangleq \measuredangle \frac{p_2}{p_1} \qquad -\pi < \Psi \leq \pi$$

yields a set of coordinates on $\mathbb{C}P^1$ analogous to latitude and longitude (Figure 10.1). Note that the subspace spanned by $e_1 = [1 \quad 0]^T$ maps to the North pole, N, and that spanned by $e_2 = [0 \quad 1]^T$ maps to the South pole, S. Thus the local trivialization T_1 is defined on fibers above all points on the sphere excepting the South pole. An analogous statement holds for T_2 and the North pole.

Now that coordinates have been assigned to the base manifold $\mathbb{C}P^1$, explicit expressions may be given for the transition functions and local sections of (10.11) and (10.12). The local sections defined by (10.12) may be written in coordinates as

$$\sigma_1(\phi,\Psi) = \begin{bmatrix} \cos\phi \\ \sin\phi \, e^{j\Psi} \end{bmatrix} \tag{10.17a}$$

and

$$\sigma_2(\phi,\Psi) = \begin{bmatrix} \cos\phi \, e^{-j\Psi} \\ \sin\phi \end{bmatrix}. \tag{10.17b}$$

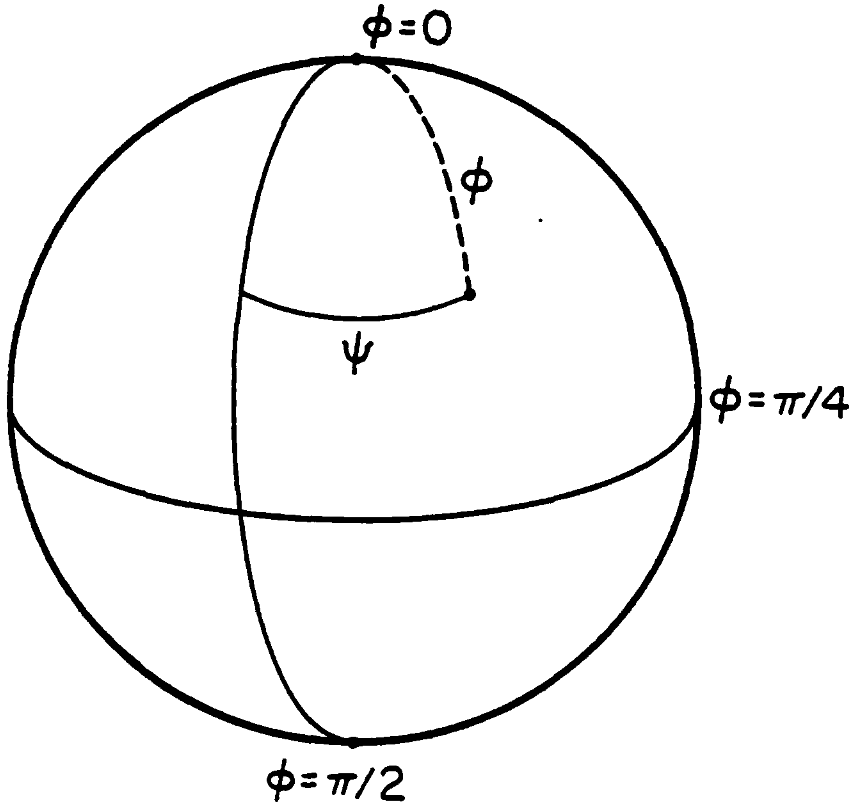

Figure 10.1. Coordinates on $\mathbb{CP}^1$.

Thus a given unit vector in $\mathbb{C}^2$ whose projection has its coordinates in $S^2 - \{N,S\}$ may be written, as in (10.8), as

$$p = \begin{bmatrix} \cos\phi \\ \sin\phi\, e^{j\Psi} \end{bmatrix} e^{j\theta_1} \quad \text{using } T_1 \tag{10.18a}$$

and

$$p = \begin{bmatrix} \cos\phi\, e^{-j\Psi} \\ \sin\phi \end{bmatrix} e^{j\theta_2} \quad \text{using } T_2. \tag{10.18b}$$

The transition functions $g_{ik}([p]) = g_{ik}(\phi,\Psi)$ are given by

$$g_{12}(\phi,\Psi) = e^{-j\Psi} \tag{10.19a}$$

and

$$g_{21}(\phi,\Psi) = e^{+j\Psi}. \tag{10.19b}$$

Note that $e^{j\theta_1} = g_{12}(\phi,\Psi)e^{j\theta_2}$ as required by Definition 10.3. Thus $\theta_2 = \theta_1 + \Psi$.

Note that the expression of S^3 as a circle bundle over S^2 is the Hopf fibration [55, p. 66]. This construction is very appealing in that it allows one to visualize the unit sphere in $\mathbb{C}^2$. In higher dimensions, visualization is no longer possible; a mathematical procedure for constructing the space $\mathbb{C}P^n$ from $\mathbb{C}P^{n-1}$ is given in [52, pp. 114-115]. For the purposes of this thesis it is sufficient to note that a set of coordinates for $S^{2n-1} \subseteq \mathbb{C}^n$ may be obtained from those for $S^{2n-3} \subseteq \mathbb{C}^{n-1}$ via the following procedure. Assume that $p \in \mathbb{C}^n$ is not orthogonal to e_1. Thus p may be written, using the local trivialization T_1 as in (10.8), as $p = \rho_1([p])e^{j\theta_1(p)}$. Then coordinates may be assigned to $\mathbb{C}P^{n-1}$ using the component p_1 to define $\cos\phi_1 = |p_1|$. Thus for $n = 2$

$$p = \begin{bmatrix} \cos\phi_1 \\ \sin\phi_1 e^{j\psi_1} \end{bmatrix} e^{j\theta_1} \tag{10.20}$$

For $n = 3$

$$p = \begin{bmatrix} \cos\phi_1 \\ \sin\phi_1 \ \cos\phi_2 \ e^{j\psi_1} \\ \sin\phi_1 \ \sin\phi_2 \ e^{j\psi_2} \end{bmatrix} e^{j\theta_1} . \tag{10.21}$$

For $n = 4$

$$p = \begin{bmatrix} \cos\phi_1 \\ \sin\phi_1 \ \cos\phi_2 \ e^{j\psi_1} \\ \sin\phi_1 \ \sin\phi_2 \ \cos\phi_3 \ e^{j\psi_2} \\ \sin\phi_1 \ \sin\phi_2 \ \sin\phi_3 \ e^{j\psi_3} \end{bmatrix} e^{j\theta_1} \tag{10.22}$$

where $\phi_i \in [0,\pi/2]$, $\Psi_i \in (-\pi,\pi]$, and $\theta_i \in (-\pi,\pi]$. Again, note that other assignments of coordinates to $\mathbb{C}P^{n-1}$ are possible (for example ϕ_1 could be defined from $\cos\phi_1 = |e_2^H p| = |p_2|$) and the phase coordinate defined using T_1 may still be chosen.

From (10.20)-(10.22) one can easily see the pattern for obtaining coordinates for $\mathbb{C}P^n$ from those for $\mathbb{C}P^{n-1}$. Note that in each case Ψ_i represents the phase difference between the (i+1)st and the 1st components of p. Thus Ψ_i is undefined if either of these components is zero. If the first component of p is zero, then of course the local trivialization T_1 cannot be used. The values of ϕ_i and Ψ_i (defined when $\phi_i \neq 0$ and $\phi_i \neq \frac{\pi}{2}$) may still be obtained, however. In particular, any point in $\mathbb{C}P^{n-1}$ may be specified by giving a set of coordinates ϕ_i and Ψ_i. Similarly to each set of values of ϕ_i and Ψ_i (noting Ψ_i is undefined when $\phi_i = 0$ or $\pi/2$) there corresponds a point of $\mathbb{C}P^{n-1}$.

To illustrate, it can easily be seen from (10.21) that for $\mathbb{C}^3$ the local trivializations T_1, T_2, and T_3 yield phase coordinates

$$\theta_1 = \measuredangle p_1 \tag{10.23a}$$

$$\begin{aligned} \theta_2 &= \measuredangle p_2 \\ &= \theta_1 + \Psi_1 \end{aligned} \tag{10.23b}$$

$$\begin{aligned} \theta_3 &= \measuredangle p_3 \\ &= \theta_1 + \Psi_2 \\ &= \theta_2 + (\Psi_2 - \Psi_1). \end{aligned} \tag{10.23c}$$

Thus the transition functions $g_{ij} \triangleq g_{ij}(\phi_1, \phi_2, \Psi_1, \Psi_2)$ are given by

$$g_{12} = e^{-j\Psi_1} \tag{10.24a}$$

$$g_{13} = e^{-j\Psi_2} \tag{10.24b}$$

$$g_{23} = e^{-j(\Psi_2 - \Psi_1)} \tag{10.24c}$$

Finally, the local sections $\rho_i(\mathbb{C}P^{n-1}) \to S^{2n-1}$, defined in (10.10), may be expressed using the above coordinates. For $\mathbb{C}^3$, the local sections $\rho_i \triangleq \rho_i(\phi_1, \phi_2, \Psi_1, \Psi_2)$ corresponding to the local sections T_1, T_2, and T_3 are

$$\rho_1 = \begin{bmatrix} \cos\phi_1 & & \\ \sin\phi_1 & \cos\phi_2 & e^{j\Psi_1} \\ \sin\phi_1 & \sin\phi_2 & e^{j\Psi_2} \end{bmatrix} \tag{10.25a}$$

$$\rho_2 = \begin{bmatrix} \cos\phi_1 \quad e^{-j\Psi_1} \\ \sin\phi_1 \quad \cos\phi_2 \\ \sin\phi_1 \quad \sin\phi_2 \quad e^{j(\Psi_2-\Psi_1)} \end{bmatrix} \tag{10.25b}$$

$$\rho_3 = \begin{bmatrix} \cos\phi_1 \quad e^{-j\Psi_2} \\ \sin\phi_1 \quad \cos\phi_2 \quad e^{j(\Psi_1-\Psi_2)} \\ \sin\phi_1 \quad \sin\phi_2 \end{bmatrix} . \tag{10.25c}$$

The above construction may be used to assign a complete set of (2n-1) real coordinates to each member of a pair of left and right singular vectors. Let these vectors be denoted by v and u, respectively. To illustrate, assume that v and u both lie in the domain of definition of T_i. Then v and u may be represented as

$$u = \rho_i([u])e^{j\theta_{iu}} \tag{10.26a}$$

$$v = \rho_i([v])e^{j\theta_{iv}}. \tag{10.26b}$$

(Note the subscript refers to the numbering of the local trivalization T_i defined using the ith standard basis vector and not to any ordering of the singular vectors.)

Recall (Appendix B) that a pair of singular vectors is not uniquely defined, even if the associated singular value has multiplicity one. If (u,v) is a choice of singular vectors, then $(\hat{u},\hat{v}) = e^{j\alpha}(u,v)$ is another choice. Thus the phase coordinates of the vectors, θ_{iu} and θ_{iv}, are not well defined; however, the phase difference coordinate

$$\tilde{\theta}_i \triangleq \theta_{iv} - \theta_{iu} \tag{10.27}$$

is well defined.

One way to give a rule specifying the singular vectors is to choose the right singular vector to be the phase zero vector in a local trivialization. The left singular vector is then uniquely determined from the equation $v = \frac{1}{\sigma} Mu$. Thus, given the local trivialization T_i, u may be chosen so that $\theta_{iu} \equiv 0$. It then follows that $\theta_{iv} = \tilde{\theta}_i$, as defined by (10.27) for arbitrary u and v. Note that these various phase coordinates may be related via the transition functions g_{ik}. From (10.11) and (10.14), it follows that, given an arbitrary pair (u,v),

$$e^{j\theta_{iv}} = g_{ik}([v])e^{j\theta_{kv}}$$

$$e^{j\theta_{iu}} = g_{ik}([u])e^{j\theta_{ku}}$$

$$\Rightarrow \quad e^{j\tilde{\theta}_i} = g_{ik}([v])\overline{g_{ik}([u])}e^{j\tilde{\theta}_k} \tag{10.28}$$

where

$$g_{ik}([u]) = \exp[j \measuredangle \bar{u}_k u_i] \tag{10.29a}$$

and

$$g_{ik}([v]) = \exp[j \measuredangle \bar{v}_k v_i]. \tag{10.29b}$$

The parameterization of singular vectors may now be completed by assigning coordinates to $\mathbb{C}P^{n-1}$. For example, with $n = 2$ and choosing the right singular vector to have phase zero, the singular vectors may be written using the local trivialization T_1 as

$$u = \begin{bmatrix} \cos \phi_{1u} \\ \sin \phi_{1u} \, e^{j\Psi_{1u}} \end{bmatrix} \tag{10.30a}$$

$$v = \begin{bmatrix} \cos\phi_{1v} \\ \sin\phi_{1v}\, e^{j\Psi_{1v}} \end{bmatrix} e^{j\tilde{\theta}_1}. \tag{10.30b}$$

Similarly, using T_2

$$u = \begin{bmatrix} \cos\phi_{1u}\, e^{-j\Psi_{1u}} \\ \sin\phi_{1u} \end{bmatrix} \tag{10.31a}$$

$$v = \begin{bmatrix} \cos\phi_{1v}\, e^{-j\Psi_{1v}} \\ \sin\phi_{1v} \end{bmatrix} e^{j\tilde{\theta}_2}. \tag{10.31b}$$

The functions in (10.28) relating different phase difference coordinates $\tilde{\theta}_i$ may be written using these coordinates on CP^{n-1}. For example, from (10.23) for $n = 3$, it follows that

$$\tilde{\theta}_2 = \tilde{\theta}_1 + \Psi_{1v} - \Psi_{1u} \tag{10.32a}$$

$$\begin{aligned} \tilde{\theta}_3 &= \tilde{\theta}_1 + \Psi_{2v} - \Psi_{2u} \\ &= \tilde{\theta}_2 + (\Psi_{2v} - \Psi_{1v}) - (\Psi_{2u} - \Psi_{1u}) \ . \end{aligned} \tag{10.32b}$$

As discussed in Chapter 6, the phase difference $\tilde{\theta}_i$ is a measure of how the ith components of the signals $v(t) = ve^{st}$ and $u(t) = ue^{st}$ interfere when added together. It was also pointed out that the most meaningful definition of phase difference is that given by $\theta = \measuredangle\, u^H v$, since this indicates how the component of $v(t)$ in the direction spanned by u will interfere with $u(t)$ when the signals are added. Local trivializations using the right singular vectors will now be developed, along with transition functions relating the resulting measures of phase difference to the measures $\tilde{\theta}_i$.

Let $\{u_i\ ;\ i=1,\ldots,n\}$ be a basis of right singular vectors. Consider the local trivialization obtained by setting $z=u_i$ in (10.5)

$$T_{u_i}(p) = ([p], e^{j\theta_{u_i}(p)}) \tag{10.33}$$

where

$$\theta_{u_i}(p) = \measuredangle\, u_i^H p. \tag{10.34}$$

Note $T_{u_i}(p)$ is defined for all p such that $u_i^H p \neq 0$. The components of the vector p written in the basis u_i are given by

$$p = U\begin{bmatrix} u_1^H p \\ \vdots \\ u_n^H p \end{bmatrix} \tag{10.35}$$

where

$$U = [u_1 \vdots \cdots \vdots u_n].$$

Since different choices of the right singular vectors will yield different values for the components $u_i^H p$ and the phase coordinate $\theta_{u_i}(p)$, it is not clear these quantities have physical significance. When the vector p in (10.33)-(10.35) is the ith left singular vector v_i, however, the coordinate

$$\theta_{u_i}(v_i) = \measuredangle\, u_i^H v_i \tag{10.36}$$

is independent of the choice of the $\{u_i\}$. (Although the components $u_k^H v_i$, $k \neq i$, are not independent.) This fact is appealing since the phase coordinates defined by (10.36) have physical significance.

Coordinates for $\mathbb{C}P^{n-1}$ may be assigned to the components of v_i written as in (10.35). In particular, it is useful to define

$$\cos \phi_i \triangleq |u_i^H v_i|. \tag{10.37}$$

Note that magnitudes of the components $u_k^H v_i$ are well-defined (assuming all singular values are distinct), but that the arguments are not. Nonetheless, given a basis of right singular vectors then coordinates Ψ_i based upon the difference between $\measuredangle\, u_k^H v_i$ and $\measuredangle\, u_i^H v_i$ may be defined.

To avoid notational difficulties, for the remainder of this section, let u and v be a pair of singular vectors corresponding to the same singular value; i.e., $Au = \sigma v$. Thus no subscript distinguishing among the singular values and vectors will be used. Define $\theta \triangleq \theta_u(v)$ as in (10.36). Assume that both u and v lie within the domain of definition of the trivialization T_i given by (10.9)-(10.10). Note that, for the remainder of this section, the subscript "i" will refer to a choice of trivialization T_i. Thus one may write (repeating (10.26)-(10.27) for convenience)

$$u = \rho_i([u])e^{j\theta_{iu}} \tag{10.38a}$$

and

$$v = \rho_i([v])e^{j\theta_{iv}}. \tag{10.38b}$$

where $\rho_i([u])$ and $\rho_i([v])$ are the local sections defined by (10.12) and

$$\theta_{iu} = \measuredangle\, e_i^H u \tag{10.39a}$$

$$\theta_{iv} = \measuredangle\, e_i^H v \tag{10.39b}$$

$$\tilde{\theta}_i \triangleq \theta_{iv} - \theta_{iu} \quad . \tag{10.39c}$$

Two different methods of measuring phase difference between the pair of left and right singular vectors v and u have now been defined. The first method is to measure $\tilde{\theta}_i$, the phase difference between the ith components of v and u, as in (10.39). The second method is to use the natural measure of phase difference $\theta = \theta_u(v)$ as in (10.36). From (10.36), (10.38) and (10.39), it may be seen that θ and $\tilde{\theta}_i$ are related by

$$\begin{aligned} \theta &= \theta_u(v) \\ &= \measuredangle\, u^H v \\ &= \tilde{\theta}_i + \measuredangle\,[\rho_i([u])]^H \rho_i([v]) \ . \end{aligned} \qquad (10.40)$$

Define the function $g_i \equiv g_i([u],[v])$ by

$$g_i = \exp\{j \measuredangle\,[\rho_i([u])]^H \rho_i([v])\} \qquad (10.41)$$

so that

$$e^{j\theta} = e^{j\tilde{\theta}_i} g_i \quad . \qquad (10.42)$$

Thus g_i may be used to relate the different measures of phase difference between pairs of singular vectors. Note in particular that g_i is a function <u>only</u> of the subspaces in which the singular vectors lie. Expressed in the coordinates for $\mathbb{C}P^1$, and the associated coordinates for S^3, defined by (10.18) the functions g_1 and g_2 are given by

$$\begin{aligned} g_1 &= g_1(\phi_u,\phi_v,\Psi_u,\Psi_v) \\ &= \exp\{j \measuredangle\,[\cos\phi_u \cos\phi_v + \sin\phi_u \sin\phi_v\, e^{j(\Psi_v-\Psi_u)}] \quad , \end{aligned} \qquad (10.43a)$$

$$\begin{aligned} g_2 &= g_2(\phi_u,\phi_v,\Psi_u,\Psi_v) \\ &= \exp\{j \measuredangle\,[\cos\phi_u \cos\phi_v\, e^{-j(\Psi_v-\Psi_u)} + \sin\phi_u \sin\phi_v]\} \ . \end{aligned} \qquad (10.43b)$$

Finally, suppose the right singular vector u_i is chosen to be that given by the local section $\rho_i([u])$:

$$u_i = \rho_i([u]) \tag{10.44}$$

(i.e., by setting $\theta_{iu} \equiv 0$ in (10.26b)). Then, from (10.27), v is given by

$$\begin{aligned} v &= \rho_i([v])e^{j\tilde{\theta}_i} \\ &= \rho_i([v])g_i^{-1}g_i e^{j\tilde{\theta}_i} \\ &= \rho([v])e^{j\theta} \end{aligned} \tag{10.45}$$

where

$$\rho([v]) \triangleq \tilde{\rho}_i([v])g_i^{-1} \quad . \tag{10.46}$$

10.3. Summary

In this chapter the mathematical structure of the space in which singular vectors lie has been studied. It has been shown that this structure is that of a principal fiber bundle; this fact in turn was used to study the existence of a global definition of phase or phase difference for singular vectors.

By using the phase or phase difference coordinates, as well as sets of coordinates assigned to complex projective space (the base space of the

fiber bundle), a complete set of coordinates for pairs of singular vectors was obtained. Rules for transforming from one coordinate system to another were also derived.

An important advantage to describing singular vectors using the fiber bundle structure is that the concept of direction of a signal can be formalized. One can assign coordinates specifying the direction of a signal; given a local trivialization, a phase coordinate may then be used to distinguish among the unit vectors lying in the same direction.

CHAPTER 11

MATHEMATICAL STRUCTURE OF SINGULAR VECTORS, II

11.1. Introduction

The purpose of this chapter is to describe the geometric structure of the differential equations governing singular vectors. The relation between singular values and various measures of phase difference between singular vectors is explored. It is shown that, locally, knowledge of the singular values and singular subspaces suffices to determine the phase difference to within a constant. The fact that the motion of the singular subspaces affects the phase difference is a multivariable system property which has been suggested by the example in Chapter 8. The generalized Cauchy-Riemann equations presented in this chapter describe this behavior mathematically. Thus the groundwork is laid for generalizing the Bode gain-phase relations in Chapter 12. Finally, a systematic method for deriving equations constraining transfer function matrices is developed. This method is appealing in that it is independent of coordinates; hence any set of coordinates may be chosen and the relevant equations derived.

11.2. Differential Equations and Connections in Fiber Bundles

As in Chapter 10, identify the unit sphere in $\mathbb{C}^n$ with the unit sphere $S^{2n-1} \subseteq \mathbb{R}^{2n}$. Consider the principal fiber bundle with total space S^{2n-1}, Lie group $U(1)$, base space $\mathbb{C}P^{n-1}$ and the projection map taking each vector w to its equivalence class $[w]$ as in Definition 10.1. In this chapter the projection map in Definition 10.2 will be written as

$$\pi(w) = ww^H \quad . \tag{11.1}$$

This is possible since there exists a one-to-one correspondence between the points of $\mathbb{CP}^{n-1}$ and the projection operators onto the one-dimensional subspaces of $\mathbb{C}^n$ corresponding to these points.

Given a point $w \in S^{2n-1}$, consider the set of curves $w(t)$ through w with the property that $w(0) = w$. The set of tangent vectors at a point $w \in S^{2n-1}$ is denoted $T_w S^{2n-1}$ and is called the tangent space at w. Given a vector $X \in T_w S^{2n-1}$, the differential form $w^H dw$ evaluated on X is given by

$$w^H dw(X) = w^H(t) \left.\frac{dw}{dt}\right|_{t=0} = w^H X \quad ,$$

where $w(t)$ is any curve satisfying $w(0) = w$ and $\left.\frac{dw}{dt}\right|_{t=0} = X$.

The tangent space to $w \in S^{2n-1}$ may be characterized as

$$T_w S^{2n-1} = \{X \in T_w \mathbb{R}^{2n} \,|\, \mathrm{Re}[w^H X] = 0\} \quad .$$

In Section 9.3 two subspaces of $T_w S^{2n-1}$ with special properties were singled out for study. These subspaces will now be characterized.

First, let $w(t)$ be a curve in S^{2n-1}. Then $w(t)$ will be called a "minimum energy" curve if the condition $w^H \frac{dw}{dt} = 0$ is satisfied for all t. The set of all tangent vectors at w with this property will be denoted by

$$H_w = \{X \in T_w S^{2n-1} \,|\, w^H X = 0\} \quad . \tag{11.2}$$

Note it follows from the definition of H_w that, for all $g \in U(1)$, the subspace $H_{wg} = (H_w)g$.

A second set of curves discussed in Section 9.3 were those of the form $w(t) = we^{j\alpha(t)}$, with w a constant unit vector. Tangent vectors to

curves with this property are given by that subspace of $T_w S^{2n-1}$ defined by

$$V_w = \{X \in T_w S^{2n-1} | ww^H X = X\} \quad . \tag{11.3}$$

Note that the circle of unit vectors in $\mathbb{C}^n$ lying in the subspace spanned by w may be identified with a great circle in S^{2n-1}. The characterization (11.3) of V_w states that the tangent vector to w(t) at w must be tangent to this great circle.

For later reference, note that V_w has the alternate characterization

$$V_w = \{X \in T_w S^{2n-1} | \pi_*(X) = 0\} \quad . \tag{11.3'}$$

To show this, first note that if w(t) is a curve with w(0) = w and $\left.\frac{dw}{dt}\right|_0 = X$ then, from (11.1),

$$\begin{aligned} \pi_*(X) &= \frac{d}{dt}\, \pi(w(t))\Big|_0 \\ &= \frac{d}{dt}\, [w(t)w^H(t)]\Big|_0 \\ &= \left.\frac{dw}{dt}\right|_0 w^H(0) + w(0) \left.\frac{dw^H}{dt}\right|_0 \\ &= Xw^H + wX^H \quad . \end{aligned}$$

The characterizations (11.3) and (11.3)' are then equivalent provided

$$ww^H X = X$$

$$\Longleftrightarrow$$

$$Xw^H + wX^H = 0 \quad .$$

To show this, note that

$$
\begin{aligned}
&Xw^H + wX^H \\
&\quad = ww^H(Xw^H + wX^H) + (I - ww^H)(Xw^H + wX^H) \\
&\quad = ww^HXw^H + wX^H + Xw^H - wX^H - ww^HXw^H + wX^H \\
&\quad = w(- w^HXw^H + X^H) + (ww^HX + X)w^H \\
&\quad = w(X^Hww^H + X^H) + (ww^HX + X)w^H \qquad (*)
\end{aligned}
$$

where the fact that $w^Hw \equiv 1 \Rightarrow X^Hw + w^HX = 0$ was used. It follows from (*) that $ww^HX + X = 0 \Rightarrow Xw^H + wX^H = 0$. Moreover (*) also implies that

$$
\begin{aligned}
(Xw^H + wX^H)w &= w(X^Hww^H + X^H)w + (ww^HX + X) \\
&= wX^Hw + wX^Hw + ww^HX + X \\
&= - ww^HX - ww^HX + ww^HX + X \\
&= X - ww^HX \quad .
\end{aligned}
$$

Hence $Xw^H + wX^H = 0 \Rightarrow X = ww^HX$.

From (11.2) and (11.3) it follows that the tangent space may be decomposed as the direct sum

$$T_wS^{2n-1} = H_w \oplus V_w \quad . \tag{11.4}$$

Again, note the subspace V_w consists of tangent vectors to that great circle in S^{2n-1} identified with the circle of unit vectors lying in the subspace of $\mathbb{C}^n$ spanned by w. The subspace H_w consists of vectors normal to this great circle.

Now consider the decomposition (11.4) applied to each member of a pair of singular vectors corresponding to the same singular value. Recall from Chapter 9 that, if the singular subspaces were constant, then the logarithm of the singular value would be a harmonic function. Hence locally the properties of the singular value would correspond completely to those of the gain of a scalar transfer function. From (11.4) the condition that the singular subspaces are constant is equivalent to the condition that the derivatives of the singular vectors v and u lie entirely in the subspaces V_v and V_u, respectively. Thus properties of the singular value deviating from those of the gain of a scalar transfer function must be due to the components of the derivatives of v and u lying in the subspaces H_v and H_u, respectively. In particular, the failure of log σ to have a harmonic conjugate implies that the measures of phase difference defined in Chapter 10 cannot be related to the singular value in the same way that phase and gain of a scalar transfer function are related. In order to get a better picture of the way in which these quantities are related, it will be convenient to introduce the notion of a connection in a fiber bundle. It will first be shown that the decomposition (11.4) satisfies the definition of a connection. Then an equivalent form of the connection will be introduced which is much more convenient for doing calculations and gaining insight. This form of writing a connection will eventually allow a generalization of the Bode gain-phase relations to be obtained in Chapter 12.

The preceding discussion may be used to show that the decomposition (11.4) satisfies the following definition. Let $\pi : P \to M$ be a principal fiber bundle with group G (in this thesis always U(1)) and base space M of real dimension n.

Definition 11.1 [54, p. 29]: A connection assigns to each $p \in P$ a subspace $H_p \subseteq T_pP$ such that for $V_p = \{X \in T_pP | \pi_*(X) = 0\}$ the decomposition $T_pP = H_p \oplus V_p$ holds. It is required that $R_{g*}(H_p) = H_{pg}$ and that there exist n vector fields (defined on a neighborhood U of p) that span H_q $\forall$ $q \in U$. The subspace V_p is termed the vertical subspace of T_pP and H_p is termed the horizontal subspace. ∎

In the present case the map $R_g : P \to P$ is given by $R_g(w) = we^{j\alpha}$, for $g = e^{j\alpha}$. Thus $R_{g*}(X) = Xe^{j\alpha}$ and, from the definition (11.2) of H_{wg}, it follows that $R_{g*}(H_w) = H_w = H_{wg}$. Thus the decomposition (11.4) is indeed a connection.

Definition 11.1 describes a connection as a decomposition of the tangent space to S^{2n-1}. From (11.2) and (11.3) it may be seen that the linear operator $\omega : T_wS^{2n-1} \to \{j\alpha | \alpha \in \mathbb{R}\}$ defined by

$$\omega_w(X) = w^H dw(X) = w^H X \tag{11.5}$$

decomposes T_wS^{2n-1} into the null space of ω, (i.e., H_w) and its orthogonal complement, (i.e., V_w).

In [54, pp. 29-30] a definition of a connection equivalent to Definition 11.1 is given; this definition focuses on the linear operator (11.5) rather than T_wS^{2n-1}. For the purposes of this thesis it suffices to note that ω defined by (11.5) is a connection one-form defined on the total space P. It will prove useful to have yet another equivalent definition of a connection as defined on the base space M rather than the total space.

First, some notation will be introduced. If G is a Lie group, then denote the Lie algebra [54, p. 18] of G by $\mathfrak{G}$. In the present case $G = U(1) = \{e^{j\delta} | \delta \in \mathbb{R}\}$ and $\mathfrak{G} = \mathfrak{U}(1) \triangleq \{j\delta | \delta \in \mathbb{R}\}$.

Definition 11.2 [54, pp. 30-31]: A connection assigns to each local trivialization $T_\alpha : \pi^{-1}(U_\alpha) \to U_\alpha \times G$ a $\mathfrak{G}$-valued one-form ω_α on U_α. If T_β is another local trivialization and $g_{\alpha\beta} : U_\alpha \cap U_\beta \to G$ is the transition function from T_α to T_β, then it is required that

$$\omega_\beta = g_{\alpha\beta}^{-1}\, dg_{\alpha\beta} + g_{\alpha\beta}^{-1}\omega_\alpha g_{\alpha\beta} \quad . \tag{11.6}$$

■

From the proof in [54, p. 32] it follows that the connection forms ω_α in Definition 11.2 may be obtained from the connection one-form ω using local sections corresponding to local trivializations as in the proof of Theorem 10.5. Consider a point $x \in \mathbb{C}P^{n-1}$ with x in U_α, the domain of definition of the local trivialization T_χ, and let $Y_x \in T_x\mathbb{C}P^{n-1}$. Then ω_α can be defined by

$$\begin{aligned} \omega_\alpha(Y_x) &= \rho_\alpha^* \omega(Y_x) \\ &= \omega_{\rho_\alpha(x)}(\rho_{\alpha *} Y_x) \\ &= \rho_\alpha{}^H(x)\, d\rho_\alpha(Y_x) \end{aligned}$$

or, dropping the dependence on x and Y_x,

$$\omega_\alpha = \rho_\alpha{}^H d\rho_\alpha \quad , \tag{11.7}$$

where ρ_α is the local section (10.7) defined using the local trivialization T_α. Recall that different local sections are related via the transition functions as

$$\rho_\beta(x) = \rho_\alpha(x) g_{\alpha\beta}(x) \quad . \tag{11.8}$$

Thus it follows that

$$\begin{aligned} d\rho_\beta &= d\rho_\alpha g_{\alpha\beta} + \rho_\alpha dg_{\alpha\beta} \\ \rho_\beta{}^H d\rho_\beta &= \rho_\beta{}^H d\rho_\alpha g_{\alpha\beta} + \rho_\beta{}^H \rho_\alpha dg_{\alpha\beta} \\ &= \bar{g}_{\alpha\beta}\rho_\alpha{}^H d\rho_\alpha g_{\alpha\beta} + \bar{g}_{\alpha\beta} dg_{\alpha\beta} \quad . \end{aligned} \tag{11.9}$$

Since in the present case $g_{\alpha\beta} \in U(1)$, it follows that $\bar{g}_{\alpha\beta} = g_{\alpha\beta}^{-1}$; hence, (11.9) reduces to

$$\begin{aligned} \rho_\beta{}^H d\rho_\beta &= g_{\alpha\beta}^{-1} dg_{\alpha\beta} + g_{\alpha\beta}^{-1}\rho_\alpha{}^H d\rho_\alpha g_{\alpha\beta} \\ &= g_{\alpha\beta}^{-1} dg_{\alpha\beta} + \rho_\alpha{}^H d\rho_\alpha \quad . \end{aligned} \tag{11.10}$$

Thus condition (11.6) is satisfied.

Before applying the various definitions of a connection to the study of singular vectors one, further definition will be helpful. The following paragraph is based on [54, p. 37].

Given a connection one-form ω on the principal fiber bundle $\pi : P \to M$ with group G, any vector $X \in T_pP$ may be written as $X = X^V + X^H$, where $X^V \in V$, the vertical subspace, and $X^H \in H$, the horizontal subspace.

<u>Lemma 11.3 [54, p. 37]</u>: Given a vector field X on M, there exists a unique vector field $\tilde{X}$ on P such that $\omega(\tilde{X}) \equiv 0$ and $\pi_*(\tilde{X}_p) = X_{\pi(p)}$ for all $p \in P$. The vector field $\tilde{X}$ is called the horizontal lift of X. ■

To apply the preceding definitions, let w be a unit vector in $\mathbb{C}^n$, and assume that $e_i^H w \neq 0$, so that the local trivialization T_i (10.9) may be applied. Then w may be written as

$$w = \rho_i e^{j\theta_i} \quad , \tag{11.11}$$

where $\theta_i = \theta_i(w)$ is the phase coordinate given by (10.10) and $\rho_i = \rho_i([w])$ is the reference vector given by the local section (10.12).

Let $\alpha : (-\varepsilon,\varepsilon) \to S^{2n-1}$ be a curve with $\alpha(0) = w$ and let X be the tangent vector to α at t=0:

$$X = \frac{d}{dt}\,\alpha(t)\Big|_{t=0} \quad . \tag{11.12}$$

Then writing $\alpha(t) = \rho_i(t)e^{j\theta_i(t)}$, where $\rho_i(t) \triangleq \rho_i([w(t)])$ and $\theta_i(t) \triangleq \theta_i(w(t))$, gives

$$X = \left[\frac{d\rho_i}{dt} e^{j\theta_i} + \rho_i e^{j\theta_i} \left(j \frac{d\theta_i}{dt}\right)\right]\Bigg|_{t=0} \quad . \tag{11.13}$$

The condition used to define the horizontal subspace (11.2) may then be expressed as

$$\begin{aligned} w^H dw(X) &= \rho_i^H \frac{d\rho_i}{dt} + j\frac{d\theta_i}{dt} \\ &= 0 \quad . \end{aligned} \tag{11.14}$$

Thus the connection one-form can be written as

$$w^H dw = (\rho_i^H d\rho_i)\circ\pi_* + j\; d\theta_i \quad . \tag{11.15}$$

It follows that the horizontal subspace may be characterized in terms of the local trivialization T_i as

$$H_w = \{X \in T_w S^{2n-1} \,|\, \rho_i^H \frac{d\rho_i}{dt} + j\frac{d\theta_i}{dt} = 0\} \quad . \tag{11.16}$$

Recall the differential equations developed in Section 9.3 to describe the motion of the singular vectors. These differential equations will now be examined using the concept of a connection.

Let $\gamma(t) = x(t) + jy(t)$, $t \in [0,1]$ be an analytic function of t. Assume the image of γ lies in an open connected subset of the complex plane over which the singular values of M(s) are distinct. By this assumption, at each point of $\gamma(t)$ there exist n uniquely defined right singular subspaces of complex dimension one. Let the singular values of M be given the usual ordering $\sigma_1 > \sigma_2 > \ldots > \sigma_n$ and denote the right singular subspace corresponding to $\sigma_i(t)$ by $\mathfrak{U}_i(t) = \mathfrak{U}_i(\gamma(t))$.

In Section 9.3 the problem of determining a (nonunique) right singular vector given, a well-defined right singular subspace, was posed. In the terminology introduced in Chapter 10 it can be said that the min-max property (6.15) determines curves $\mathfrak{U}_i(t)$ in the base space $\mathbb{C}P^{n-1}$ and the problem consists of how to "lift" these curves to the total space S^{2n-1}. Motivated by the terminology of Lemma 11.3, the choice of right singular vector obtained by fixing an initial condition $u_i(0)$, setting $u_i^H \frac{du_i}{dt} \equiv 0$, and integrating the differential equation

$$\frac{du_i}{dt} = \sum_{k \neq i} u_k \left(u_k^H \frac{du_i}{dt} \right)$$

$$u_k^H \frac{du_i}{dt} = \left(\frac{1}{\sigma_i^2 - \sigma_k^2} \right) \{ \sigma_i u_k^H \frac{dM^H}{dt} v_i + \sigma_k v_k^H \frac{dM}{dt} u_i \}$$

along $\gamma(t)$ will be termed the horizontal lift of $\mathfrak{U}_i(t) \in \mathbb{C}P^{n-1}$ to S^{2n-1} with initial condition $u_i(0)$. Note the right singular vector obtained in this fashion is a "minimum energy" singular vector discussed in Section 9.3; as in

that section, denote this vector by $u_i^*(t)$. Observe there exists a family of "minimum energy" singular vectors above $\mathcal{U}_i(t)$, indexed by the initial condition $u_i(0)$.

Suppose now that $\gamma(t)$ is a closed curve, $\gamma(1) = \gamma(0)$. Recall from Section 9.3 that the condition $u^{*H} \frac{du^*}{dt} \equiv 0$ was interpreted as meaning that u^* does not "spin" as it moves. (Until further notice, the subscript "i" will be omitted.) It was pointed out that if the singular subspace $\mathcal{U}(t)$ is constant, then it necessarily follows that $u^*(t)$ not spinning implies that $u^*(1) = u^*(0)$. If $\mathcal{U}(t)$ is <u>not</u> constant, however, then no results were given. It can now be shown, using characterization (11.16) of the horizontal subspace, that in general $u^*(1) \neq u^*(0)$. To see this, assume for simplicity that $e_1^H u^*(t) \neq 0 \quad \forall t \in [0,1]$. Then the local trivialization T_1 may be used to characterize H_{u^*}. Equation (11.14) implies

$$u^*(1) = e^{j\beta}\, u^*(0)$$

where

$$j\beta = -\int_0^1 \left(\rho^H \frac{d\rho}{dt}\right) dt \tag{11.17a}$$

$$= -\int_0^1 \left(\rho^H \frac{\partial\rho}{\partial x}\,\frac{dx}{dt} + \rho^H \frac{\partial\rho}{\partial y}\,\frac{dy}{dt}\right) dt \tag{11.17b}$$

$$= -\int_\gamma \rho^H \frac{\partial\rho}{\partial x}\, dx + \rho^H \frac{\partial\rho}{\partial y}\, dy \tag{11.17c}$$

and $\rho \triangleq \rho_1$ is the local section defined in (10.12).

From (11.17a) it follows that the phase discrepancy β is a function solely of the path traced out in $\mathbb{C}P^{n-1}$ by the subspace $\mathcal{U}(t) = \mathcal{U}(\gamma(t))$.

Thus (11.17) may be rewritten

$$j\beta = -\int_{\mathbb{U}(t)} \rho^H \, d\rho \quad . \tag{11.18}$$

Note the integrand of (11.18) is the connection form described in Definition 11.2. For later reference, expressions for this form in terms of the coordinates on $\mathbb{C}P^1$ and $\mathbb{C}P^2$ given in Chapter 10 are now derived. For n=2, it follows from (10.17a) that coordinates in $\mathbb{U}$ are given by (ϕ,ψ) and

$$\rho = \begin{bmatrix} \cos\phi \\ \sin\phi \; e^{j\psi} \end{bmatrix} \tag{11.19}$$

$$\Rightarrow \quad d\rho = \begin{bmatrix} -\sin\phi \\ \cos\phi \; e^{j\psi} \end{bmatrix} d\phi + \begin{bmatrix} 0 \\ \sin\phi \; e^{j\psi} \end{bmatrix} j d\psi \tag{11.20}$$

$$\Rightarrow \quad \rho^H d\rho = j \sin^2\phi \; d\psi \quad . \tag{11.21}$$

(Note it is still assumed that local trivialization T_1 is being applied.) For n=3, it follows from (10.25a) that coordinates on $\mathbb{U}$ are given by $(\phi_1,\psi_1,\phi_2,\psi_2)$ and

$$\rho = \begin{bmatrix} \cos\phi_1 \\ \sin\phi_1 \; \cos\phi_2 \; e^{j\psi_1} \\ \sin\phi_1 \; \sin\phi_2 \; e^{j\psi_2} \end{bmatrix} \tag{11.22}$$

$$\Rightarrow \quad \rho^H d\rho = j \sin^2\phi_1 (\cos^2\phi_2 d\psi_1 + \sin^2\phi_2 d\psi_2) \quad . \tag{11.23}$$

Elsewhere in this thesis interpretations of the parameters ϕ_i and ψ_i were presented. In examples it may be possible to identify these parameters

with elements of the transfer function matrix written in standard coordinates. In such cases the expression for the phase discrepancy in terms of the ϕ_i and ψ_i may prove useful. This will become more clear later.

In order to apply Stokes' Theorem [49, p. 124] to Equation (11.17), assume that $\gamma(t)$ is a simple closed curve analytic in t. Then the set $C = \{\gamma(t) \; ; \; t \in [0,1]\}$ is the boundary of a compact subset $D \subseteq \mathbb{C}$. Since it was assumed that the singular values of M(s) were distinct over D, it follows that at each point $s = x + jy \in D$ the right singular subspaces are well-defined. Assume that $e_1^H u^*(x,y) \neq 0$ for $(x,y) \in D$. Thus the local trivialization T_1 may be used to characterize H_{u*} over D. Write

$$\begin{aligned} u^* &= \rho e^{j\theta} \\ &= \rho_1(x,y) e^{j\theta(x,y)} \quad . \end{aligned}$$

From (11.17c) and the special case of Stokes' Theorem known as Green's Theorem [49, p. 134]

$$\begin{aligned} j\beta &= -\int_C \rho^H \frac{\partial \rho}{\partial x} dx + \rho^H \frac{\partial \rho}{\partial y} dy \\ &= -\int_D d[\rho^H \frac{\partial \rho}{\partial x} dx + \rho^H \frac{\partial \rho}{\partial y} dy] \\ &= -\int_D \left[-\left(\frac{\partial \rho^H}{\partial y} \frac{\partial \rho}{\partial x} + \rho^H \frac{\partial^2 \rho}{\partial x \partial y} \right) + \left(\frac{\partial \rho^H}{\partial x} \frac{\partial \rho}{\partial y} + \rho^H \frac{\partial^2 \rho}{\partial y \partial x} \right) \right] dx \wedge dy \\ &= -\int_D \left(\frac{\partial \rho^H}{\partial x} \frac{\partial \rho}{\partial y} - \frac{\partial \rho^H}{\partial y} \frac{\partial \rho}{\partial x} \right) dx \wedge dy \\ &= -2j \iint_D \mathrm{Im} \left[\frac{\partial \rho^H}{\partial x} \frac{\partial \rho}{\partial y} \right] dxdy \end{aligned} \qquad (11.24)$$

where the fact that mixed second partial derivatives are equal (Appendix G) was used. Using (11.21) it may be shown that

$$\beta = \iint_D \sin^2\phi \left(\frac{\partial \phi}{\partial x} \frac{\partial \psi}{\partial y} - \frac{\partial \phi}{\partial y} \frac{\partial \psi}{\partial x} \right) dxdy \quad . \qquad (11.25)$$

Formulas similar to (11.25) hold for $n > 2$ as well. An alternate method of computing β which considers only the set $\mathbb{U}(D) \subseteq \mathbb{C}P^{n-1}$ will now be developed. The cases $n=2$ and $n > 2$ must be considered separately.

First consider the case $n=2$ and the mapping $\mathbb{U} : D \to \mathbb{C}P^1$. Denote the image of C under the map $\mathbb{U} : C \to \mathbb{C}P^1$ by Γ and assume that Γ is a simple closed curve in the domain of ρ. Since $\mathbb{C}P^1$ is a compact connected manifold of real dimension two [52, p. 115], it follows that Γ separates $\mathbb{C}P^1$ into two subsets; moreover, Γ is the boundary of each of these subsets. It is a fact that $\mathbb{C}P^n$ is orientable [52, p. 119]; given an orientation of $\mathbb{C}P^1$, it follows that each of the two subsets has an orientation inherited from that for $\mathbb{C}P^1$. Each of these in turn induces an orientation of Γ and these induced orientations are opposite in direction. Choose the subset of $\mathbb{C}P^1$ yielding the induced orientation of Γ which agrees with the direction travelled along Γ by $\mathbb{U}(t)$. Denote this subset by Δ. Stokes Theorem [49, p. 124] then shows that

$$\begin{aligned} j\beta &= -\int_\Gamma \rho^H d\rho \\ &= -\int_\Delta d(\rho^H d\rho) \\ &= -\int_\Delta (d\rho)^H \wedge d\rho \quad . \end{aligned} \tag{11.26}$$

Using (11.21)

$$\begin{aligned} \beta &= -\int_\Gamma \sin^2\phi \; d\psi \\ &= -\int_\Delta \sin 2\phi \; d\phi \wedge d\psi \quad . \end{aligned} \tag{11.27}$$

Note that β may be computed with knowledge only of Γ and its orientation. Further knowledge of the mapping $\mathbb{U} : D \to \mathbb{C}P^1$ is unnecessary.

One further interpretation of (11.27) is available. Recall that $\mathbb{C}P^1$ is homeomorphic to $S^2 \subseteq \mathbb{R}^3$. Coordinates for S^2 are given by

$$\begin{aligned} x_1 &= \cos 2\phi & \phi &\in [0,\pi/2] \\ x_2 &= \sin 2\phi \cos\psi & \psi &\in (-\pi,\pi] \\ x_3 &= \sin 2\phi \sin\psi & & . \end{aligned} \tag{11.28}$$

From Spivak [49, p. 131] it follows that the element of surface area on S^2 is

$$\eta = x_1 dx_2 \wedge dx_3 + x_2 dx_3 \wedge dx_1 + x_3 dx_1 \wedge dx_2 \tag{11.29}$$

or

$$= 2\sin 2\phi \, d\phi \wedge d\psi \quad . \tag{11.30}$$

Let Γ_s denote the curve in S^2 mapped out by the image of $\Gamma \subseteq \mathbb{C}P^1$, and let Δ_s denote the interior of Γ_s. Then from (11.17a)

$$\begin{aligned} j\beta &= - \int_0^1 \rho^H \frac{d\rho}{dt} \, dt \\ &= -j \int_0^1 \sin^2\phi \frac{d\psi}{dt} \, dt \\ &= -j \int_{\Gamma_s} \sin^2\phi \, d\psi \\ &= -j \int_{\Delta_s} \sin 2\phi \, d\phi \wedge d\psi \\ &= -\frac{j}{2}[\text{area of } \Delta_s \subseteq S^2] \quad . \end{aligned}$$

Thus the phase discrepancy β is proportional to the area of the subset of S^2 enclosed by Γ_s. Hence if the change in the subspace $\mathcal{U}$ is small, the area enclosed will be small, and so will the phase discrepancy.

In the general case $n > 2$, the mapping from $D \subseteq \mathbb{C}$ into $\mathbb{C}P^{n-1}$ is a mapping from a space with real dimension 2 into a space with real dimension $2n-2$ (>2 for $n>2$). Thus $\Gamma = \Pi(C)$ is not the boundary of any subset of $\mathbb{C}P^{n-1}$. However, under certain conditions [49, pp. 109-114], the image $\Delta' = \Pi(D)$ is a submanifold of $\mathbb{C}P^{n-1}$ with boundary C. (Methods for verifying these conditions hold are available; however, this will not be pursued in this thesis. Rather they will be assumed to hold in order to illustrate the type of results available.)

Stokes Theorem may be applied to show

$$\begin{aligned} j\beta &= -\int_{\Gamma} \rho^H d\rho \\ &= -\int_{\Delta'} d(\rho^H d\rho) \\ &= -\int_{\Delta'} (d\rho)^H \wedge d\rho \quad . \end{aligned} \tag{11.31}$$

(Note the definition of Δ' in (11.31) is different from that of Δ in (11.26)). For $n=3$, (11.23) shows that the integrand of (11.31) is

$$\begin{aligned} (d\rho)^H \wedge d\rho = j[&\sin 2\phi_1(\cos^2\phi_2 d\phi_1 \wedge d\psi_1 + \sin^2\phi_2 d\phi_1 \wedge d\psi_2) \\ &+ \sin^2\phi_1 \sin 2\phi_2(-d\phi_2 \wedge d\psi_1 + d\phi_2 \wedge d\psi_2)] \quad . \end{aligned} \tag{11.32}$$

Again, it follows that β is a function solely of the image of Γ in $\mathbb{C}P^{n-1}$, not of the original curve $\gamma(t)$ bounding $D \subseteq \mathbb{C}$. Note, moreover, that since $\omega = \rho^H d\rho$ is a connection with values

in a scalar Lie algebra, it follows [54, pp. 37-39] that $d\omega = (d\rho)^H \wedge d\rho$ is the curvature of ω. Thus in all cases $n \geq 2$ it follows that β is obtained by integrating the curvature of a connection over an appropriate surface.

The preceding observations may now be used to interpret the meaning of the differential form

$$A_i \triangleq j[-\frac{\partial \log\sigma_i}{\partial y} dx + \frac{\partial \log\sigma_i}{\partial x} dy]$$

$$= \frac{j}{\sigma_i} \mathrm{Im}[v_i^H \frac{\partial M}{\partial x} u_i]dx + \frac{j}{\sigma_i} \mathrm{Im}[v_i^H \frac{\partial M}{\partial y} u_i]dy$$

$$= [v_i^H \frac{\partial v_i}{\partial x} - u_i^H \frac{\partial u_i}{\partial x}]dx + [v_i^H \frac{\partial v_i}{\partial y} - u_i^H \frac{\partial u_i}{\partial y}]dy \quad . \tag{11.33}$$

It will be seen (Equations (11.47) and (11.48)) that A_i governs how the measures of phase difference θ_i and $\tilde{\theta}_i$ change as a function both of the singular values and the singular subspaces.

First, note that the Laplacian of log σ_i may be obtained from

$$dA_i = j\left(\frac{\partial^2 \log\sigma_i}{\partial x^2} + \frac{\partial^2 \log\sigma_i}{\partial y^2}\right) dx\wedge dy \quad . \tag{11.34}$$

It was shown in Section 9.4 that (11.34) does not in general equal zero; moreover, the deviation from zero is related to the motion of the singular vectors. This may also be seen from

$$\nabla^2 \log\sigma_i = 2\{\mathrm{Im}[\frac{\partial v_i^H}{\partial x} \frac{\partial v_i}{\partial y}] - \mathrm{Im}[\frac{\partial u_i^H}{\partial x} \frac{\partial u_i}{\partial y}]\} \quad . \tag{11.35}$$

(From now on, the subscript "i" will be suppressed when convenient.) Assume for simplicity that both $e_k^H u \neq 0$ and $e_k^H v \neq 0$. Then u and v may be written in terms of the phase coordinates and local sections given by the local trivialization T_k defined using the standard basis vector e_k as in (10.38)-(10.39):

$$u = \rho_{ku}\, e^{j\theta_{ku}}$$

and (11.36)

$$v = \rho_{kv}\, e^{j\theta_{kv}} \quad ,$$

where $\rho_{ku} \triangleq \rho_k([u(s)])$ and $\rho_{kv} \triangleq \rho_k([v(s)])$. (Note that ρ_{ku} is a local section, not of the original bundle over $\mathbb{C}P^{n-1}$, but of its pullback along the map $[u] : D \to \mathbb{C}P^{n-1}$. A similar comment holds for ρ_{kv}.) If u is chosen so that $\theta_{ku} \equiv 0$, then (11.36) becomes

$$u = \rho_{ku}$$

and (11.37)

$$v = \rho_{kv}\, e^{j\tilde{\theta}_k}$$

with

$$\tilde{\theta}_k \triangleq \theta_{kv} - \theta_{ku} \quad .$$

The form A may be rewritten as

$$\begin{aligned} A &= j[-\frac{\partial \log\sigma}{\partial y}\, dx + \frac{\partial \log\sigma}{\partial x}\, dy] \\ &= [\rho_{kv}^H \frac{\partial \rho_{kv}}{\partial x} - \rho_{ku}^H \frac{\partial \rho_{ku}}{\partial x} + j\, \frac{\partial \tilde{\theta}_k}{\partial x}]dx \\ &\quad + [\rho_{kv}^H \frac{\partial \rho_{kv}}{\partial y} - \rho_{ku}^H \frac{\partial \rho_{ku}}{\partial y} + j\, \frac{\partial \tilde{\theta}_k}{\partial y}]dy \quad . \end{aligned} \tag{11.38}$$

From (10.45) it follows that v may be rewritten in terms of the phase difference $\theta \triangleq \measuredangle u^H v$:

$$v = \rho_v\, e^{j\theta} \quad , \tag{11.39}$$

where $\rho_v \triangleq \rho([v(s)])$. Using the function g_k (10.41) it follows from (10.42) that

$$j \frac{\partial \theta}{\partial x} = j \frac{\partial \tilde{\theta}_k}{\partial x} + g_k^{-1} \frac{\partial g_k}{\partial x} \tag{11.40}$$

and from (10.46) that

$$\rho_v^H \frac{\partial \rho_v}{\partial x} = \rho_{kv}^H \frac{\partial \rho_{kv}}{\partial x} - g_k^{-1} \frac{\partial g_k}{\partial x} \quad . \tag{11.41}$$

Using (11.40) and (11.41) and similar equations for derivatives with respect to y, it follows that (11.38) equals

$$\begin{aligned} A &= j[- \frac{\partial \log\sigma}{\partial y} dx + \frac{\partial \log\sigma}{\partial x} dy] \\ &= [\rho_v^H \frac{\partial \rho_v}{\partial x} - \rho_{ku}^H \frac{\partial \rho_{ku}}{\partial x} + j \frac{\partial \theta}{\partial x}]dx \\ &+ [\rho_v^H \frac{\partial \rho_v}{\partial y} - \rho_{ku}^H \frac{\partial \rho_{ku}}{\partial y} + j \frac{\partial \theta}{\partial y}]dy \quad . \end{aligned} \tag{11.42}$$

Rearranging the form (11.38) yields

$$\begin{aligned} & - j \left(\frac{\partial \log\sigma}{\partial y} + \frac{\partial \tilde{\theta}_k}{\partial x}\right) dx + j \left(\frac{\partial \log\sigma}{\partial x} - \frac{\partial \tilde{\theta}_k}{\partial y}\right) dy \\ &= [\rho_{kv}^H \frac{\partial \rho_{kv}}{\partial x} - \rho_{ku}^H \frac{\partial \rho_{ku}}{\partial x}]dx + [\rho_{kv}^H \frac{\partial \rho_{kv}}{\partial y} - \rho_{ku}^H \frac{\partial \rho_{ku}}{\partial y}]dy \end{aligned} \tag{11.43}$$

and rearranging the form (11.42) yields

$$\begin{aligned} & - j \left(\frac{\partial \log\sigma}{\partial y} + \frac{\partial \theta}{\partial x}\right) dx + j \left(\frac{\partial \log\sigma}{\partial x} - \frac{\partial \theta}{\partial y}\right) dy \\ &= [\rho_v^H \frac{\partial \rho_v}{\partial x} - \rho_{ku}^H \frac{\partial \rho_{ku}}{\partial x}]dx + [\rho_v^H \frac{\partial \rho_v}{\partial y} - \rho_{ku}^H \frac{\partial \rho_{ku}}{\partial y}]dy \quad . \end{aligned} \tag{11.44}$$

Suppose $\sigma e^{j\tilde{\theta}_k}$ (respectively, $\sigma e^{j\theta}$) were analytic. Then log σ and $\tilde{\theta}_k$ (respectively, log σ and θ) would necessarily satisfy the Cauchy-Riemann equations. This is possible, however, only if the right hand sides of (11.43) (respectively, (11.44)) are equal to zero. These equations quantify the extent by which motion of the singular subspaces prevents $\sigma e^{j\tilde{\theta}_k}$ and $\sigma e^{j\theta}$ from satisfying the local gain-phase relations given by the Cauchy-Riemann equations.

Indeed, if $\gamma(t)$ is a curve in $\mathbb{C}$, then the left and right singular subspaces map $\gamma(t)$ to curves $\mathfrak{V}(t)$ and $\mathfrak{U}(t)$ in $\mathbb{C}P^{n-1}$.

Recall now that a left singular vector $v(t) \in S^{2n-1}$ is said to be "minimum energy" if $v^H \frac{dv}{dt} \equiv 0$. Given a curve $\mathfrak{V}(t) \in \mathbb{C}P^{n-1}$ determined by a left singular subspace, a minimum energy left singular vector above $\mathfrak{V}(t)$ will be denoted by $v^*(t)$. From Lemma 11.3 it follows that requiring $v^*(t)$ to be minimum energy above $\mathfrak{V}(t)$ is equivalent to requiring that the vector field tangent to the curve $v^*(t) \in S^{2n-1}$ be the horizontal lift of the vector field tangent to the curve $\mathfrak{V}(t) \in \mathbb{C}P^{n-1}$. Now, from the characterization (11.16) of the horizontal subspace, it follows that the rate of change of the phase coordinate assigned to $v^*(t)$ by some choice of local trivialization is determined by the rate of change of the corresponding local section ρ with respect to a minimum energy vector. This latter rate of change is given by the difference between the tangent vector to $\rho(t) \in S^{2n-1}$ and the horizontal lift of the tangent vector to $\mathfrak{V}(t) \in \mathbb{C}P^{n-1}$. Moreover, the value of this rate of change may be found by evaluating the connection form $\rho^H d\rho$ on the tangent vector to $\mathfrak{V}(t)$. A similar discussion can be made concerning $u^*(t)$, a minimum energy singular vector above the right singular subspace $\mathfrak{U}(t)$.

Now consider the forms (11.43) and (11.44), which show how the functions $\sigma e^{j\tilde{\theta}_k}$ and $\sigma e^{j\theta}$ fail to satisfy the Cauchy-Riemann equations. Evaluating these forms along a tangent vector to a curve $\gamma(t) \in \mathbb{C}$ shows that this failure is quantified by the difference between the deviations of the local sections above $\mathfrak{V}(t)$ and $\mathfrak{U}(t)$ from minimum energy vectors above these curves. Hence $\mathfrak{V}(t)$ and $\mathfrak{U}(t)$ are the images in $\mathbb{C}P^{n-1}$ of the curve $\gamma(t)$ in $\mathbb{C}$ under the maps $[v] : \gamma \to \mathbb{C}P^{n-1}$ and $[u] : \gamma \to \mathbb{C}P^{n-1}$, respectively. These latter maps are those which determine, via the mini-max principle (6.15), the

singular subspaces in which the left and right singular vectors are constrained to lie. From the discussion following Equations (11.36), it follows that the connection forms which measure the failure of the local sections to be minimum energy vectors are now no longer defined in the original circle bundle over $\mathbb{C}P^{n-1}$, but in its pullback along the maps $[v] : \gamma \to \mathbb{C}P^{n-1}$ and $[u] : \gamma \to \mathbb{C}P^{n-1}$, respectively.

One method used to gain insight into the behavior of scalar transfer functions was to use an analogy with two-dimensional potential theory [27]. This analogy is also used in explaining theory of harmonic and analytic functions [56,63]. An interpretation of $\nabla^2 \log\sigma$ is now given using such an analogy.

Think of the gradient vector $\nabla\log\sigma = \left(\frac{\partial\log\sigma}{\partial x}, \frac{\partial\log\sigma}{\partial y}\right)$ as being the velocity vector field of a fluid flowing in steady state along the surface of the complex plane, and identify $\mathbb{C}$ with $\mathbb{R}^2$. Let C be a simple closed curve in $\mathbb{R}^2$ parameterized by $\gamma(t) = (x(t), y(t))$, $a \le t \le b$. Assume that γ is traversed counterclockwise and that $\left\|\frac{d\gamma}{dt}\right\|_2 = 1$. Then the outward pointing unit normal to $\gamma(t)$ is given by $N = \left(\frac{dy}{dt}, -\frac{dx}{dt}\right)$. Thus, if $\nabla\log\sigma \cdot N = \left(-\frac{\partial\log\sigma}{\partial y}\frac{dx}{dt} + \frac{\partial\log\sigma}{\partial x}\frac{dy}{dt}\right)$ is positive at a point of C, then fluid is flowing out of D (the interior of C) at that point. The net fluid flowing out of D is given by the integral

$$\text{net flow} = \int_C \left(\frac{\partial\log\sigma}{\partial x}, \frac{\partial\log\sigma}{\partial y}\right)\cdot(dy,-dx) \tag{11.45a}$$

$$= \int_C \left(-\frac{\partial\log\sigma}{\partial y}\,dx + \frac{\partial\log\sigma}{\partial x}\,dy\right) \tag{11.45b}$$

$$= \int_a^b \left(-\frac{\partial\log\sigma}{\partial y}\frac{dx}{dt} + \frac{\partial\log\sigma}{\partial x}\frac{dy}{dt}\right)dt \quad . \tag{11.45c}$$

Using Stokes' Theorem,

$$\text{net flow} = \int_D \left(\frac{\partial^2 \log\sigma}{\partial x^2} + \frac{\partial^2 \log\sigma}{\partial y^2} \right) dx \wedge dy \quad . \tag{11.46}$$

Thus if log σ were harmonic, the net fluid flow would be zero. For the largest singular value, (9.25) shows that $\nabla^2 \log \bar{\sigma} \geq 0$. Thus the net fluid flow out of D is positive. Similarly, for the smallest singular value $\nabla^2 \log \underline{\sigma} \leq 0$. Thus the net fluid flow out of D is negative. For intermediate singular values no general statement may be made. However, since det M(s) is an analytic function it follows that $\log|\det M| = \prod_{i=1}^{n} \log\sigma_i$ is harmonic. Thus the sum of the net flows (11.46) over all singular values must be equal to zero. For example, in the case n=2, it is as though the excess fluid entering the region D from the flow $\nabla \log \underline{\sigma}$ is somehow transferred and leaves D in the flow $\nabla \log \bar{\sigma}$.

From (11.43) and (11.44) it follows that equations analogous to the Cauchy-Riemann equations for $\sigma e^{j\tilde{\theta}_k}$ and $\sigma e^{j\theta}$ are given by

$$j \left(\frac{\partial \log\sigma}{\partial x} - \frac{\partial \tilde{\theta}_k}{\partial y} \right) = \rho_{kv}^H \frac{\partial \rho_{kv}}{\partial y} - \rho_{ku}^H \frac{\partial \rho_{ku}}{\partial y}$$

$$j \left(\frac{\partial \log\sigma}{\partial y} + \frac{\partial \tilde{\theta}_k}{\partial x} \right) = -\rho_{kv}^H \frac{\partial \rho_{kv}}{\partial x} + \rho_{ku}^H \frac{\partial \rho_{ku}}{\partial x} \tag{11.47}$$

and

$$j \left(\frac{\partial \log\sigma}{\partial x} - \frac{\partial \theta}{\partial y} \right) = \rho_v^H \frac{\partial \rho_v}{\partial y} - \rho_{ku}^H \frac{\partial \rho_{ku}}{\partial y} \quad .$$

$$j \left(\frac{\partial \log\sigma}{\partial y} + \frac{\partial \theta}{\partial x} \right) = -\rho_v^H \frac{\partial \rho_v}{\partial x} + \rho_{ku}^H \frac{\partial \rho_{ku}}{\partial x} \quad . \tag{11.48}$$

Note the right hand side of (11.48) may be obtained from that of (11.47) using the function g_k:

$$\rho_{kv}^{H}\frac{\partial\rho_{kv}}{\partial x} = \rho_{v}^{H}\frac{\partial\rho_{v}}{\partial x} + g_k^{-1}\frac{\partial g_k}{\partial x}$$

$$\rho_{kv}^{H}\frac{\partial\rho_{kv}}{\partial y} = \rho_{v}^{H}\frac{\partial\rho_{v}}{\partial y} + g_k^{-1}\frac{\partial g_k}{\partial y} \tag{11.49}$$

where it may be shown from (11.40) and (10.41) that

$$g_k^{-1}\frac{\partial g_k}{\partial x} = \frac{\partial}{\partial x}\{j \measuredangle\, \rho_{ku}^{H}\rho_{kv}\}$$

$$g_k^{-1}\frac{\partial g_k}{\partial y} = \frac{\partial}{\partial y}\{j \measuredangle\, \rho_{ku}^{H}\rho_{kv}\} \quad . \tag{11.50}$$

Equations (11.47) and (11.48) may be expressed in coordinates on $\mathbb{C}P^{n-1}$. For the case n=2, k=1:

$$\frac{\partial \log\sigma}{\partial x} - \frac{\partial\tilde{\theta}_1}{\partial y} = \sin^2\phi_v \frac{\partial\psi_v}{\partial y} - \sin^2\phi_u \frac{\partial\psi_u}{\partial y}$$

$$\frac{\partial \log\sigma}{\partial y} + \frac{\partial\tilde{\theta}_1}{\partial x} = -\sin^2\phi_v \frac{\partial\psi_v}{\partial x} + \sin^2\phi_u \frac{\partial\psi_u}{\partial x} \tag{11.51}$$

and

$$\frac{\partial \log\sigma}{\partial x} - \frac{\partial\theta}{\partial y} = \sin^2\phi_v \frac{\partial\psi_v}{\partial y} - \sin^2\phi_u \frac{\partial\psi_u}{\partial y}$$
$$- \frac{\partial}{\partial y}\measuredangle[\cos\phi_v \cos\phi_v + \sin\phi_u \sin\phi_v\, e^{j(\psi_v-\psi_u)}]$$

$$\frac{\partial \log\sigma}{\partial y} + \frac{\partial\theta}{\partial x} = -\sin^2\phi_v \frac{\partial\psi_v}{\partial x} + \sin^2\phi_u \frac{\partial\psi_u}{\partial x}$$
$$+ \frac{\partial}{\partial x}\measuredangle[\cos\phi_u \cos\phi_v + \sin\phi_u \sin\phi_v\, e^{j(\psi_v-\psi_u)}] \quad . \tag{11.52}$$

Similar equations may be derived for $n > 2$ and for other local trivializations T_k.

A differential one-form $\omega(x,y) = A(x,y)dx + B(x,y)dy$ called <u>exact</u> if there exists a function $f(x,y)$ such that $df = \omega = \frac{\partial f}{\partial x}dx + \frac{\partial f}{\partial y}dy$. If mixed

second partial derivatives of f are equal, then $d\omega = d^2 f = (\frac{\partial^2 f}{\partial y \partial x} - \frac{\partial^2 f}{\partial x \partial y})\cdot$ $dx \wedge dy = 0$ and ω is said to be closed (Spivak [49, p. 91]). A standard result is that all exact forms are closed. Thus if two one-forms ω_1 and ω_2 differ by an exact form, it follows that $d\omega_1 = d\omega_2$. Recall it was shown in Appendix G that, at points where the singular values are distinct, partial derivatives of all orders of the singular values and vectors exist. Moreover, away from singularities in the coordinate systems used to describe the singular vectors, this property is preserved so that, in particular, mixed second partial derivatives of $\theta, \tilde{\theta}_k$, ϕ_v, ϕ_u, etc. are equal.

Now, consider the forms (11.43) and (11.44). Since $d\tilde{\theta}_k$ and $d\theta$ appear on the left hand side of these forms it follows that (11.43) and (11.44) differ from the form A in (11.33) by an exact differential. Thus taking d of the left-hand side of (11.43) or (11.44) yields the Laplacian of log σ just as in (11.34). Using (11.51) in (11.43) and taking d gives the Laplacian in coordinates

$$\nabla^2 \log\sigma = \sin 2\phi_v \left(\frac{\partial \phi_v}{\partial y} \frac{\partial \psi_v}{\partial x} - \frac{\partial \phi_v}{\partial x} \frac{\partial \psi_v}{\partial y} \right) - \sin 2\phi_u \left(\frac{\partial \phi_u}{\partial x} \frac{\partial \psi_u}{\partial y} - \frac{\partial \phi_u}{\partial y} \frac{\partial \psi_u}{\partial x} \right) . \tag{11.53}$$

Equations for $\nabla^2 \tilde{\theta}_k$ and $\nabla^2 \theta$ may also be derived from (11.43) or (11.44). Thus what can be done using the star operator [54]? For our purposes it suffices to define * for one-forms on $\mathbb{R}^2$. Let $\omega = Adx + Bdy$ with A and B real valued functions of (x,y); then $*\omega = -Bdx + Ady$. Note that if $\omega = df = \frac{\partial f}{\partial x} dx + \frac{\partial f}{\partial y} dy$, then $\omega \wedge *\omega = [(\frac{\partial f}{\partial x})^2 + (\frac{\partial f}{\partial y})^2] dx \wedge dy$. Note also that the integrand of (11.45a) is just $*d(\log \sigma)$.

Applying the operator * to (11.43) and using coordinates yields (for n=2 and k=1)

$$\left(\frac{\partial\tilde{\theta}_1}{\partial y} - \frac{\partial \log\sigma}{\partial x}\right)dx - \left(\frac{\partial \log\sigma}{\partial y} + \frac{\partial\tilde{\theta}_1}{\partial x}\right)dy$$
$$= -\left(\sin^2\phi_v \frac{\partial\psi_v}{\partial y} - \sin^2\phi_u \frac{\partial\psi_u}{\partial y}\right)dx + \left(\sin^2\phi_v \frac{\partial\psi_v}{\partial x} - \sin^2\phi_u \frac{\partial\psi_u}{\partial x}\right)dy \quad . \tag{11.54}$$

An equation for $\nabla^2\tilde{\theta}_1$ may be obtained from (11.54) by taking d of both sides:

$$\nabla^2\tilde{\theta}_1 = -\sin 2\phi_v\left(\frac{\partial\phi_v}{\partial y}\frac{\partial\psi_v}{\partial y} + \frac{\partial\phi_v}{\partial x}\frac{\partial\psi_v}{\partial x}\right)$$
$$+ \sin 2\phi_u\left(\frac{\partial\phi_u}{\partial y}\frac{\partial\psi_u}{\partial y} + \frac{\partial\phi_u}{\partial x}\frac{\partial\psi_u}{\partial x}\right)$$
$$- \sin^2\phi_v\left(\frac{\partial^2\psi_v}{\partial x^2} + \frac{\partial^2\psi_v}{\partial y^2}\right) + \sin^2\phi_u\left(\frac{\partial^2\psi_u}{\partial x^2} + \frac{\partial^2\psi_u}{\partial y^2}\right) \quad . \tag{11.55}$$

Note that in general $\nabla^2\tilde{\theta}_1 \neq \nabla^2\theta$; the form (11.54) and the analogous form obtained from (11.44) do not differ by an exact differential.

11.3. Cauchy's Integral Theorem and a Simple Method for Deriving Differential Equations

In Section 11.2 and Chapter 9, a number of differential equations were derived constraining the properties of a matrix transfer function. The basic strategy was to obtain differential equations for the singular values and vectors of a matrix M(s) in terms of $\frac{\partial M}{\partial x}$ and $\frac{\partial M}{\partial y}$. By then observing that M(s) must satisfy the Cauchy-Riemann equations, it was shown that the singular values and vectors are not mutually independent functions. By assigning coordinates to the singular vectors it could be shown, for

example, that knowledge of the singular values and singular subspaces determines the phase difference parameters θ_i and $\tilde{\theta}_i$ to within an arbitrary constant.

It should be pointed out that the generalized Cauchy-Riemann equations (11.47) or (11.48) are not the only ones constraining the behavior of the transfer function matrix. Lemma 9.6 may be used in conjunction with the differential equations (9.17)-(9.22) to show that additional constraints on the singular vectors, and thus the coordinates ϕ_{ui}, ϕ_{vi}, ψ_{ui} and ψ_{vi}, must be satisfied. Rather than list examples, a systematic method for deriving a complete set of generalized Cauchy-Riemann equations will now be presented. The basic philosophy is that constraints on system properties imposed by local analyticity of transfer functions are completely known. However, this knowledge is expressed in standard coordinates for the matrix, while other coordinates are more meaningful in assessing feedback properties. Thus the goal is to study how constraints imposed by local analyticity manifest themselves after coordinate transformations.

In addition to the Cauchy-Riemann equations, locally analytic functions must satisfy Cauchy's Integral Theorem [26,48]. Let $f(s) = g(s) + jh(s)$ be locally analytic in s over a simply connected region $G \subseteq \mathbb{C}$, let C be a simple closed curve in G, and let D denote the interior of C. Then

$$\int_C f(s)ds = 0 \quad . \qquad (11.56)$$

One way of proving (11.56) is to use the Cauchy-Riemann Equations (9.1) and Stokes' Theorem [49, pp. 105-106]. Thus

$$\int_C f(s)ds = \int_D df \wedge ds \qquad , \tag{11.57}$$

where

$$\begin{aligned} df \wedge ds &= \left(\frac{\partial f}{\partial x} dx + \frac{\partial f}{\partial y} dy \right) \wedge (dx + j\ dy) \\ &= j \left(\frac{\partial f}{\partial x} + j \frac{\partial f}{\partial y} \right) dx \wedge dy \\ &= 0 \end{aligned}$$

by (9.1). When applied to the nonanalytic function $\log \sigma + j\ \theta$, Stokes' Theorem yields

$$\begin{aligned} \int_C (\log \sigma + j\ \theta) ds &= \int_D d\log\sigma \wedge ds + j\ d\theta \wedge ds \\ &= j \int_D \left[\left(\frac{\partial \log\sigma}{\partial x} - \frac{\partial \theta}{\partial y} \right) + j \left(\frac{\partial \log\sigma}{\partial y} + \frac{\partial \theta}{\partial x} \right) \right] dx \wedge dy . \end{aligned} \tag{11.58}$$

If θ is given by (11.39), then the generalized Cauchy-Riemann equations (11.48) show that (11.58) does not generally equal zero. Thus the same motion of singular subspaces which prevents $\sigma e^{j\theta}$ from satisfying the Cauchy-Riemann equations also prevents Cauchy's Integral Theorem from being satisfied. Similar remarks hold for the function $\sigma e^{j\tilde{\theta}_k}$, with $\tilde{\theta}_k$ defined as in (11.37) and generalized Cauchy-Riemann equations given by (11.47).

Since each element of a transfer function matrix M(s) written in standard coordinates is locally analytic, it follows that, under the conditions on C given prior to (11.56),

$$\int_C M\ ds = 0 \qquad . \tag{11.59}$$

Equivalently,

$$dM \wedge ds = 0 \ , \ \forall s \in D \qquad . \tag{11.60}$$

Condition (11.60) is the key to seeing how the property of analyticity generalizes to nonstandard coordinates. Write M in terms of its singular value decomposition

$$M = V \Sigma U^H \qquad . \tag{11.61}$$

Then

$$0 = dM \wedge ds = (dV \wedge ds)\Sigma U^H + V(d\Sigma \wedge ds)U^H + V\Sigma(dU^H \wedge ds)$$

$$\Rightarrow \qquad [dV\Sigma U^H + Vd\Sigma U^H + V\Sigma dU^H]\wedge ds = 0$$

$$\Rightarrow \qquad \Sigma^{-1} d\Sigma \wedge ds = -\ [dU^H U + \Sigma^{-1} V^H dV \Sigma]\wedge ds \qquad . \tag{11.62}$$

By writing, e.g., $d\Sigma = \frac{\partial \Sigma}{\partial x} dx + \frac{\partial \Sigma}{\partial y} dy$, (11.62) reduces to $2n^2$ partial differential equations which must be satisfied by the singular values and vectors of M(s). For example, writing

$$\begin{aligned} \Sigma &= \mathrm{diag}[\sigma_i] \ , \quad \sigma_1 \geq \sigma_2 \geq \ldots \geq \sigma_n \\ V &= [v_1 \mid \ldots \mid v_n] \\ U &= [u_1 \mid \ldots \mid u_n] \end{aligned} \tag{11.63}$$

yields (assuming n=2 for simplicity):

$$\begin{bmatrix} d\log\sigma_1 & 0 \\ 0 & d\log\sigma_2 \end{bmatrix} \wedge ds = -\left\{ \begin{bmatrix} du_1{}^H u_1 & du_1{}^H u_2 \\ du_2{}^H u_1 & du_2{}^H u_2 \end{bmatrix} + \begin{bmatrix} v_1{}^H dv_1 & \frac{\sigma_2}{\sigma_1} v_1{}^H dv_2 \\ \frac{\sigma_1}{\sigma_2} v_2{}^H dv_1 & v_2{}^H dv_2 \end{bmatrix} \right\} \wedge ds \quad . \tag{11.64}$$

Taking real and imaginary parts of the four components of (11.64) yields the eight desired equations. If so desired, coordinates may be assigned to the singular vectors. Then the diagonal elements of (11.62) yield generalized Cauchy-Riemann equations relating the singular values to measures of phase difference between the left and right singular vectors.

Note also that the same technique may be used to obtain differential equations which must be satisfied by other decompositions of a transfer matrix. Examples are the polar decomposition [14] and eigenvalue-eigenvector decompositions.

Note also that $2n^2$ equations analogous to the Laplacian may be derived using the "d" and the "*" operators. From (11.61) it follows that

$$dM = dV\Sigma U^H + Vd\Sigma U^H + V\Sigma dU^H$$

$$\Rightarrow \quad V^H dMU = V^H dV\Sigma + d\Sigma + \Sigma dU^H U$$

$$\Rightarrow \quad \Sigma^{-1} V^H dMU = \Sigma^{-1} V^H dV\Sigma + \Sigma^{-1} d\Sigma + dU^H U$$

$$\Rightarrow \quad U^H M^{-1} dMU = \Sigma^{-1} V^H dV\Sigma + \Sigma^{-1} d\Sigma + dU^H U \tag{11.65}$$

assuming that M^{-1} exists. Note that the diagonal elements of $\Sigma^{-1}d\Sigma$ are given by

$$d\log\sigma_i = \frac{\partial\log\sigma_i}{\partial x} dx + \frac{\partial\log\sigma_i}{\partial y} dy \quad . \tag{11.66}$$

Applying * to (11.66):

$$*d(\log\sigma_i) = -\frac{\partial\log\sigma_i}{\partial y} dx + \frac{\partial\log\sigma_i}{\partial x} dy \quad . \tag{11.67}$$

Applying d to (11.67):

$$d{*}d(\log\sigma_i) = \left(\frac{\partial^2 \log\sigma_i}{\partial x^2} + \frac{\partial^2 \log\sigma_i}{\partial y^2}\right) dx \wedge dy \ . \tag{11.68}$$

Since M(s) satisfies Laplace's equation, taking d* of (11.65) yields a matrix equation which must be satisfied by the second partial derivatives of the singular values and vectors. In particular, the real parts of the diagonal elements of the equation give formulas for $\nabla^2 \log\sigma_i$.

11.4. Summary

The purpose of this chapter has been to explore the mathematical structure of the differential equations governing singular values and vectors. It was shown that geometric ideas lend themselves readily to the analysis of properties of these equations whose study was originally motivated by the thought experiments in Chapter 9.

Finally, it should be pointed out that the differential equations discussed in Chapter 9 and in this chapter group themselves into two distinct sets. One set, which will be termed analysis equations (e.g., (9.12), (9.13), (9.19), (9.20), and (9.25)), may be used to obtain the derivatives of singular values and vectors in terms of derivatives of the transfer function matrix. Thus they are useful in determining the properties of a specific matrix.

The other set of equations (e.g., (11.43), (11.44), (11.51), (11.52), (11.53), and (11.55)), which will be termed design equations, give relations among the derivatives of the singular values and vectors which must be satisfied by any matrix transfer function. Thus these equations, in

principle, play the same role as do the Bode integral relations. They constrain the behavior of physical systems and thus limit the properties which may be achieved in feedback design. The difficulty, of course, is that it is very hard to get any insight from the differential equations. Thus in the next chapter a generalization of Bode gain-phase relations to multivariable system is pursued.

CHAPTER 12

GENERALIZATION OF BODE GAIN-PHASE RELATION TO MULTIVARIABLE SYSTEMS

12.1. Introduction

In the previous chapters the concept of a local trivialization has been used to express the left and right singular vectors in coordinates. The resulting sets of parameters each included a measure of phase difference between the left and right singular vectors. In Chapter 8, an example was presented which suggested that the function $\sigma e^{j\theta}$ could be related to feedback properties in much the same way as could a scalar open loop transfer function. The relation between σ and θ, however, was clearly not that between the gain and phase of a stable minimum-phase rational transfer function. This motivated the study of just how these two functions were related. Towards this end, differential equations analogous to the Cauchy-Riemann equations were derived. These equations showed, in principle, that θ and σ were related as a function of the singular subspaces. It was not clear, however, that such generalized Cauchy-Riemann equations provide much insight into the nature of this relation. Motivated by the Bode gain-phase relations for scalar feedback systems, which provide more insight than the scalar Cauchy-Riemann equations, one is naturally led to ask whether analogous integral relations may be obtained for relating θ and $\log \sigma$. The purpose of this chapter is to provide such a generalization and, in particular, to study the effect of motion of the singular subspaces.

12.2. Integral Relations Among Singular Values, Phase Differences, and Singular Subspaces

In Chapter 11 the one-form

$$\begin{aligned} A_i &= j[-\frac{\partial \log \sigma_i}{\partial y} dx + \frac{\partial \log \sigma_i}{\partial x} dy] \\ &= \frac{j}{\sigma_i} \mathrm{Im}[v_i^H \frac{\partial M}{\partial x} u_i]dx + \frac{j}{\sigma_i} \mathrm{Im}[v_i^H \frac{\partial M}{\partial y} u_i]dy \\ &= [v_i^H \frac{\partial v_i}{\partial x} - u_i^H \frac{\partial u_i}{\partial x}]dx + [v_i^H \frac{\partial v_i}{\partial y} - u_i^H \frac{\partial u_i}{\partial y}]dy \end{aligned} \tag{12.1}$$

was studied. It was shown that (12.1) relates the singular values to various measures of phase difference between the singular vectors. Assume that both the left and right singular vectors may be assigned phase coordinates using the local trivialization T_z, as in (10.5). (For the remainder of this chapter, the subscript "i" used in (12.1) to distinguish among singular values will be suppressed unless a specific singular value or singular vector pair is being discussed.) Then, using T_z, the left and right singular vectors may be written as in (10.8)

$$\begin{aligned} v(s) &= \rho_z([v(s)])e^{j\theta_z(v(s))} \\ u(s) &= \rho_z([u(s)])e^{j\theta_z(u(s))} \quad , \end{aligned} \tag{12.2}$$

where in this local trivialization the phase difference is given by

$$\Delta\theta_z(s) \triangleq \theta_z(v(s)) - \theta_z(u(s)) \quad . \tag{12.3}$$

Two examples of local trivializations were singled out in Chapters 10 and 11. The first used one of the standard basis vectors to define the phase of a vector w by $\theta_k(w) = \measuredangle e_k^H w$ as in (10.10). The second used a right singular vector u to define phase as $\theta_u(w) = \measuredangle u^H w$ as in (10.34).

In the remainder of this chapter, the subscript "z" will be suppressed in (12.2)-(12.3) unless a specific local trivialization is being discussed. Given any local trivialization, writing the singular vectors in terms of the local sections and phase difference coordinates as in (12.2) and substituting into (12.1) yields:

$$\frac{\partial \Delta\theta}{\partial x}\,dx + \frac{\partial \Delta\theta}{\partial y}\,dy = -\frac{\partial \log \sigma}{\partial y}\,dx + \frac{\partial \log \sigma}{\partial x}\,dy + j[\,\rho_v^H \frac{\partial \rho_v}{\partial x} - \rho_u^H \frac{\partial \rho_u}{\partial x}]dx$$
$$+ j[\,\rho_v^H \frac{\partial \rho_v}{\partial y} - \rho_u^H \frac{\partial \rho_u}{\partial y}]dy \qquad (12.4)$$

where $\rho_v \triangleq \rho[v(s)]$, $\rho_u \triangleq \rho[u(s)]$, and $\Delta\theta \triangleq \Delta\theta(s)$.

In principle (12.4) may be used to calculate $\Delta\theta(j\omega)$ as a function of the singular values and singular subspaces; i.e., assuming that the images of the left and right singular subspaces lie within the domain of definition of the section ρ, then

$$\Delta\theta(j\omega) = \int_{-\infty}^{\omega} [\frac{\partial \log \sigma}{\partial x} + j(\,\rho_v^H \frac{\partial \rho_v}{\partial y} - \rho_u^H \frac{\partial \rho_u}{\partial y})]dy + \Delta\theta(-j\infty) \qquad (12.5a)$$

and

$$\Delta\theta(j\omega) = \int_{\infty}^{\omega} [\frac{\partial \log \sigma}{\partial x} + j(\,\rho_v^H \frac{\partial \rho_v}{\partial y} - \rho_u^H \frac{\partial \rho_u}{\partial y})]dy + \Delta\theta(j\infty). \qquad (12.5b)$$

Hence

$$\Delta\theta(j\omega) - \frac{1}{2}[\Delta\theta(-j\infty) + \Delta\theta(j\infty)] = \frac{-1}{2}[\int_{\omega}^{-\infty} \frac{\partial \log \sigma}{\partial x}\,dy + \int_{\omega}^{\infty} \frac{\partial \log \sigma}{\partial x}\,dy]$$
$$\frac{-j}{2}\,[\int_{\omega}^{-\infty} (\,\rho_v^H \frac{\partial \rho_v}{\partial y} - \rho_u^H \frac{\partial \rho_u}{\partial y})dy + \int_{\omega}^{\infty} (\,\rho_v^H \frac{\partial \rho_v}{\partial y} - \rho_u^H \frac{\partial \rho_u}{\partial y})dy]. \qquad (12.6)$$

If $\sigma e^{j\Delta\theta}$ were a stable minimum phase proper rational transfer function, or if the singular subspaces were constant, then the second term

on the right hand side of (12.6) would not be present. Thus (12.6) would show that the value of $\Delta\theta$ is completely determined by σ, and Cauchy's integral theorem could be applied to show the function $\sigma e^{j\Delta\theta}$ must satisfy a Bode gain-phase relation as in Theorem 2.2.

In general, however, $\sigma e^{j\Delta\theta}$ is not analytic and Cauchy's Integral Theorem cannot be applied. However, an integral equation analogous to the Bode gain-phase relation may still be derived using Stokes' Theorem.

First, the behavior at infinity of the singular value decomposition will be discussed. Generally, the singular values will not be distinct at $s=\infty$; in fact, in many cases of interest they will all be equal to zero. The followsin Lemma states conditions under which it remains possible to uniquely define one-dimensional singular subspaces at $s=\infty$.

<u>Lemma 12.1</u>: Let the matrix $M(s)$ taking values in $\mathbb{C}^{n\times n}$ have entries which are proper rational transfer functions. Assume that $\det M(s) \not\equiv 0$ and that the singular values of $M(s)$ are distinct in the closed right half plane (CRHP). (Note this implies that the singular values may be ordered so that, $\forall s \in \text{CRHP}$, $\sigma_1[M(s)] > \sigma_2[M(s)] > \cdots > \sigma_n[M(s)]$.). Then there exist constants $k_i \geq 0$ and $c_i > 0$ such that for any $\alpha \in [-\pi/2, \pi/2]$

$$\lim_{R\to\infty} R^{k_i}\sigma_i[M(Re^{j\alpha})] = c_i. \tag{12.7}$$

Next assume, $\forall i$ and j, that if $k_i = k_j$, then $c_i \neq c_j$. Then $\forall i$ there exists a pair of unit vectors w_i and z_i, lying in uniquely defined one-dimensional subspaces $\mathbb{W}_i$ and $\mathbb{Z}_i$, such that for any $\alpha \in [-\pi/2, \pi/2]$

$$c_i = \lim_{R\to\infty} (Re^{j\alpha})^{k_i} w_i^H M(Re^{j\alpha}) z_i. \tag{12.8}$$

■

<u>Proof</u>: See Appendix I. ■

Suppose that the vectors w_i and z_i in (12.8) exist, and that these vectors both lie in the domain of definition of some local trivialization T. Then, by continuity, there exists a neighborhood of infinity such that the left and right singular vectors v_i and u_i also each lie within the domain of definition of T. Let $\Delta\theta_i$ be the phase difference (12.3) between v_i and u_i as measured in this trivialization. Then as $s \to \infty$ along the ray $Re^{j\alpha}$, $\alpha \in [-\pi/2, \pi/2]$

$$\Delta\theta_i \to \theta(w_i) - \theta(z_i) - k_i\alpha.$$

This follows from (12.8) since, as $R \to \infty$, the right singular vector may be chosen so that $u_i(Re^{j\alpha}) \to z_i$; the left singular vector must then satisfy $v_i(Re^{j\alpha}) \to (\frac{1}{e^{j\alpha}})^{k_i} w_i = (\frac{1}{c_i})R^{k_i} M(Re^{j\alpha}) z_i$.

Theorem 12.2: Let the matrix M(s), caking values in $\mathbb{C}^{n\times n}$, have entries which are proper rational transfer functions. Assume at each point in the closed right half plane (CRHP) that M(s) satisfies

(i) M(s) is analytic

(ii) $\det M(s) \neq 0$

(iii) M(s) has n distinct singular values.

Note that at each point $s \in$ CRHP there exists a local trivialization whose domain of definition includes both members of the ith pair of singular vectors u_i and v_i.

(iv) Assume that there exists a local trivialization T such that, $\forall s \in$ CRHP, $u_i(s)$ and $v_i(s)$ both lie within the domain of definition of T.

Finally, assume*

(v) in Lemma 12.1, if $k_i = k_j$, $i \neq j$, then $c_i \neq c_j$

(vi) the domain of definition of the local trivialization T given in (iv) also includes the vectors w_i and z_i given by Lemma 12.1.

Let T be a local trivialization satisfying (iv) and (vi). Note that at each point $s \in$ CRHP the left and right singular vectors and the phase difference corresponding to the singular value σ may be written as

$$v = \rho_v e^{j\theta_v} \triangleq \rho([v])e^{j\theta(v)} \tag{12.9a}$$

$$u = \rho_u e^{j\theta_u} \triangleq \rho([u])e^{j\theta(u)} \tag{12.9b}$$

$$\Delta\theta \triangleq \theta(v) - \theta(u) \quad . \tag{12.9c}$$

Assume the local trivialization has the property that $\rho([w]) = \overline{\rho([\overline{w}])}$. Then $\sigma\exp[j\Delta\theta]$ is conjugate symmetric, $\Delta\theta(0) = k\pi$, k an integer, and for each $\omega_o > 0$

$$\Delta\theta(j\omega_o) - \Delta\theta(0) = \frac{1}{\pi}\int_{-\infty}^{\infty} \frac{d \log \sigma}{d\nu} \{\log \coth \frac{|\nu|}{2}\} d\nu$$

$$+ \frac{1}{j\pi} \int_{CRHP} (\rho_v^H \frac{\partial\rho_v}{\partial r} - \rho_u^H \frac{\partial\rho_u}{\partial r}) dr \wedge d\alpha \tag{12.10}$$

$$\nu = \log(\frac{\omega}{\omega_o}) \quad . \tag{12.11}$$

■

<u>Proof</u>: See Appendix I. ■

Theorem 12.2 shows that the measure of phase difference $\Delta\theta(j\omega)$ may be computed from knowledge of the associated singular value and singular

*These assumptions may be relaxed.

AD-A161 452 ISSUES IN FREQUENCY DOMAIN FEEDBACK CONTROL(U) ILLINOIS UNIV AT URBANA DECISION AND CONTROL LAB J S FREUDENBERG MAY 85 DC-81 N00014-84-C-0149 4/5

UNCLASSIFIED F/G 9/3 NL

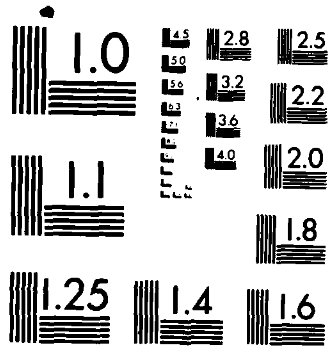

MICROCOPY RESOLUTION TEST CHART
NATIONAL BUREAU OF STANDARDS-1963-A

subspaces. Thus in one respect, $\Delta\theta(j\omega)$ is similar to the phase of a scalar transfer function. Once enough of the other properties of a system are specified, there is no freedom remaining to specify $\Delta\theta(j\omega)$. There does exist an important difference, however. The phase difference $\Delta\theta(j\omega)$ is a function, not only of the gain σ along the $j\omega$-axis, but also of the way in which the input and output directions vary over the right half plane.

An interpretation of the integrand of the second integral in (12.10) will now be developed. Consider the differential form A_i in (12.1) evaluated along a curve $\gamma(t) \in \mathbb{C}$. Then, suppressing the subscript "i" used to distinguish among singular values, this yields

$$j\left[\frac{-\partial \log\sigma}{\partial y}\frac{dx}{dt} + \frac{\partial \log\sigma}{\partial x}\frac{dy}{dt}\right] = \frac{j}{\sigma}\,\mathrm{Im}\left[v^H \frac{dM}{dt} u\right]$$

$$= v^H \frac{dv}{dt} - u^H \frac{du}{dt} \quad . \qquad (12.12)$$

The discussion will proceed by showing how the right hand side of (12.12) is related to the integrand of the second integral in (12.10). First, given an arbitrary unit vector w, the meaning of the term $w^H \frac{dw}{dt}$ (the component of the derivative of the vector lying along the vector itself) will be explored. Let the unit vector in question be written as

$$w(t) = \rho(t)e^{j\theta(t)} \qquad (12.13a)$$

where

$$\rho(t) \triangleq \rho([w(t)]) \qquad (12.13b)$$

is the local section corresponding to the local trivialization used to assign the measure of phase

$$\theta(t) \triangleq \theta(w(t)) \quad . \qquad (12.13c)$$

Then,

$$w^H \frac{dw}{dt} = \rho^H \frac{d\rho}{dt} + j\,\frac{d\theta}{dt} \quad . \tag{12.14}$$

To explore the significance of (12.14), first recall that a unit vector defined along a curve through $\mathbb{C}P^{n-1}$ is said to be "minimum energy" if $w^H \frac{dw}{dt} \equiv 0$. This condition, in turn, implies that the vector changes along the curve by only the amount needed to remain in the appropriate subspace of $\mathbb{C}^n$.

Consider first the case in which the subspace spanned by w(t) is constant. Since the local section ρ is a function of (and only of) this subspace, it follows that $\frac{d\rho}{dt} = 0$. Thus, in this case, the "excess energy" measured by a nonzero value of $w^H \frac{dw}{dt}$ translates completely into a change in the phase θ. In this way, the vector w(t) is analogous to a scalar allpass function (i.e., a function whose magnitude is constant with t). (Note also the condition that the subspace spanned by w(t) is constant implies that w(t) moves along the great circle of S^{2n-1} identified with the circle of unit vectors of $\mathbb{C}^n$ lying in the subspace spanned by w.)

Now recall the thought experiments discussed in Chapter 9. These suggested that there exists a component of the motion of a unit vector analogous to "spinning," and that the measure of spinning is given by $w^H \frac{dw}{dt}$. Hence, minimum energy vectors are those which do not "spin" as they move. It was further conjectured that the spinning of a unit vector might be related to some measure of the changing phase of the vector. Moreover, when a pair of left and right singular vectors was considered, the difference $v^H \frac{dv}{dt} - u^H \frac{du}{dt}$, interpreted as the difference in the rates of spinning of the vectors, was conjectured to be related to some measure of changing phase difference between

the vectors. In Chapter 9, these conjectures could not be investigated, since no rigorous notions of phase of a vector, or of phase difference between vectors, were yet available. Using the ideas about phase developed in Chapters 10 and 11, these conjectures will now be explored. The essential equation is (12.14).

Now, as has just been pointed out, in the special case where the subspace spanned by $w(t)$ is constant, the value of $w^H \frac{dw}{dt}$ is indeed equal to the rate of change of θ, the measure of phase. Moreover, this conclusion is independent of the trivialization used to measure θ. Recall next another special case introduced in Chapter 9, i.e., that in which the vector w is minimum energy (but the subspace it spans is not necessarily constant). From (12.14) it follows immediately that the measure of phase θ may change even if $w^H \frac{dw}{dt} = 0$. A necessary and sufficient condition for this to occur is that the section ρ not be minimum energy; i.e., that $\rho^H \frac{d\rho}{dt} \neq 0$. Note another necessary condition for $w^H \frac{dw}{dt} \neq j \frac{d\theta}{dt}$ is that the subspace $[w(t)]$ not be constant. This is not a sufficient condition, however, since the component $\rho^H \frac{d\rho}{dt}$ must also be nonzero.

Finally, consider the general case, in which $w^H \frac{dw}{dt} \neq 0$ and the subspace spanned by $w(t)$ also is changing (implying that $\frac{d\rho}{dt} \neq 0$). It follows that the value of $w^H \frac{dw}{dt}$ measures, not the rate of change of the phase θ, but rather the rate of change of the difference between θ and the phase θ^* of a minimum energy vector $w^*(t)$ traversing the same path through $\mathbb{C}P^{n-1}$. This may be seen easily from (12.14), from which it follows that the rate of change of the phase of $w^*(t)$ is given by $j \frac{d\theta^*}{dt} = - \rho^H \frac{d\rho}{dt}$. In the general case, therefore, $j \frac{d\theta}{dt} = w^H \frac{dw}{dt} + j \frac{d\theta^*}{dt}$.

Note that the value of $w^H \frac{dw}{dt}$ is independent of the local trivialization used to define phase. The rate of change of the difference $\theta - \theta^*$, however, is not so independent. This is because the rate of change of the phase θ^* of a minimum energy vector is a function of the local trivialization used, as is the value of the component $\rho^H \frac{d\rho}{dt}$ of the derivative of the corresponding local section. Thus, from (12.14), the value of the rate of change of $\dot{\theta}$ is equal to the difference between the component $w^H \frac{dw}{dt}$ and the value of the connection one-form $\rho^H d\rho$ evaluated on the tangent vector to the curve through $\mathbb{C}P^{n-1}$ traversed by $[w(t)]$. This latter term, of course, quantifies the amount by which the section ρ itself deviates from being a "minimum energy" vector. Finally, observe that once a local trivialization with which to measure the phase of w has been chosen, then the discrepancy between $w^H \frac{dw}{dt}$ and $\frac{d\theta}{dt}$ is a function solely of the path through $\mathbb{C}P^{n-1}$ along which $w(t)$ is constrained to travel (equivalently, the way in which the subspace $[w(t)]$ changes.) This follows since choosing a local trivialization implies a choice of rule for defining the local section ρ, which in turn is a function solely of the subspace in which the vector w lies. In some sense, it may be said that changes in the phase θ arise from two sources. One source is the value of the component $w^H \frac{dw}{dt}$, while the other source is the motion of the subspace $[w(t)]$. This latter source will now be studied further.

It is instructive to write ρ in coordinates so that insight may be gained into how motion of the subspaces produces a change in phase. Assume that the local trivialization used to compute θ is given by $\theta = \theta_{z_1}(w) = \measuredangle z_1^H w$, where z_1 is a constant unit vector. Choose constant vectors z_i, $i=2,\ldots,n$, so that $\{z_i \; ; \; i=1,\ldots,n\}$ is an orthonormal basis for $\mathbb{C}^n$. Then

$$\rho = \rho_{z_1}([w]) = \sum_{i=1}^{n} z_i(z_i^H \rho) \tag{12.14}$$

where $z_1^H \rho$ is a positive real number. Thus

$$\frac{d\rho}{dt} = \sum_{i=1}^{n} z_i(z_i^H \frac{d\rho}{dt}) \tag{12.15}$$

$$\Rightarrow \qquad \rho^H \frac{d\rho}{dt} = \sum_{i=1}^{n} (\rho^H z_i)(z_i^H \frac{d\rho}{dt}) \quad . \tag{12.16}$$

Write

$$r_i e^{j\alpha_i} \triangleq z_i^H \rho \quad , \tag{12.17}$$

where $\sum_{i=1}^{n} r_i^2 \equiv 1$ since $\{z_i\}$ is an orthonormal basis and ρ is a unit vector. Note, also that $\alpha_1 \equiv 0$, since $\alpha_1 = \measuredangle z_1^H \rho$, and this component of ρ is positive real since the vector z_1 was used to define the local trivialization for which ρ is the local section. These facts imply, in turn, that $\sum_{i=1}^{n} r_i \frac{dr_i}{dt} = \frac{1}{2}\frac{d}{dt}\sum_{i=1}^{n} r_i^2 = 0$, and that $\frac{d\alpha_1}{dt} = 0$. Thus, since the z_i's are constant,

$$\begin{aligned}
z_i^H \frac{d\rho}{dt} &= \frac{d}{dt}(z_i^H \rho) \\
&= \frac{dr_i}{dt} e^{j\alpha_i} + r_i e^{j\alpha_i} j \frac{d\alpha_i}{dt} \\
\Rightarrow \quad \rho^H \frac{d\rho}{dt} &= \sum_{i=1}^{n} (r_i e^{-j\alpha_i})[\frac{dr_i}{dt} e^{j\alpha_i} + j\, r_i e^{j\alpha_i} \frac{d\alpha_i}{dt}] \\
&= \sum_{i=1}^{n} [r_i \frac{dr_i}{dt} + j\, r_i^2 \frac{d\alpha_i}{dt}] \quad ,
\end{aligned}$$

$$\Rightarrow \quad \rho^H \frac{d\rho}{dt} = j \sum_{i=2}^{n} r_i^2 \frac{d\alpha_i}{dt} \quad . \tag{12.18}$$

Let the subspace spanned by w be denoted [w]. Equation (12.18) reveals a condition necessary for motion of [w] to produce a change in $\measuredangle z_1^H w$; i.e., in the

phase of that component of w used to define θ via the local trivialization under discussion. First, note that (12.14) implies w may be written as

$$
\begin{aligned}
w &= \rho e^{j\theta} \\
&= \sum_{i=1}^{n} z_i (z_i^H \rho e^{j\theta}) \\
&= Z \begin{bmatrix} z_1^H w \\ z_2^H w \\ \vdots \\ z_n^H w \end{bmatrix} = Z \begin{bmatrix} r_1 \\ r_2 \; e^{j\alpha_2} \\ \vdots \\ r_n \; e^{j\alpha_n} \end{bmatrix} e^{j\theta} \quad ,
\end{aligned} \tag{12.19}
$$

where $Z = [z_1 \mid \cdots \mid z_n]$, $\theta = \measuredangle z_1^H w$, and $\alpha_i = \measuredangle z_i^H w - \measuredangle z_1^H w$. Observe that each α_i equals the difference in phase between the components $z_i^H w$ and $z_1^H w$. (Hence, α_1 is identically equal to zero and $e^{j\alpha_1} \equiv 1$.) Next, note that (12.13) and (12.18) taken together imply

$$
\begin{aligned}
w^H \frac{dw}{dt} &= j \frac{d\theta}{dt} + j \sum_{i=2}^{n} r_i^2 \frac{d\alpha_i}{dt} \\
&= j \sum_{i=1}^{n} r_i^2 \frac{d\theta}{dt} + j \sum_{i=2}^{n} r_i^2 \frac{d\alpha_i}{dt} \\
&= j \sum_{i=1}^{n} r_i^2 \left(\frac{d\theta}{dt} + \frac{d\alpha_i}{dt}\right)
\end{aligned} \tag{12.20}
$$

where the last equality holds since α_1 is constant. Equation (12.20) reveals a condition <u>necessary</u> for the motion of the subspace [w] to cause the value of $\frac{d\theta}{dt}$ to deviate from that of $w^H \frac{dw}{dt}$. The condition is that the rate of change of the difference in phase between $z_1^H w$ and at least one of the other components $z_i^H w$, i=2,...,n, must be nonzero. That is, it is necessary that $\frac{d\alpha_i}{dt} \neq 0$ for at

least one value of i, $2 \leq i \leq n$. Moreover, note that this condition is necessary no matter what choice of vectors $\{z_i \ ; \ i=2,\ldots,n\}$ is used to complete the orthonormal basis in (12.14). (Recall the vector z_1 is determined by the local trivialization and hence is fixed.) Thus, if there exists <u>any</u> choice of $\{z_i \ ; \ i=2,\ldots,n\}$ for which $\frac{d\alpha_i}{dt} = 0 \ \ \forall \ i=2,\ldots,n$, it follows that $\rho^H \frac{d\rho}{dt} = 0$ (i.e., $\rho(t) = \rho_{z_1}([w(t)])$ is a minimum energy vector) and the motion of [w] does not affect θ. (The converse to this statement is not true, however. It may well be that, for some choice of basis, $\rho^H \frac{d\rho}{dt} = 0$ due to cancellations among nonzero terms on the right hand side of (12.18).) Note, in particular, that if the motion of [w] produces changes only in the relative <u>magnitudes</u> of the various components of w, then no effect upon θ is produced. To summarize, a necessary condition for motion of the subspace [w] to affect the value of θ is that $\exists i$, $2 \leq i \leq n$, for which $\frac{d\alpha_i}{dt} \neq 0$. A sufficient condition is that the weighted sum $\sum_{i=2}^{n} r_i^2 \frac{d\alpha_i}{dt} \neq 0$.

The preceding remarks may also be viewed in terms of the decomposition of the tangent space into horizontal and vertical subspaces, as discussed in Chapter 11. Consider $X \in T_w S^{2n-1}$ and decompose X into its horizontal and vertical components as in (11.4): $X = X^V + X^H$. Evaluating the form $w^H dw$ on the vertical component X^V yields

$$\begin{aligned} w^H dw(X^V) &= \rho^H d\rho(\pi_* X^V) + j \ d\theta(X^V) \\ &= j \ d\theta(X^V) \end{aligned} \qquad (12.21)$$

because $\pi_* X^V = 0$ by the characterization (11.3)' of the vertical subspace. Furthermore, note that (11.3)' implies $\frac{d\rho}{dt} = 0$ along any curve whose tangent vector lies in the vertical subspace. Thus, since $\rho = \sum_{i=1}^{n} z_i (r_i \ e^{j\alpha_i})$, it

follows that $\frac{d\alpha_i}{dt} = 0$ along such curves and that $w^H \frac{dw}{dt} = j \sum_{i=1}^{n} r_i^2 \frac{d\theta}{dt} = j \frac{d\theta}{dt}$ by (12.20) and the fact that w is a unit vector. Consequently, the vertical component of a tangent vector can produce only <u>equal</u> changes in the phase of each component of w.

The horizontal component of a tangent vector, on the other hand, can <u>never</u> produce equal nonzero changes in the phase of each of the components of w. This fact follows from the characterization (11.2) of the horizontal subspace and Equation (12.20). Together, these expressions yield

$$\begin{aligned} w^H dw(X^H) &= j\, d\theta(X^H) + \rho^H d\rho(\pi_* X^H) \\ &= j\, d\theta(X^H) + j \sum_{i=2}^{n} r_i^2\, d\alpha_i(\pi_* X^H) \\ &= 0 \quad . \end{aligned} \tag{12.22}$$

Equation (12.22) shows that along a curve whose tangent vector lies in the horizontal subspace, $\frac{d\theta}{dt} = 0$ unless $\frac{d\alpha_i}{dt} \neq 0$ for at least one α_i, $i=2,\ldots,n$. From the definition of α_i, it follows that along such a curve the phases of each component cannot change by an equal nonzero amount. Hence, in order that X^H produce a nonzero value of $\frac{d\theta}{dt}$, it is necessary that the subspace spanned by w(t) change. Moreover, from (12.20), it follows that the rates of change in phase of the components are constrained by the weighted sum

$$\sum_{i=1}^{n} r_i^2 \left(\frac{d\theta}{dt} + \frac{d\alpha_i}{dt}\right) = 0 \quad , \tag{12.23}$$

where $\theta = \measuredangle z_1^H w$ and $\theta + \alpha_i = \measuredangle z_i^H w$, $i=2,\ldots,n$.

There are thus two mechanisms for producing changes in θ, corresponding to the decomposition of the tangent space into vertical and

horizontal subspaces. The change due to the vertical component X^V is analogous to the change one would expect were w(t) a scalar-valued curve. This is reasonable since curves whose tangent vectors lie in the vertical subspace span a constant one-dimensional subspace of $\mathbb{C}^n$. The change due to X^H, on the other hand, is due solely to the fact that w(t) is a vector-valued curve. This too is reasonable since changes in phase can be produced in this fashion only if the subspace spanned by w(t) is not constant. Since the net change in θ is due to the sum of these effects, it follows that the discrepancy between the behavior of θ and that of the phase of a scalar allpass function is quantified by the term

$$d\theta(X^H) = -\sum_{i=2}^{n} r_i^2 \, d\alpha_i(\pi_* X^H) \quad . \tag{12.24}$$

An interpretation of (12.24) is that the horizontal component can cause phase to be transferred from one component of w to another, although the net (weighted) sum of the rates of phase change must equal zero; i.e.,

$$0 = \sum_{i=1}^{n} r_i^2 \left(\frac{d\theta}{dt} + \frac{d\alpha_i}{dt}\right) \quad . \tag{12.25}$$

This interpretation will be applied shortly to discuss how phase lead and lag may be transferred among the loops of a linear multivariable system.

Consider again (12.12), the differential form in (12.1) evaluated along a curve $\gamma(t) \in \mathbb{C}$. The preceding discussion may be extended to show how this form relates a singular value to various measures of phase difference between its associated pair of singular vectors. Let the left and right singular vectors be written in a local trivialization as in (12.2)-(12.3). Using the abbreviated notation defined immediately following (12.4) yields

$$v = \rho_v \, e^{j\theta_v} \tag{12.26a}$$

$$u = \rho_u \, e^{j\theta_u} \tag{12.26b}$$

$$\Delta\theta = \theta_v - \theta_u \quad . \tag{12.26c}$$

Substituting (12.26) into (12.12) yields

$$j\left[\frac{-\partial \log\sigma}{\partial y}\frac{dx}{dt} + \frac{\partial \log\sigma}{\partial x}\frac{dy}{dt}\right] = \frac{j}{\sigma}\,\mathrm{Im}[v^H \frac{dM}{dt} u]$$

$$= v^H \frac{dv}{dt} - u^H \frac{du}{dt}$$

$$= \rho_v^H \frac{d\rho_v}{dt} - \rho_u^H \frac{d\rho_u}{dt} + j\,\frac{d\Delta\theta}{dt} \quad . \tag{12.27}$$

Equation (12.27) is the key to understanding the relation among a singular value, the subspaces spanned by the associated pair of singular vectors, and various measures of phase difference between these vectors. Thus a number of questions originally posed in Chapter 9 may now be resolved. Note, in particular, that the term $\frac{j}{\sigma}\,\mathrm{Im}[v^H \frac{dM}{dt} u]$ is not generally equal to the rate of change of the phase difference $\Delta\theta$. Another way of viewing this is to consider an arbitrary pair of minimum energy vectors lying above the paths through $\mathbb{C}P^{n-1}$ traversed by the left and right singular subspaces. Let these vectors be denoted by v^* and u^*, respectively, where

$$v^* = \rho_v \, e^{j\theta_v^*} \tag{12.28a}$$

$$u^* = \rho_u \, e^{j\theta_u^*} \tag{12.28b}$$

and

$$\Delta\theta^* = \theta_v^* - \theta_u^* \tag{12.28c}$$

is the phase difference between the pair of minimum energy vectors. From the discussion of minimum energy vectors a few paragraphs back, it follows

that the phases of v^* and u^* are related to the sections ρ_v and ρ_u via the rules

$$j \frac{d\theta_v^*}{dt} = - \rho_v^H \frac{d\rho_v}{dt} \tag{12.29a}$$

and

$$j \frac{d\theta_u^*}{dt} = - \rho_u^H \frac{d\rho_u}{dt} \quad . \tag{12.29b}$$

Hence, the difference in the phases of the minimum energy vectors is related to the sections by

$$j \frac{d\Delta\theta^*}{dt} = - (\rho_v^H \frac{d\rho_v}{dt} - \rho_u^H \frac{d\rho_u}{dt}) \quad . \tag{12.30}$$

Using (12.30) in (12.27) yields

$$\begin{aligned} \frac{d\Delta\theta}{dt} &= \frac{1}{\sigma} \operatorname{Im}[v^H \frac{dM}{dt} u] + \frac{d\Delta\theta^*}{dt} \\ &= [\frac{-\partial \log\sigma}{\partial y} \frac{dx}{dt} + \frac{\partial \log\sigma}{\partial x} \frac{dy}{dt}] + \frac{d\Delta\theta^*}{dt} \quad . \end{aligned} \tag{12.31}$$

Equation (12.31) shows that the term $\frac{1}{\sigma} \operatorname{Im}[v^H \frac{dM}{dt} u]$ determines, not $\frac{d\Delta\theta}{dt}$, the rate of change of phase difference between the associated pair of singular vectors, but rather the discrepancy between $\frac{d\Delta\theta}{dt}$ and $\frac{d\Delta\theta^*}{dt}$, the rate of change of phase difference between a pair of minimum energy vectors traversing the paths $\mathfrak{V}(t)$ and $\mathfrak{U}(t)$ throuch $\mathbb{C}P^{n-1}$ traversed by the left and right singular subspaces. In the scalar case the latter term is, of course, not present, and the usual relation between gain and phase difference is obtained. In the general multiple loop case, the relation between the measure of gain given by a singular value and the measure of phase difference given by $\Delta\theta$ is influenced by the difference in the two paths $\mathfrak{V}(t)$ and $\mathfrak{U}(t)$. Recall the singular subspaces are constrained to traverse these subspaces as a consequence of the min-max property (6.15).

It is instructive to write the local sections ρ_v and ρ_u in coordinates so that insight may be gained into how motion of the singular subspaces affects the phase difference $\Delta\theta$. As in the discussion of Equations (12.14)-(12.20), let the local trivialization used to compute phase difference be given by $\theta_{z_1}(w) = \measuredangle z_1^H w$, where z_1 is a constant unit vector. Hence, from (12.26), $\Delta\theta = \theta_v - \theta_u$, where $\theta_v \equiv \theta_{z_1}(v) = \measuredangle z_1^H v$ and $\theta_u \equiv \theta_{z_1}(u) = \measuredangle z_1^H u$. Again, choose constant vectors z_i, $i=2,\ldots,n$, so that $\{z_i \,;\, i=1,\ldots,n\}$ is an orthonormal basis for $\mathbb{C}^n$. Then

$$\rho_v \equiv \rho_{z_1}([v]) = \sum_{i=1}^{n} z_i(z_i^H \rho_v) \tag{12.32a}$$

$$\rho_u = \rho_{z_1}([u]) = \sum_{i=1}^{n} z_i(z_i^H \rho_u) \tag{12.32b}$$

where $z_1^H \rho_v$ and $z_1^H \rho_u$ are positive real numbers. Thus, writing

$$r_{iv}\, e^{j\alpha_{iv}} \triangleq z_i^H \rho_v \tag{12.33a}$$

and

$$r_{iu}\, e^{j\alpha_{iu}} \triangleq z_i^H \rho_u \tag{12.33b}$$

yields, as in (12.18)

$$\rho_v^H \frac{d\rho_v}{dt} = j \sum_{i=2}^{n} r_{iv}^2 \frac{d\alpha_{iv}}{dt} \tag{12.34a}$$

and

$$\rho_u^H \frac{d\rho_u}{dt} = j \sum_{i=2}^{n} r_{iu}^2 \frac{d\alpha_{iu}}{dt} \quad . \tag{12.34b}$$

Consequently, as in (12.20),

$$v^H \frac{dv}{dt} - u^H \frac{du}{dt} = j \frac{d\Delta\theta}{dt} + \rho_v^H \frac{d\rho_v}{dt} - \rho_u^H \frac{d\rho_u}{dt}$$

$$= j\,\frac{d\Delta\theta}{dt} + j\sum_{i=2}^{n}\left[r_{iv}^2\,\frac{d\alpha_{iv}}{dt} - r_{iu}^2\,\frac{d\alpha_{iu}}{dt}\right]$$

$$= j\left[-\frac{\partial\log\sigma}{\partial y}\,\frac{dx}{dt} + \frac{\partial\log\sigma}{\partial x}\,\frac{dy}{dt}\right] \quad . \tag{12.35}$$

Equation (12.35) reveals a necessary, but not sufficient, condition for motion of the singular subspaces to cause the value of $\frac{d\Delta\theta}{dt}$ to deviate from that of $\frac{-\partial\log\sigma}{\partial y}\,\frac{dx}{dt} + \frac{\partial\log\sigma}{\partial x}\,\frac{dy}{dt}$ (in other words, to cause the relation between σ and $\Delta\theta$ to deviate from that between scalar gain and phase). This necessary condition is that one or more of the terms $[r_{iv}^2\,\frac{d\alpha_{iv}}{dt} - r_{iu}^2\,\frac{d\alpha_{iu}}{dt}]$ be nonzero. For example, if motion of the singular subspaces produces only changes in the relative magnitudes of the components of each singular vector, so that $\frac{d\alpha_{iv}}{dt} = \frac{d\alpha_{iu}}{dt} = 0$, $i=2,\ldots,n$, then the relation between σ and $\Delta\theta$ is not affected. Furthermore, suppose the magnitudes of the ith components of the singular vectors are the same (so that $r_{iv} = r_{iu}$, $i=2,\ldots,n$) and that the derivatives of the coordinates α_{vi} and α_{ui} are the same ($\frac{d\alpha_{iv}}{dt} = \frac{d\alpha_{iu}}{dt}$, $i=2,\ldots,n$). In this case also it follows that motion of the singular subspaces does not affect the relation between σ and $\Delta\theta$. Finally, note in particular that if $\rho_v = \rho_u$, so that the singular vectors are eigenvectors, then $r_{iv} = r_{iu}$, $i=2,\ldots,n$ and $\alpha_{iv} = \alpha_{iu}$, $i=2,\ldots,n$. It follows that, locally, the discrepancy between σ and $\Delta\theta$ and scalar gain and phase can be significant only if the singular vectors do not well approximate eigenvectors of M(s). This observation should have some significance for design methods based upon eigenvalues and eigenvectors of transfer function matrices [33].

It is instructive to view the relation between changes in the singular vectors and changes in phase difference in terms of the decomposition of the tangent space. Let $\gamma(t)$ be a curve in the complex plane, and let

X_v and X_u be the tangent vectors to the corresponding paths through $\mathbb{C}P^{n-1}$ traversed by the left and right singular vectors. Furthermore, let these vectors be decomposed into vertical and horizontal components as $X_v = X_v^V + X_v^H$ and $X_u = X_u^V + X_u^H$, respectively. Evaluating the differential form (12.1) on the tangent vector to γ yields the following string of equalities:

$$
\begin{aligned}
j\left[-\frac{\partial \log\sigma}{\partial y}\frac{dx}{dt} + \frac{\partial \log\sigma}{\partial x}\frac{dy}{dt}\right] &= \frac{j}{\sigma}\,\mathrm{Im}\left[v^H \frac{dM}{dt} u\right] \\
&= v^H \frac{dv}{dt} - u^H \frac{du}{dt} \\
&= \rho_v^H d\rho_v(\pi_* X_v) + j\ d\theta_v(X_v) \\
&\quad - \rho_u^H d\rho_u(\pi_* X_u) - j\ d\theta_u(X_u) \\
&= \rho_v^H d\rho_v(\pi_* X_v^V) - \rho_u^H d\rho_u(\pi_* X_u^V) \\
&\quad + [\rho_v^H d\rho_v(\pi_* X_v^H) + j\ d\theta_v(X_v^H)] \\
&\quad - [\rho_u^H d\rho_u(\pi_* X_u^H) + j\ d\theta_u(X_u^H)] \\
&\quad + j\ d\theta_v(X_v^V) - j\ d\theta_u(X_u^V) \quad . \qquad (12.36)
\end{aligned}
$$

Recalling the discussion of Equation (12.21), it is seen that the first two terms on the right-hand side of (12.36) equal zero. Moreover, recalling the discussion of Equation (12.22), the second two terms are also seen to equal zero. Thus, (12.12) reduces to

$$j[-\frac{\partial \log\sigma}{\partial y}\frac{dx}{dt} + \frac{\partial \log\sigma}{\partial x}\frac{dy}{dt}] = \frac{j}{\sigma}\,\mathrm{Im}[v^H \frac{dM}{dt} u]$$

$$= v^H \frac{dv}{dt} - u^H \frac{du}{dt}$$

$$= j[d\theta_v(X_v^V) - d\theta_u(X_u^V)] \quad . \qquad (12.37)$$

Equation (12.37) shows quite clearly that the form $j[-\frac{\partial \log\sigma}{\partial y}dx + \frac{\partial \log\sigma}{\partial x}dy]$ fails to completely describe the behavior of the phase difference $\Delta\theta$. In particular, this form provides no information about the effect motion of the singular subspaces has upon phase difference. This effect is determined by the horizontal components of the tangent vectors and is given by

$$j[d\theta_v(X_v^H) - d\theta_u(X_u^H)] = -[\rho_v^H d\rho_v(\pi_* X_v^H) - \rho_u^H d\rho_u(\pi_* X_u^H)] \quad . \qquad (12.38)$$

To summarize, the vertical components of the tangent vectors produce changes in phase difference entirely analogous to the scalar case. This is because these components do not affect the singular subspaces. Note also that the effect the vertical components have upon phase difference is completely determined by the behavior of the singular value. Hence, the resulting change in $\Delta\theta$ does not depend upon which components of the singular vectors are used to measure phase difference; i.e., upon the choice of local trivialization in the discussion preceding (12.14). Another way of stating this is that the vertical components produce equal changes in the phase difference between any two components of the singular vectors. The horizontal components, on the other hand, which are not present in the scalar case (or are identically zero if the singular subspaces are constant) are responsible for $\sigma e^{j\Delta\theta}$ not being analytic, and thus for the failure of the scalar gain-phase relations to describe the behavior of this function. An argument similar to that preceding (12.25) shows that the horizontal components may be interpreted

as causing phase to be transferred among the components of the singular vectors, subject to the constraints

$$j\, d\theta_v(X_v^H) + \rho_v^H d\rho_v(\pi_* X_v^H)$$

$$= j\, d\theta_v(X_v^H) + j \sum_{i=2}^{n} r_{iv}^2\, d\alpha_{iv}(X_v^H)$$

$$= 0 \tag{12.39a}$$

and

$$j\, d\theta_u(X_u^H) + \rho_u^H d\rho_u(\pi_* X_u^H)$$

$$= j\, d\theta_u(X_u^H) + j \sum_{i=2}^{n} r_{iu}^2\, d\alpha_{iu}(X_u^H)$$

$$= 0 \quad . \tag{12.39b}$$

The horizontal components of the tangent vectors are thus apparently responsible for multiple loop system phenomena having no analogue in scalar systems.

Note that if the basis $\{z_i\}$ is that given by the standard basis vectors $\{e_i\}$, then the coordinates r_{iv} and r_{iu} may be reparameterized by ϕ_{iv} and ϕ_{iu} as in Chapter 10. Similarly, the coordinates α_{iv} and α_{iu} may be replaced by ψ_{iv} and ψ_{iu}, and $\Delta\theta$ becomes $\tilde{\theta}_1$. (Note, the subscript "1" refers to the components of v and u used to define phase difference, and not to any ordering of the singular values.)

Now recall that the standard basis vectors correspond to the physical loops of the system. The above discussion shows that it is possible to interpret the failure of $\sigma e^{j\tilde{\theta}_1}$ to satisfy the scalar Bode gain-phase relations as being due to phase lead or lag being transferred

to the first loop of the system from other loops. Moreover, transfer of phase lead or lag must <u>necessarily</u> be present if the gain-phase relations are to be violated. The additional lead or lag produced in $\tilde{\theta}_1$ via loop interactions must be accompanied by lag or lead being produced in loops of the system other than the first. Obviously, this discussion may easily be modified to apply when the ith components of v and u (written in the standard basis) are used to measure the phase difference $\tilde{\theta}_i$.

Note how coupling between loops manifests itself in the integral relation (12.10). The value of $\Delta\theta(j\omega_o)$ deviates from the value it would attain if the singular subspaces were constant as a result of phase being transferred among loops of the system. The <u>net</u> effect of this phase transfer upon $\Delta\theta(j\omega_o)$ is obtained by <u>averaging</u> the value of the effect contributed, by integrating the function governing phase transfer, $\rho_v^H \frac{\partial \rho_v}{\partial r} - \rho_u^H \frac{\partial \rho_u}{\partial r}$, along each ray extending from $j\omega_o$ to the point at infinity.

The discussion of the preceding two paragraphs was based upon local trivializations using constant vectors to define phase. As discussed in earlier chapters, a more physically meaningful definition of phase utilized the right singular vectors, which are not constant. In the examples discussed in this thesis, this fact presents no difficulty since the right singular subspaces are approximately constant and equal to the standard basis directions. Thus the above analysis can be applied. In general, this will not be true. Thus the above discussion needs to be extended to the general case, although this will not be pursued in this thesis. Instead of coupling between physical loops of the system, as in the case when the standard basis vectors are used to define phase, coupling between input and output directions given by the singular vectors will appear in the equations.

One way of transforming the differential equations involving the phases $\tilde{\theta}_i$ into those involving $\theta = \measuredangle u^H v$ is to use the functions g_i as in (11.51)-(11.52). Since the two definitions of phase difference are related by an exact form, however, it is simpler to just use g_i, given by (10.41), directly in the integral relation (12.10). To illustrate, consider (12.10) in coordinates for the case n=2. Using coordinates on the ith local section (10.17) to write the ith pair of singular vectors in coordinates yields

$$\tilde{\theta}_i(j\omega_o) - \tilde{\theta}_i(0) = \frac{1}{\pi}\int_{-\infty}^{\infty} \frac{d \log \sigma}{d\nu}\{\log \coth \frac{|\nu|}{2}\}d\nu$$

$$- \frac{(-1)^i}{\pi}\int_{CRHP}(\sin^2\phi_v \frac{\partial\Psi_v}{\partial r} - \sin^2\phi_u \frac{\partial\Psi_u}{\partial r})dr\wedge d\alpha \quad . \qquad (12.40)$$

Using the function g_i in coordinates (10.43) yields

$$\theta(j\omega_o) = \tilde{\theta}_1(j\omega_o) + \measuredangle[\cos\phi_u \cos\phi_v + \sin\phi_u \sin\phi_v e^{j(\Psi_v - \Psi_u)}]\Big|_{j\omega_o}$$

and (12.41a)

$$\theta(j\omega_o) = \tilde{\theta}_2(j\omega_o) + \measuredangle[\cos\phi_u \cos\phi_v e^{-j(\psi_v - \psi_u)} + \sin\phi_u \sin\phi_v]\Big|_{j\omega_o} \quad .$$

(12.41b)

Finally, recall that the scalar Bode gain-phase relations contained a weighting function showing that the dependence of phase upon gain decreased rapidly away from the frequency in question. Note the same weighting function appears in the first integral in (12.10).

It will now be shown that the second integral in (12.10) implicitly contains a weighting function. This follows since the element of surface area in the right half plane is given by $rdr\Lambda d\alpha$. Thus the integral may be rewritten as

$$\frac{1}{\pi}\int_{CRHP}(\rho_v^H \frac{\partial\rho_v}{\partial r} - \rho_u^H \frac{\partial\rho_u}{\partial r})dr\Lambda d\alpha = \frac{1}{\pi}\int_{CRHP}\frac{1}{r}(\rho_v^H \frac{\partial\rho_v}{\partial r} - \rho_u^H \frac{\partial\rho_u}{\partial r})(rdr\Lambda d\alpha). \tag{12.42}$$

Writing the integral in this way shows that the effect of the motion of the singular subspaces at a point in the right half plane upon the value of $\theta(j\omega_o)$ decreases as the inverse of the distance from the point to $j\omega_o$. Thus coupling among loops is most effective in altering the value of $\theta(j\omega_o)$ if this coupling takes place near the frequence $j\omega_o$.

12.3. Summary

In this chapter the differential equations generalizing the Cauchy-Riemann equations have been translated into generalized gain-phase relations via Stokes' Theorem. Some insights into implications for system properties were discussed. Much work remains to be done; this is discussed in the conclusion section of Chapter 13.

CHAPTER 13

ANALYSIS OF AN EXAMPLE USING NEW INTEGRAL RELATIONS

13.1. Introduction

In Section 8.4 an example of a two-input two-output feedback system was discussed. This example exhibited properties markedly different from those of a scalar feedback system. In particular, it was found that the gain in one loop could be rolled off at 40 db/decade near crossover while the sensitivity function remained bounded less than 10 db. In addition, a new tradeoff between system properties in different frequency ranges was observed. It appeared that the anomalous behavior of this example was due to some sort of interaction between the loops of the system, although no theoretical basis for this hypothesis was available. The purpose of this chapter is to provide an extensive analysis of this example using the integral relation developed in Theorem 12.2. By identifying parameters describing the singular value decomposition of L(s) with the individual components $L_{ij}(s)$ the notion of helpful loop interaction will be quantified. A tentative explanation of the behavior of this example will be presented.

13.2. Preliminary Analysis of Example

In this chapter the feedback system with open loop transfer function

$$L(s) = \begin{bmatrix} \frac{150 \times 10^3}{(s+10)} & \frac{.78}{(s+.01)^2} \\ \frac{-7071 \times 10^3 (s+.1)}{(s+10)^3} & \frac{.64}{(s+.01)^2} \end{bmatrix} \tag{13.1}$$

will be studied. It may be verified that the feedback system with sensitivity function $S(s) = 1/(1+L(s))$ is stable.

The gain in the second loop of this system (which is approximately equal to $\left|\frac{1}{(s+.01)^2}\right|$) is large until $\omega = .01$ rad/sec, and thereafter decreases with a two-pole roll-off ($\approx$ 40 db/decade). Note the gain in the second loop is approximately equal to one at $\omega = 1$ rad/sec. The gain in the first loop is large until $\omega = 10$ rad/sec and thereafter decreases with a one-pole roll-off ($\approx$ 20 db/decade). In Section 8.4 several properties of $L(s)$ and the associated sensitivity function were noted. These will now be examined in detail.

First, denote the columns of $L(s)$ by

$$\begin{aligned} L &= [L_1 \mid L_2] \\ &= \begin{bmatrix} L_{11} & L_{12} \\ L_{21} & L_{22} \end{bmatrix} \end{aligned} \tag{13.2}$$

Let the singular value decomposition of L be denoted by

$$\begin{aligned} L &= V\Sigma U^H \\ &= [v_1 \mid v_2] \begin{bmatrix} \sigma_1 & 0 \\ 0 & \sigma_2 \end{bmatrix} [u_1 \mid u_2]^H \\ &= \begin{bmatrix} v_{11} & v_{12} \\ v_{21} & v_{22} \end{bmatrix} \begin{bmatrix} \sigma_1 & 0 \\ 0 & \sigma_2 \end{bmatrix} \begin{bmatrix} u_{11} & u_{12} \\ u_{21} & u_{22} \end{bmatrix}^H . \end{aligned} \tag{13.3}$$

From the min-max property of singular values it follows that, at each value of s,

$$\bar{\sigma}[L(s)] \geq \|L_1(s)\| \tag{13.4a}$$

$$\underline{\sigma}[L(s)] \leq \|L_2(s)\| \quad . \tag{13.4b}$$

It can readily be verified that $\|L_1(s)\| > \|L_2(s)\|$ for all s in the closed right half plane (CRHP). Thus the singular values of L(s) are distinct in the CRHP and may be numbered $\sigma_1 = \bar{\sigma}$, $\sigma_2 = \underline{\sigma}$. Since

$$Lu_i = \sigma_i v_i \tag{13.5}$$

it follows that

$$\sigma_1 v_1 = u_{11} \cdot L_1 + u_{21} \cdot L_2 \tag{13.6a}$$

$$\sigma_2 v_2 = u_{12} \cdot L_1 + u_{22} \cdot L_2 \quad . \tag{13.6b}$$

From (13.6a) it follows that

$$\begin{aligned} \sigma_1 &\leq |u_{11}| \cdot \|L_1\| + |u_{21}| \cdot \|L_2\| \\ &\leq |u_{11}| \cdot \|L_1\| + \|L_2\| \quad . \end{aligned} \tag{13.7}$$

Together (13.4a) and (13.7) imply

$$1 - \frac{\|L_2\|}{\|L_1\|} \leq |u_{11}| \quad . \tag{13.8}$$

Since $\|L_2(s)\| < \|L_1(s)\|$ in the CRHP, it follows that $|u_{11}| > 0$ there and, since U is unitary, $|u_{22}| = |u_{11}|$. Thus $\forall s \in$ CRHP $u_i(s)$ may be written using the local trivialization T_i from (10.26). (Note the correspondence between singular values and the standard basis directions implies that

numbered subscripts in this section refer both to the ordering of the singular values and to the standard basis vectors used to construct the trivializations.)

Next, (13.6a) yields

$$\sigma_1 v_{21} = u_{11} L_{11} + u_{21} L_{12} \tag{13.9}$$

$$\Rightarrow \qquad |v_{11}| \geq \frac{1}{\sigma_1} \Big| |u_{11}| \cdot |L_{11}| - |u_{21}| \cdot |L_{12}| \Big| \quad . \tag{13.10}$$

It may readily be verified that $|L_{11}| > |L_{12}|$, $\forall s \in$ CRHP, and that $(1 - \frac{\|L_2\|}{\|L_1\|})^2 > 1/2$, $\forall s \in$ CRHP. The latter fact implies that $|u_{11}|^2 > 1/2$, which, since U is unitary, implies in turn that $|u_{11}| > |u_{21}|$, $\forall s \in$ CRHP. It follows from these bounds and (13.10) that $|v_{11}| > 0$. Hence, $\forall s \in$ CRHP, $v_i(s)$ may also be written using the local trivialization T_i.

The preceding remarks show that for all $s \in$ CRHP the matrix L(s) may be assigned the coordinates

$$L = [\rho_{v_1} \mid \rho_{v_2}] \begin{bmatrix} \sigma_1 e^{j\tilde{\theta}_1} & 0 \\ 0 & \sigma_2 e^{j\tilde{\theta}_2} \end{bmatrix} [\rho_{u_1} \mid \rho_{u_2}]^H \tag{13.11}$$

or

$$L = \begin{bmatrix} \cos\phi_v & -\sin\phi_v \, e^{-j\psi_v} \\ \sin\phi_v \, e^{j\psi_v} & \cos\phi_v \end{bmatrix} \cdot \begin{bmatrix} \sigma_1 e^{j\tilde{\theta}_1} & 0 \\ 0 & \sigma_2 e^{j\tilde{\theta}_2} \end{bmatrix} \tag{13.12}$$

$$\cdot \begin{bmatrix} \cos\phi_u & -\sin\phi_u \, e^{-j\psi_u} \\ \sin\phi_u \, e^{j\psi_u} & \cos\phi_u \end{bmatrix}^H \quad .$$

The properties of L(s) used to guarantee the existence of the parameterization (13.12) may also be used to approximate the values of

these parameters. In particular, such an approximation in the frequency range over which $\sigma_1 >> \sigma_2$ will be of interest.

First, from (13.8) it follows that at frequencies for which $\frac{\|L_2\|}{\|L_1\|} << 1$, the angle

$$\phi_u \approx 0 \quad . \tag{13.13}$$

Moreover, at such frequencies $\cos \phi_u \approx 1$, so that (13.6a), (13.11), and (13.12) imply

$$\begin{aligned} \sigma_1 e^{j\tilde{\theta}_1} \rho_{v_1} &= \sigma_1 e^{j\tilde{\theta}_1} \begin{bmatrix} \cos\phi_v \\ \sin\phi_v \, e^{j\psi_v} \end{bmatrix} \\ &\approx L_1 \quad . \end{aligned} \tag{13.14}$$

From (13.14) it follows that

$$\sigma_1 \approx \|L_1\| \tag{13.15a}$$

$$\tilde{\theta}_1 \approx \measuredangle L_{11} \tag{13.15b}$$

$$\phi_v \approx \arctan \frac{|L_{21}|}{|L_{11}|} \tag{13.15c}$$

$$\psi_v \approx \measuredangle L_{21} - \measuredangle L_{11} \quad . \tag{13.15d}$$

Together (13.13) and (13.15) show that five of the eight coordinates in (13.12) may be readily approximated in terms of the component transfer functions of L(s). Since ψ_u is discontinuous at $\phi_u = 0$, it is not possible to approximate this parameter. This fact presents no difficulty, however, since ψ_u has little physical significance when $\phi_u \approx 0$.

Now recall that (13.4b) shows that $\sigma_2 \leq \|L_2\|$. It is not possible, however, to use (13.6b) to approximate σ_2 as (13.6a) was used to show $\sigma_1 \approx \|L_1\|$. This follows since the first term on the right hand side of (13.6b) is the product of a small number, $|u_{12}|$, and a vector of large magnitude. Meanwhile, the second term is the product of a number approximately equal to one and a vector whose magnitude is also approximately equal to one at frequencies of interest. Thus the left singular vector v_2 (corresponding to choosing the right singular vector $u_2 = [-\sin\phi_u \; e^{-j\psi_u} | \cos\phi_u]^T$) cannot be approximated from (13.6b). The subspace in which v_2 lies may be approximated from (13.6a) and the fact that v_1 and v_2 are orthogonal. The phase difference $\tilde{\theta}_2$ still cannot be approximated, however, since the condition $v_1^H v_2 = 0$ does not constrain this parameter.

The inability to approximate $\tilde{\theta}_2$ is inconvenient, as it was shown in Section 8.4 that feedback properties depend critically on its value. Moreover, this parameter behaves in unusual ways which are related to the anomalous properties of the sensitivity function of this system. Thus it would be very desirable to be able to predict, a priori, what the value of $\tilde{\theta}_2$ would be. This, of course, could be of potential use in design.

First, note that Equations (13.13) and (13.15) may be used to determine how changes in the functions $L_{ij}(s)$ affect the various parameters. Recall that the Bode gain-phase relations for scalar feedback systems show that increasing the gain over a frequency interval necessarily causes positive phase lead, (e.g., see the Bode plot of a phase lead filter as in [57, p. 297]). Equations (13.15a) and (13.15b) show that the gain in the first loop of the system (hence $\sigma_1[L]$) may be increased without causing $\tilde{\theta}_1$ to change. This may

be done simply by increasing $|L_{21}(j\omega)|$ over an interval while leaving $|L_{11}(j\omega)|$ constant. From (13.15c) it follows that ϕ_v will increase. Moreover, since increasing $|L_{21}(j\omega)|$ causes $\measuredangle L_{21}(j\omega)$ to increase while holding $|L_{11}(j\omega)|$ constant leaves $\measuredangle L_{11}(j\omega)$ unchanged, the difference in phase between $L_{21}(j\omega)$ and $L_{11}(j\omega)$ will increase. By (13.15d) it follows that ψ_v will increase. Thus an increase in the gain σ_1 is accompanied by phase lead, but not necessarily in all components of the output. As just shown, it is possible to increase the gain in <u>one</u> loop of the system by increasing only the magnitude of that component of the output being fed into the <u>other</u> loop. Thus phase lead is produced, but only in one component of the output. The value of phase in the other component is unaffected.

Now increasing the ratio $\frac{|L_{21}|}{|L_{11}|}$, which causes ϕ_v to increase, also affects the direction of outputs due to inputs in the direction of the singular vector u_2. This follows since

$$Lu_2 = \sigma_2 e^{j\tilde{\theta}_2} \begin{bmatrix} -\sin\phi_v e^{-j\psi_v} \\ \cos\phi_v \end{bmatrix} \tag{13.16}$$

Increasing ϕ_v thus leaves the value of the gain σ_2 unchanged; however, the magnitude of that component of the output fed into the first loop of the system increases while that of the other component decreases. In addition, the phase of the first component lags that of the second by an amount $\pi - \psi_v$.

The preceding discussion showed that the lead filter present in $L_{21}(s)$ can be associated with various changes in the parameters of (13.12). What effect, if any, this has on $\tilde{\theta}_2$ is still unclear, since an approximation to $\tilde{\theta}_2$ cannot be obtained. If $\sigma_2 e^{j\tilde{\theta}_2}$ were analytic, however, this problem

would not exist. The Bode gain-phase relations would show that $\tilde{\theta}_2$ would approach -90N°, where 20N°db/decade is the rate at which σ_2 rolls off.

The claims of the preceding discussion may be substantiated in the present example by examining plots of the various parameters. For each reference, Figures 8.1-8.7 are reproduced as Figures 13.1-13.7. Figures 13.8.a-13.11.b are Bode plots of $L_{11}(s)$, $L_{12}(s)$, $L_{21}(s)$ and $L_{22}(s)$, respectively. Figure 13.1 shows how the singular values of L may indeed be identified with the gain in the two physical loops of the system, (i.e., the magnitudes of the columns of L). Figure 13.5 shows that the right singular subspaces do indeed become aligned with the standard basis directions (which in turn correspond to the physical loops). Note the correlation between the plot of σ_2 and the Bode plots of L_{12} and L_{22} in Figures 13.9 and 13.11. Similarly, note the relation between σ_1 and the functions $L_{11}(s)$ and $L_{21}(s)$, as shown by Figures 13.8 and 13.10. Note, in particular, the peak in σ_1 (Figure 13.1) due to the peak in L_{21}. As the approximations discussed earlier show, this means of obtaining a peak in σ_1 should leave the phase difference the same as if $\tilde{\theta}_1$ actually equalled $\measuredangle L_{11}$. That this is indeed the case may be verified from Figures 13.7 and 13.8. Moreover, Figure 13.6 shows there is a peak in ϕ_v due to the peak in $|L_{21}|/|L_{11}|$. The associated phase lead in ψ_v may also be seen.

Finally, the phase difference $\tilde{\theta}_2$, which could not be approximated, is plotted along with $\tilde{\theta}_1$ in Figure 13.7. It may be seen that $\tilde{\theta}_2$ increases, or experiences phase lead, near the frequency range over which ϕ_v is increasing. This would suggest that the phase lead in L_{21}, which produces phase lead in ψ_v, also affects $\tilde{\theta}_2$. In Section 13.3 this effect will be analyzed quantitatively using the generalization of the Bode gain-phase relations presented in Chapter 12.

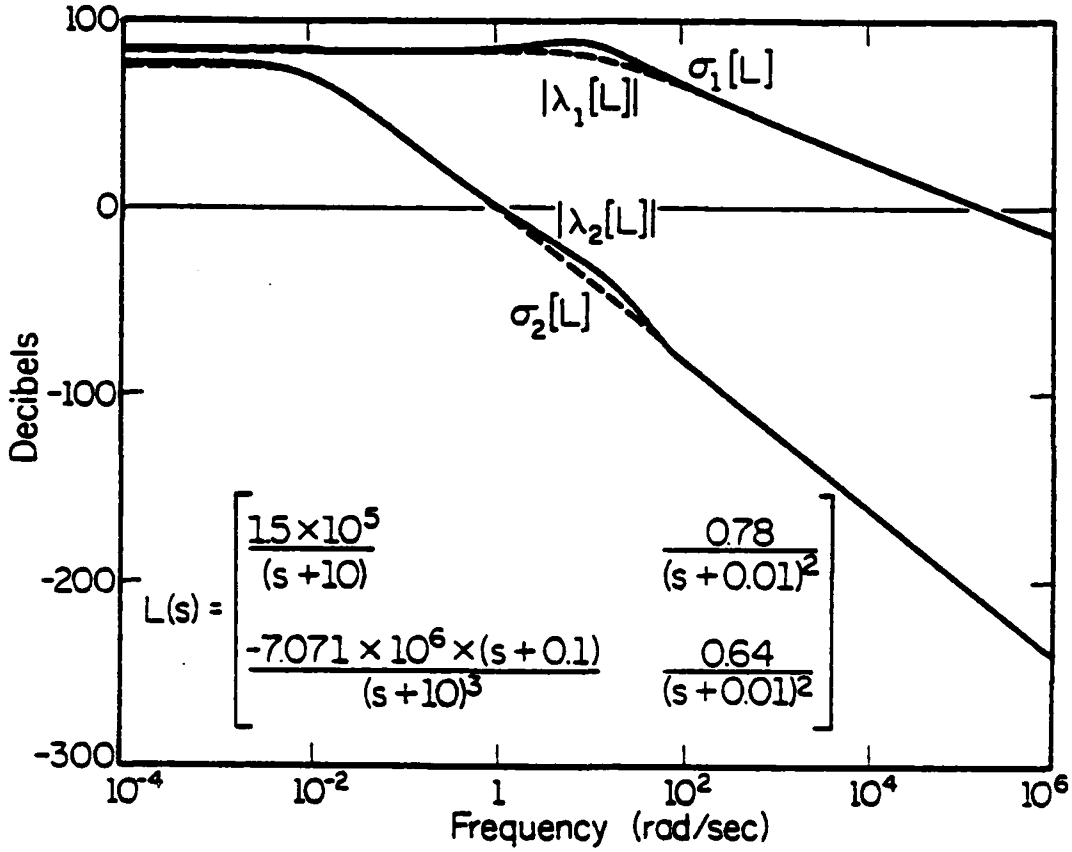

Figure 13.1. Singular values and magnitudes of eigenvalues - open loop system.

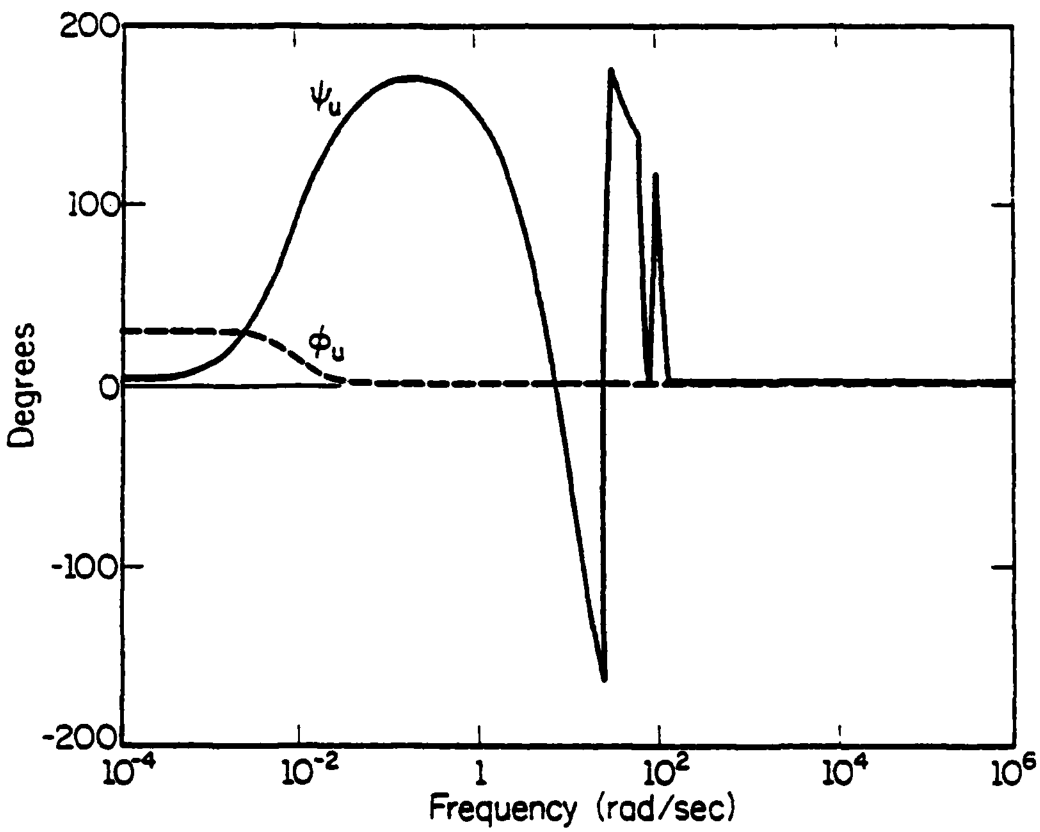

Figure 13.2. Right singular subspaces - open loop system.

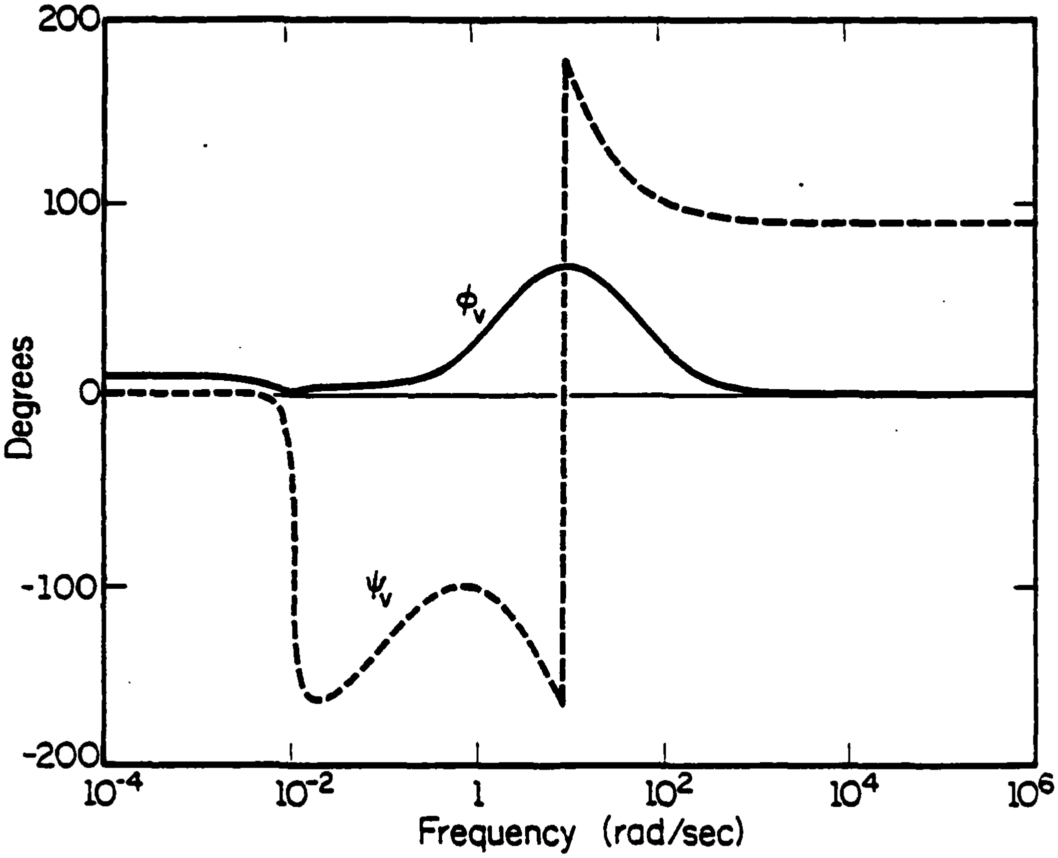

Figure 13.3. Left singular subspaces - open loop system.

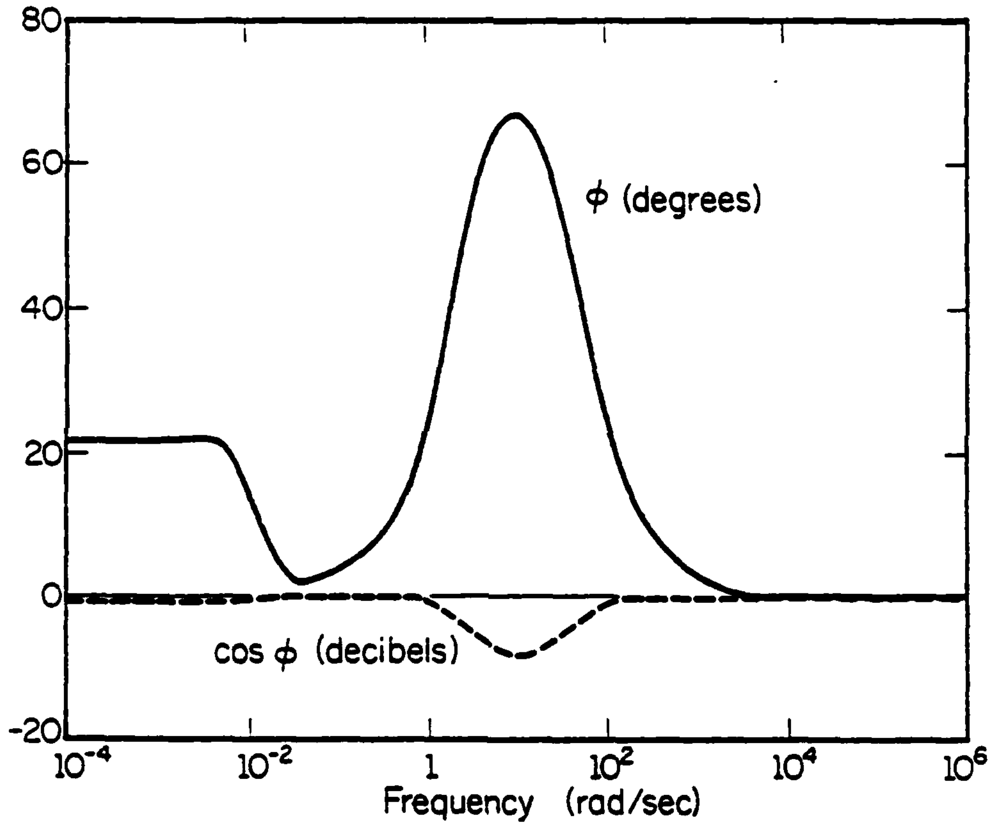

Figure 13.4. Angle between singular subspaces - open loop system.

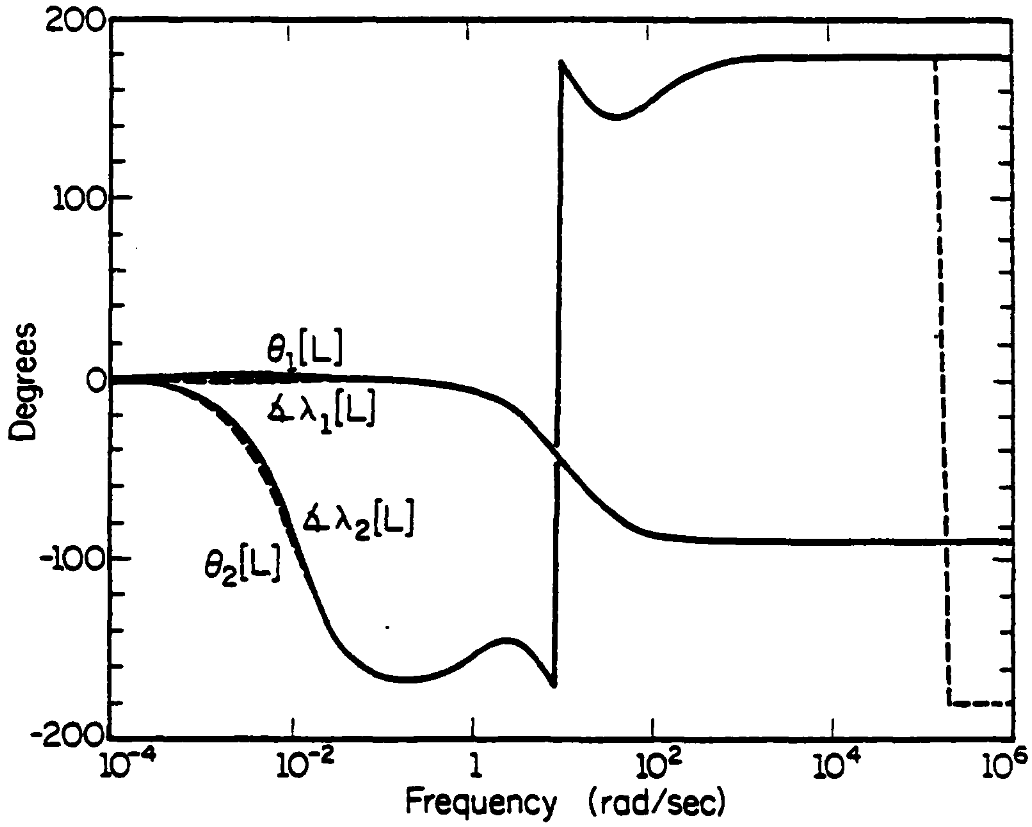

Figure 13.5. Measures of phase difference between singular vectors and phases of eigenvalues - open loop system.

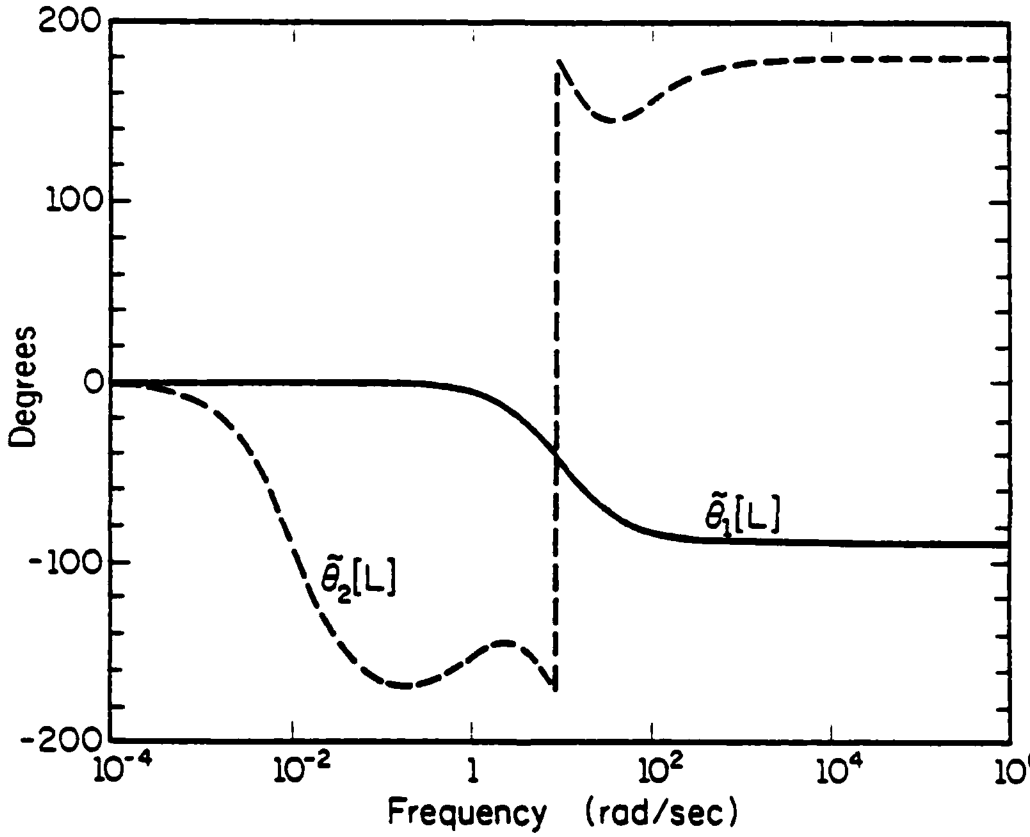

Figure 13.6. Phase differences between "ith" components of "ith" pair of singular vectors - open loop system.

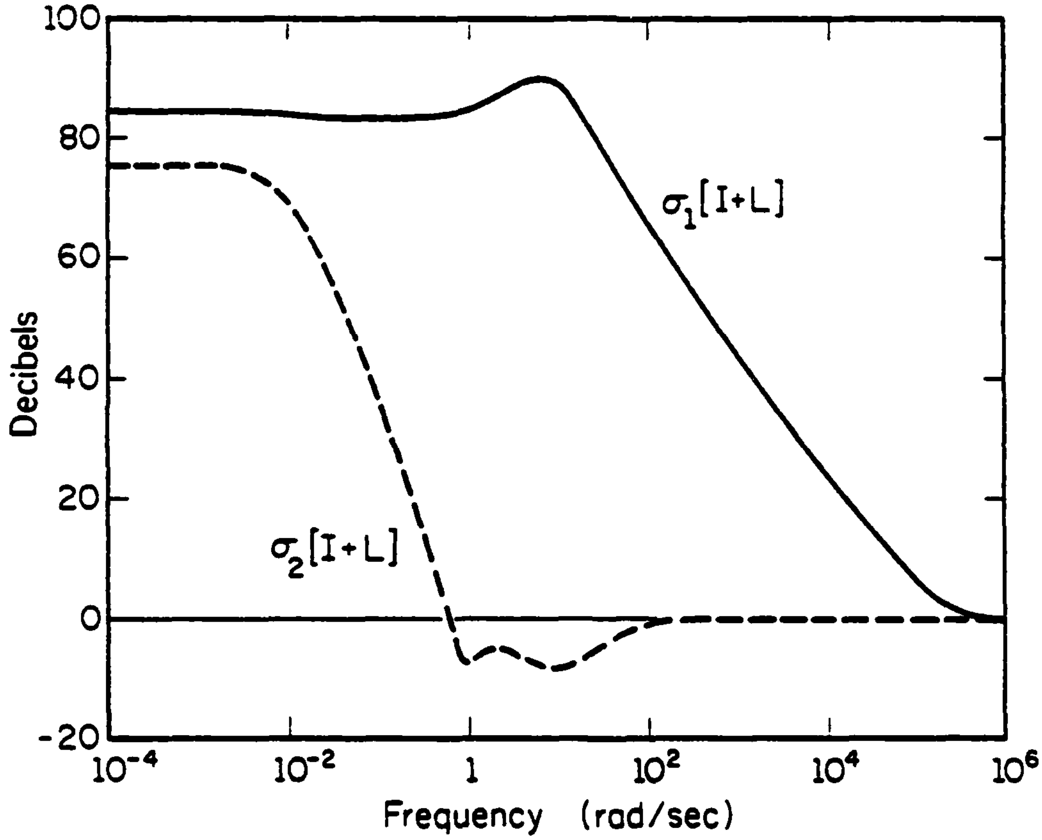

Figure 13.7. Singular values of return difference matrix.

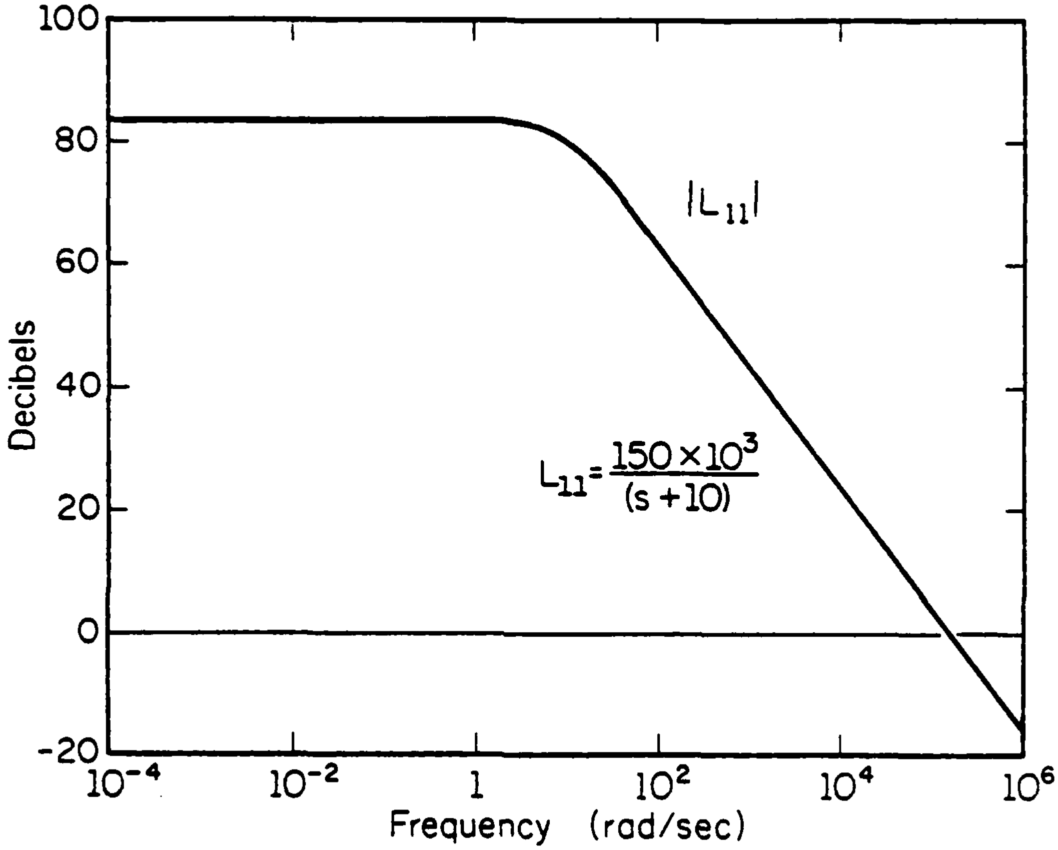

Figure 13.8.a. Gain of L_{11}.

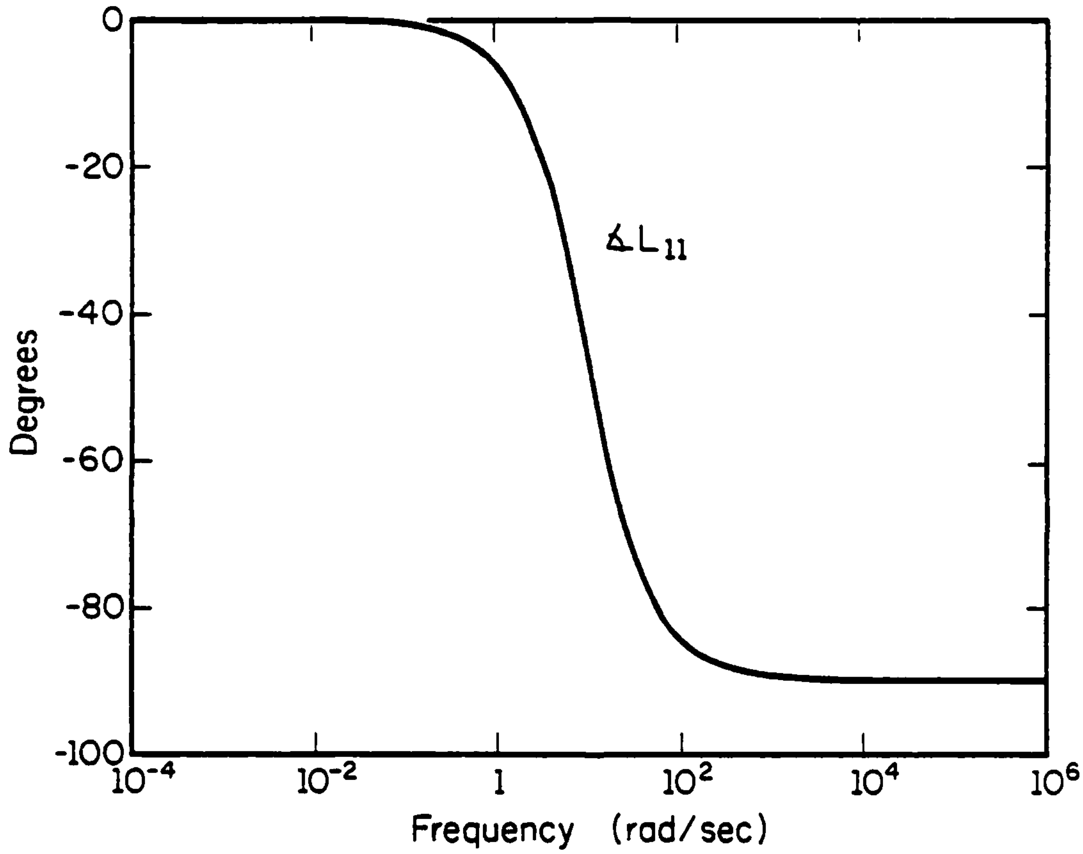

Figure 13.8.b. Phase of L_{11}.

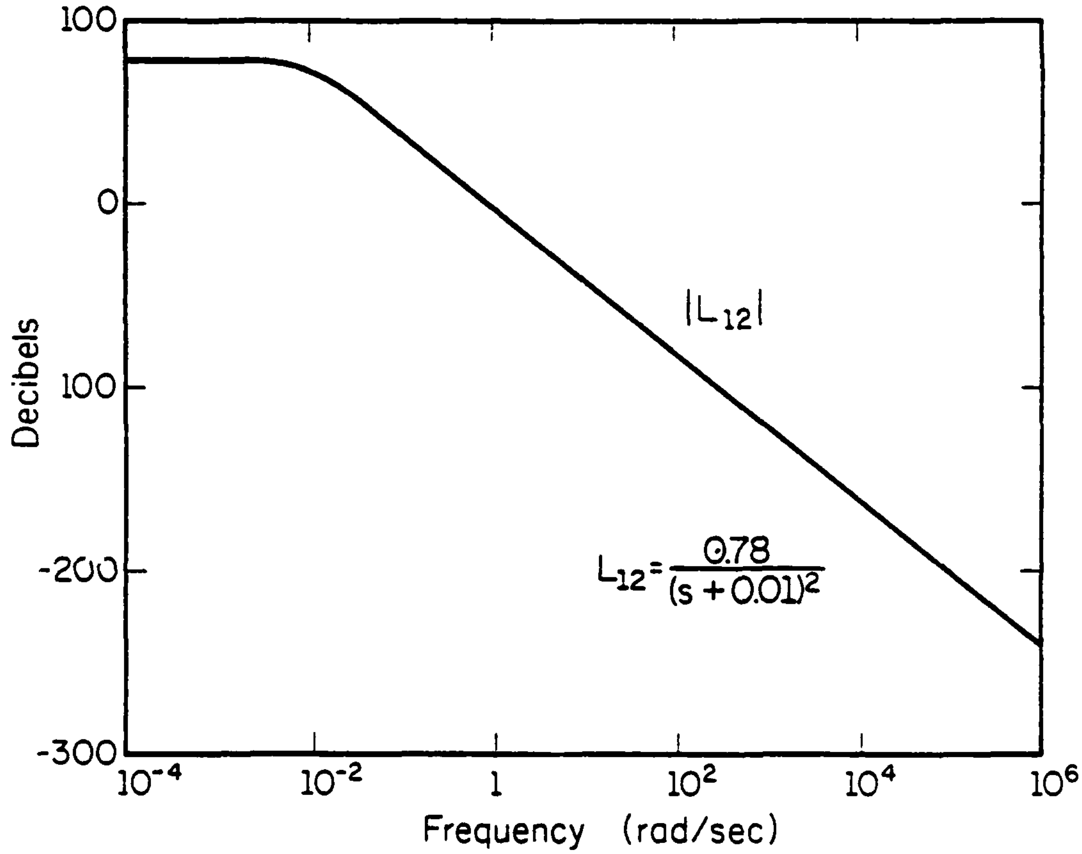

Figure 13.9.a. Gain of L_{12}.

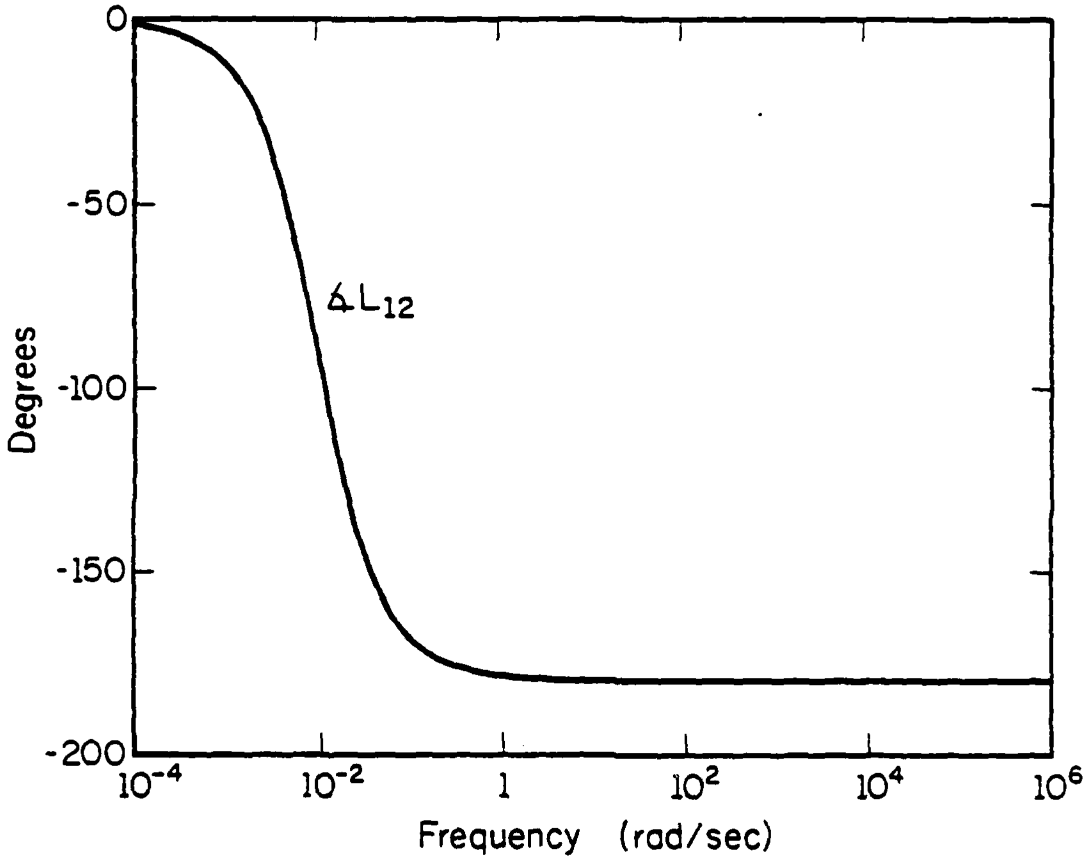

Figure 13.9.b. Phase of L_{12}.

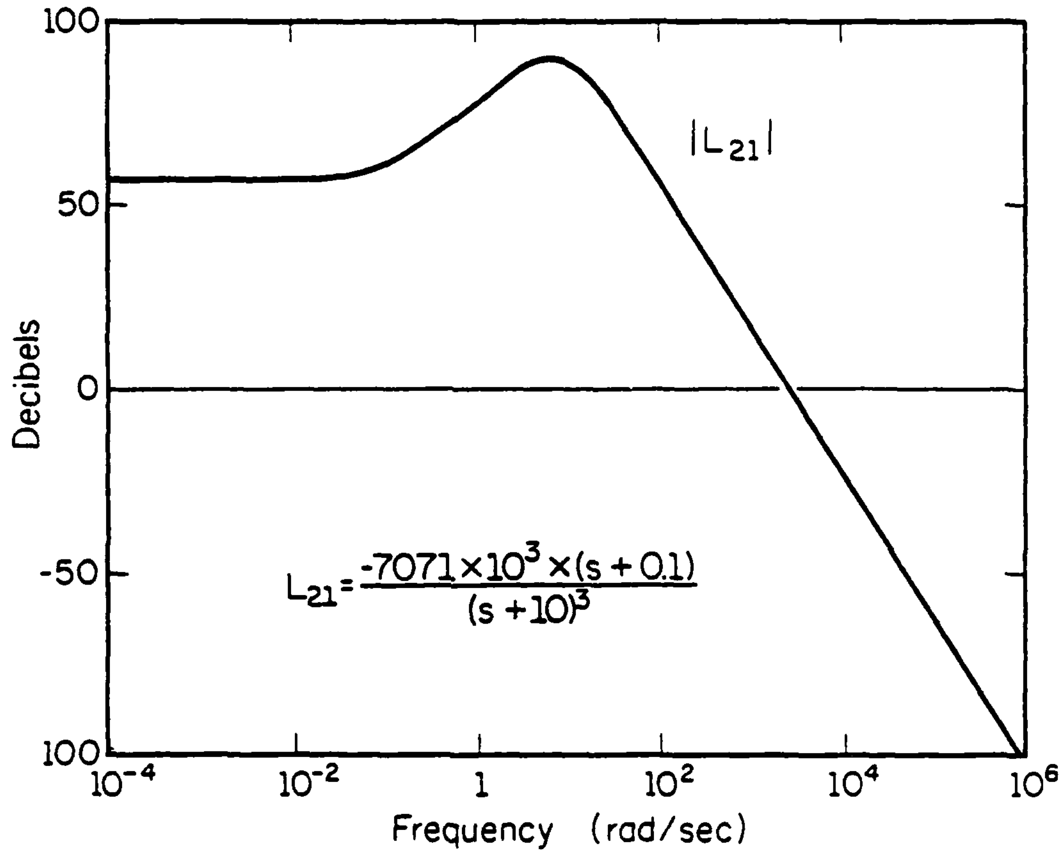

Figure 13.10.a. Gain of L_{21}.

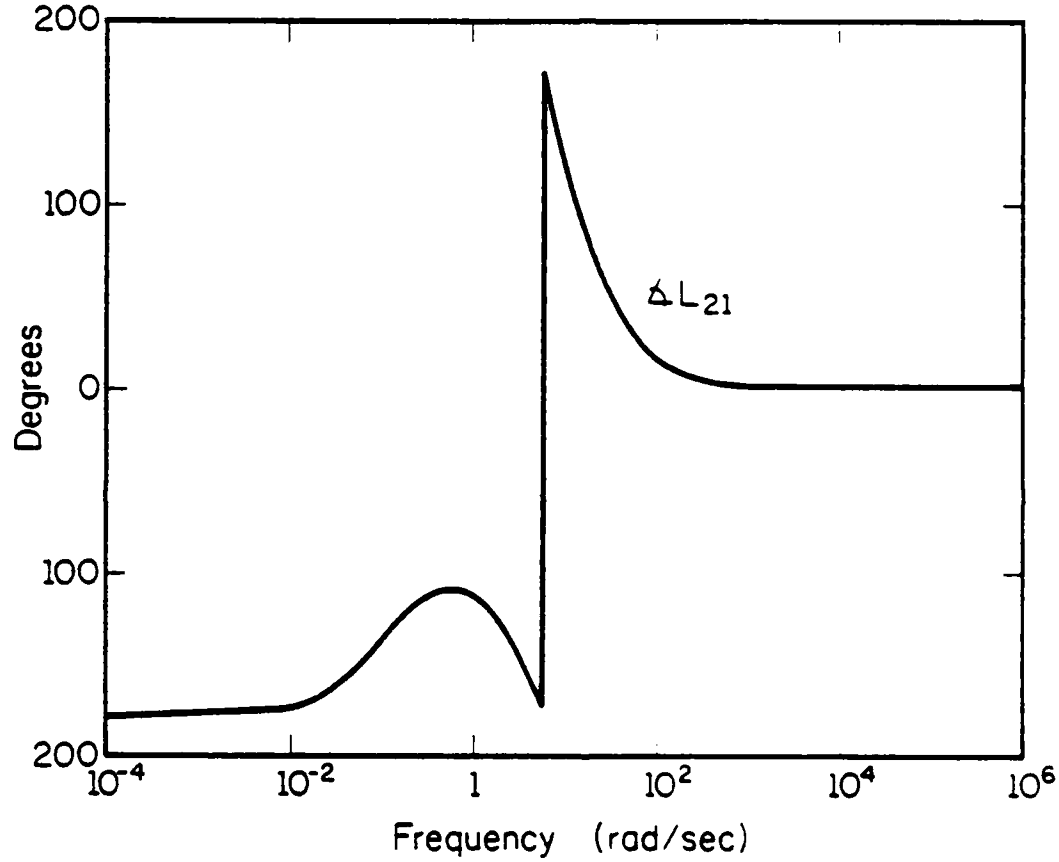

Figure 13.10.b. Phase of L_{21}.

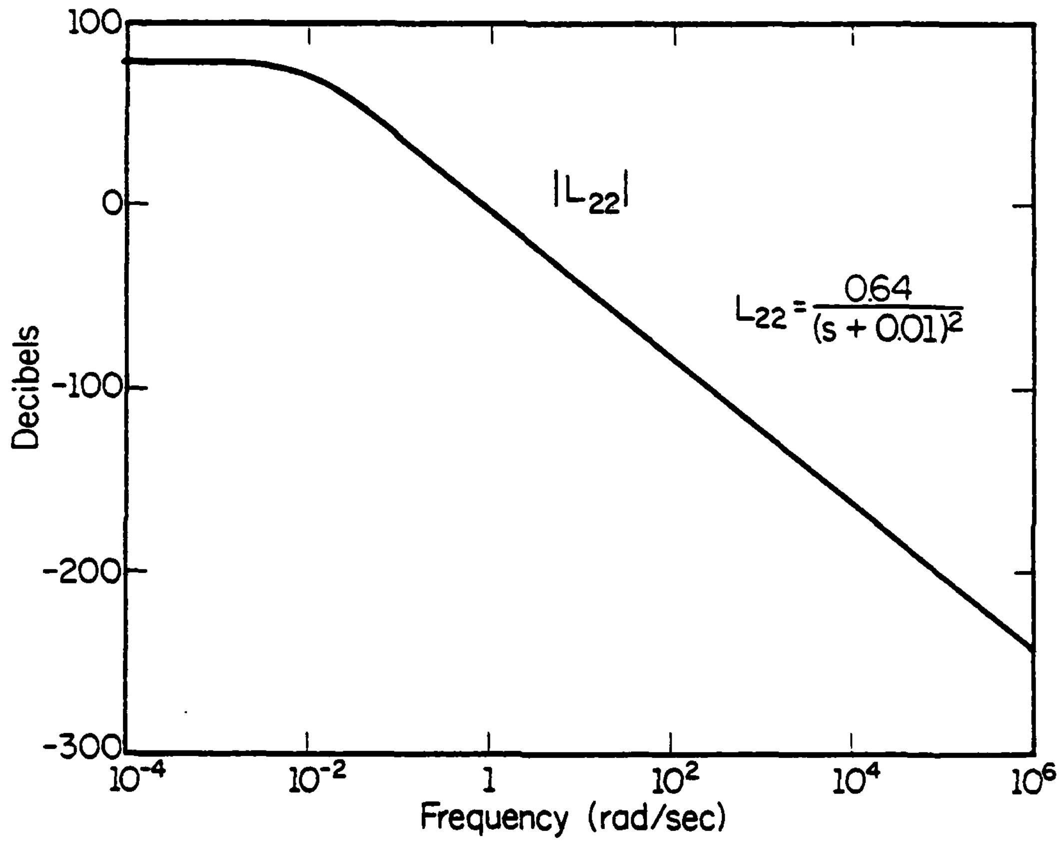

Figure 13.11.a. Gain of L_{22}.

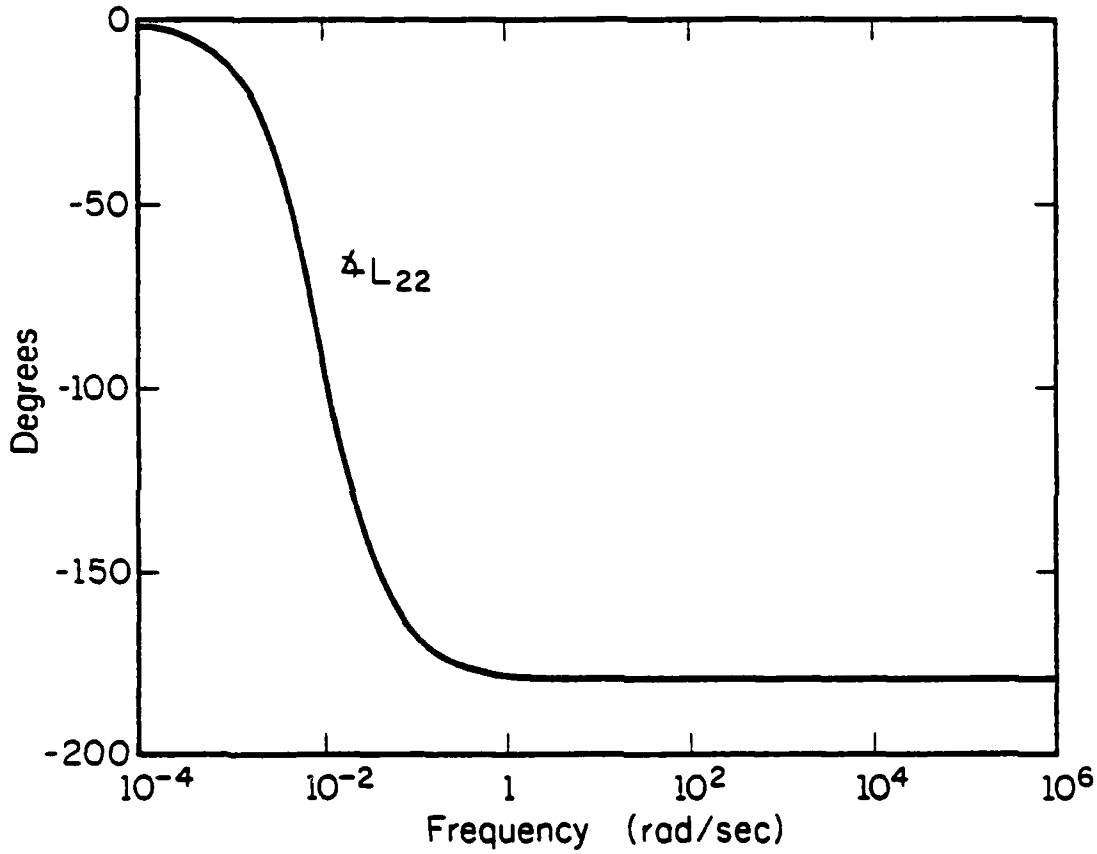

Figure 13.11.b. Phase of L_{22}.

Finally, recall that the analysis of Chapter 8 showed that the angle ϕ between singular subspaces and the phase differences $\theta_i = \measuredangle u_i^H v_i$ are important in determining feedback properties. For the example being analyzed, it was pointed out in Section 8.4 that $\theta_2 \approx \tilde{\theta}_2$ and $\phi \approx \phi_v$, so that the latter parameters may be used reliably in their place. This may also be seen using the local trivializations. From

$$u_2^H v_2 = \rho_{u_2}^H \rho_{v_2} e^{j\tilde{\theta}_2}$$

it follows that

$$\cos\phi = |\rho_{u_2}^H \rho_{v_2}|$$

$$= |\sin\phi_u \sin\phi_v e^{j(\psi_v - \psi_u)} + \cos\phi_u \cos\phi_v| \quad . \qquad (13.17)$$

Similarly, θ_2 and $\tilde{\theta}_2$ are related by the function (10.41):

$$\theta_2 = \tilde{\theta}_2 + \measuredangle g_2$$

$$= \tilde{\theta}_2 + \measuredangle[\cos \phi_u \cos \phi_v e^{-j(\Psi_v - \Psi_u)} + \sin \phi_u \sin \phi_v]. \qquad (13.18)$$

Now, since $\phi_u \approx 0$, it follows from (13.17) and (13.18) that $\phi \approx \phi_v$ and $\theta_2 \approx \tilde{\theta}_2$.

13.3. Analysis Using New Gain-Phase Relations

In the preceding section approximations to some parameters describing the singular value decomposition of L(s) were described. These approximations were based upon the algebraic relation between the various parameters and the

components $L_{ij}(s)$. Algebraic relations are based upon equations which must be satisfied at each value of frequency. Analytic relations, such as the classical Bode relations, relate the value of a parameter at one frequency to values of other parameters over the entire range of frequencies. For example, this accounts for the fact that the phase lead in the L_{21} element is necessarily accompanied by an increase in the gain of that element.

Recall that an algebraic approximation could not be obtained for $\tilde{\theta}_2$. In this section, the integral relations from Chapter 12 will be used to show that the value of $\tilde{\theta}_2(j\omega)$ is completely determined by the singular value σ_2 and by the left and right singular subspaces. Since these latter quantities can be approximated algebraically, in principal it should be possible to estimate $\tilde{\theta}_2$ via its analytic dependence upon σ_2 and the subspaces. Rules of thumb based upon the new integral relations are not yet available; thus it is not possible at the present time to estimate $\tilde{\theta}_2$ directly without numerically evaluating a surface integral. It is possible, however, to obtain an indirect estimate. In addition, some qualitative insights into the system behavior needed to produce the observed phase lead in $\tilde{\theta}_2$ are obtained.

In order to apply Theorem 12.2 certain conditions must be satisfied. The matrix L(s) obviously has no poles in the CRHP; it may easily be verified that det[L(s)] is nonzero there also. It was shown in Section 13.2 that the singular values of L(s) are distinct and that each pair of singular vectors u_i, v_i may be written using the local trivialization T_1. In addition, the constants k_i are given by $k_1 = 1$, $k_2 = 2$ and the singular vectors may be chosen so that $u_1 \to e_1$, $u_2 \to e_2$, $v_1 \to \frac{|s|}{s} e_1$ and $v_2 \to \frac{|s|^2}{s^2} e_2$. Thus all conditions

necessary to apply Theorem 12.2 are satisfied. The phase differences $\tilde{\theta}_i$ must therefore satisfy (noting $\tilde{\theta}_i(0) = 0$)

$$\tilde{\theta}_i(j\omega_o) = \frac{1}{\pi}\int_{-\infty}^{\infty} \frac{d\log\sigma_i}{d\nu}\{\log\coth\frac{|\nu|}{2}\}d\nu + \frac{1}{\pi}\int_{CRHP}(\rho_{v_i}{}^H\frac{\partial\rho_{v_i}}{\partial r} - \rho_{u_i}{}^H\frac{\partial\rho_{u_i}}{\partial r})dr\wedge d\alpha \qquad (13.19)$$

using a polar coordinate system defined by $s = j\omega_o + re^{j\alpha}$. In coordinates on $\mathbb{C}P^1$, (13.19) reduces to

$$\tilde{\theta}_i(j\omega_o) = \frac{1}{\pi}\int_{-\infty}^{\infty} \frac{d\log\sigma_i}{d\nu}\{\log\coth\frac{|\nu|}{2}\}d\nu - \frac{(-1)^i}{\pi}\int_{CRHP}(\sin^2\phi_v\frac{\partial\psi_v}{\partial r} - \sin^2\phi_u\frac{\partial\psi_u}{\partial r})dr\wedge d\alpha \quad . \qquad (13.20)$$

The first integral in (13.19)-(13.20) is similar to the scalar Bode gain-phase relation. Associated with this integral is the rule of thumb that a 20N db/decade roll-off rate produces a 90N° phase lag. The second term in (13.19)-(13.20) quantifies the amount by which motion of the singular subspaces causes the gain-phase relations to be violated. In this example it is clear that the violation of the gain-phase relations is due to interactions between the physical loops of the system. To see this, recall the fact that $\phi_u \approx 0$ implied that the right singular subspaces were aligned with the standard input directions. Thus any contribution from the surface integral must arise from the left singular subspaces changing with frequency. This manifests itself in changing loop interactions due to changes in the way outputs from the high and low gain subsystems are fed back to the input.

Note from (13.20) that the values of $\tilde{\theta}_1(j1)$ and $\tilde{\theta}_2(j1)$ should deviate from those expected from the SISO gain-phase relations by amounts

of equal magnitude and opposite sign. Thus an alternative to computing the surface integral directly would be to estimate its value by comparing the value of $\tilde{\theta}_1(j1)$ with that of the phase of a transfer function F(s) which satisfies $|F(j\omega)| \approx \sigma_1(j\omega)$. Since $\sigma_1(j\omega) \approx \|L_1(j\omega)\|$, F(s) will be constructed so that $\|F(j\omega)\| = \|L_1(j\omega)\|$. Using spectral factorization techniques, it may be shown that

$$F(s) = \frac{(150 \times 10^2)(s + 2)(s + 49)}{(s + 10)^3} \tag{13.21}$$

is a suitable function. Inspection of the numerical values of $\sigma_1(j\omega)$ and $\|F(j\omega)\|$ shows that the two functions are very nearly equal. The Bode plot of F(s) is shown in Figure 13.12. As expected from classical techniques, the peak in $|F(j\omega)|$ near $\omega = 10$ rad/sec is accompanied by phase lead at lower frequencies. At $\omega = 1$ rad/sec, $\measuredangle F(j1) = 10.6°$. But $\tilde{\theta}_1(j1) \approx -5.7°$. Thus the surface integral must contribute $\approx -16.3°$ phase lag, and the value of $\tilde{\theta}_2(j1)$ should be larger than that predicted by the roll off rate of $\sigma_2(j\omega)$ near $\omega = 1$ rad/sec by $\approx 16.3°$. From Figure 13.1 it appears that σ_2 has approximately a 40 db/decade roll off for well over a decade on either side of $\omega = 1$ rad/sec. Closer inspection (Figure 13.13) reveals that a more accurate estimate would be $\approx$ 38 db/decade, while the numerical values of σ_2 indicate that very near $\omega = 1$ rad/sec, σ_2 rolls off at $\approx$ 37 db/decade. Thus if the surface integral was not present $\tilde{\theta}_2(j1)$ would be roughly -165° to -172°. The loop interaction term shows that $\tilde{\theta}_2(j1)$ should lie roughly in the interval -150° to -156°. This agrees well with the actual value of $\tilde{\theta}_2(j1) \approx -154°$.

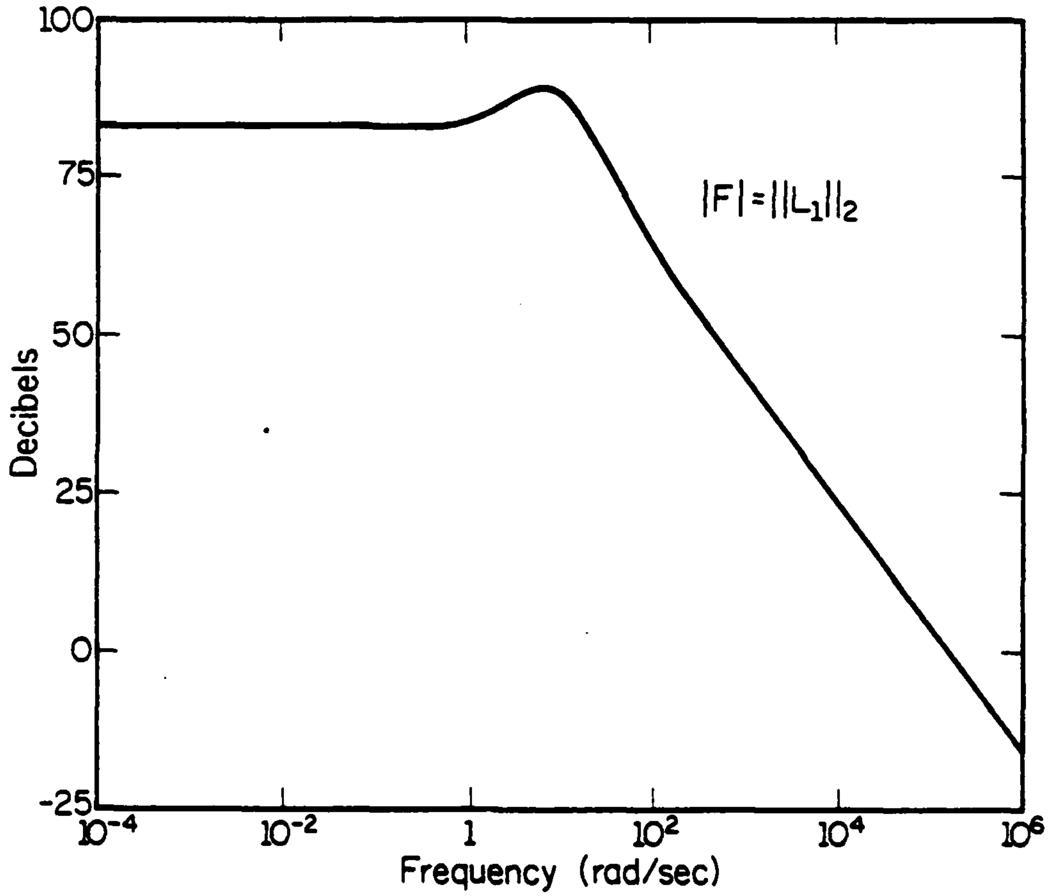

Figure 13.12.a. Gain of F.

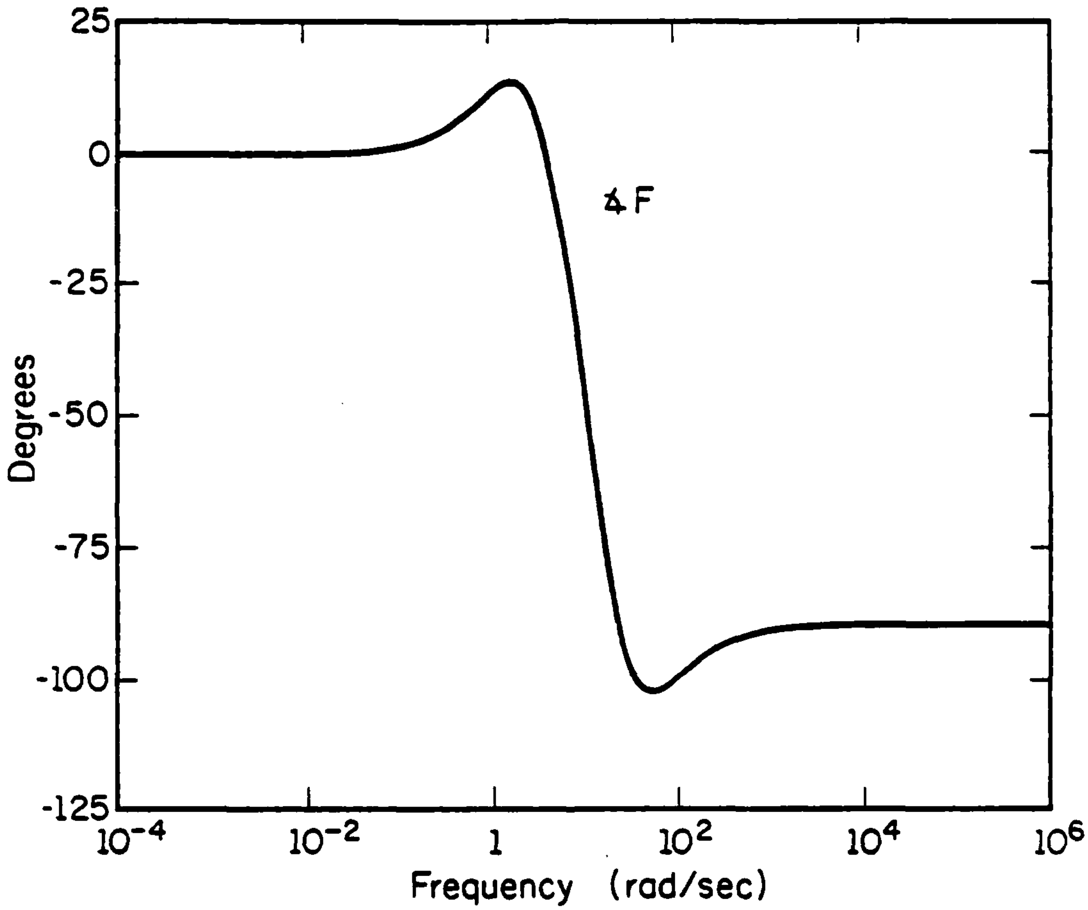

Figure 13.12.b. Phase of F.

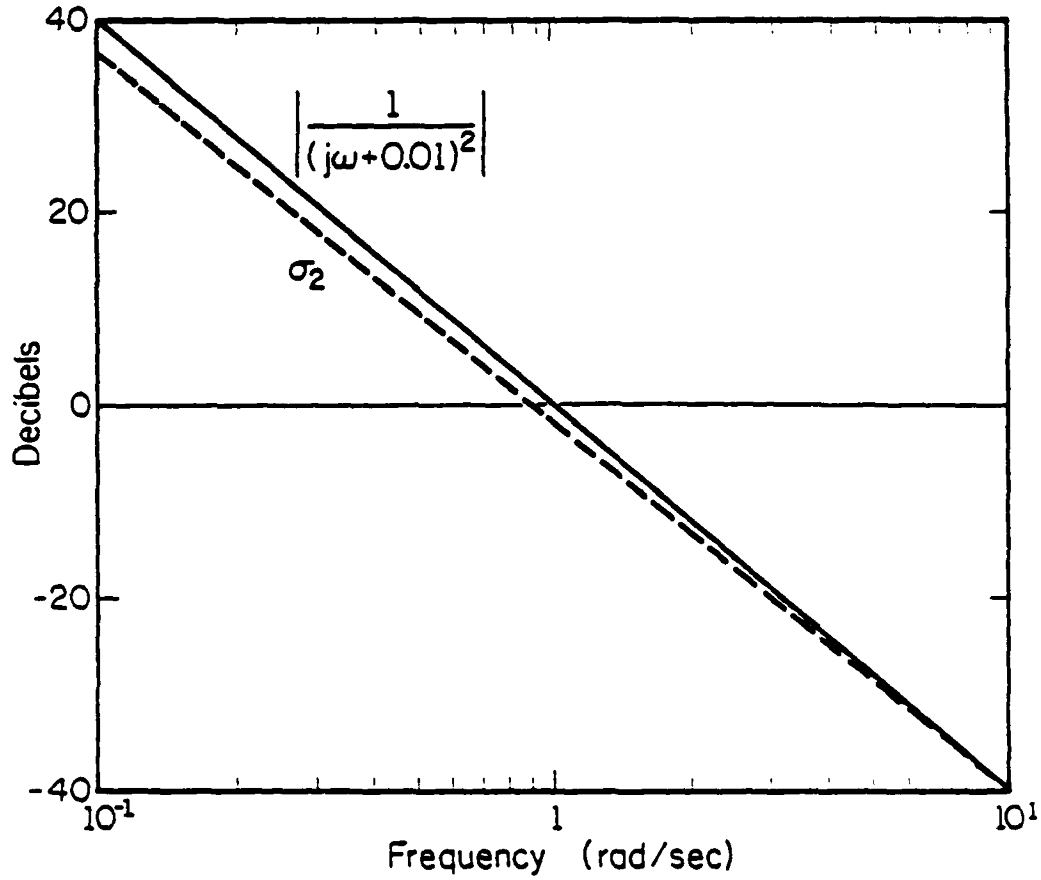

Figure 13.13. Smallest singular value vs. gain in second loop, $\|L_2\|_2$.

The integral relations may also be used to gain qualitative information about the properties of the system if loop coupling is to produce phase lead in $\tilde{\theta}_2$. First, the value of the integrand averaged over the right half plane must be negative. Since $\phi_u \approx 0$ due to the structure of the example, it follows that $\frac{\partial \psi_v}{\partial r}$ must take negative values over at least a portion of the right half plane. Moreover, ϕ_v must be sufficiently greater than zero in this region if the negative values of $\frac{\partial \psi_v}{\partial r}$ are to have an appreciable effect. Finally, since the surface integral essentially weights the integrand by a factor of $(1/r)$, it follows that ϕ_v and ψ_v must attain the appropriate values in the vicinity of $s = j1$. Since the values of both ϕ_v and ψ_v are determined by $L_{21}(s)$, it follows that the coupling introduced by this element is critical to producing the desired phase lead. Thus a large value of ϕ_v seems necessary to achieve the phase lead resulting in the first peak in the sensitivity function being only 8 db. Recall also the large value of ϕ_v results in the second peak in sensitivity being as large as 8 db. Thus it is reasonable to conjecture that the tradeoff between the levels of these two peaks cannot be avoided within the basic structure of this problem.

Finally, recall the discussion in Chapter 12 concerning the two mechanisms by which changes in the phase difference parameter $\tilde{\theta}_2$ may be produced. Clearly both are demonstrated in this example. At low and high frequencies the change in $\tilde{\theta}_2$ is dominated by the first mechanism; i.e., the fact that $\sigma_2(j\omega)$ is rolling off. In the mid-frequency range, however, the second mechanism has a significant effect. Recall this mechanism was due to a transfer of phase between the loops of the system. This transfer is

clearly demonstrated in this example, since the phase lead in $L_{21}(s)$ does not produce phase lead in $\tilde{\theta}_1$ but rather in $\tilde{\theta}_2$. The interaction between loops is present in the form of a significantly large value of ϕ_v. Moreover, the fact that the change in phase is not equal in all components of the left singular vectors (choosing the right singular vectors as $u_i = e_i$) is demonstrated by the significant change in ψ_v over the frequency interval in which $\tilde{\theta}_2$ experiences phase lead, while $\tilde{\theta}_1$ does not. Clearly, the effect in the phase difference parameters $\tilde{\theta}_i$ is contrary to what one would expect were each $\sigma_i e^{j\tilde{\theta}_i}$ a rational transfer function.

13.4. Conclusions

In this chapter the integral relations derived in Chapter 12 have been used to analyze the example in Section 8.4. The same type of analysis could be performed on the realistic example of Section 8.5, although the nature of the loop coupling in the latter example does not produce any phase lead in $\tilde{\theta}_2$. Even in the example considered, more work remains to be done. The parameters of the lead filter in $L_{21}(s)$ need to be varied in order to gain an understanding of their relation with ϕ_v and ψ_v. Especially needed is some knowledge of how these parameters are affected at points in the open right half plane.

Another task remaining is to numerically evaluate the surface integral. By evaluating the integral in steps some insight would be gained into how fast the weighting function decays the effect of the integrand.

The effect of singularities also needs to be studied. Recall Theorem 12.2 is applicable only to those matrices with distinct singular values in the right half plane. Yet, by reducing the gain in the first loop by a constant, a system with the same phase lead in $\tilde{\theta}_2$ may be obtained and for which the singular values cross over. This suggests the assumption of distinct singular values might be removed.

Another observation was that changing the sign of $L_{21}(s)$ did not affect the values of $\sigma_2(j\omega)$, ϕ_v, or $\frac{\partial\psi_v}{\partial r}$. Yet the phase leading effect was no longer present. Further inspection revealed that $\sigma_2(s)$ was zero at two points in the open right half plane. Thus the new integral relations, as expected, exhibit the effects of nonminimum phase plants. One difference, however, is that the integral relation for $\sigma_1 e^{j\tilde{\theta}_1}$ is still valid; only that for $\sigma_2 e^{j\tilde{\theta}_2}$ is affected.

Finally, the ability to independently manipulate ϕ_v, ψ_v, ϕ_u, and ψ_u is also constrained by a set of differential equations. These were not stated in Chapter 11, but a procedure with which to derive them was presented in Section 11.3. Further study into these equations is also needed.

CHAPTER 14

SUMMARY AND CONCLUSIONS

For a summary of the results of this thesis, the reader is referred to Chapter 1 and to the concluding sections of each chapter.

This thesis comprises an incomplete* attempt to generalize some ideas from classical control theory to multiple-loop feedback systems. Significant aspects of the classical theory were the quantifications of various algebraic and analytic tradeoffs among feedback properties. Investigating how these tradeoffs extend was a major task of this thesis. As even the most casual reader must have recognized, much substantial work remains to be done. Specific areas needing further research could be discussed here, but Bode's invincible fatigue is beginning to set in. Suffice it to say that the essential tools — the approximation techniques from Chapter 8 and the mathematical theory from Chapters 9-12 — appear to be at hand.

*Although hopefully not insignificant

APPENDIX A

PROOFS OF THEOREMS IN CHAPTER 3

The following lemma follows from a minor modification of the well-known Poisson Integral Formulas [26,27] for the recovery of a function analytic in the right half plane from its values on the imaginary axis. The proof found in [26] is modified to show that singularities of log f(s) at $j\omega$-axis zeros of f(s) do not contribute to the values of the integrals. As the required modification is slight, the proof will only be sketched.

Lemma A.1: Let f(s) be analytic and nonzero in the closed right half plane except for possible zeros on the imaginary axis. Assume that $\frac{d^i}{ds^i} \log f(s)$ is in class $\mathcal{R}$, i=0,1,... .

Then at each point $s_o = x_o + jy_o$, $x_o > 0$ it follows that

$$\log|f(s_o)| = \frac{1}{\pi} \int_{-\infty}^{\infty} \log|f(j\omega)| \frac{x_o}{x_o^2+(y_o-\omega)^2} d\omega \tag{A.1}$$

$$\measuredangle f(s_o) = \frac{1}{\pi} \int_{-\infty}^{\infty} \measuredangle f(j\omega) \frac{x_o}{x_o^2+(y_o-\omega)^2} d\omega \tag{A.2}$$

$$\left.\frac{d^i}{ds^i} \log f(s)\right|_{s_o} = \frac{1}{\pi} \int_{-\infty}^{\infty} \left.\frac{d^i}{ds^i} \log f(s)\right|_{s=j\omega} \frac{x_o}{x_o^2+(y_o-\omega)^2} d\omega. \tag{A.3}$$

Proof: Define the contour C_δ to be the imaginary axis traversed from $+j\infty$ to $-j\infty$ with semicircular indentations of radius δ into the right half plane at the $j\omega$-axis zeros of f(s). Then f(s) is analytic and nonzero to the right of C_δ. It follows that log f(s) and its derivatives are analytic in this region also.

The proof of the Poisson Integral Formulas in [26] may be followed to show that for each point s_o in the open right half plane there exists δ sufficiently small so that

$$\log f(s_o) = \frac{1}{j\pi} \int_{C_\delta} \log f(\zeta) \frac{x_o}{(\zeta - s_o)(\zeta + \bar{s}_o)} d\zeta \quad . \tag{A.4}$$

A straightforward calculation shows that in the limit as $\delta \to 0$ the integrals taken around the semicircular indentations vanish. Thus, setting $\zeta = j\omega$ in (A.4) yields

$$\log f(s_o) = \frac{1}{\pi} \int_{-\infty}^{\infty} \log f(j\omega) \frac{x_o}{x_o^2 + (y_o - \omega)^2} d\omega \quad . \tag{A.5}$$

Similarly,

$$\left. \frac{d^i}{ds^i} \log f(s) \right|_{s_o} = \frac{1}{\pi} \int_{-\infty}^{\infty} \left. \frac{d^i}{ds^i} \log f(s) \right|_{s=j\omega} \frac{x_o}{x_o^2 + (y_o - \omega)^2} d\omega \tag{A.6}$$

where the improper integrals are defined using Cauchy principal values [26, pp. 203-204]. The result follows by taking real and imaginary parts of (A.5). ∎

<u>Proof of Theorem 3.1</u>: Follows from Lemma A.1 by setting $f(s) = \tilde{S}(s)$ and noting $\tilde{S}(z) = B_p^{-1}(z)$. ∎

<u>Proof of Theorem 3.2</u>: Follows from Lemma A.1 by setting $f(s) = \tilde{T}(s)$ and noting $\tilde{T}(p) = B_z^{-1}(p)e^{p\tau}$. ∎

It should be pointed out that formulas relating $\log|f(s_o)|$ to a weighted integral of $\measuredangle f(j\omega)$ and $\measuredangle f(s_o)$ to a weighted integral of $\log|f(j\omega)|$ may also be obtained. These follow from the <u>conjugate</u> Poisson Integral Formulas [26, pp. 225-226] and may also have implications for feedback design. However, such implications will not be pursued further at this time.

Theorem 3.3 could be verified directly using contour integration in the right half plane with branch cuts extending from the zeros of S(s) to infinity deleted. Care must be taken to deal correctly with the fact that $\measuredangle S(s)$ jumps by a multiple of 2π across these cuts. (This led to the incorrect result in [9]). An alternative procedure is to prove Theorem 3.3 as a limiting case of the integral relation (A.1).

<u>Proof of Theorem 3.3</u>: Evaluating (A.1) for $f(s) = \tilde{S}(s)$ and $s = x > 0$ yields (noting conjugate symmetry of $S(j\omega)$ implies $S(j\omega) = \overline{S(-j\omega)}$):

$$\log|\tilde{S}(x)| = \frac{2}{\pi}\int_0^\infty \log|S(j\omega)| \frac{x}{x^2+\omega^2}\, d\omega \quad . \tag{A.7}$$

Observing that $\log|S(j\omega)| \dfrac{x^2}{x^2+\omega^2}$ converges to $\log|S(j\omega)|$ pointwise as x approaches infinity suggests that

$$\lim_{x\to+\infty} x\log|\tilde{S}(x)| = \lim_{x\to+\infty} \frac{2}{\pi}\int_0^\infty \log|S(j\omega)| \frac{x^2}{x^2+\omega^2}\, d\omega \tag{A.8}$$

might be used to evaluate

$$\int_0^\infty \log|S(j\omega)|d\omega \quad . \tag{A.9}$$

The proof of this conjecture consists of three parts. First, it is shown that (A.9) may be approximated arbitrarily closely by $\int_0^{\bar{\omega}} \log|S(j\omega)|d\omega$ for $\bar{\omega}$ sufficiently large. Next, it is shown that for $\omega \in [0,\bar{\omega}]$ the sequence $\frac{n^2}{n^2+\omega^2}$ converges uniformly to 1 as n approaches infinity. Together these facts show that the limit on the right-hand side of (A.8) is finite and equal to (A.9). Finally, the limit on the left-hand side of (A.8) is evaluated.

The power series expansion of $\log S(s) = -\log[1+L(s)]$ for $|L(s)| < 1$ is given by [58, p. 158]

$$\log S(s) = -L(s) + \frac{L^2(s)}{2} + \text{ higher order terms.}$$

Thus, by (3.22) $\omega \log|S(j\omega)|$ approaches zero at infinity. This implies that there exist a frequency ω_o and positive constants M_o and δ such that $|\log|S(j\omega)|| \le \frac{M_o}{\omega^{1+\delta}}$ for $\omega > \omega_o$. For $\bar{\omega} > \omega_o$,

$$\int_{\bar{\omega}}^{\infty} |\log|S(j\omega)||d\omega \le \int_{\bar{\omega}}^{\infty} \frac{M_o}{\omega^{1+\delta}} d\omega = \frac{M_o}{\delta\bar{\omega}^{\delta}} \quad . \tag{A.10}$$

From (A.10) it follows that for any $\varepsilon > 0$ there exists a frequency $\bar{\omega}$ such that

$$\int_{\bar{\omega}}^{\infty} \log|S(j\omega)|d\omega < \varepsilon \quad . \tag{A.11}$$

On the interval $\omega \in [0,\bar{\omega}]$ it is easy to verify that the sequence $\frac{n^2}{n^2+\omega^2}$ converges uniformly to one as n approaches infinity. If L(s) has no $j\omega$-axis poles, then uniform convergence of the integrand suffices to show that [48, p. 71]

$$\lim_{x\to\infty} \int_0^{\bar{\omega}} \log|S(j\omega)| \frac{x^2}{x^2+\omega^2} d\omega = \int_0^{\bar{\omega}} \log|S(j\omega)| d\omega \quad . \tag{A.12}$$

(If L(s) has poles in $[0,\bar{\omega}]$, then it is necessary to consider indentations into the right half plane as in the proof of the Lemma; these details are omitted.)

Together (A.11) and (A.12) imply that

$$\lim_{x\to\infty} \int_0^{\infty} \log|S(j\omega)| \frac{x^2}{x^2+\omega^2} d\omega = \int_0^{\infty} \log|S(j\omega)| d\omega \quad . \tag{A.13}$$

It remains to evaluate $\lim_{x\to\infty} x \log|\tilde{S}(x)|$. By definition

$$\log|\tilde{S}(x)| = \log|B_p^{-1}(x)| + \log|S(x)|$$

$$= \sum_{i=1}^{N_p} \log\left|\frac{\bar{p}+x}{p-x}\right| + \log|S(x)| \quad . \tag{A.14}$$

Since $\lim_{x\to\infty} x \log|S(x)| = 0$, it follows that

$$\lim_{x\to\infty} x \log|\tilde{S}(x)| = \sum_{i=1}^{N_p} \lim_{x\to\infty} x \log\left|\frac{\bar{p}_i+x}{p_i-x}\right| \quad . \tag{A.15}$$

From the power series expansions [58, p. 158]

$$\log(1 + \frac{\bar{p}}{x}) = \frac{\bar{p}}{x} - \frac{1}{2} (\frac{\bar{p}}{x})^2 + \ldots \qquad \left|\frac{\bar{p}}{x}\right| < 1$$

$$\log(1 - \frac{p}{x}) = - \frac{p}{x} - \frac{1}{2} (\frac{p}{x})^2 + \ldots \qquad \left|\frac{p}{x}\right| < 1$$

it follows that for $x > |p|$

$$\log \frac{\bar{p}_i + x}{x - p_i} = \log \left(\frac{1 + \frac{\bar{p}_i}{x}}{1 - \frac{p_i}{x}} \right)$$

$$= \frac{\bar{p}_i + p_i}{x} + \text{higher order terms.}$$

Thus,

$$\lim_{x \to \infty} x \log \left| \frac{\bar{p}_i + x}{p_i - x} \right| = 2 \operatorname{Re}[p_i] \quad . \tag{A.16}$$

Substituting (A.16) into (A.15) yields

$$\lim_{x \to \infty} x \log |\tilde{S}(x)| = \sum_{i=1}^{N_p} 2 \operatorname{Re}[p_i] \quad . \tag{A.17}$$

Substituting (A.17) into (A.8) and using (A.13) yields

$$\pi \sum_{i=1}^{N_p} \operatorname{Re}[p_i] = \int_0^\infty \log |S(j\omega)| d\omega \quad .$$ ∎

<u>Proof of Corollary</u>: At each frequency $\omega \geq \omega_c$

$$|S(j\omega)| = \left| \frac{1}{1 + L(j\omega)} \right| \leq \frac{1}{1 - |L(j\omega)|} \quad .$$

This follows since $|L(j\omega)| < 1$ for $\omega \geq \omega_c$ by (3.24). Moreover, since $|L(j\omega)| \leq \frac{M}{\omega^{1+k}} < 1$ for $\omega > \omega_c$

$$|S(j\omega)| \leq \frac{1}{1 - \frac{M}{\omega^{1+k}}} \quad .$$

Expanding $\log \left(\frac{1}{1 - \frac{M}{\omega^{1+k}}} \right)$ in a power series yields (for $\omega > \omega_c$)

$$\log\left[\frac{1}{1-\frac{M}{\omega^{1+k}}}\right] = \sum_{n=1}^{\infty}\frac{\left(\frac{M}{\omega^{1+k}}\right)^n}{n} = \frac{1}{\omega^{1+k}}\sum_{n=1}^{\infty}\frac{\left(\frac{M}{\omega^{1+k}}\right)^n\omega^{1+k}}{n} .$$

The infinite sum attains its maximum for $\omega = \omega_c$. Define

$$M_o \triangleq \sum_{n=1}^{\infty}\frac{\left(\frac{M}{\omega^{1+k}}\right)^n\omega^{1+k}}{n} = \log\left[\frac{1}{1-\frac{M}{\omega_c^{1+k}}}\right]\omega_c^{1+k} .$$

Thus, $\omega > \omega_c$ implies that

$$\log|S(j\omega)| \leq \frac{M_o}{\omega^{1+k}} .$$

Thus,

$$\int_{\omega_c}^{\infty} \log|S|d\omega \leq \int_{\omega_c}^{\infty}\frac{M_o}{\omega^{1+k}}d\omega$$

$$= \frac{M_o}{k\omega_c^{k}} .$$

Substituting M_o:

$$\frac{M_o}{k\omega_c^k} = \frac{\log\left[\frac{1}{1-\frac{M}{\omega_c^{1+k}}}\right]\omega_c^{1+k}}{k\omega_c^k} .$$

Since $\frac{M}{\omega_c^{1+k}} = \epsilon$, this reduces to

$$\int_{\omega_c}^{\infty} \log|S(j\omega)|d\omega \leq \frac{\log\left[\frac{1}{1-\epsilon}\right]\omega_c}{k} .$$

APPENDIX B

PROPERTIES OF THE SINGULAR VALUE DECOMPOSITION

The purpose of this Appendix is to state some properties of the singular value decomposition which are used in this thesis. The exposition is based upon that of Stewart [37, Section 6.6]; the reader is referred to this source for proofs and further details.

Let $A \in \mathbb{C}^{n\times n}$. Then there exist unitary matrices U and V such that

$$V^H AU = \Sigma \tag{B.1}$$

where $\Sigma = \mathrm{diag}[\sigma_1, \sigma_2, \ldots, \sigma_n]$ and $\sigma_1 \geq \sigma_2 \geq \ldots \geq \sigma_n \geq 0$. The numbers σ_i are referred to as the singular values of A. The columns of $U = [u_1 \mid \ldots \mid u_n]$ and $V = [v_1 \mid \ldots \mid v_n]$ are referred to as the right and left singular vectors, respectively. The singular values and vectors must satisfy the equations

$$Au_i = \sigma_i v_i \tag{B.2}$$

$$v_i^H A = u_i^H \sigma_i \quad . \tag{B.3}$$

Moreover, the numbers σ_i^2 are the eigenvalues of the matrix $A^H A$. The right singular vectors are eigenvectors of this matrix. Thus,

$$A^H AU = U\Sigma^2 \quad . \tag{B.4}$$

In addition, the numbers σ_i^2 are the eigenvalues of the matrix AA^H. The left singular vectors are eigenvectors of this matrix. Thus,

$$AA^H V = V\Sigma^2 \quad . \tag{B.5}$$

The singular values of A are uniquely defined. The singular vectors, however, are not. If $A^H A$ han an eigenvalue σ^2 with multiplicity k, then the corresponding columns of U may be chosen as any orthonormal basis for the eigenspace of $A^H A$ corresponding to σ^2. If $\sigma^2 > 0$ then, once the right singular vectors are chosen in this fashion, the left singular vectors are uniquely determined from (B.2). (Similar arguments starting with the left singular vectors can, of course, be made using (B.5) and (B.3).)

Note, in particular, that there exists a degree of freedom in choosing even a right singular vector corresponding to a singular value, σ_i, of multiplicity one. Let u_i be a right singular vector corresponding to σ_i, and let v_i be the corresponding left singular vector. Then, from (B.2), it follows that choosing $\hat{u}_i = e^{j\alpha}u_i$, $\alpha \in \mathbb{R}$, as a new right singular vector yields $\hat{v}_i = e^{j\alpha}v_i$ as the corresponding new left singular vector. Analogous statements hold for singular values of multiplicity greater than one.

Let $\bar{\sigma} \triangleq \sigma_1$, the largest singular value, and let $\underline{\sigma} \triangleq \sigma_n$, the smallest singular value. Then,

$$\bar{\sigma} = \|A\|_2 \qquad \text{(B.6)}$$

where $\|\cdot\|_2$ denotes the matrix norm induced by the standard Euclidean vector norm. Assume $\det A \neq 0$, so that A^{-1} exists. Then,

$$\underline{\sigma} = \frac{1}{\|A^{-1}\|_2} \quad . \qquad \text{(B.7)}$$

The Frobenius norm of a matrix is defined as

$$\|A\|_F = \sqrt{\sum_{i,j} |a_{ij}|^2} \quad . \qquad \text{(B.8)}$$

The singular values satisfy

$$\|A\|_F = \sqrt{\sum_i \sigma_i^2} \quad . \tag{B.9}$$

The singular values of A are related to the eigenvalues of A by

$$\bar{\sigma} \geq |\lambda_i| \geq \underline{\sigma} \ , \ \forall_i \quad . \tag{B.10}$$

Moreover, if A is normal (e.g., if A is Hermitian or unitary), then the eigenvalues of A may be ordered so that $\sigma_i = |\lambda_i|$.

Since the singular values of A are the nonnegative square roots of a Hermitian matrix, they inherit many of the interesting properties of such matrices. Among these are the following min-max property:

$$\sigma_i = \min_{\mathcal{S}_i} \max_{\substack{u \in \mathcal{S}_i \\ u \neq 0}} \frac{\|A\|_2}{\|u\|_2} \qquad \dim \mathcal{S}_i = n-i+1 \quad . \tag{B.11}$$

The minimum in (B.9) is taken over all subspaces of $\mathbb{C}^n$ with the appropriate dimension. In particular,

$$\bar{\sigma}[A] = \max_{\substack{u \in \mathbb{C}^n \\ u \neq 0}} \frac{\|Au\|_2}{\|u\|_2} \tag{B.12}$$

$$\Rightarrow \qquad \bar{\sigma}[A] \geq \frac{\|Au\|_2}{\|u\|_2} \qquad \forall u \in \mathbb{C}^n \quad . \tag{B.13}$$

In addition,

$$\underline{\sigma}[A] = \min_{\substack{u \in \mathbb{C}^n \\ u \neq 0}} \frac{\|Au\|_2}{\|u\|_2} \quad . \tag{B.14}$$

$$\Rightarrow \qquad \underline{\sigma}[A] \leq \frac{\|Au\|_2}{\|u\|_2} \qquad \forall u \in \mathbb{C}^n \quad . \tag{B.15}$$

Finally, one other property which singular values share with eigenvalues of Hermitian matrices is that they are numerically well-conditioned. In fact, given A, $\Delta A \in \mathbb{C}^{n \times n}$, then

$$\underline{\sigma}[A + \Delta A] \geq \underline{\sigma}[A] - \bar{\sigma}[\Delta A] \quad .$$

Thus, if $\bar{\sigma}[\Delta A] < \underline{\sigma}[A]$ and A is nonsingular, then $A + \Delta A$ is also nonsingular. In fact, given A nonsingular, the matrix ΔA of smallest magnitude for which $A + \Delta A$ is singular has magnitude $\bar{\sigma}[\Delta A] = \underline{\sigma}[A]$. One such matrix is given by $\Delta A = - \underline{\sigma}\ \underline{v}\ \underline{u}^H$, where $\underline{\sigma}$, $\underline{v}$, and $\underline{u}$ are the smallest singular values and corresponding singular vectors of A.

APPENDIX C

PROOFS OF THEOREMS IN CHAPTER 5

Proof of Theorem 5.1: Note the sensitivity matrix $S(s) = [I + L(s)]^{-1}$ has no poles in the closed right half plane by assumption of closed loop stability. The function det $S(s)$ thus has no poles in the closed right half plane but has zeros at the open right half plane poles $\{p_i \; ; \; i=1,\ldots,N_p\}$ of $L(s)$. It is necessary to remove these zeros. Define

$$D(s) \triangleq B_p^{-1}(s) \cdot \det S(s) \tag{C.1}$$

where $B_p(s)$ is the Blaschke product

$$B_p(s) = \prod_{i=1}^{N_p} \frac{p_i - s}{\bar{p}_i + s} \quad . \tag{C.2}$$

Then $D(s)$ has no zeros in the open right half plane, $\log D(s)$ is analytic there, and $\log|D(s)| = \log|\det S(s)|$. A little analysis reveals that

$$\begin{aligned} \log \det S(s) &= - \log \det [I + L(s)] \\ &= - \log [1 + \Sigma(\text{products of } L_{ij}(s))] \quad . \end{aligned} \tag{C.3}$$

The fact that (5.24) is satisfied implies that the $\Sigma(\cdot)$ term on the right-hand side of (C.3) goes to zero as $\omega \to \infty$. In particular, there exists a frequency ω_1 such that $|\Sigma(\cdot)| < 1$ for $\omega > \omega_1$. At these frequencies (C.3) has the power series expansion

$$\log \det S(s) = - \Sigma(\cdot) + \frac{\Sigma^2(\cdot)}{2} + \text{higher order terms.} \tag{C.4}$$

Thus, $\omega \log|\det S(j\omega)|$ also approaches zero as $\omega \to \infty$. At this point the proof of Theorem 3.3 may be followed to yield the result. ∎

<u>Proof of Corollary 5.2</u>: Follows from the fact that

$$|\det S(s)| = \prod_{i=1}^{n} \sigma_i[S(j\omega)] \quad .$$ ∎

Note that a result similar to the Corollary in Chapter 3, Section 3.3 is available in the MIMO use. Suppose the design constraint

$$\bar{\sigma}[L(j\omega)] \leq \frac{M}{\omega^{1+k}} \leq \varepsilon < 1, \; \omega \geq \omega_c \tag{C.5}$$

is imposed, where $k > 0$ and $\frac{M}{\omega_c^{1+k}} = \varepsilon$. Then, straightforward manipulations yield, for all $\omega > \omega_c$;

$$\bar{\sigma}[S(j\omega)] = \frac{1}{\underline{\sigma}[I + L(j\omega)]}$$

$$\leq \frac{1}{1 - \bar{\sigma}[L(j\omega)]} \tag{C.6}$$

$$\bar{\sigma}[S(j\omega)] \leq \frac{1}{1 - \frac{M}{\omega^{1+k}}} \quad .$$

The proof of the Corollary in Appendix A can be followed to yield

$$\int_{\omega_c}^{\infty} \log \sigma_i[S(j\omega)] \leq \frac{\log[\frac{1}{1-\varepsilon}]\omega_c}{k} \quad . \tag{C.7}$$

APPENDIX D

CANONICAL ANGLES BETWEEN SUBSPACES

First, some facts about the angles between singular subspaces are stated and used to prove some identities involving the matrices $U_j^H V_i$. Denote the column spaces of U_i and V_i by $\mathfrak{U}_i$ and $\mathfrak{V}_i$, respectively. Then, from (8.1), $\mathfrak{U}_1$ and $\mathfrak{V}_1$ are k-dimensional subspaces of $\mathbb{C}^n$. From [36 and 59, Theorem 2.3] it follows that there exist unitary matrices

$$\hat{U} = [\hat{U}_1 \mid \hat{U}_2] \text{ and } \hat{V} = [\hat{V}_1 \mid \hat{V}_2]$$

such that the columns of U_i and V_i span $\mathfrak{U}_i$ and $\mathfrak{V}_i$, respectively, and so that (assuming $2k \leq n$):

$$U^H V = \begin{bmatrix} U_1^H V_1 & U_1^H V_2 \\ U_2^H V_1 & U_2^H V_2 \end{bmatrix} = \left[\begin{array}{c|cc} \bar{C} & \bar{S} & 0 \\ \hline -\bar{S} & \bar{C} & 0 \\ 0 & 0 & I_{n-2k} \end{array}\right] . \tag{D.1}$$

(If $2k > n$, then the identity block appears in the upper left hand corner.) The matrices $\bar{C} = \mathrm{diag}[\cos\alpha_i]$ and $\bar{S} = \mathrm{diag}[\sin\alpha_i]$, $i=1,\ldots,k$, contain the cosines and sines of the canonical angles between the subspaces $\mathfrak{U}_1$ and $\mathfrak{V}_1$. The canonical angles between subspaces are characterized as follows.

<u>Definition D.1</u>: [36] Let $\mathfrak{U}$ and $\mathfrak{V}$ be subspaces of $\mathbb{C}^n$ with

$$d_U \triangleq \dim \mathfrak{U} \geq d_V \triangleq \dim \mathfrak{V} \geq 1 \quad . \tag{D.2}$$

The canonical angles $\phi_m \in [0,\pi/2]$ between $\mathfrak{U}$ and $\mathfrak{V}$ are defined for $m=1,\ldots,d_V$ by

$$\cos\phi_m = \max_{u \in \mathfrak{U}} \max_{v \in \mathfrak{V}} |u^H v| = u_m^H v_m \tag{D.3}$$

with $\|u\|_2 = 1$, $\|v\|_2 = 1$ and subject to the constraints

$$u_i^H u = 0 \ , \ v_i^H v = 0 \qquad i=1,\ldots,m-1 \quad .$$

The vectors u_m and v_m, $m=1,\ldots,q$ are called the canonical vectors of the pair of subspaces. ■

<u>Remarks</u>:

(1) The canonical angles are uniquely defined; the canonical vectors, however, in general, are not.

(2) With the above numbering, ϕ_1 is the largest canonical angle and is computed from $\cos\phi_1 = \max\limits_{u \in \mathfrak{U}} \max\limits_{u \in \mathfrak{V}} u^H v$, with $\|u\|_2 = \|v\|_2 = 1$.

(3) The vectors $\{v_i;\ i=1,\ldots,d_V\}$ form an orthonormal basis for $\mathfrak{V}$. The vectors $\{u_i;\ i=1,\ldots,d_V\}$ may be augmented with $d_U - d_V$ vectors so that the expanded set $\{u_i;\ i=1,\ldots,d_U\}$ forms an orthonormal basis for $\mathfrak{U}$. In [36] it is claimed that the condition

$$u_i^H v_j \ , \ i \neq j;\ i=1,\ldots,d_U;\ j=1,\ldots,d_V \tag{D.4}$$

holds. ■

Note that k of the canonical angles between the subspaces $\mathfrak{U}_2$ and $\mathfrak{V}_2$ are the same as those between $\mathfrak{U}_1$ and $\mathfrak{V}_1$. In addition there are guaranteed to exist n-2k angles equal to zero. This follows since the assumption $2k \le n$ implies that the dimension of $\mathfrak{U}_2 \cap \mathfrak{V}_2$ is at least n-2k.

Since the columns of U_i and $\hat{U}_i$ both span $\mathfrak{U}_i$, there exist unitary matrices P_i such that

$$[U_1 \mid U_2] = [\hat{U}_1 \mid \hat{U}_2] \begin{bmatrix} P_1^H & 0 \\ 0 & P_2^H \end{bmatrix} \qquad \begin{array}{l} P_1 \in \mathbb{C}^{k\times k} \\ P_2 \in \mathbb{C}^{(n-k)\times(n-k)} \end{array} \tag{D.5}$$

Similarly there exist Q_i such that

$$[V_1 \mid V_2] = [\hat{V}_1 \mid \hat{V}_2] \begin{bmatrix} Q_1^H & 0 \\ 0 & Q_2^H \end{bmatrix} \qquad \begin{array}{l} Q_1 \in \mathbb{C}^{k\times k} \\ Q_2 \in \mathbb{C}^{(n-k)\times(n-k)} \end{array} . \tag{D.6}$$

Equations (D.1), (D.5) and (D.6) may be used to obtain expressions for the singular value decompositions of the matrices $U_i^H V_j$. Simple calculations yield

$$U^H V = \begin{bmatrix} U_1^H V_1 & U_1^H V_2 \\ U_2^H V_1 & U_2^H V_2 \end{bmatrix}$$

$$\left[\begin{array}{c|c} P_1 \bar{C} Q_1^H & P_1 [\bar{S} \quad 0] Q_2^H \\ \hline P_2 \begin{bmatrix} -\bar{S} \\ 0 \end{bmatrix} Q_1^H & P_2 \begin{bmatrix} \bar{C} & 0 \\ 0 & I \end{bmatrix} Q_2^H \end{array}\right] . \tag{D.7}$$

The singular value decomposition (SVD) of $U_j^H V_i$ is the (i,j)-th block of (D.7).

The SVD's of $U_i^H V_j$ can be used to derive, through straightforward manipulations, the following identities:

$$-(U_1^H V_1)^{-1}(U_1^H V_2) = (V_1^H U_2)(V_2^H U_2)^{-1} \qquad (D.8)$$

$$(U_2^H V_1)(U_1^H V_1)^{-1} = -(V_2^H U_2)^{-1}(V_2^H U_1) \qquad (D.9)$$

$$(U_2^H V_2) + (U_2^H V_1)(V_1^H U_2)(V_2^H U_2)^{-1} = (V_2^H U_2)^{-1} . \qquad (D.10)$$

Finally, it is easy to verify that the singular values of the matrix products on either side of (D.8) and (D.9) are equal to the tangents of the canonical angles.

<u>Lemma D.1</u>: Assume that $\det[U_2^H V_2] \neq 0$. Then

$$I - U_2(V_2^H U_2)^{-1} V_2^H = V_1(U_1^H V_1)^{-1} U_1^H \qquad . \qquad (D.11)$$

■

<u>Proof</u>: Note the fact that $\det[U_2^H V_2] \neq 0$ implies that $\det[U_1^H V_1] \neq 0$. Now

$$\begin{aligned} I - U_2(V_2^H U_2)^{-1} V_2^H &= I - [V_1 V_1^H + V_2 V_2^H] U_2 (V_2^H U_2)^{-1} V_2^H \\ &= I - V_1(V_1^H U_2)(V_2^H U_2)^{-1} V_2 - V_2 V_2^H \\ &= V_1 V_1^H - V_1(V_1^H U_2)(V_2^H U_2)^{-1} V_2^H \qquad . \end{aligned}$$

Using (D.8) yields

$$\begin{aligned} I - U_2(V_2^H U_2)^{-1} V_2^H &= V_1 V_1^H + V_1(U_1^H V_1)^{-1}(U_1^H V_2) V_2^H \\ &= V_1(U_1^H V_1)^{-1}(U_1^H V_1) V_1^H + V_1(U_1^H V_1)^{-1}(U_1^H V_2) V_2^H \\ &= V_1(U_1^H V_1)^{-1} U_1^H \qquad . \end{aligned}$$

■

APPENDIX E

PROOFS OF THEOREMS IN CHAPTER 8

Proof of Lemma 8.2: Condition (8.13) implies that $\underline{\sigma}[U_1^H V_1 \Sigma_1] >> 1$ which, from (8.7a), implies that A^{-1} exists and

$$\begin{aligned} A^{-1} &= (I + U_1 V_1 \Sigma_1)^{-1} \\ &\approx \Sigma_1^{-1}(U_1^H V_1)^{-1} \quad . \end{aligned} \tag{E.1}$$

Using this approximation in (8.7b-d) yields

$$B \approx \Sigma_1^{-1}(U_1^H V_1)^{-1} U_1^H V_2 \Sigma_2 \tag{E.2}$$

$$C \approx I + [U_2^H V_2 - U_2^H V_1 (U_1^H V_1)^{-1} U_1^H V_2] \Sigma_2 \tag{E.3}$$

$$D \approx U_2^H V_1 (U_1^H V_1)^{-1} \tag{E.4}$$

Using (D.10) in (E.3) yields

$$C \approx (V_2^H U_2)^{-1} [V_2^H U_2 + \Sigma_2] \quad . \tag{E.5}$$

Using the above approximations to (A)-(D) in (8.6) yields (8.14):

$$\tilde{S}_{11} \approx \Sigma_1^{-1}(U_1^H V_1)^{-1}[I + U_1^H V_2 \Sigma_2 (V_2^H U_2 + \Sigma_2)^{-1} (V_2^H U_2)(U_2^H V_1)(U_1^H V_1)^{-1}] \ . \tag{E.6}$$

Using (D.9) in (E.6) yields (8.14a)

$$\tilde{S}_{12} \approx -\Sigma_1^{-1}(U_1^H V_1)^{-1} U_1^H V_2 \Sigma_2 (V_2^H U_2 + \Sigma_2)^{-1} V_2^H U_2 \tag{E.7}$$

$$\tilde{S}_{21} \approx -(V_2^H U_2 + \Sigma_2)^{-1} (V_2^H U_2)(U_2^H V_1)(U_1^H V_1)^{-1} \quad . \tag{E.8}$$

Using (D.9) in (E.8) yields (8.14c)

$$\tilde{S}_{22} \approx (V_2^H U_2 + \Sigma_2)^{-1}(V_2^H U_2) \quad .$$

■

<u>Proof of Theorem 8.3</u>: Approximation (8.15a) follows from (8.14) by requiring that

$$\underline{\sigma}[\Sigma_1] >> \bar{\sigma}\{(U_1^H V_1)^{-1}[I - (U_1^H V_2)\Sigma_2(V_2^H U_2 + \Sigma_2)^{-1}(V_2^H U_1)]\} \tag{E.9}$$

and

$$\underline{\sigma}[\Sigma_1] >> \bar{\sigma}\{(U_1^H V_1)^{-1}(U_1^H V_2)\Sigma_2(V_2^H U_2 + \Sigma_2)^{-1}(V_2^H U_2)\} \tag{E.10}$$

so that $\tilde{S}_{11} \approx 0$ and $\tilde{S}_{12} \approx 0$. Using the resulting approximations to $\tilde{S}$ and transforming into standard coordinates yields (8.15b)

$$S \approx U_2(V_2^H U_2 + \Sigma_2)^{-1}(V_2^H U_1)U_1^H + U_2(V_2^H U_2 + \Sigma_2)^{-1}(V_2^H U_2)U_2^H \quad .$$

Using the identity $U_1U_1^H + U_2U_2^H = I$ yields (8.15a) and the identity $V_1V_1^H + V_2V_2^H = I$ yields (8.15c).

Approximation (8.16a) follows from

$$T \approx T_{app} \triangleq I - U_2(V_2^H U_2 + \Sigma_2)^{-1}V_2^H \quad .$$

Note that

$$V_2^H U_2(V_2^H U_2 + \Sigma_2)^{-1} + \Sigma_2(V_2^H U_2 + \Sigma_2)^{-1} = I \tag{E.11}$$

$$\Rightarrow \quad (V_2^H U_2 + \Sigma_2)^{-1} + (V_2^H U_2)^{-1}\Sigma_2(V_2^H U_2 + \Sigma_2)^{-1} = (V_2^H U_2)^{-1}$$

$$\Rightarrow \quad T_{app} = I - U_2(V_2^H U_2)^{-1}V_2^H + U_2(V_2^H U_2)^{-1}\Sigma_2(V_2^H U_2 + \Sigma_2)^{-1}V_2^H \quad .$$

Using Lemma D.1

$$T_{app} = V_1(U_1{}^HV_1)^{-1}U_1{}^H + U_2(V_2{}^HU_2)^{-1}\Sigma_2(V_2{}^HU_2 + \Sigma_2)^{-1}V_2{}^H$$

which is the desired result.

To obtain (8.16b) note

$$T_{app} = V_1(U_1{}^HV_1)^{-1}\ [(U_1{}^HV_1)V_1{}^H + (U_1{}^HV_2)V_2{}^H]$$
$$+ [V_1(V_1{}^HU_2) + V_2(V_2{}^HU_2)]\ (V_2{}^HU_2)^{-1}\Sigma_2(V_2{}^HU_2 + \Sigma_2)^{-1}V_2{}^H$$

$$\begin{aligned} T_{app} &= V_1V_1{}^H + V_2\Sigma_2(V_2{}^HU_2 + \Sigma_2)^{-1}V_2{}^H \\ &+ V_1[(U_1{}^HV_1)^{-1}(U_1{}^HV_2) + (V_1{}^HU_2)(V_2{}^HU_2)^{-1}\Sigma_2(V_2{}^HU_2 + \Sigma_2)^{-1}]V_2{}^H\ . \end{aligned} \tag{E.12}$$

Using (E.11) in (E.12) yields

$$\begin{aligned} T_{app} &= V_1V_1{}^H + V_2\Sigma_2(V_2{}^HU_2 + \Sigma_2)^{-1}V_2{}^H \\ &+ V_1[(U_1{}^HV_1)^{-1}(U_1{}^HV_2) + (V_1{}^HU_2)(V_2{}^HU_2)^{-1} - (V_1{}^HU_2) \\ &\cdot (V_2{}^HU_2 + \Sigma_2)^{-1}]V_2{}^H\ . \end{aligned} \tag{E.13}$$

Using (D.8) in (E.13) yields the result. Expression (8.16c) is obtained similarly. ■

<u>Proof of Theorem 8.1</u>: First note that (8.9) implies $(V_2{}^HU_2 + \Sigma_2)^{-1} \approx (V_2{}^HU_2)^{-1}$. Using this approximation in (8.15a) yields (8.10a). Expressions (8.10b) and (8.10c) follow easily. Using (D.11) in (8.10a) yields (8.11a) from which (8.11b) and (8.11c) follow easily. ■

Proof of Lemma 8.4: It may easily be verified that an alternate expression for $\tilde{S}$ is given by (assuming E^{-1} and G^{-1} exist):

$$\tilde{S} = \begin{bmatrix} G^{-1} & -G^{-1}H \\ -FG^{-1} & E^{-1} + FG^{-1}H \end{bmatrix} \tag{E.14}$$

where

$$E = I + U_2^H V_2 \Sigma_2 \tag{E.15a}$$

$$F = (I + U_2^H V_2 \Sigma_2)^{-1}(U_2^H V_1 \Sigma_1) \tag{E.15b}$$

$$G = I + U_1^H V_1 \Sigma_1 - (U_1^H V_2 \Sigma_2)(I + U_2^H V_2 \Sigma_2)^{-1}(U_2^H V_1 \Sigma_1) \tag{E.15c}$$

$$H = (U_1^H V_2 \Sigma_2)(I + U_2^H V_2 \Sigma_2)^{-1} \quad . \tag{E.15d}$$

Condition (8.19) implies that $(I + U_2^H V_2 \Sigma_2)^{-1}$ exists and

$$E \approx I \tag{E.16a}$$

$$F \approx U_2^H V_1 \Sigma_1 \tag{E.16b}$$

$$G \approx I + U_1^H V_1 \Sigma_1 - (U_1^H V_2 \Sigma_2)(U_2^H V_2 \Sigma_2) \tag{E.16c}$$

$$H \approx U_1^H V_2 \Sigma_2 \quad . \tag{E.16d}$$

The approximations (E.16) imply that (8.20) holds. ∎

Proof of Theorem 8.5: From (8.20) it follows that if $\bar{\sigma}[\Sigma_2]$ is sufficiently small, then the appropriate inverses exist and

$$\tilde{S}_{11} \approx (I + U_1^H V_1 \Sigma_1)^{-1} \tag{E.17a}$$

$$\tilde{S}_{12} \approx 0 \tag{E.17b}$$

$$\tilde{S}_{21} \approx -(U_2^H V_1 \Sigma_1)(I + U_1^H V_1 \Sigma_1)^{-1} \quad \text{(E.17c)}$$

$$\tilde{S}_{22} \approx I \quad \text{(E.17d)}$$

From (E.17) the matrix S is given in standard coordinates by

$$S \approx U_1(I + U_1^H V_1 \Sigma_1)^{-1} U_1^H - U_2(U_2^H V_1 \Sigma_1)(I + U_1^H V_1 \Sigma_1)^{-1} U_1^H + U_2 U_2^H \quad \text{(E.18)}$$

which implies

$$T \approx U_1 U_1^H - U_1(I + U_1^H V_1 \Sigma_1)^{-1} U_1^H + U_2(U_2^H V_1 \Sigma_1)(I + U_1^H V_1 \Sigma_1)^{-1} U_1^H \quad . \quad \text{(E.19)}$$

Note that

$$I - (I + U_1^H V_1 \Sigma_1)^{-1} = U_1^H V_1 \Sigma_1 (I + U_1^H V_1 \Sigma_1)^{-1} \quad . \quad \text{(E.20)}$$

Using (E.20) in (E.19) yields

$$T \approx U_1(U_1^H V_1)\Sigma_1(I + U_1^H V_1 \Sigma_1)^{-1} U_1^H + U_2(U_2^H V_1 \Sigma_1)(I + U_1^H V_1 \Sigma_1)^{-1} U_1^H \quad \text{(E.21)}$$

or

$$T \approx V_1 \Sigma_1 (I + U_1^H V_1 \Sigma_1)^{-1} U_1^H \quad \text{(E.22)}$$

from which (8.22b) and (8.22c) easily follow. To obtain (8.21a) from (8.22a) define

$$S_{app} \triangleq I - V_1 \Sigma_1 (I + U_1^H V_1 \Sigma_1)^{-1} U_1^H \quad \text{(E.23)}$$

and note

$$U_1^H V_1 \Sigma_1 (I + U_1^H V_1 \Sigma_1)^{-1} + (I + U_1^H V_1 \Sigma_1)^{-1} = I \tag{E.24}$$

$$\Rightarrow \quad \Sigma_1 (I + U_1^H V_1 \Sigma_1)^{-1} + (U_1^H V_1)^{-1} (I + U_1^H V_1 \Sigma_1)^{-1} = (U_1^H V_1)^{-1} \tag{E.25}$$

$$S_{app} = I - V_1 (U_1^H V_1)^{-1} U_1^H + V_1 (U_1^H V_1)^{-1} (I + U_1^H V_1 \Sigma_1)^{-1} U_1^H \quad . \tag{E.26}$$

Using (D.11) in (E.26) yields

$$S_{app} = U_2 (V_2^H U_2)^{-1} V_2^H + V_1 (U_1^H V_1)^{-1} (I + U_1^H V_1 \Sigma_1)^{-1} U_1^H \quad . \tag{E.27}$$

To obtain (8.21b) note

$$S_{app} = U_2 (V_2^H U_2)^{-1} [(V_2^H U_1) U_1^H + (V_2^H U_2) U_2^H] + [U_1 (U_1^H V_1) + U_2 (U_2^H V_1)] \cdot (U_1^H V_1)^{-1} (I + U_1^H V_1 \Sigma_1)^{-1} U_1^H ,$$

or

$$S_{app} = U_2 U_2^H + U_1 (I + U_1^H V_1 \Sigma_1)^{-1} U_1^H + U_2 [(V_2^H U_2)^{-1} (V_2^H U_1) + (U_2^H V_1)(U_1^H V_1)^{-1} \cdot (I + U_1^H V_1 \Sigma_1)^{-1}] U_1^H \quad . \tag{E.28}$$

Using (E.24) in (E.28) yields

$$\begin{aligned} S_{app} = {} & U_2 U_2^H + U_1 (I + U_1^H V_1 \Sigma_1)^{-1} U_1^H \\ & + U_2 [(V_2^H U_2)^{-1} (V_2^H U_1) + (U_2^H V_1)(U_1^H V_1)^{-1} \\ & - (U_2^H V_1) \Sigma_1 (I + U_1^H V_1 \Sigma_1)^{-1}] U_1^H \quad . \end{aligned}$$

From (D.9) it follows that

$$S_{app} = U_2U_2^H + U_1(I + U_1^HV_1\Sigma_1)^{-1}U_1^H - U_2(U_2^HV_1)\Sigma_1(I + U_1^HV_1\Sigma_1)^{-1}U_1^H \quad .$$

From which (8.21b) follows.

To derive (8.21c) from (E.27) first note

$$\begin{aligned}(U_1^HV_1)^{-1}(I + U_1^HV_1\Sigma_1)^{-1} &= [(I + U_1^HV_1\Sigma_1)(U_1^HV_1)]^{-1} \\ &= [(U_1^HV_1)(I + \Sigma_1U_1^HV_1)]^{-1} \\ &= (I + \Sigma_1U_1^HV_1)^{-1}(U_1^HV_1)^{-1} \quad . \end{aligned} \tag{E.29}$$

Using (E.29) in (E.27) yields

$$\begin{aligned} S_{app} &= U_2(V_2^HU_2)^{-1}V_2^H + V_1(I + \Sigma_1U_1^HV_1)^{-1}(U_1^HV_1)^{-1}U_1^H \\ &= [V_1(V_1^HU_2) + V_2(V_2^HU_2)](V_2^HU_2)^{-1}V_2^H \\ &\quad + V_1(I + \Sigma_1U_1^HV_1)^{-1}(U_1^HV_1)^{-1}[(U_1^HV_1)V_1^H + (U_1^HV_2)V_2^H] \\ &= V_2V_2^H + V_1(I + \Sigma_1U_1^HV_1)^{-1}V_1^H \\ &\quad + V_1[(V_1^HU_2)(V_2^HU_2)^{-1} + (I + \Sigma_1U_1^HV_1)^{-1}(U_1^HV_1)^{-1}(U_1^HV_2)]V_2^H \quad . \end{aligned} \tag{E.30}$$

Using the identity

$$(I + \Sigma_1U_1^HV_1)^{-1} = I - (I + \Sigma_1U_1^HV_1)^{-1}\Sigma_1U_1^HV_1$$

yields

$$\begin{aligned} S_{app} &= V_2V_2^H + V_1(I + \Sigma_1U_1^HV_1)^{-1}V_1^H \\ &\quad + V_1[(V_1^HU_2)(V_2^HU_2)^{-1} + (U_1^HV_1)^{-1}(U_1^HV_2) - (I + \Sigma_1U_1^HV_1)^{-1}\Sigma_1U_1^HV_2]V_2^H \quad . \end{aligned}$$

From (D.8) it follows that

$$S_{app} = V_2V_2^H + V_1(I + \Sigma_1U_1^HV_1)^{-1}V_1^H$$
$$- V_1[(I + \Sigma_1U_1^HV_1)^{-1}\Sigma_1U_1^HV_2]V_2^H$$

which is the desired result. ∎

APPENDIX F

COUNTEREXAMPLE TO CONJECTURE THAT LOG σ IS HARMONIC

Let

$$M(s) = \begin{bmatrix} s & 0 \\ 2 & s \end{bmatrix} . \tag{F.1}$$

Then the singular values of M(s) are the nonnegative square roots of the eigenvalues of

$$[M(s)]^H M(s) = \begin{bmatrix} \bar{s} & 2 \\ 0 & \bar{s} \end{bmatrix} \begin{bmatrix} s & 0 \\ 2 & s \end{bmatrix}$$

$$= \begin{bmatrix} |s|^2 + 4 & 2s \\ 2\bar{s} & |s|^2 \end{bmatrix} \tag{F.2}$$

$$\det[\lambda I - [M(s)]^H M(s)] =$$

$$\lambda^2 - 2(|s|^2 + 2)\lambda + |s|^4 = 0$$

$$\Rightarrow \quad \lambda_{1,2} = |s|^2 + 2 \pm 2\sqrt{|s|^2 + 1} \tag{F.3}$$

$$\Rightarrow \quad \sigma_1 = 1 + \sqrt{|s|^2 + 1}$$

$$\sigma_2 = -1 + \sqrt{|s|^2 + 1} .$$

Define

$$\gamma \triangleq |s|^2 = x^2 + y^2 . \tag{F.4}$$

Then, (F.3) yields

$$\sigma_1 = 1 + \sqrt{\gamma + 1}$$
$$\sigma_2 = -1 + \sqrt{\gamma + 1} \quad . \tag{F.5}$$

Dropping the subscript on σ:

$$\frac{\partial^2 \log\sigma}{\partial x^2} = \frac{\partial}{\partial x}\left[\frac{1}{\sigma}\frac{\partial\sigma}{\partial x}\right]$$
$$= \frac{-1}{\sigma^2}\left(\frac{\partial\sigma}{\partial x}\right)^2 + \frac{1}{\sigma}\left(\frac{\partial^2\sigma}{\partial x^2}\right) \quad .$$
$$\frac{\partial^2 \log\sigma}{\partial x^2} = \frac{1}{\sigma^2}\left[\sigma\,\frac{\partial^2\sigma}{\partial x^2} - \left(\frac{\partial\sigma}{\partial x}\right)^2\right] \tag{F.6}$$
$$\frac{\partial^2 \log\sigma}{\partial y^2} = \frac{1}{\sigma^2}\left[\sigma\,\frac{\partial^2\sigma}{\partial y^2} - \left(\frac{\partial\sigma}{\partial y}\right)^2\right] \quad ,$$

so that

$$\nabla^2 \log\sigma \triangleq \frac{\partial^2 \log\sigma}{\partial x^2} + \frac{\partial^2 \log\sigma}{\partial y^2}$$
$$= \frac{1}{\sigma^2}\left[\sigma\left(\frac{\partial^2\sigma}{\partial x^2} + \frac{\partial^2\sigma}{\partial y^2}\right) - \left(\frac{\partial\sigma}{\partial x}\right)^2 - \left(\frac{\partial\sigma}{\partial y}\right)^2\right] \quad . \tag{F.7}$$

From (F.5)

$$\frac{\partial\sigma_1}{\partial x} = \frac{\partial\sigma_2}{\partial x} = \frac{x}{\sqrt{\gamma + 1}}$$
$$\frac{\partial\sigma_1}{\partial y} = \frac{\partial\sigma_2}{\partial y} = \frac{y}{\sqrt{\gamma + 1}} \qquad \text{(F.8)}$$

$$\Rightarrow \quad \left(\frac{\partial\sigma_1}{\partial x}\right)^2 = \left(\frac{\partial\sigma_2}{\partial x}\right)^2 = \frac{x^2}{\gamma + 1}$$
$$\left(\frac{\partial\sigma_1}{\partial y}\right)^2 = \left(\frac{\partial\sigma_2}{\partial y}\right)^2 = \frac{y^2}{\gamma + 1} . \qquad \text{(F.9)}$$

From (F.8)

$$\frac{\partial^2\sigma_1}{\partial x^2} = \frac{\partial^2\sigma_2}{\partial x^2} = \frac{1}{\gamma + 1}\left[\sqrt{\gamma + 1} - \frac{x^2}{\sqrt{\gamma + 1}}\right]$$
$$\frac{\partial^2\sigma_1}{\partial y^2} = \frac{\partial^2\sigma_2}{\partial y^2} = \frac{1}{\gamma + 1}\left[\sqrt{\gamma + 1} - \frac{y^2}{\sqrt{\gamma + 1}}\right] . \qquad \text{(F.10)}$$

Also,

$$\sigma_1\left(\frac{\partial^2\sigma_1}{\partial x^2}\right) = \frac{1}{\gamma + 1}\left[\gamma + 1 + \sqrt{\gamma + 1} - \frac{1 + \sqrt{\gamma + 1}}{\sqrt{\gamma + 1}}(x^2)\right]$$
$$\sigma_1\left(\frac{\partial^2\sigma_1}{\partial y^2}\right) = \frac{1}{\gamma + 1}\left[\gamma + 1 + \sqrt{\gamma + 1} - \frac{1 + \sqrt{\gamma + 1}}{\sqrt{\gamma + 1}}(y^2)\right] . \qquad \text{(F.11)}$$

Define

$$K_1 \triangleq \frac{1}{\sigma_1^{\,2}(\gamma + 1)} \qquad \text{(F.12)}$$

Then, combining (F.7), (F.9) and (F.11) yields

$$\frac{\partial^2 \log\sigma_1}{\partial x^2} + \frac{\partial^2 \log\sigma_1}{\partial y^2} = K_1[2(\gamma + 1 + \sqrt{\gamma + 1}\,) - \frac{1 + \sqrt{\gamma + 1}}{\sqrt{\gamma + 1}}(x^2 + y^2)$$

$$- (x^2 + y^2)]$$

$$= K_1\left[\frac{\gamma + 2 + 2\sqrt{\gamma + 1}}{\sqrt{\gamma + 1}}\right] \tag{F.13}$$

$$= K_1\left[\frac{\sigma_1{}^2}{\sqrt{\gamma + 1}}\right]$$

$$\nabla^2 \log\sigma_1 = \left(\frac{1}{\sqrt{|s|^2 + 1}}\right)^3 \quad .$$

Similarly,

$$\nabla^2 \log\sigma_2 = -\left(\frac{1}{\sqrt{|s|^2 + 1}}\right)^3 \quad . \tag{F.14}$$

APPENDIX G

DIFFERENTIABILITY OF SINGULAR VALUES AND VECTORS

In this Appendix, various results concerning the differentiability properties of singular values and vectors are presented. These results are based upon properties of eigenvalues and eigenvectors of Hermitian matrices; these properties are discussed extensively in Kato [32]. There is some overlap between this Appendix and earlier results by Freudenberg, Looze and Cruz [10] and MacFarlane and Hung [60]. This overlap will be pointed out in the discussion.

Singular values are by definition real valued functions of the complex frequency variable $s = x + jy$. It follows [48] that they cannot be even locally analytic in this variable. Recall one characterization of analytic functions is the existence, at each point in the domain of analyticity, of a convergent power series expansion with nonzero radius of convergence [48]. Lack of analyticity implies the nonexistence of a power series expansion in s; however, it can be shown that such an expansion exists in the two separate variables x and y. This, in turn, shows that singular values are analytic in these two variables. This fact was pointed out by MacFarlane and Hung [60]. The results of [60] concerned only analyticity, however, and were limited to the case of distinct singular values. This is inconvenient when studying properties of repeated singular values. In particular, the present motivation for discussing analyticity in the two variables is that analyticity implies the existence and continuity of partial derivatives of all orders. The converse is not

true, however, and the present results can be used to discuss existence of partial derivatives even for multiple singular values for which no power series expansion is possible. First some definitions will be presented.

Definition G.1: A function f defined in a neighborhood of a point $x=(x_1,x_2)\in\mathbb{R}^2$ is of class C^k at (x,y) if the kth order partial derivatives $\frac{\partial^k f}{\partial x_1^{a_1}\partial x_2^{a_2}}$, $a_1+a_2=k$, exist and are continuous at x. Functions in C^k are said to be k-times continuously differentiable. ∎

Definition G.2 [61, p. 2]: A complex-valued function f defined on an open subset $D\subseteq\mathbb{C}^2$ is analytic in D if each point $w=(w_1,w_2)\in D$ has an open neighborhood N, $w\in N\subseteq D$, such that the function f has a power series expansion

$$f(z) = \sum_{k,\ell=0}^{\infty} c_{k\ell}\,(z_1-\omega_1)^k(z_2-\omega_2)^\ell \tag{G.1}$$

which converges for all $z=(z_1,z_2)\in N$. ∎

Definition G.3: A complex valued function f defined on a neighborhood of a point $w=(w_1,w_2)\in\mathbb{C}^2$ is analytic at w if there exists an open neighborhood N, $w\in N\subseteq D$, such that the function f has a power series expansion (G.1) at w which converges for all $z\in N$. ∎

Thus, a singular value σ_i is analytic at (x_o,y_o) provided σ_i has a power series expansion

$$\sigma_i(x,y) = \sum_{k,\ell=0}^{\infty} c_{k\ell}\,(x-x_o)^k(y-y_o)^\ell \tag{G.2}$$

which converges for all (x,y) in a neighborhood of (x_o,y_o) in $\mathbb{C}^2$. Note that for real values of (x,y) and (x_o,y_o) the series (G.2) sums to the

value of $\sigma_i[M(s = x + jy)]$, where $M(s)$ is the matrix being studied. This fact implies that the $c_{k\ell}$ are real numbers.

Given the expansion (G.2), the partial derivatives at (x_o, y_o) with respect to x and y may be determined from the $c_{k\ell}$. Even if an expansion (G.2) does not exist, however, the partial derivatives may still exist and be continuous. Results will also be presented for the singular projections and singular vectors.

Definition G.4: Let $\mathfrak{U}_i(s)$ be a right singular subspace of $M(s)$. (Note $\mathfrak{U}_i(s)$ is not necessarily one-dimensional.) The orthogonal projection [32, p.57] onto $\mathfrak{U}_i(s)$ is denoted by P_{u_i} and is termed the singular projection onto the subspace $\mathfrak{U}_i$. Similarly, P_{v_i} will denote the singular projection onto the left singular subspace $\mathfrak{V}_i$. ∎

Theorem G.5: Let $M(s)$ be a matrix taking values in $\mathbb{C}^{n\times n}$ whose elements are functions of the complex variable $s = x + jy$. Let $D \in \mathbb{C}$ be a simply connected region of the complex plane. Assume that:

(i) For all $s \in D$ each element $M_{ij}(s)$ is analytic in s.

(ii) The number of distinct singular values is constant in D.

Note this implies that the singular values of $M(s)$ can be ordered so that $\sigma_1[M(s)] \geq \sigma_2[M(s)] \geq \dots \geq \sigma_n[M(s)]$ for all $s \in D$. Moreover, if two singular values are equal at any point of D they are equal $\forall s \in D$.

If (i) and (ii) are satisfied, then at each point $s_o = x_o + jy_o \in D$:

(1) If $\sigma_i[M(s_o)] \neq 0$, then σ_i is of class C^∞. That is, partial derivatives of all orders exist and are continuous.

(2) Each right and left singular projection is of class C^∞.

Let condition (ii) be replaced by:

(ii)' The singular values of $M(s)$ are distinct for all $s \in D$.

If (i) and (ii)' are satisfied, then at each point $s_o = x_o + jy_o \in D$:

(1)' If $\sigma_i[M(s_o)] \neq 0$, then σ_i has an expansion of the form (G.2) and is thus analytic in the sense of Definition G.3.

(2)' Each right and left singular projection is analytic. ∎

Proof: At each point $s_o = x_o + jy_o \in D$ it follows from (i) that M(s) has a power series expansion

$$M(s) = \sum_{i=0}^{\infty} M_i (s-s_o)^i \quad . \tag{G.3}$$

Now, consider M as a function of the two variables x and y, where these variables may assume complex values. It will now be shown that M(x,y) is analytic in (x,y) at (x_o, y_o).

Note that (G.3) shows M(x,y) is continuous in x and y. By Osgood's Lemma [61, p. 2] it follows that if M(x,y) is analytic in x and y separately, then M(x,y) is analytic in (x,y). First, setting $y = y_o$ in (G.3) yields a power series expansion in x:

$$M(x,y_o) = \sum_{i=0}^{\infty} \tilde{M}_i (x-x_o)^i \quad . \tag{G.4}$$

This power series has a nonzero radius of convergence since: (a) the series (G.3) has radius of convergence $R > 0$; (b) the series (G.4) converges for real values of x with $|x-x_o| < R$; (c) by Theorem 1.3, Chapter III of Conway [48] it follows that $M(x,y_o)$ in fact converges for all complex values of x with $|x-x_o| < R$. Thus M(x,y) is analytic in x at (x_o,y_o). A similar argument shows that M(x,y) is analytic in y at (x_o,y_o). As remarked above, Osgood's Lemma then implies that M(x,y) is analytic in (x,y) at (x_o,y_o).

Define the matrix

$$\hat{M}(x,y) = \sum_{i=0}^{\infty} M_i^H (x - jy - s_o)^i \quad . \tag{G.5}$$

Note that for <u>real</u> values of x and y

$$\hat{M}(x,y) = [M(x,y)]^H \triangleq \overline{M^T(s)} \tag{G.6}$$

where "$\overline{\quad\quad}$" denotes complex conjugation. Thus, $\hat{M}$ is <u>not</u> analytic in s, yet $\hat{M}$ is analytic in (x,y) by the same argument used for M(x,y). This, of course, is a consequence of the definition of $\hat{M}$; the definition <u>does not</u> involve taking the complex conjugates of x or y.

Next, the matrices

$$M_R(x,y) \triangleq \hat{M}(x,y)M(x,y) \tag{G.7}$$

and

$$M_L(x,y) \triangleq M(x,y)\hat{M}(x,y) \tag{G.8}$$

are also analytic in (x,y). Moreover, the singular values of $M(s_o)$, $s_o = x_o + jy_o$, are the nonnegative square roots of the eigenvalues of $M_R(x_o,y_o)$ and $M_L(x_o,y_o)$; the right singular subspaces of $M(s_o)$ are the eigenspaces of M_R and the left singular subspaces are the eigenspaces of M_L.

To summarize, at each point $s_o = x_o + jy_o \in D$, the matrices $M_L(x,y)$ and $M_R(x,y)$ are analytic functions of (x,y) in some neighborhood N of $(x_o,y_o) \in \mathbb{R}^2$. Note this implies these matrices are C^∞ in x and y. By Kato [32, p. 134, Theorem 5.13a] the eigenvalues and eigenprojections of M_L and M_R are also C^∞ functions of (x,y) in the neighborhood N of (x_o,y_o). Note the

eigenprojections of M_L are the left singular projections of M and the eigenprojections of M_R are the right singular projections of M. This proves (2).

If $\sigma_i[M(s_o)] \neq 0$, then by continuity there exists a neighborhood $N' \subseteq N$ of (x_o,y_o) such that $\sigma_i[M(x,y)] \neq 0 \ \forall (x,y) \in N' \subseteq N$. Since $\sigma_i[M(x,y)] = +\sqrt{\lambda_i[M_R(x,y)]}$ $(= +\sqrt{\lambda_i[M_L(x,y)]})$, it follows that $\sigma_i[M(x,y)]$ is C^∞ in N'. This proves (1).

Now, suppose that (ii)' holds. Allow (x,y) to take values in $\mathbb{C}^2$ rather than $\mathbb{R}^2$. By continuity, (ii)' implies that the eigenvalues of $M_L(x,y)$ and $M_R(x,y)$ are distinct in some complex neighborhood of each point (x_o,y_o) with x_o and y_o real. Thus, by Kato [32, p. 134, Remark 5.13b] it follows that the eigenvalues and eigenprojections of M_L and M_R are analytic in (x,y). Conclusions (1)' and (2)' follow. ∎

The preceding theorem shows that, away from points where the number of distinct singular values changes, partial derivatives of all orders of the singular values exist and are continuous (in both x and y). Thus the computation of the partial derivative of a singular value which was performed in Chapter 9 can be rigorously justified. The above theorem also shows that the orthogonal projections onto the singular subspaces possess continuous partial derivatives of all orders. As pointed out earlier, the choice of singular vectors is not unique. Kato [32] and MacFarlane and Hung [60] each give a method for constructing singular vectors. First Kato's method will be discussed.

Let $\mathfrak{U}_i(x,y)$ be the right singular subspace of $M(s = x + jy)$ corresponding to the singular value $\sigma_i(x,y)$. Assume that σ_i satisfies (i) and (ii) or (ii)'. Then, there exists a right singular projection $P_{u_i}(x,y)$ satisfying (2) or (2)'. Let the columns of $U_i(x_o,y_o)$ be a set of right singular vectors; i.e., an orthonormal basis for $\mathfrak{U}_i(x_o,y_o)$. Then, [32, pp. 110-114], the columns of $U_i(x,y)$ defined by

$$U_i(x,y) = W(x,y)U_i(x_o,y_o)$$

$$W(x,y) = [I - (P_{u_i}(x,y) - P_{u_i}(x_o,y_o))^2]^{-1/2} \cdot \qquad \text{(G.9)}$$

$$\cdot\ [P_{u_i}(x,y)P_{u_i}(x_o,y_o) + (I - P_{u_i}(x,y))(I - P_{u_i}(x_o,y_o)]$$

are a set of right singular vectors spanning the right singular subspace $\mathfrak{U}_i(x,y)$. Note this formula is only guaranteed to be valid locally; this is because the condition

$$\|P_{u_i}(x,y) - P_{u_i}(x_o,y_o)\|_2 < 1 \qquad \text{(G.10)}$$

must be satisfied. This condition implies that the right singular subspace $\mathfrak{U}_i(x,y)$ can contain no vector orthogonal to the subspace $\mathfrak{U}_i(x_o,y_o)$. If (G.10) is satisfied then the square root in (G.9) is defined by [32, p. 34]

$$(I - A)^{-1/2} = \sum_{n=0}^{\infty} \binom{-1/2}{n} (-A)^n \qquad \text{(G.11)}$$

where

$$\binom{-1/2}{n} \triangleq \frac{(-\frac{1}{2})(-\frac{1}{2} - 1)\cdots(-\frac{1}{2} - (n-1))}{n!}$$
$$\binom{-1/2}{0} \triangleq 1 \qquad \text{(G.12)}$$

The set of singular vectors (G.9) is, of course, not unique; one can multiply $U_i(x,y)$ by any other unitary matrix which leaves the subspaces $\mathfrak{U}_i(x,y)$ and $\mathfrak{U}_i^{\perp}(x,y)$ invariant. If $\sigma_i[M(x_o,y_o)] \neq 0$, then a set of left singular vectors can be obtained from

$$V_i(x,y) = \frac{1}{\sigma_i(x,y)} M(x,y)U_i(x,y) \quad . \tag{G.13}$$

If (ii) is satisfied, then the singular vectors so defined are C^{∞}; if (ii)' is satisfied, the vectors are analytic in (x,y). This shows it is possible to choose these vectors to have continuous partial derivatives of all orders.

MacFarlane and Hung [60] propose a method for constructing singular vectors analytic in (x,y) when the singular value has multiplicity one. The construction is again valid only locally, although this is not pointed out in [60]. (The construction assumes a matrix in $\mathbb{C}^{\ell\times\ell}$ has ℓ-1 linearly independent rows and that these are the <u>first</u> ℓ-1 rows. This latter assumption can be made, without loss of generality, at a point, and continuity implies it holds in a neighborhood. However, a more general claim cannot be made. It appears that the same difficulty is present here as in the construction of Kato. Namely, the singular subspace $\mathfrak{U}_i(x,y)$ may become orthogonal to $\mathfrak{U}_i(x_o,y_o)$. In Chapter 10 the ability to construct a set of singular vectors which form a basis for a given singular subspace and which are continuous is studied. It is shown that, in general, this is possible only locally; thus, the deficiency in Kato's and MacFarlane and Hung's constructions cannot be overcome.)

An alternative approach to the construction of sets of singular vectors can be based on other results in Kato [32]. These results can be used to give singular vectors along a curve $\gamma(t) = x(t) + jy(t)$ in the complex plane. This construction is valid only along a path and not over an open set in the plane. However, the construction has other convenient features; no assumption similar to (G.10) need be made, and the number of distinct singular values is allowed to change.

While Theorem G.5 used no special properties of Hermitian matrices, the next result does; these properties are necessary to be able to treat points where the number of distinct singular values changes. These results were presented in [10] but are repeated here for completeness.

Theorem G.6: Let $M(s)$ be a matrix taking values in $\mathbb{C}^{n\times n}$ whose elements are functions of the complex variable $s = x + jy$. Let $\gamma(t) = x(t) + jy(t)$, $-\infty \leq t_1 \leq t \leq t_2 \leq +\infty$, be a curve in the complex plane. Assume that:

(i) $\gamma(t)$ is analytic in t; i.e., at each value of $t_o \in (t_1, t_2)$ there exists a power series expansion with nonzero radius of convergence

$$\gamma(t) = \sum_{i=0}^{\infty} c_i (t-t_o)^i \quad . \tag{G.14}$$

(ii) Each element $M_{ij}(s)$ is analytic in s at all points of the image of $\gamma(t)$. Let $t_o \in (t_1, t_2)$ and let $\sigma(t_o)$ be a nonzero singular value of $M[\gamma(t_o)]$ with multiplicity k. Then there exists an open neighborhood N such that $t_o \in N \subseteq (t_1, t_2)$ and analytic functions of t

$$\sigma_\ell : N \subseteq \mathbb{R} \to \mathbb{R}^+$$

$$u_\ell : N \subseteq \mathbb{R} \to \mathbb{C}^n$$

$$v_\ell : N \subseteq \mathbb{R} \to \mathbb{C}^n \;, \quad \ell=1,\ldots,k$$

such that

(1) $\sigma_\ell(t)$, $t \subseteq N$, is a singular value of $M[\gamma(t)]$ with left singular vector $v_\ell(t)$ and right singular vector $u_\ell(t)$.

(2) $\sigma_\ell(t_o) = \sigma(t_o)$.

(3) The columns of the matrices

$$u_\sigma(t) \triangleq [u_1(0) \mid \cdots \mid u_k(0)]$$

and

$$v_\sigma(t) \triangleq [v_1(0) \mid \cdots \mid v_k(0)]$$

are respectively orthonormal bases for the right and left k-dimensional singular subspaces $\mathfrak{U}_\sigma$ and $\mathfrak{V}_\sigma$ of $M[\gamma(t_o)]$ corresponding to $\sigma(t_o)$. ■

Note there is no assumption that the number of distinct singular values is constant along $\gamma(t)$. Thus care must be taken in numbering the singular values and vectors near exceptional points, (i.e., points where the number of distinct singular values changes). For this reason the singular values in Theorem G.6 are not numbered according to, say, decreasing order of magnitude. Note also that there exist singular projections P_{u_σ} and P_{v_σ} which are analytic in t. Further discussion is found in [10].

Proof of Theorem G.6: Assumptions (i) and (ii) show that the matrix M is analytic in t. Thus, M can be expanding in a power series

$$M(t) = \sum_{i=0}^{\infty} M_i(t-t_o)^i \quad . \tag{G.15}$$

By a construction similar to that in the proof of Theorem G.5 there exist matrices $M_L(t)$ and $M_R(t)$ which, for real values of t, are equal to $M(t)[M(t)]^H$ and $[M(t)]^H M(t)$, respectively. By Kato [32, p. 139, Theorem 6.1] the eigenvalues of $M_L(t)$ and $M_R(t)$ are analytic at each real value of t. Thus the nonzero singular values of M(t) are also analytic at real values of t. The result in Kato also shows the singular projections are analytic in t and on page 140 of [32] sets of basis vectors for the projections are constructed. These basis vectors are analytic in t and are obtained as the solution of differential equations along $\gamma(t)$. One can use this construction to obtain a set of right singular vectors; the left singular vectors are then given by

$$v_\ell(t) = \frac{1}{\sigma_\ell(t)} M[\gamma(t)]u_\ell(t) \quad .$$

Thus singular vectors with the desired properties exist; uniqueness is not guaranteed, of course. ■

Note that derivatives of all orders of the functions σ_ℓ, u_ℓ and v_ℓ with respect to t exist and are continuous in t. By letting $\gamma(t) = x_o + jy_o + t$ and $\gamma(t) = x_o + jy_o + jt$, the partial derivatives of the singular values and vectors with respect to x and y can be evaluated at $s_o = x_o + jy_o$. These

partial derivatives are guaranteed to be continuous only along the respective curve $\gamma(t)$, however. In particular, mixed partial derivatives do not necessarily exist. Of course, if s_o is not an exceptional point, (i.e., a point where the number of distinct singular values changes) continuity in both x and y and the existence of mixed partial derivatives of all orders follows from Theorem G.5. The behavior of singular values and vectors near exceptional points will need further study if it is desired to extend the results of this thesis (in particular, the Bode integral relations) to more general situations.

The results of Theorems G.5 and G.6 can be used to obtain formulas for the partial derivatives, with respect to x and y, of the singular values and vectors. These formulas were stated in Chapter 9 for the case of distinct singular values, but are here derived rigorously.

Theorem G.7: Let $M(s)$ satisfy the assumptions of Theorem G.6. Let $\sigma(s_o)$ be a singular value of $M(s_o)$ with multiplicity k. Let $\gamma(t) = [t_1,t_2] \to \mathbb{C}$ be a curve satisfying the assumptions of Theorem G.6 such that $\gamma(t_o) = s_o$, $t_1 < t_o < t_2$. Define

$$\Sigma(t) \triangleq \mathrm{diag}[\sigma_1(t) \mid \cdots \mid \sigma_k(t)] \tag{G.16}$$

$$U_\sigma(t) \triangleq [u_1(t) \mid \cdots \mid u_k(t)] \tag{G.17}$$

and

$$V_\sigma(t) \triangleq [v_1(t) \mid \cdots \mid v_k(t)] \tag{G.18}$$

where the σ_ℓ, u_ℓ and v_ℓ are guaranteed to exist by Theorem G.6. Then,

$$\left.\frac{d\Sigma}{dt}\right|_{t=t_o} = \mathcal{R}e[V_\sigma^H \frac{dM}{dt} U_\sigma]\Big|_{t=t_o} \tag{G.19}$$

where

$$\mathcal{R}e[A] \triangleq \frac{1}{2}[A + A^H] \quad . \tag{G.20}$$

Since the functions $\sigma_\ell(t)$, $u_\ell(t)$ and $v_\ell(t)$, $\ell=1,\ldots,k$, are equal to k of the singular values and vectors of M(s) along $\gamma(t)$, it follows that the partial derivatives of these singular values and vectors can be computed from those of these functions. Thus, setting $\gamma_x(t) = s_o + t$, $t \in (-\varepsilon,\varepsilon)$ and $\gamma_y(t) = s_o + jt$, $t \in (-\varepsilon,\varepsilon)$, allows the computation of the partial derivatives $\{\frac{\partial\sigma_\ell}{\partial x}, \frac{\partial u_\ell}{\partial x}, \frac{\partial v_\ell}{\partial x}\}$ and $\{\frac{\partial\sigma_\ell}{\partial y}, \frac{\partial u_\ell}{\partial y}, \frac{\partial v_\ell}{\partial y}\}$, respectively. Moreover, this construction shows that continuous partial derivatives <u>in one variable</u> of all orders exist. For singular values of multiplicity one, a construction using the results of Theorem G.5 shows that continuous <u>mixed</u> partial derivatives of all orders exist.

<u>Proof of Theorem G.7</u>: Properties of the singular values and vectors imply that, for real t,

$$U_\sigma^H(t)M^H(t)M(t)U_\sigma(t) - \Sigma^2(t) = 0 \quad . \tag{G.21}$$

It follows from (G.21) that (dropping dependence on t)

$$\begin{aligned} &\frac{dU_\sigma^H}{dt} M^H M U_\sigma + U_\sigma^H M^H M \frac{dU_\sigma}{dt} \\ &+ U_\sigma^H \frac{dM^H M}{dt} U_\sigma - \frac{d\Sigma^2}{dt} = 0 \end{aligned} \tag{G.22}$$

$$\Rightarrow \qquad \frac{dU_\sigma{}^H}{dt} U_\sigma \Sigma^2 + \Sigma^2 U_\sigma{}^H \frac{dU_\sigma}{dt}$$

$$+ U_\sigma{}^H \frac{dM^H M}{dt} U_\sigma - \frac{d\Sigma^2}{dt} = 0 \quad . \tag{G.23}$$

At $t=t_o$, $\Sigma^2(t_o) = \sigma^2(t_o) I_{k\times k}$. Thus, the first two terms of (G.23) yield:

$$\left[\frac{dU_\sigma{}^H}{dt} U_\sigma \Sigma^2 + \Sigma^2 U_\sigma{}^H \frac{dU_\sigma}{dt}\right]\Bigg|_{t=t_o} = \sigma^2(t_o) \left[\frac{dU_\sigma{}^H}{dt} U_\sigma + U_\sigma{}^H \frac{dU_\sigma}{dt}\right]\Bigg|_{t=t_o} . \tag{G.24}$$

From the identity

$$U_\sigma{}^H U_\sigma \equiv I_{k\times k} \quad ,$$

it follows that

$$\frac{dU_\sigma{}^H}{dt} U_\sigma + U_\sigma{}^H \frac{dU_\sigma}{dt} = 2\mathrm{Re}[U_\sigma{}^H \frac{dU_\sigma}{dt}]$$

$$= 0 \quad . \tag{G.25}$$

Substituting (G.25) into (G.23) and using various properties of singular values yields:

$$\frac{d\Sigma^2}{dt} = U_\sigma{}^H \frac{dM^H M}{dt} U_\sigma$$

$$\Rightarrow \qquad 2\Sigma \frac{d\Sigma}{dt} = U_\sigma{}^H \frac{dM^H}{dt} V_\sigma \Sigma + \Sigma V_\sigma{}^H \frac{dM}{dt} U_\sigma$$

$$= 2\Sigma \ \mathrm{Re}[V_\sigma{}^H \frac{dM}{dt} U_\sigma] \tag{G.26}$$

$$\Rightarrow \qquad \frac{d\Sigma}{dt} = \mathrm{Re}[V_\sigma{}^H \frac{dM}{dt} U_\sigma]$$

which was to be proven. ∎

AD-A161 452 ISSUES IN FREQUENCY DOMAIN FEEDBACK CONTROL(U) ILLINOIS UNIV AT URBANA DECISION AND CONTROL LAB J S FREUDENBERG MAY 85 DC-81 N00014-84-C-0149 5/5

UNCLASSIFIED F/G 9/3 NL

END

FILMED

DTIC

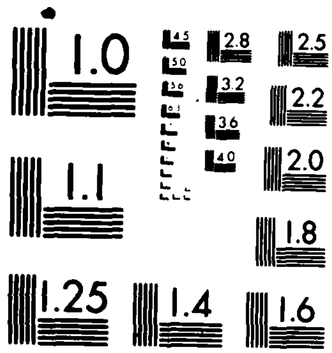

MICROCOPY RESOLUTION TEST CHART
NATIONAL BUREAU OF STANDARDS-1963-A

It should be pointed out that the derivatives $\frac{d\sigma_\ell}{dt}$ can be calculated using any orthonormal basis for the right singular subspace and the corresponding set of left singular vectors. Thus, at exceptional points $s_o = \gamma(t_o)$ there is no need to determine precisely which basis of the right singular subspace of $M(s_o)$ yields an analytic set of right singular vectors along $\gamma(t)$. This is discussed in detail in Freudenberg, Looze and Cruz [10, Theorem 2].

Explicit formulas for the derivatives of the singular vectors can also be obtained. First, some additional notations must be introduced.

Let the number of distinct singular values of $M(s_o) \in \mathbb{C}^{n\times n}$ be given by N. Let the singular values be denoted by $\sigma_i, i=1,\ldots,N$, where the multiplicity of σ_i is given by k_i. (Note $\sum_{i=1}^{N} k_i = n$.) Then there are N right singular subspaces $\mathfrak{U}_i, i=1,\ldots,N$ with $\dim(\mathfrak{U}_i)=k_i$.

<u>Theorem G.8</u>: Let M(s) satisfy the assumptions of Theorem G.6. Let $\gamma(t) : [t_1,t_2] \to \mathbb{C}$ be a curve satisfying the assumptions of Theorem G.6 such that $\gamma(t_o) = s_o$, $t_1 < t_o < t_2$. Define

$$\Sigma_i(t) \triangleq \text{diag}[\sigma_{i1}(t) \mid \cdots \mid \sigma_{ik_i}] \tag{G.27}$$

$$U_i(t) \triangleq [u_{i1}(t) \mid \cdots \mid u_{ik_i}(t)] \tag{G.28}$$

and

$$V_i(t) \triangleq [v_{i1}(t) \mid \cdots \mid v_{ik_i}(t)] \tag{G.29}$$

where the $\sigma_{i\ell}$, $u_{i\ell}$ and $v_{i\ell}$ are guaranteed to exist by Theorem G.6. Then the derivatives of U_i and V_i can be written

$$\frac{dU_i}{dt} = \sum_{m=1}^{N} U_m \cdot \left(U_m{}^H \frac{dU_i}{dt}\right) \tag{G.30}$$

and

$$\frac{dV_i}{dt} = \sum_{m=1}^{N} V_m \cdot \left(V_m{}^H \frac{dV_i}{dt}\right) \quad . \tag{G.31}$$

For $m \neq i$

$$U_m{}^H \frac{dU_i}{dt} = \left(\frac{1}{\sigma_i{}^2 - \sigma_m{}^2}\right) \left[U_m{}^H \frac{dM^H}{dt} V_i \sigma_i + \sigma_m V_m{}^H \frac{dM}{dt} U_i\right] \tag{G.32}$$

and

$$V_m{}^H \frac{dV_i}{dt} = \left(\frac{1}{\sigma_i{}^2 - \sigma_m{}^2}\right) \left[V_m{}^H \frac{dM^H}{dt} V_i \sigma_m + \sigma_i V_m{}^H \frac{dM}{dt} U_i\right] \quad . \tag{G.33}$$

Also

$$\mathrm{Re}[U_i{}^H \frac{dU_i}{dt}] = 0 \quad . \tag{G.34}$$

and

$$\mathrm{Re}[V_i{}^H \frac{dV_i}{dt}] = 0 \tag{G.35}$$

while

$$[V_i{}^H \frac{dV_i}{dt} - U_i{}^H \frac{dU_i}{dt}] = \frac{j}{\sigma_i} \mathrm{Im}[V_i{}^H \frac{dM}{dt} U_i] \tag{G.36}$$

where

$$\mathrm{Im}[A] \triangleq \frac{1}{2j} [A - A^H] \quad . \tag{G.37}$$

■

<u>Proof</u>: Using various properties of the singular value decomposition and dropping the dependence on t:

$$M^H M U_i = U_i \Sigma_i^{\,2}$$

$$\Rightarrow \quad \frac{dM^H M}{dt} U_i + M^H M \frac{dU_i}{dt} = U_i \frac{d\Sigma_i^{\,2}}{dt} + \frac{dU_i}{dt} \Sigma_i^{\,2} \quad .$$

For $m \neq i$

$$U_m^{\,H} \frac{dM^H M}{dt} U_i + \Sigma_m^{\,2} U_m^{\,H} \frac{dU_i}{dt} = 0 + U_m^{\,H} \frac{dU_i}{dt} \Sigma_i^{\,2} \quad . \tag{G.38}$$

Evaluating (G.38) at t_o yields $\Sigma_m^{\,2} = \sigma_m I_{k_m}$ and $\Sigma_i^{\,2} = \sigma_i I_{k_i}$, which in turn implies

$$U_m^{\,H} \frac{dU_i}{dt} = \left(\frac{1}{\sigma_i^{\,2} - \sigma_m^{\,2}}\right) U_m^{\,H} \frac{dM^H M}{dt} U_i$$

$$= \left(\frac{1}{\sigma_i^{\,2} - \sigma_m^{\,2}}\right) \left[U_m^{\,H} \frac{dM^H}{dt} V_i \sigma_i + \sigma_m V_m^{\,H} \frac{dM}{dt} V_i\right] \quad .$$

Thus, (G.38) is proven and (G.33) follows similarly. Equations (G.34) and (G.35) follow from (G.25). Finally, from

$$V_i^{\,H} M U_i = \Sigma_i$$

$$\Rightarrow \quad \frac{dV_i^{\,H}}{dt} V_i \Sigma_i + \Sigma_i U_i^{\,H} \frac{dU_i}{dt} + V_i^{\,H} \frac{dM}{dt} U_i = \frac{d\Sigma_i}{dt} \quad . \tag{G.39}$$

At $t = t_o$, $\Sigma_i = \sigma_i I_{k_i}$. This fact, and rearranging terms in (G.39) yields

$$\frac{1}{\sigma_i} \operatorname{Im}\left[V_i^H \frac{dM}{dt} U_i\right] = \left[V_i^H \frac{dV_i}{dt} - U_i^H \frac{dU_i}{dt}\right]$$

which proves the result. ∎

The above theorem again shows the existence of a degree of freedom in the singular vectors: $V_i^H \frac{dV_i}{dt}$ and $U_i^H \frac{dU_i}{dt}$ can be chosen as arbitrary functions analytic in t, subject to (G.36). Note also that the comments which were made following Theorem G.7 concerning the partial derivatives of the singular values with respect to x and to y also apply to the singular vectors.

Recall the construction of right singular vectors used in the proof of Theorem G.7. This construction, based upon the results of Kato [32, p. 140] yielded a set of singular vectors analytic in t, satisfying a differential equation. It is interesting to investigate the choice of singular vectors obtained from this procedure.

For simplicity assume that the singular values are distinct at s_o. Let $\gamma(t)$ be a curve through s_o and assume M(s) and $\gamma(t)$ satisfy the assumptions of Theorems G.6-G.8. Define

$$U(t_o) \triangleq [U_1(t_o) \mid \cdots \mid U_n(t_o)] \tag{G.40}$$

where $U_i(t_o)$ is a unit vector in the right singular subspace $\mathfrak{U}_i(t_o)$. A transformation function W(t) can be constructed so that, locally,

$$U_i(t) = W(t)U_i(t_o) \tag{G.41}$$

is a right singular vector in the subspace $\mathfrak{U}_i(t)$. Let $P_k(t) \equiv P_{u_k}(t)$ denote the orthogonal projection onto the subspace $\mathfrak{U}_k(t)$ and define

$$Q(t) \triangleq \sum_{k=1}^{n} P_k'(t)P_k(t) \qquad \text{(G.42)}$$

where

$$P_k'(t) = \frac{d}{dt}[P_k(t)] \quad . \qquad \text{(G.43)}$$

It can be shown that W(t) is the solution of the differential equation

$$\frac{d}{dt} W(t) = Q(t)W(t) \qquad \text{(G.44)}$$

with initial condition $W(t_o) = I$. From (G.41) and (G.44) it follows that

$$\frac{du_i(t)}{dt} = Q(t)u_i(t) \quad . \qquad \text{(G.45)}$$

Hence, supressing dependence on t:

$$\begin{aligned} u_i^H \frac{du_i}{dt} &= u_i^H Qu_i \\ &= u_i^H \sum_{k=1}^{N} P_k'P_k u_i \quad . \end{aligned} \qquad \text{(G.46)}$$

Since $P_i u_i = u_i$ and $P_k u_i = 0, k \neq i$, (G.46) reduces to

$$u_i^H \frac{du_i}{dt} = u_i^H P_i' u_i \quad . \qquad \text{(G.47)}$$

Now, for real values of t, $P_i(t) = [P_i(t)]^H$; i.e., $P_i(t)$ is Hermitian. Moreover, so is $P_i'(t)$. Thus, $u_i^H P_i' u_i$ is a real number. But since $\mathrm{Re}[u_i^H \frac{du_i}{dt}] = 0$, it follows that both sides of (G.47) equal zero. Thus, using Kato's procedure yields right singular vectors with the property that $u_i^H \frac{du_i}{dt} \equiv 0$. The constraint (G.36) implies that the left singular vectors given by

$$v_i(t) = \frac{1}{\sigma_i(t)} M(t)u_i(t) \tag{G.48}$$

must satisfy

$$v_i^H \frac{dv_i}{dt} = \frac{j}{\sigma_i} \mathrm{Im}[v_i^H \frac{dM}{dt} u_i] \quad . \tag{G.49}$$

Note, in particular, the left singular vector given by (G.48) is analytic in t. This implies that the quantity $\mathrm{Im}[v_i^H \frac{dM}{dt} u_i]$ is also analytic on t.

APPENDIX H

PROOF OF THEOREM 9.7

From (9.16) and (9.22) it follows that

$$A \triangleq j[-\frac{\partial \log\sigma_i}{\partial y}dx + \frac{\partial \log\sigma_i}{\partial x}dy] = [v_i^H \frac{\partial v_i}{\partial x} - u_i^H \frac{\partial u_i}{\partial x}]dx + [v_i^H \frac{\partial v_i}{\partial y} - u_i^H \frac{\partial u_i}{\partial y}]dy \quad , \tag{H.1}$$

which in turn yields

$$dA = j\left(\frac{\partial^2 \log\sigma_i}{\partial x^2} + \frac{\partial^2 \log\sigma_i}{\partial y^2}\right)dx\wedge dy$$

$$= -[\frac{\partial v_i^H}{\partial y}\frac{\partial v_i}{\partial x} - \frac{\partial u_i^H}{\partial y}\frac{\partial u_i}{\partial x}]dx\wedge dy + [\frac{\partial v_i^H}{\partial x}\frac{\partial v_i}{\partial y} - \frac{\partial u_i^H}{\partial x}\frac{\partial u_i}{\partial y}]dx\wedge dy \quad . \tag{H.2}$$

Thus,

$$\nabla^2 \log\sigma_i = 2\ \mathrm{Im}\{\frac{\partial v_i^H}{\partial x}\frac{\partial v_i}{\partial y} - \frac{\partial u_i^H}{\partial x}\frac{\partial u_i}{\partial y}\} \quad . \tag{H.3}$$

From (9.17) and (9.18)

$$\frac{\partial u_i}{\partial x} = \sum_{k=1}^{n} u_k(u_k^H \frac{\partial u_i}{\partial x}) \tag{H.4a}$$

$$\frac{\partial v_i}{\partial x} = \sum_{k=1}^{n} v_k(v_k^H \frac{\partial v_i}{\partial x}) \tag{H.4b}$$

$$\Rightarrow \quad \frac{\partial u_i^H}{\partial x}\frac{\partial u_i}{\partial y} = \sum_{k=1}^{n} \overline{(u_k^H \frac{\partial u_i}{\partial x})}(u_k^H \frac{\partial u_i}{\partial y}) \tag{H.5a}$$

$$\frac{\partial v_i^H}{\partial x}\frac{\partial v_i}{\partial y} = \sum_{k=1}^{n} \overline{(v_k^H \frac{\partial v_i}{\partial x})}(v_k^H \frac{\partial v_i}{\partial y}) \tag{H.5b}$$

$$\Rightarrow \quad \nabla^2 \log\sigma_i = 2 \sum_{k=1}^{n} \mathrm{Im}\{\overline{(v_k^H \frac{\partial v_i}{\partial x})}(v_k^H \frac{\partial v_i}{\partial y}) - \overline{(u_k^H \frac{\partial u_i}{\partial x})}(u_k^H \frac{\partial u_i}{\partial y})\} \quad . \tag{H.6}$$

For $k \neq i$,

$$u_k^H \frac{\partial u_i}{\partial x} = \frac{1}{(\sigma_i^2 - \sigma_k^2)} \{\sigma_i u_k^H \frac{\partial M^H}{\partial x} v_i + \sigma_k v_k^H \frac{\partial M}{\partial x} u_i\}$$

$$\Rightarrow \quad \overline{u_k^H \frac{\partial u_i}{\partial x}} = \frac{1}{(\sigma_i^2 - \sigma_k^2)} \{\sigma_i v_i^H \frac{\partial M}{\partial x} u_k + \sigma_k u_i^H \frac{\partial M^H}{\partial x} v_k\} \quad .$$

Using Lemma 9.6:

$$\overline{u_k^H \frac{\partial u_i}{\partial x}} = \frac{-j}{\sigma_i^2 - \sigma_k^2} \{\sigma_i v_i^H \frac{\partial M}{\partial y} u_k - \sigma_k u_i^H \frac{\partial M^H}{\partial y} v_k\} \quad .$$

Thus,

$$\overline{(u_k^H \frac{\partial u_i}{\partial x})} \cdot (u_k^H \frac{\partial u_i}{\partial y}) = \frac{-j}{(\sigma_i^2 - \sigma_k^2)^2} \{\sigma_i^2 |v_i^H \frac{\partial M}{\partial y} u_k|^2 - \sigma_k^2 |v_k^H \frac{\partial M}{\partial y} u_i|^2$$

$$+ \sigma_i \sigma_k \, 2j \, \mathrm{Im}[(v_i^H \frac{\partial M}{\partial y} u_k)(v_k^H \frac{\partial M}{\partial y} u_i)]\}$$

$\Rightarrow$ (H.7)

$$\mathrm{Im}\{\overline{(u_k^H \frac{\partial u_i}{\partial x})}(u_k^H \frac{\partial u_i}{\partial y})\} = \frac{-1}{(\sigma_i^2 - \sigma_k^2)^2} [\sigma_i^2 |v_i^H \frac{\partial M}{\partial y} u_k|^2 - \sigma_k^2 |v_k^H \frac{\partial M}{\partial y} u_i|^2] \quad .$$

Similarly, it can be shown that

$$\mathrm{Im}\{\overline{(v_k^H \frac{\partial v_i}{\partial x})}(v_k^H \frac{\partial v_i}{\partial y})\} = \frac{-1}{(\sigma_i^2 - \sigma_k^2)^2} [\sigma_k^2 |v_i^H \frac{\partial M}{\partial y} u_k|^2 - \sigma_i^2 |v_k^H \frac{\partial M}{\partial y} u_i|^2]. \tag{H.8}$$

Using (H.7) and (H.8) in (H.6) yields

$$\nabla^2 \log \sigma_i = 2\,\mathrm{Im}\{\overline{(v_i^H \frac{\partial v_i}{\partial x})}(v_i^H \frac{\partial v_i}{\partial y}) - \overline{(u_i^H \frac{\partial u_i}{\partial x})}\;(u_i^H \frac{\partial u_i}{\partial y})\}$$

$$+ 2 \sum_{k\neq i} \frac{1}{\sigma_i^2 - \sigma_k^2} \{|v_i^H \frac{\partial M}{\partial y} u_k|^2 + |v_k^H \frac{\partial M}{\partial y} u_i|^2\} \quad . \qquad \text{(H.9)}$$

Let the first term on the right-hand side of (H.9) be denoted (I). Then from (9.22) and Lemma 9.6

$$(\mathrm{I}) = 2\,\mathrm{Im}\{\overline{(\frac{j}{\sigma_i}\,\mathrm{Im}[v_i^H \frac{\partial M}{\partial x} u_i] + (u_i^H \frac{\partial u_i}{\partial x}))}(\frac{j}{\sigma_i}\,\mathrm{Im}[v_i^H \frac{\partial M}{\partial y} u_i] + (u_i^H \frac{\partial u_i}{\partial y}))$$

$$- \overline{(u_i^H \frac{\partial u_i}{\partial x})}(u_i^H \frac{\partial u_i}{\partial y})\}$$

$$= 2\,\mathrm{Im}\{\frac{1}{\sigma_i^2}\,\mathrm{Im}[v_i^H \frac{\partial M}{\partial x} u_i]\;\mathrm{Im}[v_i^H \frac{\partial M}{\partial y} u_i] + \overline{(u_i^H \frac{\partial u_i}{\partial x})}\;\frac{j}{\sigma_i}\,\mathrm{Im}[v_i^H \frac{\partial M}{\partial y} u_i]$$

$$+ (u_i^H \frac{\partial u_i}{\partial y})\;\frac{-j}{\sigma_i}\,\mathrm{Im}[v_i^H \frac{\partial M}{\partial x} u_i]\} \quad .$$

Since $u_i^H \frac{\partial u_i}{\partial x}$ and $u_i^H \frac{\partial u_i}{\partial y}$ are both purely imaginary numbers, it follows that (I) equals zero. Using Lemma 9.6 one more time in (H.9) yields

$$\nabla^2 \log \sigma_i = \sum_{k\neq i} \frac{1}{\sigma_i^2 - \sigma_k^2} \{|v_i^H \frac{\partial M}{\partial x} u_k|^2 + |v_i^H \frac{\partial M}{\partial y} u_k|^2$$

$$+ |v_k^H \frac{\partial M}{\partial x} u_i|^2 + |v_k^H \frac{\partial M}{\partial y} u_i|^2\}$$

which was to be proven. ∎

APPENDIX I

PROOFS OF THEOREMS IN CHAPTER 12

Proof of Lemma 12.1: For each $\alpha \in [-\pi/2, \pi/2]$, define $M_\infty(\alpha) \stackrel{\Delta}{=} \lim_{R\to\infty} M(Re^{j\alpha})$. Since $M(s)$ has proper rational entries, it follows that $M_\infty(\alpha)$ exists and is independent of α. Thus define $M_\infty \stackrel{\Delta}{=} M_\infty(\alpha)$.

First, suppose that M_∞ has rank n. Then (12.7) is satisfied, for $i=1,\ldots,n$, with $k_i=0$ and $c_i \stackrel{\Delta}{=} \sigma_i[M_\infty]$. Suppose, in addition, that $\sigma_i[M_\infty] \neq \sigma_k[M_\infty]$ for $i \neq k$. Then (12.8) is satisfied with the $\mathbb{W}_i$ and $\mathcal{Z}_i$ given by the left and right singular subspaces $\mathcal{V}_i[M_\infty]$ and $\mathcal{U}_i[M_\infty]$ and with the w_i and z_i a pair of singular vectors $v_i[M_\infty]$ and $u_i[M_\infty]$.

Next, suppose that M_∞ has rank $m < n$. Then (12.7) is satisfied for $i=1,\ldots,m$ with $k_i=0$ and $c_i \stackrel{\Delta}{=} \sigma_i[M_\infty]$. Suppose, in addition, that $\sigma_i[M_\infty] \neq \sigma_k[M_\infty]$ for $i\neq k$, $i \leq m$, $k \leq m$. Then (12.8) is satisfied by the left and right singular vectors $v_i[M_\infty]$ and $u_i[M_\infty]$, $i=1,\ldots,m$. Note that $M(s)$ may be decomposed as

$$M(s) = M_\infty + \frac{1}{s} M_1(s)$$

where $M_1(s)$ is proper. Define $P_{v\infty}$ to be the orthogonal projection onto the subspace $\mathcal{V}_\infty \subseteq \mathbb{C}^n$ spanned by $\{v_1[M_\infty],\ldots,v_m[M_\infty]\}$. Define $P_{u\infty}$ to be the orthogonal projection onto the subspace $\mathcal{U}_\infty \subseteq \mathbb{C}^n$ spanned by $\{u_1[M_\infty],\ldots,u_m[M_\infty]\}$. Similarly, let the projections onto the orthogonal complements of $\mathcal{V}_\infty$ and $\mathcal{U}_\infty$ be denoted by $P^\perp_{v\infty} = I - P_{v\infty}$ and $P^\perp_{u\infty} = I - P_{u\infty}$.

By continuity, there exist m singular values and singular subspaces $\sigma_i[M(s)]$, $\mathcal{V}_i[M(s)]$, and $\mathcal{U}_i[M(s)]$ such that $\forall\alpha \in [-\pi/2,\pi/2]$, and $i=1,\ldots,m$

$$\sigma_i[M_\infty] = \lim_{R\to\infty} \sigma_i[M(Re^{j\alpha})]$$

$$\mathfrak{V}_i[M_\infty] = \lim_{R\to\infty} \mathfrak{V}_i[M(Re^{j\alpha})]$$

$$\mathfrak{U}_i[M_\infty] = \lim_{R\to\infty} \mathfrak{U}_i[M(Re^{j\alpha})] \quad .$$

(Note that $\mathfrak{V}_\infty = \bigcup_{i=1}^{m} \mathfrak{V}_i[M_\infty]$ and $\mathfrak{U}_\infty = \bigcup_{i=1}^{m} \mathfrak{U}_i[M_\infty]$.) Again, these limits are independent of α. Similarly, define $\mathfrak{U}_\infty(s) = \bigcup_{i=1}^{m} \mathfrak{U}_i(s)$, $\mathfrak{V}_\infty(s) = \bigcup_{i=1}^{m} \mathfrak{V}_i(s)$, and projection operators $P_{v\infty}(s)$, $P_{u\infty}(s)$, $P^{\perp}_{v\infty}(s)$ and $P^{\perp}_{u\infty}(s)$. Define

$$\hat{M}_1(s) = P^{\perp}_{v\infty}(s)M_1(s)P^{\perp}_{u\infty}(s) \quad ;$$

and

$$\hat{M}_{1\infty} = \lim_{R\to\infty} \hat{M}_1(Re^{j\alpha})$$

where the limit is independent of $\alpha\in[-\pi/2,\pi/2]$. Then the n-m singular values of M(s) which approach zero as $|s|\to\infty$ satisfy $\forall\alpha\in[-\pi/2,\pi/2]$,

$$\lim_{R\to\infty} R\sigma_{m+i}(Re^{j\alpha}) = \sigma_i[\hat{M}_{1\infty}] \qquad i=1,\ldots,n-m \quad .$$

To show this, recall that by definition

$$\sigma_{m+1}[M(s)] = \max_{\|u\|=1} \|M(s)P^{\perp}_{u\infty}(s)u\| \quad .$$

$$= \max_{\|u\|=1} \|P^{\perp}_{v\infty}(s)M(s)P^{\perp}_{u\infty}(s)u\|$$

which follows since $M(s)P^{\perp}_{u\infty}(s)u\in\mathfrak{V}^{\perp}_\infty(s)$ for $u\in\mathfrak{U}^{\perp}_\infty(s)$.

Thus,

$$\sigma_{m+1}[M(s)] = \max_{\|u\|=1} \left\| P^{\perp}_{v\infty}(s)[M_\infty + \frac{1}{s} M_1(s)]P^{\perp}_{u\infty}(s)u \right\|_2$$

$$\geq \left| \underline{\sigma}[P^{\perp}_{v\infty}(s)M_\infty P^{\perp}_{u\infty}(s)] - \frac{1}{|s|} \bar{\sigma}[\hat{M}_1(s)] \right|$$

and

$$\lim_{R\to\infty} R\sigma_{m+1}[M(Re^{j\alpha})] \geq \bar{\sigma}[M_{1\infty}] \quad ,$$

since, by definition, $\lim_{R\to\infty} P^{\perp}_{v\infty}(Re^{j\alpha})M_\infty P^{\perp}_{u\infty}(Re^{j\alpha}) = 0$ for all $\alpha \in [-\pi/2, \pi/2]$. Moreover, from

$$\sigma_{k+1}[M(s)] \leq \bar{\sigma}[P^{\perp}_{v\infty}(s)M_\infty P^{\perp}_{u\infty}(s)] + \frac{1}{|s|} \bar{\sigma}[\hat{M}_1(s)]$$

it follows that

$$\lim_{R\to\infty} R\sigma_{m+1}[M(s)] = \bar{\sigma}[\hat{M}_{1\infty}] \quad .$$

Similarly, it may be shown that

$$\lim_{R\to\infty} R\sigma_{m+i}[M(s)] = \sigma_i[\hat{M}_{1\infty}] \quad , \quad i=1,\ldots,n-m \quad .$$

Let $\hat{M}_{1\infty}$ have rank m_1 (note $m_1 \leq n-m$). Then (12.7) is satisfied by setting $k_{m+i} = 1$ and $c_{m+i} = \sigma_i[\hat{M}_{1\infty}]$ for $i=1,\ldots,m_1$.

Suppose that the nonzero singular values of $\hat{M}_{1\infty}$ are distinct. Then (12.8) is satisfied by left and right singular vectors $v_i \triangleq v_i[\hat{M}_{1\infty}]$ and $u_i \triangleq u_i[\hat{M}_{1\infty}]$ for $i=m+1,\ldots,m_1$. That is

$$\sigma_i[\hat{M}_{1\infty}] = \lim_{R\to\infty} Re^{j\alpha} v_i^H M(Re^{j\alpha})u_i$$

$$= \lim_{R\to\infty} Re^{j\alpha} \frac{1}{Re^{j\alpha}} v_i^H \hat{M}_1(s) u_i^H$$

$$= v_i^H \hat{M}_{1\infty} u_i^H \quad .$$

If rank $\hat{M}_{1\infty} = m_1 = n-m$, then the above procedure gives the values of k_i and c_i in (12.7) and the z_i and w_i in (12.8) for all $i=1,\ldots,n$. If $m_1 < n-m$, then there exist singular values for which (12.7) is satisfied for $k_i \geq 2$. The above procedure can be repeated by writing

$$\hat{M}_1 = \hat{M}_{1\infty} + \frac{1}{s} M_2$$

where M_2 is proper. The singular value decomposition of $\hat{M}_{1\infty}$ may be used to obtain projection operators onto the nullspace of $\hat{M}_{1\infty}$ and its image. These in turn may be used to define $\hat{M}_2(s)$ similarly to $\hat{M}_1(s)$. Since, (a) $M(s)$ is rational, (b) $\det M(s) \not\equiv 0$, and (c) only n singular values exist, this procedure may be repeated until values of k_i, c_i, w_i, and z_i are found for all $i=1,\ldots,n$. ∎

Before proceeding with the proof of Theorem 12.2 it is necessary to present some additional Definitions and Lemmas.

Definition I.1: Let $g(s) = g(x,y)$ and $h(s) = h(x,y)$ be real valued functions of the complex frequency variable $s = x+jy$. Then $f(s) \triangleq g(s) + jh(s)$ is said to be conjugate symmetric provided

$$g(s) = g(\bar{s}) \tag{I.1a}$$

and

$$h(s) = -h(\bar{s}) \quad . \tag{I.1b}$$

Equivalently,

$$f(s) = \overline{f(\bar{s})} \quad . \tag{I.1c}$$

■

<u>Lemma I.2</u>: Assume that $f(s) = g(s) + jh(s)$ is conjugate symmetric, and that $g(x,y)$ and $h(x,y)$ have continuous partial derivatives. Then

$$\left.\frac{\partial g}{\partial x}\right|_{(x,y)} = \left.\frac{\partial g}{\partial x}\right|_{(x,-y)} \tag{I.2a}$$

$$\left.\frac{\partial g}{\partial y}\right|_{(x,y)} = - \left.\frac{\partial g}{\partial y}\right|_{(x,-y)} \tag{I.2b}$$

$$\left.\frac{\partial h}{\partial x}\right|_{(x,y)} = - \left.\frac{\partial h}{\partial x}\right|_{(x,-y)} \tag{I.2c}$$

$$\left.\frac{\partial h}{\partial y}\right|_{(x,y)} = \left.\frac{\partial h}{\partial y}\right|_{(x,-y)} \quad . \tag{I.2d}$$

■

<u>Proof</u>: By definition,

$$\begin{aligned}\left.\frac{\partial g}{\partial x}\right|_{(x,y)} &= \lim_{\Delta x \to 0} \frac{g(x+\Delta x,y) - g(x,y)}{\Delta x} \\ &= \lim_{\Delta x \to 0} \frac{g(x+\Delta x,-y) - g(x,-y)}{\Delta x} \\ &= \left.\frac{\partial g}{\partial x}\right|_{(x,-y)}\end{aligned}$$

$$\begin{aligned}\left.\frac{\partial g}{\partial y}\right|_{(x,y)} &= \lim_{\Delta y \to 0} \frac{g(x,y+\Delta y) - g(x,y)}{\Delta y} \\ &= \lim_{\Delta y \to 0} \frac{g(x,-y-\Delta y) - g(x,-y)}{\Delta y}\end{aligned}$$

$$= -\lim_{\Delta y' \to 0} \frac{g(x,-y+\Delta y') - g(x,-y)}{\Delta y'}$$

$$= - \left. \frac{\partial g}{\partial y} \right|_{(x,-y)}$$

where $\Delta y' \triangleq \Delta y$. Proof of Equations (I.2c) and (I.2d) follows similarly. ■

Lemma I.3: Let M(s) satisfy the assumptions of Theorem 12.1. Then each singular value and its associated measure of phase difference (12.3) have the property that $f(s) = \log\sigma(s) + j[\theta(s) - \theta(0)]$ is conjugate symmetric. ■

Proof: Let the singular value decomposition of $M(s) = M(x,y)$ be given by

$$M(x,y) = V(x,y)\Sigma(x,y)[U(x,y)]^H \quad . \tag{I.3}$$

Then each singular value may be written (suppressing the subscript) as $\sigma(x,y) = [v(x,y)]^H M(x,y)u(x,y)$. The left and right singular vectors v and u may be written as in (12.2), yielding

$$\sigma(x,y) \exp[j\Delta\theta(x,y)] = [\rho_v(x,y)]^H M(x,y)\rho_u(x,y) \quad . \tag{I.4}$$

Since rational functions are conjugate symmetric, it follows that $M(x,y) = \overline{M(x,-y)}$. By assumption ρ_v and ρ_u are also conjugate symmetric. Thus (I.4) implies that $\sigma(x,y) = \sigma(x,-y)$ and $\exp[j\theta(x,y)] = \exp[-j\theta(x,-y)]$. Hence $\theta(x,y) = -\theta(x,-y) + 2k\pi$ and $\theta(x,0) = k\pi$, with k even if $\exp[j\theta(x,0)] = 1$ and odd if $\exp[j\theta(x,0)] = -1$. Finally, the assumptions of Theorem 12.2 yield that $\theta(x,0)$ is constant in x. Denoting this constant by $\theta(0)$ yields the result. ■

Next, if $\mathbb{C}$ is identified with $\mathbb{R}^2$, a basis for the cotangent space to a point $s = x+jy \in \mathbb{C}$ is given by $\{dx,dy\}$. A complex basis for the cotangent space is given by

$$\{ds = dx + jdy,\ d\bar{s} = dx - jdy\} \quad .$$

The dual basis for the tangent space is given by [62, p. 2]

$$\{\frac{\partial}{\partial s} \triangleq \frac{1}{2}(\frac{\partial}{\partial x} - j\frac{\partial}{\partial y}) \ ,\ \frac{\partial}{\partial \bar{s}} \triangleq \frac{1}{2}(\frac{\partial}{\partial x} + j\frac{\partial}{\partial y})\} \quad . \tag{I.5}$$

Let $g(s) = g(x,y)$ and $h(s) = h(x,y)$ be C^∞ in (x,y). Then $f(s) \triangleq g(s) + jh(s)$ is analytic iff $\frac{\partial f}{\partial \bar{s}} = 0$, where

$$\begin{aligned}\frac{\partial f}{\partial \bar{s}} &= \frac{1}{2}[\frac{\partial f}{\partial x} + j\frac{\partial f}{\partial y}] \\ &= \frac{1}{2}[(\frac{\partial g}{\partial x} + j\frac{\partial h}{\partial x}) + j(\frac{\partial g}{\partial y} + j\frac{\partial h}{\partial y})] \\ &= \frac{1}{2}[(\frac{\partial g}{\partial x} - \frac{\partial h}{\partial y}) + j(\frac{\partial h}{\partial x} + \frac{\partial g}{\partial y})] \quad .\end{aligned} \tag{I.6}$$

Thus the condition $\frac{\partial f}{\partial \bar{s}} = 0$ is equivalent to the Cauchy-Riemann equations being satisfied. Note also that Lemmas I.2 and I.3 imply $\frac{\partial f}{\partial \bar{s}}$ is conjugate symmetric. Finally, note that

$$ds \wedge d\bar{s} = -2j\ dx \wedge dy \quad . \tag{I.7}$$

It will be convenient to have an expression for the basis (I.5) in terms of polar coordinates on the closed right half plane. Let ja be a point on the $j\omega$-axis. Then a polar coordinate system is given by

$$s = ja + re^{j\alpha} \qquad r \in [0,\infty)$$
$$\alpha \in [-\pi/2, \pi/2] \quad . \tag{I.8}$$

Thus,

$$ds = e^{j\alpha}(dr + jr\ d\alpha) \tag{I.9a}$$

$$d\bar{s} = e^{-j\alpha}(dr - jr\, d\alpha) \quad , \tag{I.9b}$$

$$\frac{\partial}{\partial s} = \frac{1}{2} e^{-j\alpha}(\frac{\partial}{\partial r} - \frac{j}{r}\frac{\partial}{\partial \alpha}) \tag{I.10a}$$

$$\frac{\partial}{\partial \bar{s}} = \frac{1}{2} e^{j\alpha}(\frac{\partial}{\partial r} + \frac{j}{r}\frac{\partial}{\partial \alpha}) \quad , \tag{I.10b}$$

and

$$ds \wedge d\bar{s} = -\,2\,jr\; dr \wedge d\alpha \quad . \tag{I.11}$$

In polar coordinates, (I.6) is given by

$$\begin{aligned}\frac{\partial f}{\partial \bar{s}} &= \frac{1}{2} e^{j\alpha}(\frac{\partial f}{\partial r} + \frac{j}{r}\frac{\partial f}{\partial \alpha}) \\ &= \frac{1}{2} e^{j\alpha}[(\frac{\partial g}{\partial r} + j\,\frac{\partial h}{\partial r}) + \frac{j}{r}\,(\frac{\partial g}{\partial \alpha} + j\,\frac{\partial h}{\partial \alpha})] \\ &= \frac{1}{2} e^{j\alpha}[(\frac{\partial g}{\partial r} - \frac{1}{r}\frac{\partial h}{\partial \alpha}) + j(\frac{\partial h}{\partial r} + \frac{1}{r}\frac{\partial g}{\partial \alpha})] \quad .\end{aligned} \tag{I.12}$$

Proof of Theorem 12.2: Consider the closed curve, $C(R,\varepsilon)$, traversed counter-clockwise, pictured in Figure I.1. Denote the interior of $C(R,\varepsilon)$ by $D(R,\varepsilon)$, the large semicircle by C_R, the small semicircle by C_ε, and let C_1 and C_2 be as pictured in Figure I.1. Let $D(R,\varepsilon)$ have the orientation given by the standard basis for the tangent space to points in $\mathbb{R}^2$. Then Stokes' Theorem [49, p. 124] shows that, letting $f(s) = \log\sigma(s) + j\theta(s)$,

$$\int_{C(R,\varepsilon)} \frac{f(s)}{s-j\omega}\, ds = -\int_{D(R,\varepsilon)} \frac{\partial f}{\partial \bar{s}}\,(\frac{1}{s-j\omega})\, ds \wedge d\bar{s} \quad . \tag{I.13}$$

The proof will be broken into several steps.

Step 1: Take the limit as $\varepsilon \to 0$ in (I.13). First, consider the curve C_ε parameterized by $s(t) = j\omega + \varepsilon e^{j(\pi/2-\pi t)}$, $0 \le t \le 1$. Then $ds = \varepsilon e^{j(\pi/2-\pi t)}(-j\pi)dt$ and continuity implies

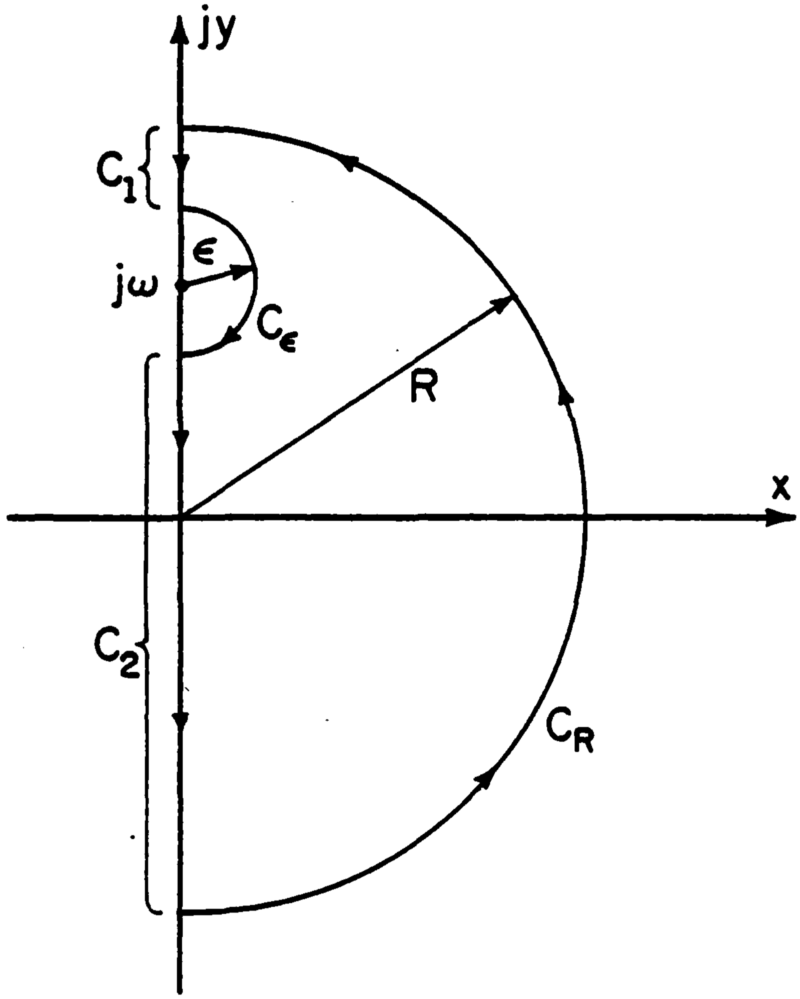

Figure I.1. The curve C(R,ε).

$$\lim_{\varepsilon\to 0} \int_{C_\varepsilon} \frac{f(s)}{s-j\omega}\,ds = -\,j\pi \int_0^1 f(j\omega + \varepsilon e^{j(\pi/2-\pi t)})dt$$

$$= -\,j\pi\, f(j\omega) \quad . \tag{I.14}$$

Thus,

$$\int_{C(R,0)} \frac{f(s)}{s-j\omega}\,ds = \lim_{\varepsilon\to 0} \int_{C(R,\varepsilon)} \frac{f(s)}{s-j\omega}\,ds$$

$$= -\,j\pi\, f(j\omega) + \int_{C_R} \frac{f(s)}{s-j\omega}\,ds$$

$$+ \lim_{\varepsilon\to 0} [\int_R^{\omega+\varepsilon} f(jy)\,\frac{dy}{y-\omega} + \int_{\omega-\varepsilon}^{-R} f(jy)\,\frac{dy}{y-\omega}] \quad . \tag{I.15}$$

Define $\int_R^{-R} f(jy)\,\frac{dy}{y-\omega}$ by the limit in (I.15), provided this limit exists and is finite. The fact that the limit indeed exists and is finite will be proven by showing that $\lim_{\varepsilon\to 0}$ of the right hand side of (I.13) exists and is finite.

First, define a polar coordinate system on the closed right half plane by

$$s = x+jy$$

$$= j\omega + re^{j\alpha} \qquad r\in [0,\infty)$$

$$\alpha\in [-\pi/2,\pi/2] \quad .$$

Then,

$$-\int_{D(R,\varepsilon)} \frac{\partial f}{\partial \bar{s}}\,(\frac{1}{s-j\omega})ds\wedge d\bar{s}$$

$$= 2j \int_{D(R,\varepsilon)} \frac{\partial f}{\partial \bar{s}}\,(e^{-j\alpha})dr\wedge d\alpha \quad . \tag{I.16}$$

Since the integrand of (I.16) is independent of ε, it follows that

$$\int_{D(R,0)} \frac{\partial f}{\partial \bar{s}} (e^{-j\alpha}) dr \wedge d\alpha \triangleq \lim_{\varepsilon \to 0} \int_{D(R,\varepsilon)} \frac{\partial f}{\partial \bar{s}} (e^{-j\alpha}) dr \wedge d\alpha$$

exists and is finite. Thus the limit in (I.15) has these properties. Rearranging yields

$$f(j\omega) = \frac{1}{j\pi} \int_{C_R} f(s) \left(\frac{1}{s-j\omega}\right) ds + \frac{1}{j\pi} \int_{R}^{-R} f(jy) \frac{dy}{y-\omega}$$

$$+ \frac{1}{j\pi} \int_{D(R,0)} \frac{\partial f}{\partial \bar{s}} \left(\frac{1}{s-j\omega}\right) ds \wedge d\bar{s} \quad . \tag{I.17}$$

Similarly, it may be shown that

$$f(-j\omega) = \frac{1}{j\pi} \int_{C_R} f(s) \left(\frac{1}{s+j\omega}\right) ds + \frac{1}{j\pi} \int_{R}^{-R} f(jy) \frac{dy}{y+\omega}$$

$$+ \frac{1}{j\pi} \int_{D(R,0)} \frac{\partial f}{\partial \bar{s}} \left(\frac{1}{s+j\omega}\right) ds \wedge d\bar{s} \quad . \tag{I.18}$$

Thus subtracting (I.18) from (I.17) yields

$$2j[\theta(j\omega) - \theta(0)] = \frac{1}{j\pi} \int_{C_R} f(s) \left[\frac{1}{s-j\omega} - \frac{1}{s+j\omega}\right] ds$$

$$+ \frac{1}{j\pi} \int_{R}^{-R} f(jy) \left[\frac{1}{y-\omega} - \frac{1}{y+\omega}\right] dy$$

$$+ \frac{1}{j\pi} \int_{D(R,0)} \frac{\partial f}{\partial \bar{s}} \left(\frac{1}{s-j\omega}\right) ds \wedge d\bar{s} - \frac{1}{j\pi} \int_{D(R,0)} \frac{\partial f}{\partial \bar{s}} \left(\frac{1}{s+j\omega}\right) ds \wedge d\bar{s}$$

or

$$\theta(j\omega) - \theta(0) = -\frac{1}{2\pi}\int_{C_R} f(s)\,[\frac{1}{s-j\omega} - \frac{1}{s+j\omega}]ds$$

$$-\frac{1}{2\pi}\int_{R}^{-R} f(jy)\,[\frac{1}{y-\omega} - \frac{1}{y+\omega}]dy$$

$$-\frac{1}{2\pi}\int_{D(R,0)} \frac{\partial f}{\partial \bar{s}}\,(\frac{1}{s-j\omega})ds\wedge d\bar{s} + \frac{1}{2\pi}\int_{D(R,0)} \frac{\partial f}{\partial \bar{s}}\,(\frac{1}{s+j\omega})ds\wedge d\bar{s} \quad . \tag{I.19}$$

<u>Step 2</u>: Show that conjugate symmetry implies

$$-\frac{1}{2\pi}\int_{D(R,0)} \frac{\partial f}{\partial \bar{s}}\,(\frac{1}{s-j\omega})ds\wedge d\bar{s} + \frac{1}{2\pi}\int_{D(R,0)} \frac{\partial f}{\partial \bar{s}}\,(\frac{1}{s+j\omega})ds\wedge d\bar{s}$$

$$= -\frac{1}{\pi}\,\mathrm{Re}[\int_{D(R,0)} \frac{\partial f}{\partial \bar{s}}\,(\frac{1}{s-j\omega})ds\wedge d\bar{s}] \quad . \tag{I.20}$$

Define the notation

$$L \triangleq \int_{D(R,0)} \frac{\partial f}{\partial \bar{s}}\,(\frac{1}{s-j\omega})ds\wedge d\bar{s} \tag{I.21a}$$

$$R \triangleq \int_{D(R,0)} \frac{\partial f}{\partial \bar{s}}\,(\frac{1}{s+j\omega})ds\wedge d\bar{s} \tag{I.21b}$$

and a polar coordinate system

$$s = j\omega + re^{j\alpha} \qquad r\in[0,\infty) \quad .$$

$$\alpha\in[-\pi/2,\pi/2] \quad .$$

Then $ds\wedge d\bar{s} = -2jr\,dr\wedge d\alpha$ and $\frac{1}{s-j\omega} = \frac{1}{r}e^{-j\alpha}$. Thus

$$L = -2j\int_{D(R,0)} \frac{\partial f}{\partial \bar{s}}\,e^{-j\alpha}\,dr\wedge d\alpha \quad . \tag{I.22}$$

Assume (with no loss of generality) that $R>\omega$. Then C_R implicitly defines r as a function of α via the equation

$$x^2 + y^2 = R^2 \quad .$$

$$\Rightarrow \quad (r \cos \alpha)^2 + (\omega + r \sin \alpha)^2 = R^2$$

$$\Rightarrow \quad r^2 + r(2\omega \sin \alpha) + \omega^2 - R^2 = 0$$

$$\Rightarrow \quad r = -\omega \sin\alpha + \sqrt{R^2 - \omega^2 \cos^2 \alpha}$$

$$\triangleq F(\alpha) \quad . \tag{I.23}$$

Thus,

$$L = -2j \int_{-\pi/2}^{\pi/2} \int_{0}^{F(\alpha)} \frac{\partial f}{\partial \bar{s}} e^{-j\alpha} \, dr \wedge d\alpha \quad . \tag{I.24}$$

Similarly, define a coordinate system by $s = -j\omega + \rho e^{j\beta}$, $\rho \in [0,\infty)$, $\beta \in [-\pi/2, \pi/2]$ and define $G(\beta) \triangleq \omega \sin \beta + \sqrt{R^2 - \omega^2 \cos^2 \beta}$.

It follows that

$$R = -2j \int_{-\pi/2}^{\pi/2} \int_{0}^{G(\beta)} \frac{\partial f}{\partial \bar{s}} e^{-j\beta} \, d\rho d\beta \quad . \tag{I.25}$$

Conjugate symmetry implies that

$$\left(\frac{\partial f}{\partial \bar{s}}\right)\Big|_{s=\rho e^{j\beta}} = \overline{\left(\frac{\partial f}{\partial \bar{s}}\right)\Big|_{s=\rho e^{-j\beta}}} \quad .$$

Then

$$R = -2j \int_{-\pi/2}^{\pi/2} \int_{0}^{G(\beta)} \overline{\frac{\partial f}{\partial \bar{s}}\Big|_{s=\rho e^{-j\beta}} e^{j\beta}} \, d\rho d\beta \quad . \tag{I.26}$$

Define a new variable of integration $\gamma = -\beta$. Then (I.26) reduces to

$$R = -2j \int_{\pi/2}^{-\pi/2} \int_{0}^{G(-\gamma)} \overline{\left.\frac{\partial f}{\partial \bar{s}}\right|_{s=\rho e^{j\gamma}} e^{-j\gamma}}\, d\rho(-d\gamma) \quad .$$

Noting

$$G(-\gamma) = \omega \sin(-\gamma) + \sqrt{R^2 - \omega^2 \cos^2\gamma}$$
$$= F(\gamma)$$

it follows that

$$R = -2j \int_{-\pi/2}^{\pi/2} \int_{0}^{F(\gamma)} \overline{\frac{\partial f}{\partial \bar{s}} e^{-j\gamma}}\, d\rho d\gamma \quad . \tag{I.27}$$

Equations (I.24) and (I.27) show that $L = -\bar{R}$ (since α and γ are merely dummy variables of integration). Thus the left hand side of (I.20) reduces to

$$-\frac{1}{2\pi} L + \frac{1}{2\pi} R = -\frac{1}{2\pi} [L - R]$$
$$= -\frac{1}{2\pi} [L + \bar{L}]$$
$$= -\frac{1}{\pi} \mathrm{Re}[L]$$

which, using (I.21a), proves (I.20).

From (I.12) and (I.22)

$$L = -2j \int_{D(R,0)} \frac{1}{2} e^{j\alpha} \left[\left(\frac{\partial \log\sigma}{\partial r} - \frac{1}{r}\frac{\partial \theta}{\partial \alpha}\right) + j\left(\frac{\partial \theta}{\partial r} + \frac{1}{r}\frac{\partial \log\sigma}{\partial \alpha}\right)\right] e^{-j\alpha}\, dr \wedge d\alpha$$

$$= \int_{D(R,0)} \left[\left(\frac{\partial \theta}{\partial r} + \frac{1}{r}\frac{\partial \log\sigma}{\partial \alpha}\right) - j\left(\frac{\partial \log\sigma}{\partial r} - \frac{1}{r}\frac{\partial \theta}{\partial \alpha}\right)\right] dr \wedge d\alpha \quad .$$

Thus,

$$-\frac{1}{\pi} \mathrm{Re}[L] = -\frac{1}{\pi} \int_{D(R,0)} \left(\frac{\partial \theta}{\partial r} + \frac{1}{r}\frac{\partial \log\sigma}{\partial \alpha}\right) dr \wedge d\alpha \quad . \tag{I.28}$$

Using (I.28) in (I.19) yields

$$\theta(j\omega) - \theta(0) = -\frac{1}{2\pi}\int_{C_R} f(s)\,[\frac{1}{s-j\omega} - \frac{1}{s+j\omega}]ds$$

$$-\frac{1}{2\pi}\int_{R}^{-R} f(jy)\,[\frac{1}{y-\omega} - \frac{1}{y+\omega}]dy$$

$$-\frac{1}{\pi}\int_{D(R,0)} (\frac{\partial\theta}{\partial r} + \frac{1}{r}\frac{\partial \log\sigma}{\partial\alpha})dr\wedge d\alpha \quad . \tag{I.29}$$

Step 3: Show that the following limits exist and are finite:

$$A \triangleq \lim_{R\to\infty} \frac{-1}{2\pi}\int_{C_R} f(s)\,[\frac{1}{s-j\omega} - \frac{1}{s+j\omega}]ds$$

$$B \triangleq \lim_{R\to\infty} \frac{-1}{2\pi}\int_{R}^{-R} f(jy)\,[\frac{1}{y-\omega} - \frac{1}{y+\omega}]dy \quad .$$

First consider

$$A = \lim_{R\to\infty} \frac{-1}{2\pi}\int_{C_R} f(s)\frac{2j\omega}{s^2+\omega^2}ds \quad .$$

Define polar coordinates $s = Re^{j\alpha}$, $R\in[0,\infty)$, $\alpha\in[-\pi/2,\pi/2]$. Then,

$$A = \lim_{R\to\infty} \frac{-j\omega}{\pi}\int_{-\pi/2}^{\pi/2} f(Re^{j\alpha})\,[\frac{Re^{j\alpha}}{R^2e^{2j\alpha} + \omega^2}]j\,d\alpha$$

$$= \lim_{R\to\infty} \frac{\omega}{\pi}\int_{-\pi/2}^{\pi/2} f(Re^{j\alpha})\,[\frac{Re^{j\alpha}}{R^2e^{2j\alpha} + \omega^2}]d\alpha \quad .$$

Define

$$M(R) \triangleq \sup_{\alpha\in[-\pi/2,\pi/2]} \left|f(Re^{j\alpha})\,[\frac{Re^{j\alpha}}{R^2e^{2j\alpha} + \omega^2}]\right|$$

$$\leq \sup_{\alpha\in[-\pi/2,\pi/2]} |f(Re^{j\alpha})|\,\frac{R}{R^2-\omega^2}$$

where $R>\omega$ is assumed with no loss of generality. From Lemma 12.1 it follows that as $R\to\infty$ $\log\sigma$ approaches infinity no faster than $\log R$ and θ remains bounded. Thus $M(R)\to 0$ as $R\to\infty$. A standard argument may then be used to show that $A=0$.

Next, consider

$$B = \lim_{R\to\infty} \frac{-1}{2\pi} \int_{R}^{-R} f(jy) \frac{2\omega}{y^2-\omega^2} dy$$

$$= \lim_{R\to\infty} \frac{\omega}{\pi} \int_{-R}^{R} f(jy) \frac{1}{y^2-\omega^2} dy \quad .$$

An argument similar to the one used to show $A=0$ may be used to show

$$B = \frac{\omega}{\pi} \int_{-\infty}^{\infty} f(jy) \frac{1}{y^2-\omega^2} dy \quad .$$

Conjugate symmetry implies

$$B = \frac{2\omega}{\pi} \int_{0}^{\infty} \log\sigma\cdot\left(\frac{1}{y^2-\omega^2}\right) dy \quad .$$

Define

$$\int_{CRHP} \left(\frac{\partial\theta}{\partial r} + \frac{1}{r}\frac{\partial\log\sigma}{\partial\alpha}\right) dr\wedge d\alpha = \lim_{R\to\infty} \int_{D(R,0)} \left(\frac{\partial\theta}{\partial r} + \frac{1}{r}\frac{\partial\log\sigma}{\partial\alpha}\right) dr\wedge d\alpha$$

where the existence and finiteness of the limit follows from (I.29) and the fact that A and B exist and are finite. Thus, (I.29) reduces to

$$\theta(j\omega) - \theta(0) = -\frac{2\omega}{\pi} \int_{0}^{\infty} \log\sigma\cdot\left(\frac{1}{\omega^2-y^2}\right) dy$$

$$-\frac{1}{\pi} \int_{CRHP} \left(\frac{\partial\theta}{\partial r} + \frac{1}{r}\frac{\partial\log\sigma}{\partial\alpha}\right) dr\wedge d\alpha \quad . \tag{I.30}$$

An argument identical to one used by Bode may be applied to the first integral in (I.30) to show

$$\theta(j\omega) - \theta(0) = \frac{1}{\pi} \int_{-\infty}^{\infty} \frac{d \log \sigma (j\omega)}{d\nu} \{\log \coth \frac{|\nu|}{2}\} d\nu$$

$$- \frac{1}{\pi} \int_{CRHP} \left(\frac{\partial\theta}{\partial r} + \frac{1}{r} \frac{\partial \log\sigma}{\partial\alpha}\right) dr \wedge d\alpha$$

where

$$\nu = \log (y/\omega) \quad .$$

The fact that

$$j \left[\frac{\partial\theta}{\partial r} + \frac{1}{r} \frac{\partial \log\sigma}{\partial\alpha}\right] = - \rho_v^H \frac{\partial \rho_v}{\partial r} + \rho_u^H \frac{\partial \rho_u}{\partial r}$$

yields the result. (Note in the statement of the theorem that ω is replaced by ω_o and y is replaced by ω.)

■

REFERENCES

[1] N. A. Lehtomaki, D. Castanon, B. Levy, G. Stein, N. R. Sandell, Jr., and M. Athans, "Robustness Tests Utilizing the Structure of Modelling Error," Proc. 20th IEEE Conf. on Decision and Control, pp. 1173-1190, San Diego, CA, December 1981.

[2] H. Kwakernaak, "Robustness Optimization of Linear Feedback Systems," Proc. 22nd IEEE Conf. on Decision and Control, pp. 618-624, San Antonio, TX, December 1983.

[3] J. B. Cruz, Jr. and W. R. Perkins, "A New Approach to the Sensitivity Problem in Multivariable Feedback System Design," IEEE Trans. Automat. Contr., Vol. AC-9, pp. 216-223, 1964.

[4] J. C. Doyle and G. Stein, "Multivariable Feedback Design: Concepts for a Classical/Modern Synthesis," IEEE Trans. Automat. Contr., Vol. AC-26, pp. 4-16, February 1981.

[5] J. C. Doyle, J. E. Wall, Jr., and G. Stein, "Performance and Robustness Analysis for Structured Uncertainty," Proc. 21st IEEE Conf. on Decision and Control, pp. 629-636, Orlando, FL, December 1982.

[6] H. Nyquist, "Regeneration Theory," Bell Syst. Tech. J., pp. 126-147, January 1932.

[7] H. W. Bode, Network Analysis and Feedback Amplifier Design, Van Nostrand, Princeton, NJ, 1945.

[8] Y. W. Lee, "Synthesis of Electric Networks by Means of the Fourier Transforms of Laguerre's Functions," J. Math. and Phys., Vol. XI, pp. 83-113, June 1932.

[9] I. M. Horowitz, Synthesis of Feedback Systems, Academic Press, NY, 1963.

[10] J. S. Freudenberg, D. P. Looze, and J. B. Cruz, Jr., "Robustness Analysis Using Singular Value Sensitivities," Int. J. Contr., Vol. 35, No. 1, pp. 95-116, 1982.

[11] J. B. Cruz, Jr., J. S. Freudenberg, and D. P. Looze, "A Relationship Between Sensitivity and Stability of Multivariable Feedback Systems," IEEE Trans. Automat. Contr., Vol. AC-26, pp. 66-74, February 1981.

[12] N. A. Lehtomaki, N. R. Sandell, Jr., and M. Athans, "Robustness Results in Linear-Quadratic Gaussian Based Multivariable Control Design," IEEE Trans. Automat. Contr., Vol. AC-26, pp. 75-92, February 1981.

[13] M. G. Safonov, A. J. Laub, and G. L. Hartman, "Feedback Properties of Multivariable Systems: The Role and Use of the Return Difference Matrix," IEEE Trans. Automat. Contr., Vol. AC-26, pp. 47-65, February 1981.

[14] I. Postlethwaite, J. M. Edmunds, and A. G. J. MacFarlane, "Principal Gains and Principal Phases in the Analysis of Linear Multivariable Feedback Systems," IEEE Trans. Automat. Contr., Vol. AC-26, pp. 32-46, February 1981.

[15] D. C. Youla, H. A. Jabr, and J. J. Bongiorno, "Modern Wiener-Hopf Design of Optimal Controllers - Parts I and II," IEEE Trans. Automat. Contr., Vol. AC-21, pp. 3-13, February 1976 and pp. 319-338, June 1976.

[16] G. Zames and B. A. Francis, "Feedback, Minimax Sensitivity, and Optimal Robustness," IEEE Trans. Automat. Contr., Vol. AC-28, No. 5, pp. 585-601, May 1983.

[17] G. Zames, "Feedback and Optimal Sensitivity: Model Reference Transformations, Multiplicative Seminorms, and Approximate Inverses," IEEE Trans. Automat. Contr., Vol. AC-26, pp. 301-320, 1981.

[18] P. M. Frank, Introduction to System Sensitivity Theory, Academic Press, NY, 1978.

[19] J. E. Wall, Jr., J. C. Doyle, and C. A. Harvey, "Tradeoffs in the Design of Multivariable Feedback Systems," 18th Allerton Conference, pp. 715-725, October 1980.

[20] M. G. Safonov and B. S. Chen, "Multivariable Stability Margin Optimization with Decoupling and Output Regulation," Proc. 21st IEEE Conf. on Decision and Control, pp. 616-622, December 1982.

[21] B. A. Francis and G. Zames, "On Optimal Sensitivity Theory for SISO Feedback Systems," IEEE Trans. Automat. Contr., Vol. AC-29, No. 1, pp. 9-16, January 1984.

[22] V. H. L. Cheng and C. A. Desoer, "Limitations on the Closed-Loop Transfer Function Due to Right-Half Plane Transmission Zeros of the Plant," IEEE Trans. Automat. Contr., Vol. AC-25, pp. 1218-1220, December 1980.

[23] J. S. Freudenberg and D. P. Looze, "Sensitivity Reduction, Nonminimum Phase Zeros, and Design Tradeoffs in Single Loop Feedback Systems," Proc. 22nd IEEE Conf. on Decision and Control, pp. 980-985, San Antonio, TX, December 1983.

[24] J. S. Freudenberg and D. P. Looze, "Limitations on Feedback Properties Imposed by Unstable Open Loop Poles," Proc. 1984 American Control Conf., pp. 582-583, June 1984.

[25] J. S. Freudenberg and D. P. Looze, "Right Half Plane Poles and Zeros and Design Tradeoffs in Feedback Systems," IEEE Trans. Automat. Contr., to appear.

[26] N. Levinson and R. M. Redheffer, Complex Variables, Holden-Day, San Francisco, CA, 1970.

[27] A. E. Guillemin, The Mathematics of Circuit Analysis, Wiley, NY, 1949.

[28] J. S. Freudenberg and D. P. Looze, "An Analysis of H^{∞}-Optimization Design Methods," Proc. 22nd IEEE Conf. on Decision and Control, pp. 560-561, San Antonio, TX, December 1983.

[29] D. P. Looze and J. S. Freudenberg, "On the Relation of Open Loop to Closed Loop Properties in Multivariable Feedback Systems," Proc. 1983 American Control Conf., pp. 272-277, San Francisco, CA, June 1983. Also IEEE/CSS Robust Control Workshop, Interlaken, Switzerland, October 1982.

[30] J. C. Doyle, "Analysis of Feedback Systems with Structured Uncertainties," IEE Proc., Vol. 129, Pt. D, No. 6, pp. 242-250, November 1982.

[31] A. G. J. MacFarlane and D. F. A. Scott-Jones, "Vector Gain," Int. J. Control, Vol. 29, pp. 65-91, 1979.

[32] T. Kato, A Short Introduction to Perturbation Theory for Linear Operators, Springer-Verlag, NY, 1982.

[33] Y. S. Hung and A. G. J. MacFarlane, Multivariable Feedback: A Quasi-Classical Approach, Lecture Notes in Control and Information Sciences, 40, Springer-Verlag, Berlin, 1982.

[34] J. S. Freudenberg and D. P. Looze, "Phase in Multivariable Feedback Systesm," Proc. 23rd IEEE Conf. on Decision and Control, pp. 313-314, Las Vegas, NV, December 1984.

[35] C. A. Desoer and J. D. Schulman, "Zeros and Poles of Matrix Transfer Functions and their Dynamical Interpretation," IEEE Trans. Circ. and Syst., Vol. CAS-21, pp. 3-8, January 1974.

[36] Å. Björck and G. H. Golub, "Numerical Methods for Computing Angles Between Linear Subspaces," Mathematics of Computation, Vol. 27, No. 123, pp. 579-594, July 1973.

[37] G. W. Stewart, Introduction to Matrix Computations, Academic Press, NY, 1973.

[38] G. Strang, Linear Algebra and Its Applications, Academic Press, NY, 1976.

[39] V. C. Klema and A. J. Laub, "The Singular Value Decomposition: Its Computation and Some Applications," IEEE Trans. Automat. Contr., Vol. AC-25, No. 2, pp. 164-176, April 1980.

[40] P. R. Halmos, Finite-Dimensional Vector Spaces, 2nd Edition, Van Nostrand, Princeton, NJ, 1958.

[41] B. D. O. Anderson, "A Simplified Viewpoint of Hyperstability," IEEE Trans. Automat. Contr., Vol. AC-13, pp. 292-294, June 1968.

[42] H. H. Rosenbrock, Computer-Aided Control System Design, Academic Press, London, 1974.

[43] I. Postlethwaite and A. G. J. MacFarlane, A Complex Variable Approach to the Analysis of Linear Multivariable Feedback Systems, Lecture Notes in Control and Information Sciences, 12, Springer-Verlag, Berlin, 1979.

[44] J. S. Freudenberg and D. P. Looze, "The Multivariable Nature of Multivariable Feedback Systems," Proc. 22nd IEEE Conf. on Decision and Control, pp. 786-787, San Antonio, TX, December 1983.

[45] J. S. Freudenberg and D. P. Looze, "The Relation Between Open Loop and Closed Loop Properties of Multivariable Feedback Systems: A Practical Example," Proc. 23rd IEEE Conf. on Decision and Control, pp. 322-323, Las Vegas, NV, December 1984.

[46] Final Technical Report TR-168-1, "Robustness Analysis of Beam Pointing Control Systems," ALPHATECH, Inc., Burlington, MA, May 1983.

[47] L. A. Zadeh and C. A. Desoer, Linear System Theory, McGraw-Hill, NY, 1963.

[48] J. B. Conway, Functions of One Complex Variable, 2nd Edition, Springer-Verlag, NY, 1978.

[49] M. Spivak, Calculus on Manifolds, Benjamin, NY, 1965.

[50] H. M. Farkas and I. Kra, Riemann Surfaces, Springer-Verlag, NY, 1980.

[51] J. W. Vick, Homology Theory, Academic Press, NY, 1973.

[52] M. J. Greenberg and J. R. Harper, Algebraic Topology, A First Course, Benjamin/Cummings, Reading, MA, 1981.

[53] H. J. Bernstein and A. V. Phillips, "Fiber Bundles and Quantum Theory," Sci. Amer., pp. 122-137, July 1981.

[54] D. Bleeker, Gauge Theory and Variational Principles, Addison-Wesley, Reading, MA, 1981.

[55] S. T. Hu, Homotopy Theory, Academic Press, NY, 1959.

[56] G. Polya and G. Latta, Complex Variables, Wiley, NY, 1974.

[57] J. J. DiStefano, III, A. R. Stubberud, and I. J. Williams, Feedback and Control Systems, Schaum's Outline Series, McGraw-Hill, NY, 1967.

[58] K. Knopp, Infinite Sequences and Series, Dover, NY, 1956.

[59] G. W. Stewart, "Error and Perturbation Bounds for Subspaces Associated with Certain Eigenvalue Problems," SIAM Review, Vol. 15, No. 4, pp. 727-764, October 1973.

[60] A. G. J. MacFarlane and Y. S. Hung, "Analytic Properties of the Singular Values of a Rational Matrix," Int. J. Control, Vol. 37, No. 2, pp. 221-234, 1983.

[61] R. C. Gunning and H. Rossi, Analytic Functions of Several Complex Variables, Prentice-Hall, Englewood Cliffs, NJ, 1965.

[62] P. Griffiths and J. Harris, Principles of Algebraic Geometry, Wiley, NY, 1978.

[63] G. Springer, Introduction to Riemann Surfaces, 2nd Edition, Chelsea, NY, 1981.

[64] L. Auslander and R. E. MacKenzie, Introduction to Differentiable Manifolds, Dover, NY, 1977.

VITA

James Scott Freudenberg was born March 31, 1956, and grew up in Gibson County, Indiana. He graduated from Rose-Hulman Institute of Technology, Terre Haute, Indiana, in May 1978, receiving Bachelor of Science degrees in Mathematics and in Physics. Following graduation, he worked one year for the Navigation Systems Technology Group of Rockwell/Collins Avionics, Cedar Rapids, Iowa. From 1979-1984 he was a graduate student at the University of Illinois, receiving Master of Science and Doctor of of Philosophy degrees in electrical engineering. Since September 1984, he has been an Assistant Professor in the Department of Electrical Engineering and Computer Science, University of Michigan, Ann Arbor, Michigan.

END

FILMED

1-86

DTIC